INTEGRATED FACIES-ANALYSIS AND STRATIGRAPHY OF THE EARLY MIOCENE NORTH ALPINE FORELAND BASIN (UPPER AUSTRIA)

Dissertation
zur Erlangung des Doktorgrades der Naturwissenschaften
an der Karl-Franzens-Universität Graz
Institut für Erdwissenschaften

vorgelegt von
Mag. rer. nat. Patrick Grunert
Graz, Juli 2011

CONTENTS

PREFACE

The present thesis results from joint projects on Upper Oligocene-Lower Miocene marine deposits of the North Alpine Foreland Basin (NAFB) that were initiated in 2007 by the Commission for the Paleontological and Stratigraphical Research of Austria (CPSA; Austrian Academy of Sciences) and Rohöl-Aufsuchungs AG (RAG). In an effort to combine the resources from academia and industry, the scientific objectives of the project bundle encompass

(1) the documentation of facies evolution and distribution in the NAFB based on microfossil assemblages (foraminifers, dinoflagellate cysts, calcareous nannoplankton) and geochemical proxies,

(2) the development of an improved age model for the NAFB derived from bio-, magneto- and sequence stratigraphic data that allow a correlation of the lithostratigraphic units to the astronomically tuned Neogene time-scale (Lourens et al., 2004), and

(3) the identification of global (eustatic sea-level, global climate change) and local (tectonics, current patterns, local climate change) signals that shaped the paleoceanographic evolution of the NAFB.

The doctoral candidate performed benthic foraminiferal analyses and various geochemical measurements and was responsible for coordination of the project activities between CPSA and RAG, the distribution of sample material to project partners and the integration of all evaluated data for publication.

The present thesis summarizes the main results for selected Early Miocene localities of the NAFB. Chapter 1 provides a brief introduction to the Central Paratethys sea, the NAFB and the Upper Austrian study area, the value of foraminifers for paleoenvironmental and stratigraphic analysis and the underlying principles of the applied geochemical proxies. Chapters 2-5 consist of four scientific articles that have been published by or submitted to international, peer-reviewed journals:

Chapter 2 Grunert, P., Harzhauser, M., Rögl, F., Sachsenhofer, R., Gratzer, R., Soliman, A., Piller, W.E. (2010). Oceanographic conditions as a trigger for the formation of an Early Miocene (Aquitanian) *Konservat-Lagerstätte* in the Central Paratethys Sea. *Palaeogeography, Palaeoclimatology, Palaeoecology* 292, 425–442.

Chapter 3 Grunert, P., Hinsch, R., Sachsenhofer, R., Ćorić, S., Harzhauser, M., Piller, W.E., Sperl, H. (submitted). Early Burdigalian upfill of the Puchkirchen Basin (North Alpine Foreland Basin, Central Paratethys): facies development and sequence stratigraphy. *Marine and Petroleum Geology*.

Chapter 4 Grunert, P., Soliman, A., Ćorić, S., Roetzel R., Harzhauser, M., Piller, W.E. (submitted). Facies development along the tide-influenced shelf of the Burdigalian Seaway: an example from the Ottnangian stratotype (Early Miocene, middle Burdigalian). *Marine Micropaleontology*.

Chapter 5 Grunert, P., Soliman, A., Ćorić, S., Scholger, R., Harzhauser, M., Piller, W.E. (2010). Stratigraphic re-evaluation of the stratotype for the regional Ottnangian stage (Central Paratethys, middle Burdigalian). *Newsletters on Stratigraphy* 44, 1–16.

Chapters 2-5 correspond to the three studied regional stages Egerian (chapter 2), Eggenburgian (chapter 3) and Ottnangian (chapter 4-5). A concluding synopsis on the stratigraphic and paleoenvironmental implications for the Early Miocene NAFB is provided in the final chapter 6.

Acknowledgements

At this point I would like to express my sincere thanks to a number of people that have contributed to the present thesis.

I am grateful to my supervisors Werner E. Piller and Mathias Harzhauser for their guidance with countless discussions, constructive comments and critical reviews over the past years. Not only did you offer me useful advice with my thesis, but you also provided me the opportunity to participate in teaching and to attend conferences, workshops and summer schools. I deeply appreciate this continuous support that was important for my growth as a person and as a scientist.

I want to thank my co-workers within the project who contributed their precious time and data to the present work: Stjepan Ćorić, Reinhard Gratzer, Ralph Hinsch, Reinhard Roetzel, Fred Rögl, Reinhard Sachsenhofer, Robert Scholger and Ali Soliman. In the course of the project, a number of people have contributed to the outcome of this thesis with intense discussions, constructive comments and thorough manuscript reviews: Ulrich Bieg, Katharina Borowski, Thierry Corrège, Sorin Filipescu, Mourad Greiss, Martin Head, Steve Hubbard, Oleg Mandic, Gonzalo Jimenez-Moreno, Michael Kaminski, Gerhard Linzer, Stefan Müllegger, Wolfgang Nachtmann, Martina Pippèrr, Bettina Reichenbacher, Markus Reuter, Sylvain Richoz, Christian Rupp, Hanns Sperl and Ludwig Wagner. Elvira Eberhard, Wolfgang Mitterlehner, Stefan Pfingstl, Claudia Puschenjak, Doris Reischenbacher, Karl Stingl and Franz Topka are acknowledged for their help with field-work, sample collection and preparation and paleomagnetic and geochemical measurements.

Finally, I want to thank my family. I am deeply grateful for your support in so many respects over the past ten years. Katrin, the passion and commitment you show in your work is inspiring, good luck in Norway! Claudia, thank you for your encouraging words and patience during the intense finish.

ABSTRACT

The herein presented thesis results from four case studies on Early Miocene facies and stratigraphy of the North Alpine Foreland Basin (NAFB) of Upper Austria. Microfossil, geochemical and sedimentary proxy records were integrated with bio-, magneto- and sequence stratigraphy in order to document facies distribution and development through time at selected localities in the study area. The achieved correlation to the global stratigraphic record allows the determination of regional and global events that affected the NAFB.

During the Early Aquitanian/late Egerian marine deposition in the NAFB was restricted to its eastern parts. The finely laminated deposits of the Ebelsberg Fm. from the section Pucking exemplarily document the paleoceanographic conditions along the northern shelf of the Puchkirchen Basin. Assemblages of foraminifers and dinoflagellate cysts together with geochemical proxies reveal an outer shelf and upper slope facies of the Puchkirchen Basin that complements previous studies on coeval shelf and basinal facies. Upwelling and episodically increased coastal runoff provided large amounts of nutrients stimulating primary productivity and triggered dysoxic-anoxic bottom waters of an oxygen minimum zone. The new data help to understand the complex oceanographic processes that led to the formation of an exceptional *Konservat-Lagerstätte* within the Ebelsberg Fm. Episodes of intensified upwelling and blooms of productivity, surface-water currents and storm events are all discussed as triggers for the accumulation of rich and well-preserved fossil assemblages that occur in distinct intervals of the section.

At the beginning of the Burdigalian/middle Eggenburgian a major transgression established a western connection of the NAFB with the Mediterranean. This new marine gateway is called the Burdigalian Seaway and existed until the middle Burdigalian/middle Ottnangian. The borehole Hochburg 1, located in the center of the Puchkirchen Basin, was selected for evaluation of the pelitic Hall Fm. The studied section comprises a complete middle Eggenburgian to lower Ottnangian sedimentary record. The revealed benthic foraminiferal assemblages and geochemical proxies document the sedimentary upfill of the Puchkirchen Basin during the early Burdigalian: with the beginning of the transgression that established the Burdigalian Seaway, the long-lived basin-axial Puchkirchen Channel System was briefly reactivated, resulting in intense reworking of Chattian-Aquitanian/Egerian deposits. Channel deposition eventually ceased in the course of the transgression and a bathyal environment with flysch-type faunas dominated by *Bathysiphon filiformis* established. Large amounts of sediment were shed into the basin by several extensive river systems that entered the basin from north, west and south. In the study area, a NE prograding delta developed that is reflected in a characteristic agglutinated foraminiferal fauna with small-sized specimens of *Ammodiscus*. High sedimentation rates finally led to the upfill of the Puchkirchen Basin by the end of the Eggenburgian. At the base of the Ottnangian, a last major transgression re-established a suboxic bathyal setting reflected in rich agglutinated foraminiferal assemblages. Subsequently, characteristic hyaline foraminiferal faunas with *Lenticulina inornata*,

Cibicidoides lopjanicus and *Ammonia beccharii* developed in the shallowing environment of the extensive early Ottnangian shelf sea.

Ottnang-Schanze, the stratotype of the Ottnangian stage, represents deposition during the maximum extent of the Burdigalian Seaway in the late early Ottnangian. A distinctive change in microfossil assemblages documents the transition from an outer neritic to bathyal towards a middle neritic paleoenvironment under the influence of currents and storm events. The development reflects the beginning of a regressive trend that culminated in the middle Ottnangian when the sea regressed entirely from the study area sea.

The integrated bio-, magneto- and sequence stratigraphic records allow a correlation to the global stratigraphic records and an evaluation of global and local events in the records of the Puchkirchen Basin. In general, the results support previous studies that suggest a primary control of eustatic sea-level on the basin rather than Alpine tectonics during the Burdigalian. Most prominently the transgression at the base of the Hall Fm. is linked to a eustatic rise in sea-level during the earliest Burdigalian that is well documented from all over the world.

For the Burdigalian, three sequences are identified in the Puchkirchen Basin that correspond to the global 3rd-order sequences Bur 1-3. The sequence stratigraphic evaluation together with nannoplankton data suggests that the hiatus between the Egerian Upper Puchkirchen Fm. and the Hall Fm. comprises the entire lower Eggenburgian and corresponds to at least 1 Ma. The new data further indicate that the lithostratigraphic boundary between Eggenburgian/Ottnangian does not correspond to the geochronological boundary. The latter, corresponding to the Bur 3 sequence boundary, is identified deep within the Hall Fm. The new stratigraphic data from Ottnang-Schanze constrain the maximum extent of the Burdigalian Seaway and the beginning of the final regressive phase to c. 18 Ma.

Finally, the present study contributes to current debates on regional biostratigraphy. The results confirm the FODs of *Elphidium felsense* and *E. ortenburgense* at the base of the middle Eggenburgian and restriction of *Lenticulina buergli* to the Eggenburgian. However, the occurence of blooms of *Uvigerina posthantkeni* in the strongly reworked Egerian deposits at the base of the Hall Fm. once more documents the problematic biostratigraphic value of this index species for the base of the Eggenburgian.

CHAPTER 1

INTRODUCTION TO THE STUDY AREA AND APPLIED METHODOLGY

1.1. The Central Paratethys sea: paleogeography and stratigraphy

From Oligocene to Middle Miocene large parts of Central Europe were covered by the Central Paratethys Sea (Fig. 1.1; Rögl, 1998; Harzhauser and Piller, 2007). This epicontinental sea came into existence around the Eocene/Oligocene boundary due to the northward movement of the African plate. The continuous rise of the Alpine mountain chain resulted in the disintegration of the ancient Tethys sea into the Paratethys sea in the North and the Mediterranean sea in the South. Paleogeography and paleoceanography of the Central Paratethys were controlled by an intense

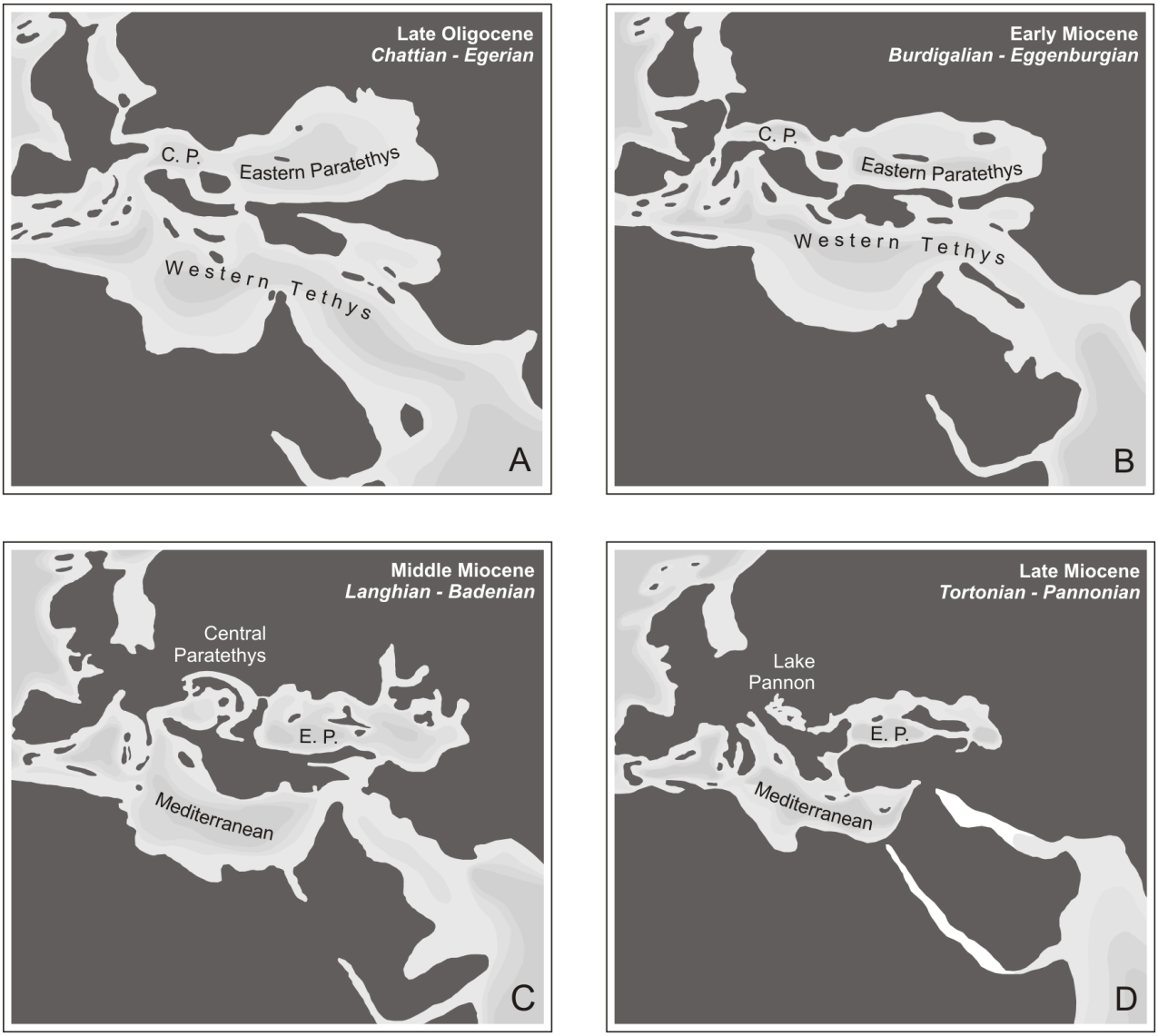

Fig. 1.1. Late Oligocene – Late Miocene paleogeographic evolution of the Paratethys and Mediterranean seas according to Rögl (1998) and Harzhauser and Piller (2007).

interplay of global sea-level changes and regional tectonics (Rögl, 1998; Harzhauser et al., 2007; Piller et al., 2007). Due to continuing restriction during the Middle Miocene the Central Paratethys finally developed into the Pannonian Lake System (Harzhauser and Piller, 2007).
The complex pattern of changing land bridges and seaways had a severe impact on the fauna and flora and resulted in distinct biogeographic patterns, recognised already by Laskarev (1924) who was the first to introduce the concept of the Paratethys (Rögl, 1998; Harzhauser et al., 2007). With the progress in understanding the unique and complex history of the Central Paratethys, efforts towards a regional stratigraphic concept were taken culminating in the series "Chronostratigraphie und Neostratotypen" (Cicha et al., 1967; Steininger and Seneš, 1971; Baldí and Seneš, 1975; Papp et al., 1973, 1974, 1978, 1985; Stevanović et al., 1990). This concept paralleling global Oligocene-Miocene stratigraphy has been applied to the Central Paratethys since then and further attempts have been made to correlate the regional stages more and more precisely to the international chronostratigraphic framework (e.g., Rögl et al., 1979; Rögl 1998; Kováč et al. 2004; Piller et al. 2007; Lirer et al. 2009; De Leeuw et al., 2010; Vasiliev et al., 2010). For each of the regional stages a holostratotype and several faciostratotypes has been selected. As the later represent characteristic facies reflecting regional environmental changes these sections do not follow the GSSP concept of the International Commission for Stratigraphy that was established somewhat later (Hedberg, 1976).

1.2. The North Alpine Foreland Basin

The North Alpine Foreland Basin (NAFB; in many studies referred to as Molasse Basin) extends from Savoy (France) in the west to Lower Austria in the east (Kuhlemann and Kempf, 2002). Mesozoic and Paleozoic rocks of the Swiss Jura Mountains, the Vosges, the Black Forest, the Franconian Platform and the Bohemian Massif confine the NAFB to the North while it is bordered by the Alps in the South (Bachmann et al., 1987; Kuhlemann and Kempf, 2002). Due to the load of the Alpine nappes the NAFB is strongly asymmetric (Bachmann et al., 1987).
The basin is filled with Paleozoic-Cenozoic sediments superimposed on the Varsician basement: a 500-1000m thick succession of upper Paleozoic and Mesozoic deposits is followed by Cenozoic sediments ("Molasse") that predominantly consist of clastic Alpine debris and locally reach a thickness of 5000m (Bachmann et al., 1987; Malzer et al., 1993; Wagner, 1998; Kuhlemann and Kempf, 2002). The Paleozoic, Mesozoic and Paleogene strata continue at least 50km below the Alpine nappes to the south (Bachmann et al., 1987).
The tectonic and paleogeographic evolution of the NAFB is strongly related to Alpine orogeny and the disintegration of the Tethys sea (Bachmann et al., 1987; Malzer et al., 1993; Berger, 1996; Rögl, 1998; Wagner, 1998; Kuhlemann and Kempf, 2002; Harzhauser and Piller, 2007): the Triassic to Eocene sediments were deposited along the northern Tethyan shelf (Bachmann et al., 1987; Wagner, 1998). During this time the continuous collision of the African and European plates resulted in the rise of the Alpine mountain chain that finally formed an archipelago. Around the

Eocene/Oligocene boundary this biogeographic barrier divided the Tethys into the northern Paratethys and the southern Mediterranean seas (Rögl, 1998; Harzhauser and Piller, 2007). Subsequently, the NAFB acted as one of the main sedimentary basins of the Central Paratethys until the upfill of the basin and a major paleogeographic reorganization led to the regression of the sea towards the east (Rögl, 1998; Wagner, 1998).

The present study focuses on the Early Miocene development of the NAFB (Fig. 1.2). At the beginning of the Aquitanian (late Egerian) the marine connection towards the Mediterranean in the west was interrupted (Wenger, 1987; Malzer et al., 1993; Berger, 1996; Wagner, 1998; Kuhlemann and Kempf, 2002). Marine sedimentation was confined to the eastern part of the NAFB with the exception of short-term marine ingressions via the Bresse-Rhône Graben during sea-level highstands (Berger, 1996; Kuhlemann and Kempf, 2002). West of Munich, terrestrial paleoenvironments developed with large river systems originating from the Alps (Untere Süßwasser Molasse/Lower Freshwater Molasse; Berger, 1996; Wagner, 1998; Kuhlemann and Kempf, 2002; Doppler et al., 2005). A major transgression re-established basin-wide marine conditions during the early Burdigalian, initiating a wave of faunal immigration from the Atlantic and Mediterranean into the Central Paratethys (Vavra, 1979; Berger, 1996; Schlunegger

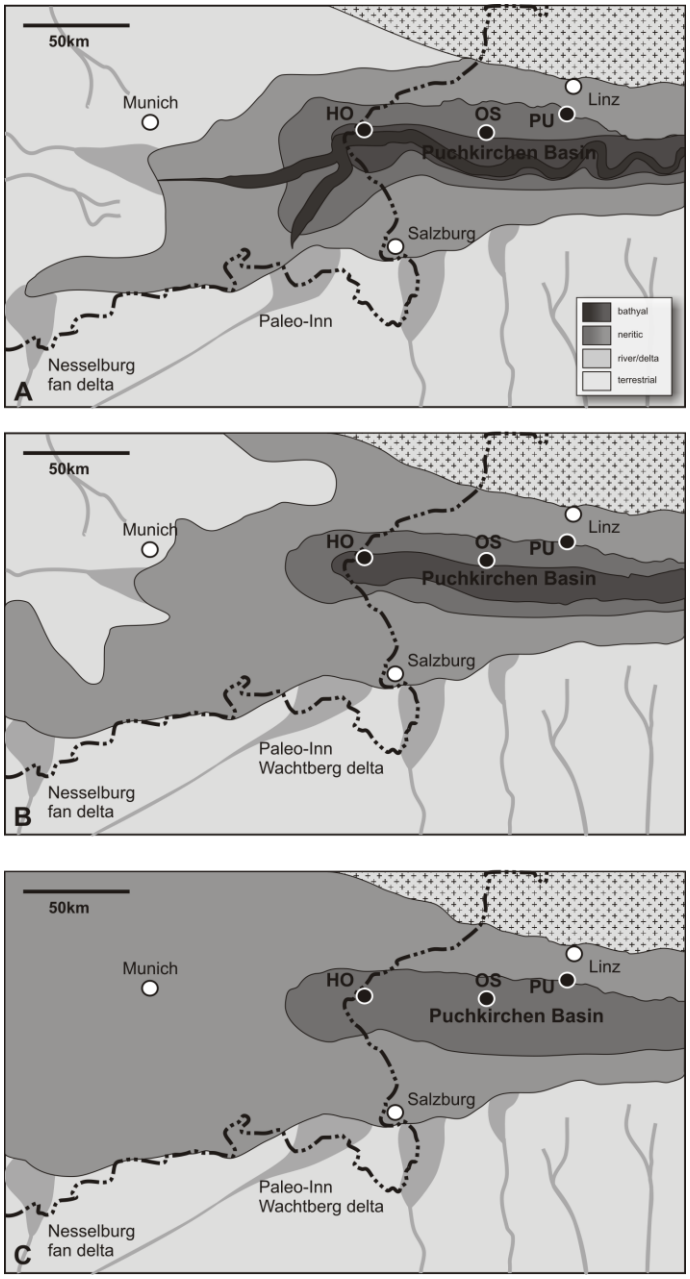

Fig. 1.2. Paleogeographic evolution of the study area during the Early Miocene. The maps are compiled from Wenger (1987), Kuhlemann and Kempf (2002), Bieg (2005) and Hinsch (2008).

A: upper Egerian-middle Eggenburgian. Restriction of marine deposition to the eastern NAFB and presence of the Puchkirchen Channel System.

B: middle-upper Eggenburgian. Transgression establishes Burdigalian Seaway, Puchkirchen Basin filled up.

C: early Ottnangian. Maximum extent of Burdigalian Seaway.

Fig. 1.3. Location of the studied sites Pucking, Hochburg 1 and Ottnang-Schanze in the Upper Austrian study area.

et al., 1997; Rögl, 1998; Kroh and Harzhauser, 1999; Mandic and Steininger, 2003; Kroh and Menkveld-Gfellner, 2006). This newly established gateway is commonly referred to as the Burdigalian Seaway (Allen et al., 1985). In contrast to the wide and deep-marine Oligocene foreland basin, the Burdigalian Seaway was a strait with extensive shelf areas narrowed by the advancing Alpine thrust front. Deep-water environments were limited to the Puchkirchen Basin and the easternmost part of the NAFB along the steep escarpment of the Bohemian Massif (Wenger, 1987; Rögl, 1998; Wagner, 1998; Kuhlemann and Kempf, 2002; Rupp and Haunold-Jenke, 2003; Roetzel et al., 2006; Grunert et al., 2010). The narrowing of the basin resulted in amplified currents that are linked to increased tides. The widespread tidal deposits along the northern shelf have become a prominent example for sedimentation under meso- and macrotidal control and complex interacting current patterns have been discussed in a number of sedimentological and modelling studies (Homewood and Allen, 1981; Allen and Homewood, 1984; Allen et al., 1985; Faupl and Roetzel, 1987; 1990; Keller, 1989; Tessier and Gigot, 1989; Lesueur et al., 1990; Krenmayr, 1991; Schaad et al., 1992; Martel et al., 1994; Sztanó, 1994; 1995; Sztanó and De Boer, 1995; Uchmann and Krenmayr, 1995; 2004; Krenmayr et al., 1996; Salvermoser, 1999; Bieg, 2005; Heimann et al., 2009; Grunert et al., 2010). Marine sedimentation in the NAFB finally ceased due to its constant upfill during the middle Burdigalian, marking the onset of a major paleogeographic reorganisation of the Central Paratethys (Berger, 1996; Rögl, 1998; Harzhauser and Piller, 2007).

The study area with the sites Pucking, Hochburg 1 and Ottnang-Schanze is located in the Upper Austrian portion of the NAFB (Fig. 1.3). In contrast to the western NAFB, marine sedimentation continued in the study area from Oligocene to Early Miocene. A deep-marine environment developed in the Puchkirchen Basin which extends from Bavaria (SE Germany) to Upper Austria and Salzburg (NE Austria) and parallels the Alpine thrust front with a west-east directed basinal axis (Malzer et al., 1993; Kuhlemann and Kempf, 2002). It is confined by the Bohemian Massif to the North and East, by the thrust complexes of the Helvetic Zone, the Rhenodanubian Flysch and the Northern Calcareous Alps to the south, and by the Bavarian shelf to the West (Wenger, 1987; Malzer et al., 1993; Wagner, 1998; Kuhlemann and Kempf, 2002; De Ruig, 2003). Large parts of

the southern Puchkirchen Basin have been incorporated in the Alpine thrust sheets as part of the tectonised "Imbricated Molasse" (De Ruig, 2003).

Vast and moderately inclined shelf and slope areas confined the deep-marine trough to the North and West, while a steep and tectonically active slope was present in the South close to the Alpine thrust front (Zweigel, 1998; Kuhlemann and Kempf, 2002; De Ruig, 2003). Sediment distribution was mainly triggered by the Puchkirchen Channel System, an extensive meandering basin-axial channel that was 3 to 5km wide and 10s of kilometers long (De Ruig, 2003; Hubbard et al., 2005; De Ruig and Hubbard, 2006; Hubbard at al., 2009). Several rivers entered the basin from the north, south and west and delivered large amounts of sediment into the basin. Increasing sedimentation rates led to the final upfill of the Puchkirchen Basin by the end of the Eggenburgian (Zweigel, 1998; Brügel et al., 2003; Hinsch, 2008; Pippèrr, 2011). Following a major transgression, the extensive Ottnangian shelf sea developed that existed until the middle Ottnangian (Kuhlemann and Kempf, 2002; Rupp et al., 2008).

Stratigraphy of the study area is based on litho- and biostratigraphy (Krenmayr and Schnabel, 2006; Rupp et al., 2008). An overview of the Lower Miocene lithostratigraphic units and biostratigraphic index species is given in Fig 1.4. The present study focuses on deposits of the basin center: the Upper Puchkirchen and Ebelsberg Fms. represent the Egerian, the Hall Fm. comprises the Eggenburgian and the sediments of the Innviertel Group belong to the Ottnangian (Aberer, 1958; Wagner, 1998; Rupp et al., 2008). Biostratigraphy in the area is based on benthic foraminifers (Wenger, 1987; Pippèrr et al., 2007; Pippèrr and Reichenbacher, 2009; 2010; Pippèrr, 2011). The concept has been established in eastern Bavaria and has been adopted for Upper Austria (Wenger, 1987; Rupp and Haunold-Jenke, 2003). Problems of biostratigraphic correlation mainly arise from facies dependency (Cicha et al., 1998; see chapter 6).

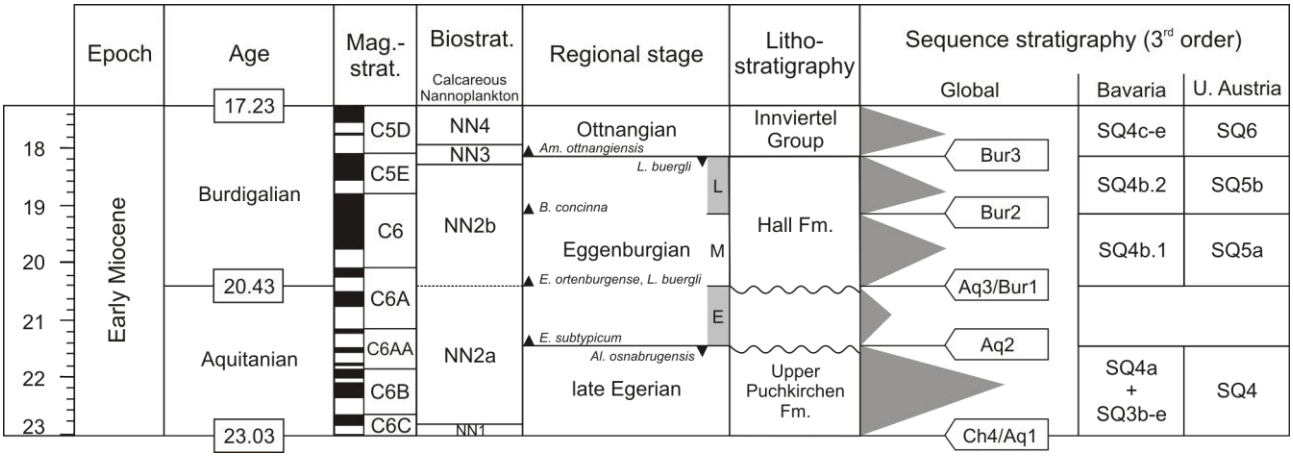

Fig. 1.4. Integrated Early Miocene stratigraphy of the study area. Correlation of the regional stages to the Neogene time-scale (Lourens et al., 2004) follows Piller et al. (2007). Regional benthic foraminiferal biostratigraphy compiled from Wenger (1987), Cicha et al. (1998) and Pippèrr and Reichenbacher (2009). Bavarian and Upper Austrian 3rd-order sequence stratigraphy is adopted from Peña (2007) and Hinsch (2008).

1.3. Foraminifers as paleoenvironmental proxies and stratigraphic markers

The present thesis is largely based on the evaluation of foraminiferal assemblages in order to obtain information on paleoenvironmental parameters and biostratigraphic constraints. Foraminifera constitute a class of amoeboid, pseudopod-bearing organisms of the kingdom Protoctista (Loeblich and Tappan, 1992; Sen Gupta, 2002). Foraminifers typically form tests that are made of various materials including organic cements, sedimentary particles and calcium carbonate (Hansen, 2002). The phylogenetic relationship of Foraminifera to other Protozoan groups is not well understood. Molecular evidence, however, suggests a close relation to the Radiolaria and Cercozoa (Cavalier-Smith, 2003).

Few foraminiferal species have been reported from freshwater environments and the vast majority lives in marine environments. There, foraminifers occupy a wide range of ecological niches in fully marine neritic, bathyal and abyssal environments as well as in restricted lagoons and estuaries (Murray, 2006). With estimated 3200-4300 extant species most foraminifers adopted a benthic lifestyle whereas only 40-50 extant species are known to occupy a planktic habitat (Sen Gupta, 2002; Murray, 2007).

In the fossil record, benthic foraminifers are documented since the Cambrian while planktic foraminifers do not appear before the Jurrassic (Sen Gupta, 2002; Spezzaferri and Spiegler, 2007). The calcareous and agglutinated tests show a high fossilization potential which makes them excellent biostratigraphic markers and paleoenvironmental proxies. Foraminifers are amongst the best-studied protozoan organisms (see e.g., Goldstein, 2002; Murray, 2006; Schiebel and Hemleben, 2007 for reviews on foraminiferal biology). Detailed biological information is available for many taxa thus providing a well-established reference archive for actualistic paleoenvironmental reconstruction from foraminiferal assemblages (Leckie and Olson, 2003; Murray, 2006; Jorrissen et al., 2007; Kucera, 2007). Planktic species give information about productivity, temperature, salinity and stratification of surface waters while benthic foraminifers are used as indicators of nutrient flux, bottom-water oxygenation, salinity and water energy. In biostratigraphy, the globally abundant planktic foraminifers serve as index fossils since the Cretaceous (Bolli et al., 1985; Gradstein et al., 2004). Larger benthic foraminifers are stratigraphically important since the late Paleozoic while smaller species are mostly used for regional correlation (Gradstein et al., 2004).

1.4. Geochemical proxies

In order to provide a multi-proxy record for a detailed reconstruction of the depositional environment various geochemical parameters of bulk sediment samples have been acquired parallel to the microfossil assemblages for the present thesis.

The quantity of organic matter (OM) in a given sample is commonly expressed as the contents of total organic carbon (**TOC**; Hunt, 1996). As there is no systematic correlation of TOC with primary

productivity observed in the present oceans many authors suggest that preservation of OM is more important for TOC than the production of OM (Demaison and Moore, 1980; Peters et al., 2005). The preservation of OM at the time of deposition primarily depends on (a) the type/origin of organic matter (terrestrial/marine), (b) the oxygenation of the water-column and the sediment, (c) the degree of bioturbation, and (d) the rate of sedimentation (Demaison and Moore, 1980; Hunt, 1996; Peters et al., 2005). Highest TOC values are thus expected in deposits of anoxic environments due to restricted circulation or a prominent oxygen minimum layer (Schulz and Zabel, 1999).

Parallel to TOC the content of **sulfur (S)** was measured. Sulfur content mainly reflects the degree of sulfate-reducing bacterial activity and serves as an indicator of bottom-water oxygenation (Peters et al., 2005). The ***TOC/S*** ratio is commonly used as an index value for coastal runoff and bottom-water oxygenation: empirical studies suggest that values < 2.8 reflect dys- and anoxic conditions while a ratio > 2.8 is related to increased coastal runoff and input of terrestrial organic matter (Berner and Raiswell, 1983; Berner, 1984; Schulz and Zabel, 1999).

Rock Eval Pyrolysis is a standard technique mainly used in hydrocarbon exploration in order to identify the type and maturity of organic matter. During Rock Eval Pyrolysis, a stream of helium passes through 100mg of the pulverized rock sample that is continuously heated to 550°C (Espitalié et al., 1977; Hunt, 1996). The resulting vapors are analysed with a flame ionization detector and four parameters are evaluated from the pyrogram (Tissot and Welte, 1984; Peters, 1986; Hunt, 1996; Peters et al., 2005):

S_1 (mg of hydrocarbon/g of rock) represents any free hydrocarbons (HC) that were thermally distilled from the rock at 300°C (Peters et al., 2005). They were present either at the time of deposition or they were generated from the kerogen since deposition (Hunt, 1996).

S_2 is the amount of HC generated through thermal cracking of the kerogen between 350 and 550°C (Peters et al., 2005). S_2 is used in combination with TOC to calculate the hydrogen index (see below; Hunt, 1996).

S_3 (mg CO_2/g of rock) is the amount of CO_2 yielded from the kerogen between 300 and 390°C (Hunt, 1996; Peters et al., 2005). S_3 is an indication of the amount of oxygen in the kerogen and is used to calculate the oxygen index (Hunt, 1996).

T_{max} represents the top of the S_2 peak which is the temperature at which the maximum of HC is released from the kerogen (Peters et al., 2005). T_{max} is an indicator for the stage of maturation of the OM (Hunt, 1996).

Several indices (hydrogen index, oxygen index and production index) can be calculated from the pyrolysis parameters (Hunt, 1996; Peters et al., 2005). In the present thesis, the **hydrogen index** is used for facies analysis in order to identify the origin of the organic matter contained in the sediments. The hydrogen index is defined as the ratio of mg HC in S_2/g TOC (Espitalié et al., 1977).

Very low values indicate major input of terrestrial-derived organic matter while high values suggest marine organic matter derived from surface water productivity (Tissot and Welte, 1984; Emeis and Kvenvolden, 1986; Davis et al., 1989). For samples with TOC below 1.5% several factors have to be considered that obscure original HI values, e.g. a significant lowering of HI values is likely due to bioturbation or the mineral-matrix effect (Espitalié et al., 1980; Orr, 1983; Pratt, 1984). An approach to overcome these problems and to estimate the "true" HI of samples with low TOC was presented by Langford and Blanc-Valleron (1990).

Biomarker analysis is commonly used to assess the origin of OM and the depositional environment (Hunt, 1996). Bio(logical) markers constitute organic compounds that can be linked to a specific group of living organisms from which they originate (Hunt, 1996). They show a high potential for preservation as they are resistant to biodegradation and high thermal maturity. Hundreds of biomarkers have been identified including n-paraffins, porphyrins, acyclic isoprenoids (pristane, phytane), terpenoids and steroids (Hunt, 1996).

Stable carbon and oxygen isotope measurements have been performed in order to evaluate trends in freshwater input, water temperature and productivity. The ratio between stable isotopes is commonly reported in the δ-notation ($\delta^{13}C$, $\delta^{18}O$).

$\delta^{13}C$ is is commonly used as an indicator for primary productivity (Marshall, 1992). Isotopic fractionation occurs as ^{12}C gets preferentially fixed during photosynthesis. Episodes of high productivity are thus reflected by a positive carbon isotope signal as ^{12}C gets increasingly exported from surface waters and the residual DIC enriched in ^{13}C (Marshall, 1992). For upwelling areas, however, this pattern might be obscured as ^{12}C is reintroduced to the surface waters by the upwelled bottom-waters which results in a more negative isotope signature compared to other eutrophic areas (Wefer et al., 1999).

$\delta^{18}O$ mainly depends on temperature and salinity (Wefer et al., 1999). Kinetic isotopic fractionation occurs during evaporation of water vapor from sea-water and condensation of rain-water (Marshall, 1992). During phases of cold climate relatively more ^{16}O gets trapped in large continental ice-sheets, thus enriching the sea-water in ^{18}O and resulting in increased values. Vice versa, high freshwater influx and lowered salinity are reflected in low ^{18}O values as freshwater is enriched by light ^{16}O (Wefer et al., 1999). In general, meteoric waters shows more negative isotopic values than sea-water (Marshall, 1992).

1.5. References

Aberer, F., 1958. Die Molassezone im westlichen Oberösterreich und in Salzburg. Mitteilungen der Geologischen Gesellschaft in Wien 50, 23–93.

Allen, P.A., Homewood, P., 1984. Evolution and mechanics of a Miocene tidal sandwave. Sedimentology 31, 63–81.

Allen, P.A., Mange-Rajetzky, M., Matter, A., Homewood, P., 1985. Dynamic palaeogeography of open Burdigalian sea-way, Swiss Molasse Basin. Eclogae Geologicae Helveticae 79, 351–381.

Baldí, T., Seneš, J., 1975. OM – Egerien. Die Egerer, Pouzdraner, Puchkirchener Schichtengruppe und die Bretkaer Formation. Chronostratigraphie und Neostratotypen, Miozän der Zentralen Paratethys 5. Verlag der Slowakischen Akademie der Wissenschaften, Bratislava, 577 p.

Bachmann, G.H., Müller, M., Weggen, K., 1987. Evolution oft he Molasse Basin (Germany, Switzerland). Tectonophysics 137, 77–92.

Berger, J.-P., 1996. Cartes paléogéographiques-palinspastiques du bassin molassique suisse (Oligocène inférieur – Miocène moyen). Neues Jahrbuch für Geologie und Paläontologie 202, 1–44.

Berner, R.A., 1984. Sedimentary pyrite formation: An update. Geochimica et Cosmochimica Acta 48, 605–615.

Berner, R.A., Raiswell, R., 1984. C/S method for distinguishing freshwater from marine sedimentary rocks. Geology 12, 365–368.

Bieg, U., 2005. Palaeooceanographic modelling in global and regional scale: An example from the Burdigalian Seaway. Ph.D. Thesis, Eberhard-Karls-Universität Tübingen, Germany, 108 p.

Bolli, H.M., Saunders, J.B., Perch-Nielsen, K., 1985. Plankton Stratigraphy Volume 1: Planktic foraminifera, calcareous nannoplankton and calpionellids. Cambridge University Press, Cambridge.

Brügel, A., Dunkl, I., Frisch, W., Kuhlemann, J., Balogh, K., 2003. Geochemistry and Geochronology of Gneiss Pebbles from Foreland Molasse Conglomerates: Geodynamic and Paleogeographic Implications for the Oligo-Miocene Evolution of the Eastern Alps. The Journal of Geology 111, 543–563.

Cavalier-Smith, T., 2003. Protist phylogeny and the high-level classification of Protozoa. European Journal of Protistology 39, 338–348.

Cicha, I., Seneš, J., Tejkal, J., 1967. M3 (Karpatien). Die Karpatische Serie und ihr Stratotypus. Chronostratigraphie und Neostratotypen, Miozän der Zentralen Paratethys 1. Verlag der Slowakischen Akademie der Wissenschaften, Bratislava, 312 p.

Cicha, I., Rögl, F., Rupp, C., Ctyroká, J., 1998. Oligocene-Miocene foraminifers of the Central Paratethys. Abhandlungen der Senckenbergischen Naturforschenden Gesellschaft 549, 1–325.

Davis, H.R., Byers, C.W., Pratt, L.M., 1989. Depositional mechanisms and organic matter in Mowry shale (Cretaceous), Wyoming. AAPG Bulletin 73, 1103–1116.

De Leeuw, A., Bukowski, K., Krijgsman, W., Kuiper, K.F., 2010. Age of the Badenian salinity crisis. Impact of Miocene climate variability on the circum-mediterranean region. Geology 38, 715–718.

Demaison, G.J., Moore, G.T., 1980. Anoxic environments and oil source bed genesis. AAPG Bulletin 64, 1179–1209.

De Ruig, M.J., 2003. Deep Marine Sedimentation and Gas Reservoir Distribution in Upper Austria. Oil Gas European Magazine 29, 64–73.

De Ruig, M.J., Hubbard, S.M., 2006. Seismic facies and reservoir characteristics of a deep marine axial channel belt in the Molasse Basin, Puchkirchen Formation, Upper Austria. AAPG Bulletin 90, 735–752.

Doppler, G., Heissig, K., Reichenbacher, B., 2005. Die Gliederung des Tertiärs im süddeutschen Molassebecken. Newsletters on Stratigraphy 41, 359–375.

Espitalié, J., Laporte, J.L., Madec, M., Marquis, F., Leplat, P., Paulet, J., Boutefeu, A., 1977. Méthode rapide de caractérisation des roches mères, de leur potentiel pétrolier et de leur degré d´évolution. Revue de l´ Institut Français du Pérole 32, 23–42.

Espitalié, J., Senga Makadi, K., Trichet, J., 1985. Role of the mineral matrix during kerogen pyrolysis. Organic Geochemistry 6, 365–382.

Faupl, P., Roetzel, R., 1987. Gezeitenbeeinflußte Ablagerungen der Innviertler Gruppe (Ottnangien) in der oberösterreichischen Molassezone. Jahrbuch der Geologischen Bundesanstalt 130, 415–447.

Faupl, P., Roetzel, R., 1990. Die Phosphoritsande und Fossilreichen Grobsande: Gezeitenbeeinflußte Ablagerungen der Innviertler Gruppe (Ottnangien) in der oberösterreichischen Molasse. Jahrbuch der Geologischen Bundesanstalt 133, 157–180.

Goldstein, S.T., 2002. Foraminifera: A Biological Overview. In: Sen Gupta, B.K. (Ed.), Modern Foraminifera, pp. 37–56. Kluwer Academic Publishers, Dordrecht-Boston-London.

Gradstein, F., Ogg, J., Smith, A., 2004. A Geologic Time Scale 2004. Cambridge University Press, Cambridge.

Grunert, P., Soliman, A., Harzhauser, M., Müllegger, S., Piller, W. E., Roetzel, R., Rögl, F., 2010. Upwelling conditions in the Early Miocene Central Paratethys sea. Geologica Carpathica 61, 129–145.

Hansen, H.J., 2002. Shell Construction in Modern Calcareous Foraminifera. In: Sen Gupta, B.K. (Ed.), Modern Foraminifera, pp. 57–70. Kluwer Academic Publishers, Dordrecht-Boston-London.

Harzhauser, M., Kroh, A., Mandic, O., Piller, W.E., Göhlich, U., Reuter M., Berning, B. 2007. Biogeographic responses to geodynamics: A key study all around the Oligo-Miocene Tethyan Seaway. Zoologischer Anzeiger - Journal of Comparative Zoology, 246, 241–256.

Harzhauser, M., Piller, W.E., 2007. Benchmark data of a changing sea. – Palaeogeography, Palaeobiogeography and Events in the Central Paratethys during the Miocene. Palaeogeography, Palaeoclimatology, Palaeoecology 253, 8–31.

Hedberg, H.D., 1976. International Stratigraphic Guide. John Wiley & Sons, New York, 200 p.

Heimann, F.U.M., Schmid, D.U., Pippèrr, M., Reichenbacher, B., 2009. Re-interpreting the Baltringer Horizont as a subtidal channel facies: implications for a new understanding of the Upper Marine Molasse “Cycles“ (Early Miocene). Neues Jahrbuch für Geologie und Paläontologie, Abhandlungen 254, 135–149.

Hinsch, R., 2008. New Insights into the Oligocene to Miocene Geological Evolution of the Molasse Basin of Austria. Oil Gas European Magazine 34, 138–143.

Homewood, P., Allen, P.A., 1981. Wave-, tide-, and current-controlled sandbodies of Miocene Molasse, Western Switzerland. AAPG Bulletin 65, 2534–2545.

Hubbard, S.M., de Ruig, M.J., Graham, S.A., 2005. Utilizing outcrop analogs to improve subsurface mapping of natural gas-bearing strata in the Puchkirchen Formation, Molasse Basin, Upper Austria. Austrian Journal of Earth Sciences 98, 52–66.

Hubbard, S.M., de Ruig, M.J., Graham, S.A., 2009. Confined channel-levee complex development in an elongate depo-center: Deep-water Tertiary strata of the Austria Molasse basin. Marine and Petroleum Geology 26, 85–112.

Hunt, J.M., 1996. Petroleum Geochemistry and Geology. W.H. Freeman and Company, New York.

Jorissen, F.J., Fontanier, C., Thomas, E., 2007. Paleoceanographical proxies based on deep-sea benthic foraminiferal assemblage characteristics. In: Hillaire-Marcel, C., de Vernal, A. (Eds.), Proxies in late Cenozoic paleocenography, pp. 263–326. Elsevier, Amsterdam.

Keller, B., 1989. Fazies und Stratigraphie der Oberen Meeresmolasse (unteres Miozän) zwischen Napf und Bodensee. Ph.D. Thesis, University of Bern, Switzerland.

Kováč, M., Barath, I., Harzhauser, M., Hlavaty, I. Hudackova, N., 2004. Miocene depositional systems and sequence stratigraphy of the Vienna Basin. Courier Forschungsinstitut Senckenberg 246, 187–212.

Krenmayr, H.-G., 1991. Sedimentologische Untersuchungen der Vöcklaschichten (Innviertler Gruppe, Ottnangien) in der oberösterreichischen Molassezone im Gebiet der Vöckla und der Ager. Jahrbuch der Geologischen Bundesanstalt 134, 83–100.

Krenmayr, H.-G., Roetzel, R., Rupp, C., 1996. Stop 2: Puchkirchen-Berg. In: Krenmayr, H.-G., Roetzel, R. (Eds.), Exkursionsführer, 11. Sedimentologentreffen, Exkursion B2, Oligozäne und miozäne Becken- und Gezeitensedimente in der Molassezone Oberösterreichs. Berichte der Geologischen Bundesanstalt 33, 1–43.

Krenmayr, H.G., Schnabel, W., 2006. Geologische Karte von Oberösterreich 1:200.000, 1 sheet, 2 additional maps. Geological Survey of Austria, Vienna.

Kroh, A., Harzhauser, M., 1999. An Echinoderm Fauna from the Lower Miocene of Austria: Paleoecology and Implications for Central Paratethys Paleobiogeography. Annalen des Naturhistorischen Museums Wien 101A, 145–191.

Kroh, A., Menkveld-Gfeller, U., 2006. Echinoids from the Belpberg Beds (Obere Meeresmolasse, Middle Burdigalian) in the area of Bern (Switzerland). Eclogae Geologicae Helvetiae 99, 193–203.

Kucera, M., 2007. Planktonic foraminifera as tracers of past oceanic environments. In: Hillaire-Marcel, C., de Vernal, A. (Eds.), Proxies in late Cenozoic paleocenography, pp. 213–262. Elsevier, Amsterdam.

Kuhlemann, J., Kempf, O., 2002. Post-Eocene evolution of the North Alpine Foreland Basin and its response to Alpine tectonics. Sedimentary Geology 152, 45–78.

Langford, F.F., Blanc-Valleron, M.-M., 1990. Interpreting Rock-Eval Pyrolysis Data Using Graphs of Pyrolizable Hydrocarbons vs. Total Organic Carbon. AAPG Bulletin 74, 799–804.

Laskarev, V.N., 1924. Sur les equivalentes du Sarmatien supérieur en Serbie. Recueil de traveaux ofert a M. Jovan Cvijic par ses amis et collaborateurs, p. 73-85.

Leckie, R.M., Olson, H.C., 2003. Foraminifera as proxies for sea-level change on siliciclastic margins. In: Olson, H.C., Leckie, R.M. (Eds.), Micropaleontologic Proxies for Sea-Level Change and Stratigraphic Discontinuities, Society for Sedimentary Geology Special Publication, vol. 75. Society for Sedimentary Geology, Tulsa, pp. 5–19.

Lesueur, J.-P., Rubino, J.-L., Giraudmaillet, M., 1990. Organisation et structures internes des dépôts tidaux du Miocène rhodanien. Bulletin de la Societe Geologique de France 6, 49–65.

Lirer, F., Harzhauser, M., Pelosi, N., Piller, W.E., Schmid, H.P., Sprovieri, M., 2009. Astronomically forced teleconnection between Paratethyan and Mediterranean sediments during the Middle and Late Miocene. Palaeogeography, Palaeoclimatology, Palaeoecology 275, 1–13.

Loeblich, A.R., Tappan, H., 1987. Foraminiferal genera and their classification. Van Nostrand Reinhold Company, New York-Wokingham-Melbourne-Agincourt.

Lourens, L., Hilgen, F., Shackleton, N.J., Laskar, J., Wilson, D., 2004. The Neogene Period. In: Gradstein, F.M., Ogg, J.G., Smith, A.G. (Eds.), A Geologic Time Scale 2004. Cambridge University Press, Cambridge, pp. 409–440.

Malzer, O., Rögl, F., Seifert, P., Wagner, L., Wessely, G., Brix, F., 1993. Die Molassezone und deren Untergrund. In: Brix, F., Schultz, O. (Eds.), Erdöl und Erdgas in Österreich. 281-357.

Mandic, O., Steininger, F.F., 2003. Computer-based mollusc stratigraphy – a case study from the Eggenburgian (Lower Miocene) type region (NE Austria). Palaeogeography, Palaeoclimatology, Palaeoecology 197, 263–291.

Martel, A.T., Allen, P.A., Slingerland, R., 1994. Use of tidal-circulation modeling of paleogeographical studies: An example from the Tertiary of the Alpine perimeter. Geology 22, 925–928.

Marshall, J.D., 1992. Climatic and oceanographic isotopic signals from the carbonate rock record and their preservation. Geological Magazine 129, 143–160.

Murray, J.W., 2006. Ecology and Applications of Benthic Foraminifera. Cambridge University Press, Cambridge.

Murray, J.W., 2007. Biodiversity of living benthic foraminifera: how many species are there? Marine Micropaleontology 64, 163–176.

Orr, W.L., 1983. Comments on pyrolytic hydrocarbon yields in source-rock evaluation. In: Bjorøy, M. (Ed.), Advances in organic geochemistry 1981, pp. 775–787. Wiley, Chichester.

Papp, A., Marinescu, F., Seneš, J., 1974. M5 – Sarmatien (sensu E. Suess, 1866). Die Sarmatische Schichtengruppe und ihr Stratotypus. Chronostratigraphie und Neostratotypen, Miozän der Zentralen Paratethys 4. 707 p.

Papp, A., Rögl, F., Seneš, J., 1973. Miozän M2 – Ottnangien. Die Innviertler, Salgotarjaner, Bantapusztaer Schichtengruppe und die Rzehakia Formation. Chronostratigraphie und Neostratotypen, Miozän der Zentralen Paratethys 3. Verlag der Slowakischen Akademie der Wissenschaften, Bratislava, 841 p.

Papp, A., Cicha, I., Seneš, J., Steininger, F., 1978. M4 – Badenien (Moravien, Wielicien, Kosovien). Chronostratigraphie und Neostratotypen, Miozän der Zentralen Paratethys 6. 594 p.

Papp, A., Jámbor, Á., Steininger, F.F., 1985. M6 – Pannonien (Slavonien und Serbien). Chronostratigraphie und Neostratotypen, Miozän der Zentralen Paratethys 7. 636 p.

Peters, K.E., Walters, C.C., Moldowan, J.M., 2005. The Biomarker Guide, Volume 2: Biomarkers and Isotopes in the Petroleum Exploration and Earth History, 2nd ed. Cambridge University Press.

Piller, W.E., Harzhauser, M., Mandic, O., 2007. Miocene Central Paratethys stratigraphy – current status and future directions. Stratigraphy 4, 151–168.

Pippèrr, M., 2011. Characterisation of Ottnangian (middle Burdigalian) palaeoenvironments in the North Alpine Foreland Basin using benthic foraminifera—A review of the Upper Marine Molasse of southern Germany. Marine Micropaleontology 79, 80–99.

Pippèrr, M., Reichenbacher, B., Witt, W., Rocholl, A., 2007. The Middle and Upper Ottnangian of the Simssee area (SE Germany): Micropaleontology, biostratigraphy and chronostratigraphy. Neues Jahrbuch für Geologie und Paläontologie 245, 353–378.

Pippèrr, M., Reichenbacher, B., 2009. Biostratigraphy and paleoecology of benthic foraminifera from the Eggenburgian "Ortenburger Meeressande" of southeastern Germany (Early Miocene, Paratethys). Neues Jahrbuch für Geologie und Paläontologie Abhandlungen 254, 41–61.

Pippèrr, M., Reichenbacher, B., 2010. Foraminifera from the borehole Altdorf (SE Germany): Proxies for Ottnangian (early Miocene) palaeoenvironments of the Central Paratethys. Palaeogeography, Palaeoclimatology, Palaeoecology 289, 62–80.

Pratt, L.M., 1984. Influence of Paleoenvironmental Factors on Preservation of Organic Matter in Middle Cretaceous Greenhorn Formation, Pueblo, Colorado. AAPG Bulletin 68, 1146–1159.

Roetzel, R., Ćorić, S., Galović, I., Rögl, F., 2006. Early Miocene (Ottnangian) coastal upwelling conditions along the southeastern scarp of the Bohemian Massif (Parisdorf, Lower Austria, Central Paratethys). Beiträge zur Paläontologie 30, 387–413.

Rögl, F., 1998. Palaeogeographic Considerations for Mediterranean and Paratethys Seaways (Oligocene to Miocene). Annalen des Naturhistorischen Museums in Wien 99A, 279–310.

Rögl, R., Hochuli, P., Muller, C., 1979. Oligocene-Early Miocene stratigraphic correlations in the Molasse Basin of Austria. Annales Geologiques des Pays Helleniques Tome hors series, 1045–1050.

Rupp, C., Haunold-Jenke, Y., 2003. Untermiozäne Foraminiferenfaunen aus dem oberösterreichischen Zentralraum. Jahrbuch der Geologischen Bundesanstalt 143, 227–302.

Rupp, C., Hofmann, T., Jochum, B., Pfleiderer, S., Schedl, A., Schindlbauer, G., Schubert, G., Slapansky, P., Tilch, N., Husen, D. van, Wagner, L., Wimmer-Frey, I., 2008. Geologische Karte der Republik Österreich 1:50.000, Blatt 47 Ried im Innkreis. Erläuterungen zu Blatt 47 Ried im Innkreis. Geological Survey of Austria, Vienna.

Salvermoser, S., 1999. Zur Sedimentologie gezeitenbeeinflußter Sande in der Oberen Meeresmolasse und Süßbrackwassermolasse (Ottnangium) von Niederbayern und Oberösterreich. Münchner Geologische Hefte A 26, 1–179.

Schaad, W., Keller, B., Matter, A., 1992. Die Obere Meeresmolasse (OMM) am Pfänder: Beispiel eines Gilbert-Deltakomplexes. Eclogae Geologicae Helveticae 85, 145–168.

Schiebel, R., Hemleben, C., 2007. Modern planktic foraminifera. Paläontologische Zeitschrift 79, 135–148.

Schlunegger, F., Leu, W., Matter, A., 1997. Sedimentary Sequences, Seismic Facies, Subsidence Analysis, and Evolution of the Burdigalian Upper Marine Molasse Group, Central Switzerland. AAPG Bulletin 81, 1185–1207.

Schulz, H.D., Zabel, M., 1999. Marine Geochemistry. Springer, Berlin-Heidelberg-New York.

Sen Gupta, B.K., 2002. Introduction to modern foraminifera. In: Sen Gupta, B.K. (Ed.), Modern Foraminifera, pp. 3–6. Kluwer Academic Publishers, Dordrecht-Boston-London.

Spezzaferri, S., Spiegler, D., 2007. Fossil planktic foraminifera (an overview). Paläontologische Zeitschrift 79, 149–167.

Steininger, F., Seneš, J., 1971. M1 – Eggenburgien. Die Eggenburger Schichtengruppe und ihr Stratotypus. Chronostratigraphie und Neostratotypen, Miozän der Zentralen Paratethys 2. Verlag der Slowakischen Akademie der Wissenschaften, Bratislava, 827 p.

Stevanović, P., Nevesskaja, L.A., Marinescu, F., Sokac, A., Jámbor, A., 1990. Pl1 – Pontien (sensu F. Le Play, N.P. Barbot, N. I. Andrusov). Chronostratigraphie und Neostratotypen, Neogen der Westlichen ("Zentralen") Paratethys 8. Verlag der Slowakischen Akademie der Wissenschaften, Bratislava, 952 p.

Sztanó, O., 1994. The tide-influenced Petervasara Sandstone, early Miocene, northern Hungary: sedimentology, paleogeography and basin development. Geologica ultraiectina 120, 1–155.

Sztanó, O., 1995. Palaeogeographic significance of tidal deposits: an example from an early Miocene Paratethys embayment, Northern Hungary. Palaeogeography Palaeoclimatology Palaeoecology 113, 173–187.

Sztanó, O., de Boer, P.L., 1995. Amplification of tidal motions in the Early Miocene North Hungarian Bay. Sedimentology 42, 665–682.

Tessier, B., Gigot, P., 1989. A vertical record of different tidal cyclicities: an example from the Miocene Marine Molasse of Digne (Haute Provence, France). Sedimentology 36, 767–776.

Tissot, B.T., Welte, D.H., 1984. Petroleum Formation and Occurrences. 2nd Edition. Springer Verlag, Berlin.

Uchmann, A., Krenmayr, H.-G., 1995. Trace fossils from Lower Miocene (Ottnangian) molasse deposits of Upper Austria. Paläontologische Zeitschrift 69, 503–524.

Uchmann, A., Krenmayr, H.-G., 2004. Trace fossils, Ichnofabrics and Sedimentary Facies in the Shallow Marine Lower Miocene Molasse of Upper Austria. Jahrbuch der Geologischen Bundesanstalt 144, 233–251.

Vasiliev, I., de Leeuw, A., Filipescu, S., Krijgsman, W., Kuiper, K., Stoica, M., Briceag, A., 2010. The age of the Sarmatian-Pannonian transition in the Transylvanian Basin (Central Paratethys). Palaeogeography Palaeoclimatology Palaeoecology 297, 54–69.

Vavra, N., 1979. Die Bryozoenfauna des österreichischen Tertiärs. Neues Jahrbuch für Geologie und Paläontologie, Abhandlungen 157, 366–392.

Wagner, L.R., 1998. Tectono-stratigraphy and hydrocarbons in the Molasse Foredeep of Salzburg, Upper and Lower Austria. In: Mascle, A., Puigdefábregas, C., Luterbach, H.P., Fernández, M., (Eds.), Cenozoic

Foreland Basins of Western Europe. Geological Society Special Publications 134. Geological Society, London, pp. 339–369.

Wefer, G., Berger, W.H., Bijma, J., Fischer, G., 1999. Clues to Ocean History: a Brief Overview of Proxies. In: Fischer, G., Wefer, G. (Eds.), Use of Proxies in Paleoceanography, pp. 1–68. Springer, Berlin-Heidelberg-New York.

Wenger, W.F., 1987. Die Foraminiferen des Miozäns der bayerischen Molasse und ihre stratigraphische sowie paläogeographische Auswertung. Zitteliana 16, 173–340.

Zweigel, J. (1998). Eustatic versus tectonic control on foreland basin fill. Contributions to Sedimentary Geology 20. Schweizerbart, Stuttgart.

CHAPTER 2

OCEANOGRAPHIC CONDITIONS AS A TRIGGER FOR THE FORMATION OF AN EARLY MIOCENE (AQUITANIAN) KONSERVAT-LAGERSTÄTTE IN THE CENTRAL PARATETHYS SEA

Patrick Grunert[a], Mathias Harzhauser[b], Fred Rögl[b], Reinhard Sachsenhofer[c], Reinhard Gratzer[c], Ali Soliman[a], Werner E. Piller[a]

[a] Institute for Earth Sciences (Geology and Paleontology), University of Graz, Heinrichstraße 26, A-8010 Graz, Austria

[b] Natural History Museum Vienna, Geological-Paleontological Department, Burgring 7, A-1014 Vienna, Austria

[c] Department of Applied Geosciences and Geophysics, Montanuniversität Leoben, Peter-Tunner Straße 5, A-8700 Leoben, Austria

Abstract

An exceptional Early Aquitanian *Konservat-Lagerstätte* with well-preserved vertebrate and invertebrate fossil assemblages has been studied in the North Alpine Foreland Basin of Upper Austria. The finely laminated sediments were deposited along the northern shelf of the Central Paratethys Sea. Micropaleontological (foraminifers, dinoflagellates) and geochemical (organic carbon, sulfur, carbonate content, biomarker, stable isotopes) proxies indicate intense upwelling. In addition, episodically increased coastal runoff provided large amounts of nutrients stimulating primary productivity. All evidence suggests deposition within dysoxic-anoxic bottom waters of an oxygen minimum zone along the outer shelf and upper slope.

Fossil assemblages show specific planktic and nektic associations in distinct intervals of the section. Various mechanisms are discussed to explain their origin: (1) Blooms of pteropods and calcareous nannoplankton reflect short-term peaks in primary productivity. Increased coastal runoff and/or intensified upwelling activity are considered as trigger mechanisms for providing the nutrients. (2) Allochthonous associations of the cephalopod *Aturia* with brown algae suggest a two-fold transport mechanism: shells of the offshore-living cephalopods were transported post mortem to the coast by surface currents and/or wind currents. Episodic flooding events and storms mixed the accumulated shells with the algae and moved them offshore. The latter process also seems to apply to several pipefish accumulations observed in the section. (3) Multi-species vertebrate accumulations of fish and dolphins are considered parautochthonous as their habitat is in good agreement with the reconstructed paleoenvironment. (4) Benthic macrofauna is scarce and of low

diversity. It mainly consists of bivalves adapted to dysoxic environments and is thus interpreted to be autochthonous.

2.1. Introduction

The fossil record is strongly biased by the preferred preservation of hard parts (Donovan and Paul, 1998). Conservation of organic material and soft tissue is generally scarce and bound to specific conditions. Such, often spectacular occurences are summarized as *Konservat-Lagerstätten* (Seilacher, 1970). Studies on their genesis are manifold. They have led to different scenarios explaining their origin and identified two primary triggers (Allison, 1988): (1) burial by rapid and/or catastrophic sedimentation (obrution) and (2) bottom-water anoxia. Due to facies prevalence and evolutionary patterns, *Konservat-Lagerstätten* are not evenly distributed through time (Allison and Briggs, 1993; Briggs, 2003). In the Cenozoic – contrasting the extensive black-shale deposits of the Mesozoic – most *Konservat-Lagerstätten* originate from marginal marine carbonate environments (e.g. Schwark et al., 2009) or limnic deposits (e.g. Wuttke, 1983) while marine shales are scarce (Allison and Briggs, 1993).

In this study we present well-preserved fossil assemblages of different composition from a shaley Early Miocene *Konservat-Lagerstätte* in the Central Paratethys. Based on an analysis of the depositional environment these accumulations will be evaluated for characteristic patterns and different scenarios for their origin will be discussed.

2.2. Geological setting and stratigraphy

The presented material comes from a temporary outcrop exposed during the construction of a hydroelectric power plant near the small town of Pucking in Upper Austria (N 48° 12’ 22”; E 14° 13’ 27”) and belong to the North Alpine Foreland Basin (NAFB) fill (Figs. 2.1, 2.2a). The c. 3-m-thick section was described by Kovar (1982), who had already documented an uneven distribution of the floral and faunal elements. In addition, one sample from a nearby section at Linz-Ebelsberg (12.5 km NE Pucking) has been included in the foraminiferal analysis. The deposits are part of the Ebelsberg Formation consisting of laminated sandy and silty clay to silty clay with mm-thick intercalations of silt (Wagner, 1998; Krenmayr and Schnabel, 2006). Single beds range from a few mm to 2-3 cm. Based on the regional stratigraphy and palynological assemblages, the Ebelsberg Formation has been considered as Upper Oligocene (Hochuli, 1978; Roetzel, 1983; Harzhauser and Mandic, 2002). Recent investigations of the herein described section near Pucking, however, proved an Aquitanian age (zone lower NN2) based on a nannoplankton assemblage with *Reticulofenestra minuta, R. pseudoumbilica* and *R. haqii* (Gregorova et al., 2009). According to the regional stage system for the Central Paratethys, the deposits are part of the upper Egerian stage (Piller et al., 2007; Fig. 2.3).

The section was situated on the northern shelf of the Central Paratethys Sea (Fig. 2.1b). During the Early Aquitanian, the NAFB was covered by a deep sea (Rögl, 1998). The Paratethys was a huge sea

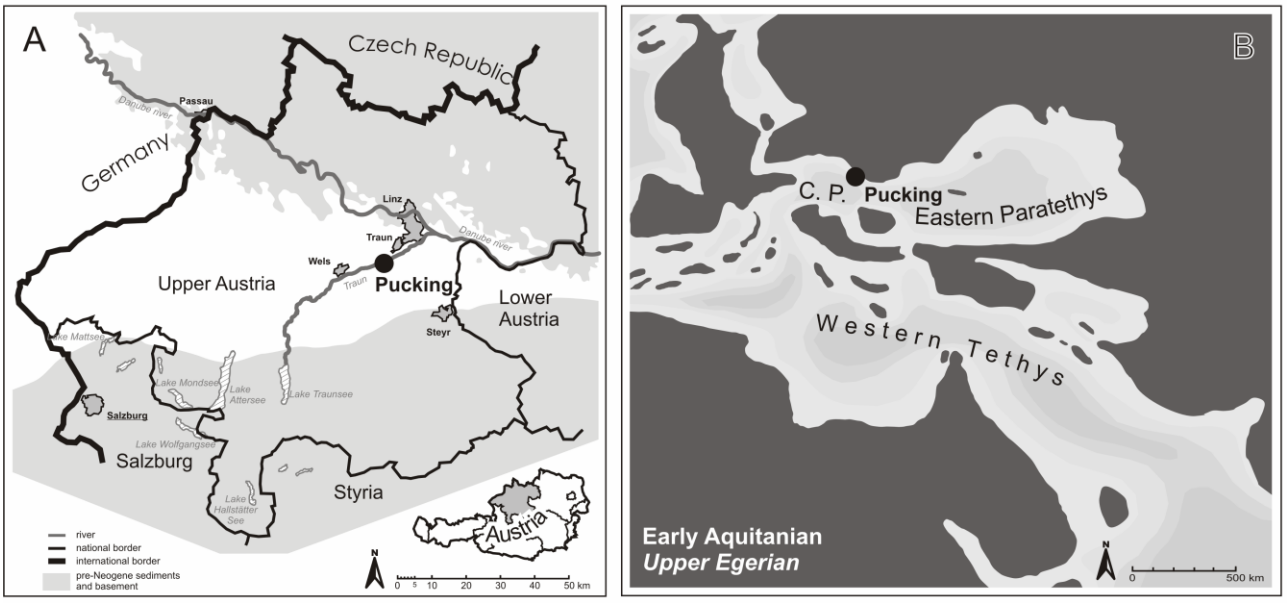

Fig. 2.1. (A) Location of the study area. (B) Paleogeographic location of the study area based on Harzhauser and Piller (2007).

at that time, reaching far into Asia. Within that system, the NAFB acted as a relatively narrow passage between the Mediterranean and the wide basins of the Carpathian Foredeep.

2.3. Material and methods

The investigated material was collected at the Pucking section in the 1980s by private and scientific collectors. One of the samples bears a specimen of the sunfish *Austromola angerhoferi* described in Gregorova et al. (2009, Fig. 2.2). High resolution sampling for micropaleontology and geochemical analyses was performed across an 8-cm-thick section on this rock slab (Fig. 2.2d).

2.3.1. Macrofauna

Well-preserved macrofossils have been recovered from various levels in the section. Rock slabs containing these fossils are stored in the collection of the Natural History Museum Vienna (NHMW; Pl. 2.1). For the present study, this material is described and paleoecologically and paleoceanographically evaluated for the first time.

Foraminifers. Thirteen samples (F1-13) have been investigated from different levels in the Pucking section (including eight samples from the sunfish horizon; Fig. 2.2a). One sample (F14) is from the Ebelsberg locality. From each sample, 100g of dried sediment were soaked in dilute H_2O_2 and wet sieved under running water with a minimum mesh size of 63µm. Planktic and benthic foraminifers have been identified based on Cicha et al. (1998). The sample material is stored at the NHMW.

2.3.2. Dinoflagellates

Two samples (D1-2) from the sunfish horizon have been analysed for dinoflagellate cysts. From each sample, 20g were treated by standard palynological techniques following Green (2001). Two

microscope slides per sample were investigated with a light microscope and the first 300 specimens were counted. Additionally, two SEM stubs were prepared from sample D2 and scanned using a DSM 982 Gemini SEM operating at a working voltage of 10kv. Dinoflagellate cyst

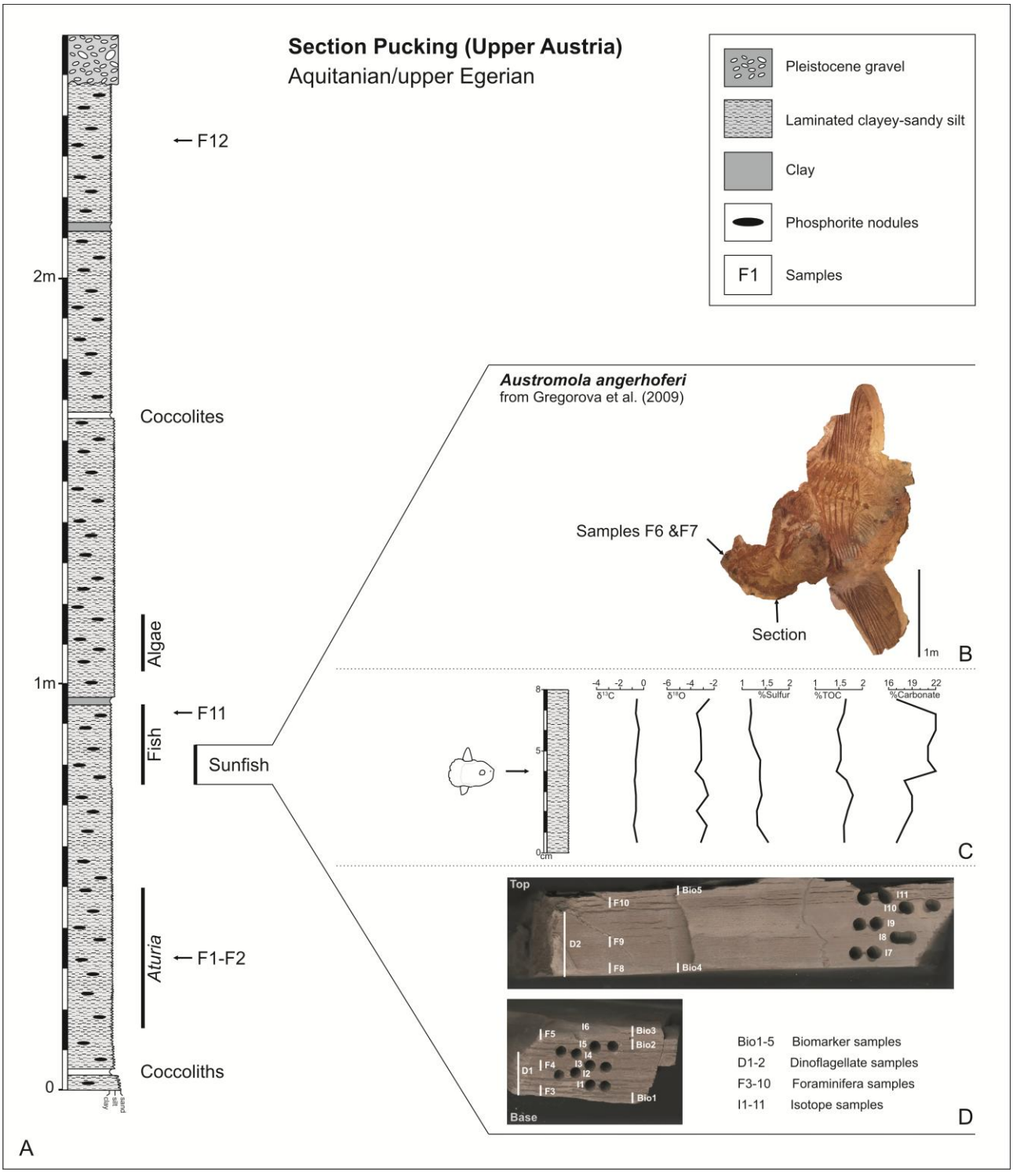

Fig. 2.2. The Pucking section. (A) Lithology and position of the fossil accumulation horizons and the micropaleontological samples. The exact position of sample F13 from a *Limacina*-accumulation above the sunfish-layer is not known. (B) Position of the section and samples F6-7 across the giant sunfish *Austromola angerhoferi*. (C) Results for the geochemical evaluation ($\delta^{18}O$, $\delta^{13}C$, TOC, S, carbonate) of samples I1-11. Stable isotope ratios relative to VPDB. (D) Position of the samples within the sunfish layer.

nomenclature generally follows Fensome and Williams (2004) and Fensome et al. (2008). The material is stored in the collection of the Institute for Earth Sciences at the University of Graz.

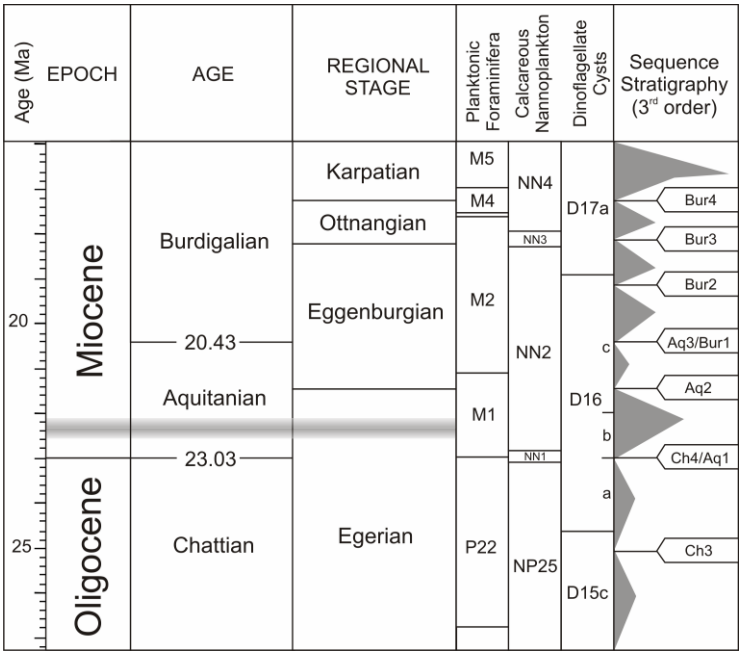

Fig. 2.3. Lower Miocene stratigraphy for the Central Paratethys based on Piller et al. (2007). The stratigraphic position of the studied sections is indicated by grey bar. Geochronology, biozonations of planktic foraminifers, calcareous nannoplankton and dinoflagellate cysts after Lourens et al. (2004), sequence stratigraphy and sea level curve after Hardenbol et al. (1998).

2.3.3. Geochemical analyses

Eleven bulk sediment samples (I1-11) from the sunfish horizon were measured for $\delta^{18}O$ and $\delta^{13}C$ at the Institute for Earth Sciences at the University of Graz, using an automatic Kiel II preparation line and a Finnigan MAT Delta Plus mass spectrometer. Samples were dried and reacted with 100% phosphoric acid at 70°C. Analytical precision, based on replicate analysis of international standards NBS-19 and NBS-18 and an internal laboratory standard, is better than 0.08‰ for $\delta^{18}O$ and 0.04‰ for $\delta^{13}C$. Results are reported in conventional δ-notation relative to the Vienna Pee Dee Belemnite standard (VPDB) in ‰ units.

Five samples (Bio1-5) from the sunfish horizon were selected for biomarker analysis. Representative portions of these samples were extracted for 1h using dichloromethane in a Dionex ASE 200 accelerated solvent extractor at 75°C and 50bar. Asphaltenes were precipitated from a hexane-dichloromethane solution (80:1 according to volume) and separated by centrifugation. The fractions of the hexane-soluble organic matter were separated into saturated and aromatic hydrocarbons and resins using medium-pressure liquid chromatography with a Köhnen-Willsch MPLC instrument (Radke et al., 1980). The hydrocarbon fractions were analysed by a gas chromatograph equipped with a 30m DB-5MS fused silica capillary column (i.d. 0.25mm; 0.25µm film thickness) coupled to a Finnigan MAT GCQ ion trap mass spectrometer. The oven temperature was programmed from 70 to 300°C at a rate of 4°C min^{-1} followed by an isothermal period of 15min. Helium was used as the carrier gas. The mass spectrometer was operated in the EI (electron ionisation) mode over a mass range from *m/z* 50 to *m/z* 650 (0.7s total scan time). Identification of individual compounds was accomplished on the basis of retention times in the total ion current chromatogram and comparison of mass spectra with published data.

Additionally, samples I1-11 and Bio1-5 were powdered and analysed for sulphur (S), total carbon

(TC), and total organic carbon contents (TOC, after acidification of samples to remove carbonate) using a Leco CS-300 analyser. The difference between TC and TOC is the total inorganic carbon content (TIC). TIC contents were used to calculate calcite equivalent percentages (= 8.34*TIC).
RockEval pyrolysis (Espitalié et al., 1977) for samples Bio1-5 was carried out using a Rock-Eval 2+ instrument. By this method, the amount of hydrocarbons (mgHC/grock) present in the rock sample (S1) and released from kerogen during gradual heating (S2) were determined. The S2 content was normalised against TOC to give the Hydrogen Index (HI = S2*100/TOC). T_{max} was measured as a thermal maturation indicator.

2.4. Results

2.4.1. Fossil mass-occurrences

Only the palynoflora and leaf flora of Pucking and associated outcrops have been studied previously (Hochuli, 1978; Kovar, 1982). A detailed description of the fauna is largely missing aside from single descriptions of a rare echinoid (Kroh, 2005), a razorbill (Mlíkovský, 1987) and the giant sunfish *Austromola* (Gregorova et al., 2009).
The survey of the collections of the NHMW clearly showed that the Pucking section is outstanding in the composition of the fauna and sheer number of species. Although total diversity is impressive, taxa are not distributed evenly. They appear in distinct associations in peculiar layers, sometimes forming nearly monospecific occurrences with the exception of driftwood associations.
In the basal part of the section, several horizons occur with accumulations of the nautilid cephalopod *Aturia* (Fig. 2.2a; Pl. 2.1, Fig. 9). The shells are distinctly larger than those of the widespread Miocene *Aturia aturi* (Basterot, 1825) and might represent an undescribed species. The compressed mode of preservation, however, hampers serious taxonomic analysis. All *Aturia* accumulations are associated with thalli of the brown seaweed *Cystoseirites altoaustriacus* Kovar, 1982 and other unidentified thalli of phycophytes.
A second type of accumulation consists mainly of fish skeletons (Pl. 2.1, Figs. 2-4). These are largely articulated, although most specimens display initial stages of decay (e.g. scales are detached). An analysis of the fish fauna has yet to be undertaken, but some comments are given by Pfeil (1983). Based on the collections of the NHMW, the diversity is moderate, with about 10 common taxa out of which four predominate: pipefish (Syngnathidae), hake (Merlucciidae), herring (Clupeidae) and mackerel (Scombridae). The syngnathids tend to form monospecific accumulations, whereas the other fishes are less exclusive. Comber (Serranidae), jack fish (Carangidae) and boarfish (Caproidae) are distinctly less frequent. Most eye catching is the occurrence of at least three almost complete specimens of the giant sunfish *Austromola angerhoferi* Gregorova et al. (2009), which attained a diameter up to c. 3 m. This is the largest fossil Cenozoic teleost known so far. Sharks are represented only by few isolated teeth. Within the same horizon, a near complete dolphin skeleton (undescribed; Pl. 2.1, Fig. 1) and a skeleton of the razorbill *Petralca austriaca* Mlíkovský, 1987 have been found.

Pteropod mass occurences consisting either of *Limacina* sp. or of *Clio* sp. are intercalated several times within the section (Pl. 2.1, Figs. 6-7). These horizons lack fish skeletons or *Aturia* shells but may contain algal thalli.

Aside from these accumulations, several mollusc taxa are found throughout the section. The mollusc fauna is of low diversity and dominated by few species. Among the gastropods, a single unidentified turrid species and the naticid *Euspira helicina* (Brocchi, 1814) predominate. Bivalves are represented by the lucinid *Megaxinus bellardianus* (Mayer, 1864), the nuculid *Nucula,* and the small pectinid *Deletopecten*. Most bivalves are articulated with only slightly gaping valves (Pl. 2.1, Fig. 10). Lucinids occur in life position perpendicular to the bedding.

Echinoderms are rare at Pucking. Only few specimens of spatangoids and *Linthia summesbergeri* Kroh (2005) have been reported (Kroh, 2005).

Frequently found are centimetre to decimetre long pieces of lignite which are often completely penetrated by teredinid bivalves (Pl. 2.1, Fig. 5). These are interpreted as driftwood falls. The bivalves *Perna aquitanica* (Mayer-Eymar, 1858) and an isognomid bivalve are also typical driftwood associates along with unidentified bryozoans and polychaetes. At least two species of probably undescribed barnacles of the family Lepadidae occur attached to the driftwood.

2.4.2. Foraminifers

The distribution of foraminifers is summarized in Tables 2.1 and 2.2. Benthic assemblages at Pucking are dominated by *Haplophragmoides laminatus, Bolivina* spp., *Caucasina* spp., *Eoeponidella* spp., *Myllostomella advena* and *Pseudoparella* spp. throughout the section (Pl. 2.2). The sample from Ebelsberg revealed a similar benthic fauna dominated by *Bolivina* spp., *Caucasina* spp., *Globocassidulina subglobosa*, *Lenticulina* spp., nonionids, *Plectofrondicularia* sp. and *Pseudoparella exigua*. The observed foraminifers display very small test sizes.

Planktic assemblages consist of globigerinid and microperforate tenuitellid species. While the latter are dominant in the samples from the *Aturia* and sunfish horizons in the lower part of the section, globigerinids predominate in samples F11-13. The sample from Ebelsberg (F14) revealed a planktic fauna dominated by globigerinids.

The composition of the assemblages differs according to the macrofaunal accumulations with which they are associated. From the *Aturia* accumulations only few foraminifers were revealed. *Caucasina schischkinskayae* and the agglutinated species *Haplophragmoides laminatus* and *Gaudryinopsis austriacus* dominate the benthic assemblages. Planktic foraminifers are scarce, with only two tenuitellid species documented from sample F2. In contrast, the samples from the sunfish horizon revealed a rich fauna. Benthic communities are dominated by small species of *Bolivina*, *Caucasina*, *Eoeponidella*, *Escornebovina* and *Myllostomella*. Mass-occurrences of tenuitellid species are recorded while globigerinids occur only in small numbers. Finally, benthic foraminifers from a *Limacina* accumulation (F13) are dominated by *Haplophragmoides*

laminatus, *Bolivina trunensis*, *Caucasina* spp. and *Pseudoparella* spp. Tenuitellid and globigerinid species are equally abundant.

2.4.3. Dinoflagellates

The two investigated samples revealed fairly well preserved specimens. The recorded assemblages are mainly composed of *Cordosphaeridium cantharellus*, *Glaphyrocysta* spp., *Homotryblium tenuispinosum*, *Lejeunecysta* spp., *Lingulodinium machaerophorum*, *Polysphaeridium zoharyi*, *Selenopemphix* spp., *Spiniferites/Achomosphaera* spp. and round brown cysts (*Brigantedinium*? spp.) (Tab. 2.3; Pl. 2.3). Other dinoflagellate cyst taxa occur only in small numbers. Additionally, acritarchs (*Paralecaniella indentata* and *Cyclopsiella* spp.) and foraminiferal test linings are common.

Many of the revealed taxa have a long biostratigraphic range and extend from Paleogene to mid-Miocene (e.g., *Apteodinium spiridoides*, *Cleistosphaeridium placacanthum*, *Cordosphaeridium cantharellus*, *Cribroperidinium* spp., *Distatodinium paradoxum*, *Glaphyrocysta* spp., *Homotryblium tenuispinosum*, *Hystrichokolpoma* spp., *Reticulatosphaera actinocoronata*, *Thalassiphora pelagica* and *Tuberculodinium vancampoae*). However, in agreement with the calcareous nannoplankton data of Gregorova et al. (2009), the co-occurrence of *Deflandrea phosphoritica*, *Distatodinium apenninicum*?*, Hystrichosphaeropsis obscura* and *Stoveracysta conerae* suggests an Early Miocene, most likely Aquitanian age (Biffi and Manum, 1988; Brinkhuis et al., 1992; Zevenboom, 1995; de Verteuil and Norris, 1996; Lourens et al., 2004; Munsterman and Brinkhuis, 2004).

The highest occurrence of *Deflandrea phosphoritica* has been used to define the top of dinocyst zone DN1 (latest Oligocene-earliest Miocene) of the eastern U.S.A. (de Verteuil and Norris, 1996). Accordingly, Munsterman and Brinkhuis (2004) recorded the highest occurrence of *D. phosphoritica* within their SNSM1a subzone of latest Chattian–earliest Aquitanian age from the Southern North Sea Basin. In the Lemme section of northern Italy, *D. phosphoritica* extends into the Early Miocene *Membranilarnacia*? *picena* (Mpi) Interval Zone (Zevenboom, 1995). The highest occurrence of *Distatodinium apenninicum* has been used to identify the base of the Early Miocene Dap Interval Subzone of northern Italy (Brinkhuis et al., 1992). Thus, the co-occurrence of *D. phosphoritica* and *D. apenninicum* indicates an Early Miocene age (Zevenboom, 1995; Williams et al., 2004).

Biffi and Manum (1988) used the lowest occurrence of *Stoveracysta conerae* to define the base of their Early Miocene DM2 Zone of northern Italy. In the NW Atlantic, the lowest occurrence of *S. conerae* is recorded within DN1 and its highest occurrence defines the top of the DN2 Interval Zone (early-middle Early Miocene; de Verteuil and Norris, 1996). *Hystrichosphaeropsis obscura* has been recorded in DN2 (de Verteuil and Norris, 1996) and SNSM2 Zone (Munsterman and Brinkhuis; 2004).

2.4.4. Geochemistry

2.4.4.1. Stable isotopes

Stable isotope ratios are rather constant, ranging from -0.8‰ to -0.41‰ (mean: -0.62‰) for $\delta^{13}C$ and -2.55‰ to -3.69‰ (mean: -3.12‰) for $\delta^{18}O$ (Tab. 2.4). No distinct change or trend is observed.

2.4.4.2. Organic carbon, sulphur and carbonate content

The evaluation of organic carbon, sulphur and carbonate content revealed relatively uniform results (Tab. 2.4; Fig. 2.2c; TOC: 1.5-1.9%; S: 1.0-1.6%; carbonate: 17-22; TOC/S: 1-1.7). While TOC and S do not show distinctive trends, a slight rise in carbonate content is documented for the upper part of the section. TOC/S ratios in the order of 1.1 to 1.7 suggest oxygen depleted conditions during deposition of the sediments (Berner, 1984).

2.4.4.3. Biomarker composition

GC traces of the five samples studied are very similar (Tab. 2.5). Representative examples of the distribution of revealed compounds are given in Figs. 2.4 and 2.5.

n-Alkanes and isoprenoids. All samples are characterized by bimodal *n*-alkane distributions with similar contributions of short-chain (C_{15}-C_{19}) and long-chain (C_{27}-C_{31}) *n*-alkanes relative to the sum of total *n*-alkanes (C_{15}-C_{33}). This suggests a contribution of both, algal material and higher terrestrial plants (Peters et al., 2005). Pristane/phytane (Pr/Ph) ratios vary in a narrow range between 0.9 and 1.4. According to Didyk et al. (1978), Pr/Ph ratios below 1.0 indicate anaerobic conditions during early diagenesis, and values between 1.0 and 3.0 reflect dysaerobic environments. However, Pr/Ph ratios are known to be affected also by maturation (Tissot and Welte, 1984) and by differences in the precursors of acyclic isoprenoids (i.e. bacterial origin; Volkman and Maxwell, 1986, ten Haven et al., 1987). Moreover, a bacterial origin for phytane from phytanyl ether lipids found in archaebacteria, as well as the formation of pristane from tocopherols (vitamin-E) or chromans (Goossens et al., 1984), cannot be excluded. Maturity variations within the studied sample set can be excluded. Therefore and because oxygen depleted conditions are supported by very low TOC/S ratios, we consider Pr/Ph ratios as an appropriate redox indicator in the present case.

Sesquiterpenoids. In all samples, aromatic sesquiterpenoids of the cadinane-type, dominated by cadalene (Fig. 2.5), are observed (Simoneit and Mazurek, 1982). This compound, together with retene, is specific for resinous input from higher plants.

Steroids and hopanoids. There is little variation in the relative amounts of C_{27}, C_{28} and C_{29} steranes. All samples are dominated by C_{29} steranes (55-60%), which are typically related to land plants (Volkman, 1986). In contrast, relative abundances of C_{28} steranes are low (12-21%). Whereas high amounts of C_{27} steranes are indicative of algal material, C_{28} steranes have been related to phytoplankton including diatoms, coccolithophorides and dinoflagellates (Grantham and Wakefield, 1988).

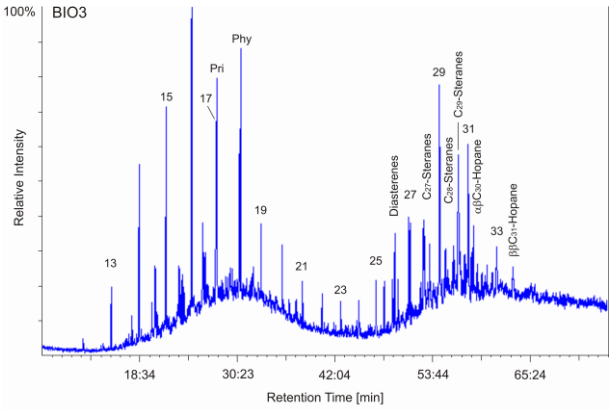

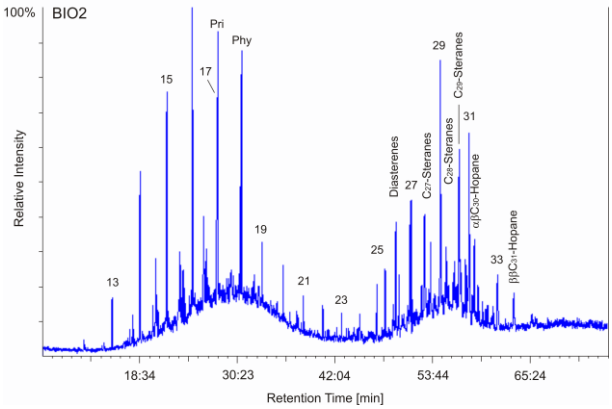

Fig. 2.4. Gas chromatograms (total ion current) of the saturated hydrocarbon fractions of samples Bio2 and Bio3. *n*-alkanes are labelled according to their carbon number.

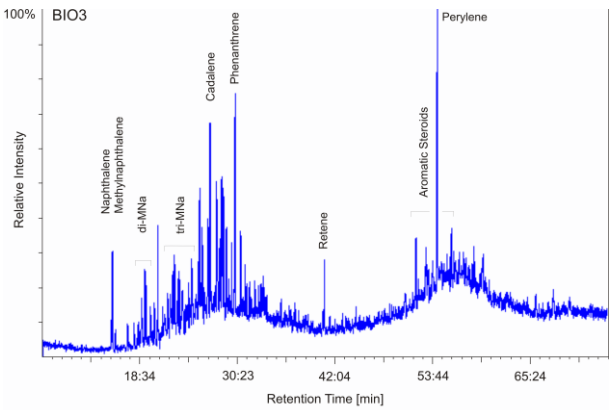

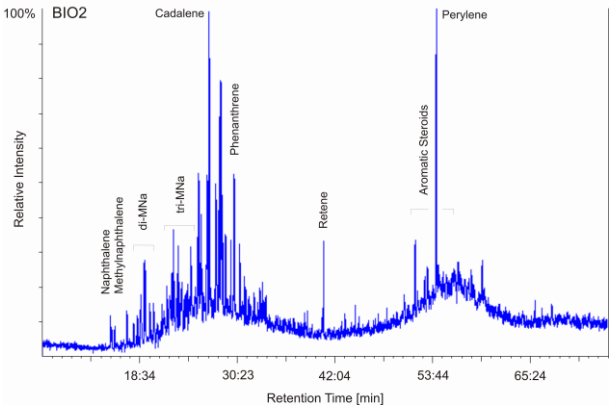

Fig. 2.5. Gas chromatograms (total ion current) of the aromatic hydrocarbon fractions of samples Bio2 and Bio3.

The steranes/hopanes ratio is a measure of organic matter production by autotrophic eukaryotes (e.g. algae, land plants) versus bacterial activity. The determined ratios (0.9-1.0) are nearly identical in all samples. Nevertheless a positive correlation between the steranes/hopanes ratio and the relative contribution of long-chain *n*-alkanes can be observed (correlation coefficient r^2: 0.78), suggesting that the ratio is mainly controlled by the relative input of land plants.

Chromans. In all samples 2,5,7,8-tetramethyl-2-(4',8',12'-trimethyltridecyl) chroman (tri-MTTC) predominates over the 2,5,8-trimethyl-2-(4',8',12'-trimethyltridecyl) chroman (di-MTTC). Although the origin of methylated MTTCs is not yet understood, methylated MTTCs have been widely used for palaeosalinity reconstruction (Sinninghe Damsté et al., 1993; Barakat and Rullkötter, 1997). The ratio between tri-MTTC and the sum of MTTCs is proportional to salinity. The detected ratios (0.6-1.0) suggests normal saline conditions.

2.4.4.4. Rock eval pyrolysis

Hydrogen Index values ranging from 170 mgHC/gTOC to 200 mgHC/gTOC indicate a type III kerogen. Calculated T_{max}-values around 425°C suggest that the organic matter is thermally immature.

2.5. Discussion

2.5.1. The paleoceanographic setting

2.5.1.1. Paleogeography

The investigated section was situated on the northern shelf of the NAFB (Fig. 2.1b). The Aquitanian coastline of the Paratethys Sea in the area of the Bohemian Massif cannot be reconstructed due to erosion. Nevertheless a minimum distance of the Pucking section to the coast can be calculated on the ancient coastline represented by the escarpment of the Bohemian Massif in the Linz area. This formed the coast, with characteristic lithologies and fauna, during the late Oligocene (Harzhauser and Mandic, 2002), whereas during the Aquitanian the coast was located further to the NNE due to the transgressive character of the Ebelsberg Formation. This assumption suggests an offshore position of the Pucking section at the time of deposition, at a minimum distance of c. 10 km to the north and c. 20 km to the northeastern coast. In any case, the Pucking section is located offshore of the many tectonically induced embayments, such as the Linz Bay, the Gallneukirchen Bay and others that structured the rocky shore. To the west and the south the shelf passed into the deep North Alpine Foreland Basin with estimated depths of 1,000-1,500m (Rögl et al., 1979).

Depth estimates for the investigated deposits are not precise due to the wide range of bathymetric distributions of the revealed benthic foraminifers. The common occurrence of *Haplophragmoides* indicates a water depth greater than 100m (Murray, 2006). The scarce occurrence of the shallow-water taxa *Ammonia* and *Elphidium* is interpreted as transport from the coast. Furthermore, recent tenuitellids are exclusively described from offshore sites in basins deeper than 100m (Li and McGowran, 1998) and from oceanic environments (Li et al., 1992). This interpretation is in good agreement with an outer shelf to slope position for the Ebelsberg Formation suggested by Wagner (1998).

2.5.1.2. Upwelling-induced primary productivity as trigger of an oxygen minimum zone

Low oxygen conditions prevailed on the shelf, favouring the preservation of organic matter. The benthic foraminiferal assemblages, dominated by bolivinids and buliminids, bear strong evidence of oxygen depleted environments with concentrations below 1ml/l (Bernhard and Sen Gupta, 1999). The agglutinated taxa *Gaudryinopsis* and *Haplophragmoides* have been reported previously from dysoxic environments in the Central Paratethys (Spezzaferri et al., 2002). The scarce occurrence of epifaunal taxa seems to be linked to low oxygen conditions too (Murray, 2001): for recent benthic communities it has been shown that the critical oxygen concentration for epifaunal taxa is around 1ml/l. Below this threshold only infaunal foraminifers better adapted to low-oxygen environments occur. Finally, the overall small test size points to stressful conditions hampering carbonate precipitation.

Accordingly, the extremely depleted mollusc fauna with the sulphur-oxidizing bacterial symbiosis of the lucinids documents a low oxygen environment (Schweimanns and Felbeck, 1985). The presence of sulphur bacteria, indirectly recorded by pyrite framboids, further supports this interpretation. Finally, the absence of bioturbation documents that the sediment was probably dysoxic from a few mm downwards. Oxygen depletion culminated in repeated episodes of anaerobic conditions in the bottom water, allowing the preservation of fish corpses. This is clearly indicated by the revealed low TOC/S and PR/Ph ratios from the sunfish horizon (Berner, 1984).

Two models have been established to explain the development of anoxic bottom waters and the deposition of organic-rich shales (see e.g., Rohling, 1994; Rullkötter, 2000; Negri et al., 2009 for reviews): (1) the stagnation model emphasizes a strong stratification of the water-column limiting mixing of surface and bottom waters. Restricted connections to open-ocean waters and increased freshwater input by rivers or intensified rainfall force a permanent halocline that hampers ventilation (Meyers, 2006). The development of anoxic bottom waters thus triggers the preservation of organic matter. Restricted basins such as the Black Sea are modern analogues for such conditions. Schulz et al. (2005) suggested similar conditions for the Early Oligocene Central Paratethys. For the Ebelsberg Fm., however, such a scenario is unlikely since broad connections to the Mediterranean and Atlantic seas did exist (Rögl, 1998). A major input of freshwater should result in an upper water-layer with reduced salinity. The planktic foraminifers, however, do not show any indications of diluted surface waters, and the distribution of chromans also indicates normal salinity.

(2) The productivtiy model focuses on the importance of high primary productivity in surface waters creating elevated levels of organic matter accumulation. Large amounts of sinking biomass consume much oxygen during decay and thus cause anoxic conditions in the water-column. Such conditions are often associated with upwelling, where an oxygen minimum zone (OMZ) is established covering the outer shelf and upper slope (e.g. Maas, 2000; Gooday, 2003; Schumacher et al., 2007).

In the present case, a scenario favouring the productivity model has been suggested by Wagner (1996, 1998). He links the deposition of fish shales and intercalated diatomites in the Upper Austrian NAFB during the Oligocene and Early Miocene to upwelling activity along the northern slope. This model is clearly supported by our data. Indications of cool and highly productive surface waters are observed in planktic foraminifers which revealed blooms of cold-water tenuitellids (Li et al., 1992), opportunistic high-productivity taxa such as *Globigerina praebulloides* and cold-water indicators including *G. ottnangiensis*. These are all commonly associated with upwelling sites (e.g. Peeters et al., 2002; Roetzel et al., 2006; Grunert et al., in press). The temperate surface water conditions indicated by both groups contrast the subtropical climate suggested by Kovar (1982) and thus further document the influence of cold currents. High export rates of organic matter are indicated by the dominance of bolivinid species. Observations from recent upwelling sites in the Indian Ocean have shown that their peak abundance is restricted

to the upper OMZ (Schumacher et al., 2007). A relationship between foraminiferal assemblages dominated by calcitic taxa and the hypoxic environment of an OMZ has been reported from the same study area (Larkin and Gooday, 2009). Studies by Gooday (1993) and Kawagata (2001) further showed that increased abundances of buliminds, *Myllostomella* spp. and *Pseudoparella exigua* are linked to elevated surface-water productivity and intermittent food supply. Highly productive surface-waters are also documented in the heterotrophic dinoflagellate taxa *Lejeunecysta* spp., *Paralecaniella indentata*, *Selenopemphix* spp., *Xandarodinium thanxum* and round brown cysts (*Brigantedinium* spp.) reaching an abundance of 30-32% (Dale, 1996; Louwye and Laga, 2008). Furthermore, the absence of oceanic dinoflagellate cyst taxa, usually adapted to oligotrophic conditions, can be linked to surface waters enriched in nutrients (Devillers and de Vernal, 2000). The common occurrence of phosphorite nodules throughout the section also points to increased nutrient flux as they are often described from upwelling sites (e.g. Schenau et al., 2000). Finally, the revealed bulk stable isotope data are close to those of a mid-Burdigalian upwelling site in the NAFB (Grunert et al., 2010).

2.5.1.3. Coastal runoff

The faunas indicate that most of the nutrient input was caused by upwelling of deeper water masses. However, the sediments also bear evidence for at least episodically strong coastal runoff providing an additional source of nutrients. Deposits of the ancient coast-line are lost due to erosion, and information on the hinterland is sparse. Leaf communities (Kovar, 1982) and the palynoflora (Hochuli, 1978) from Pucking and adjacent outcrops point to a warm, humid climate with a precipitation maximum in the warmest months and a lack of dry seasons. The annual precipitation may have ranged between 1100 and 2000 mm (Kovar, 1982).

Episodic flooding events are indicated by the dinoflagellate cysts: in contrast to the foraminiferal fauna, the occurrence of thermophilic dinoflagellate taxa such as *Lingulodinium machaerophorum*, *Melitasphaeridium choanophorum*, *Polysphaeridium zoharyi*, *Selenopemphix nephroides* and *Tuberculodinium vancampoae* suggest warm surface water conditions (Marret and Zonneveld, 2003). As most of these taxa are associated with a neritic or inner neritic environment (Dale, 1996), transport from marginal areas close to the coast towards the outer shelf is a plausible explanation. This is further supported by the observation that most revealed species related to high productivity do not belong to the thermophilic taxa. A considerable input of land plants is also indicated by the distributions of steranes and sesquiterpenoids in the samples from the sunfish layer.

2.5.2. Types of fossil mass-occurrences

The fossil mass-occurrences can be divided into planktic and nektic ones. The planktic ones are formed by pteropod and nannoplankton blooms. The nektic category is threefold: *Aturia*-algae

accumulations, pipefish mass-occurrences and multi-species vertebrate accumulations. The different compositions of the mass-occurrences point to quite different trigger mechanisms.

2.5.2.1. Blooms of pteropods and nannoplankton

The pteropods *Limacina* and *Clio* are adapted to pelagic life in the upper ocean layers. They are diel migrants with nocturnal upward migration and produce large mucous webs to catch suspended organic material (Mackas and Galbraith, 2002; Gilmer and Harbison, 1986). Fossil pteropod blooms have been linked to flooding events (Gürs and Janssen, 2004) allowing immigrations from adjacent ecosystems. Similarly, recent blooms are suggested to result from climate driven eddy intensification and the northward shift of warm-water fauna into subarctic waters (Tsurumi et al., 2005). Both mechanisms focus on import from a distant source area and are inadequate to explain the blooms in the subtropical Paratethys Sea with its wide oceanic connections.

An alternative scenario is described from Quaternary settings in the Red Sea, the Gulf of Aqaba, the Arabian Sea and the Sargasso Sea (Almogi-Labin, 1982; Almogi-Labin et al., 1986; 1988; Mohan et al., 2006). According to these studies, high primary productivity is the main trigger for large standing stocks of pteropods. Highly productive areas such as upwelling regions and boundary currents are favourable for many *Limacina* species. A correlation of *Limacina* blooms with abundance peaks of the upwelling index foraminifer *Globigerina bulloides,* coccolithophorid blooms, and a rise of buliminid foraminifers, indicating low oxygen bottom conditions, has been observed frequently (Almogi-Labin, 1982; Mohan et al., 2006). This pattern can also be observed in the fossil record of the Central Paratethys, as *Limacina* accumulations have been reported from Oligocene and Middle Miocene shales in the Carpathian Foredeep and related to anoxic environments (Báldi, 1986; Báldi, 2006).

Thus, the episodic occurrence of pteropod and nannoplankton blooms suggests temporarily changing conditions. These short-term events might either be related to intensification of upwelling or increased coastal runoff.

2.5.2.2. Allochthonous accumulations of Aturia and brown algae

Aturia is interpreted the most active and deeply living Cenozoic nautiloid, judging from the shell's large size, streamlining, and siphuncle configuration (Ward, 1987). Although many findings derive from coastal settings (Lukeneder and Harzhauser, 2002), the original habitat of *Aturia* was most likely deep water. However, the specimens from Pucking are frequently associated with brown algae, which grew in littoral environments. Therefore, the mass-occurrences might have resulted from a complex succession of processes. First, the *Aturia*-shells floated post mortem to the surface and were transported by surface currents and/or wind to the coast. Examples from recent nautiloid shells show that transport over large distances is a common phenomenon (e.g. Toriyama et al., 1964). There, they became mixed with the algae and became transported offshore at the surface.

The same coastal area was probably also the origin for the monospecific pipefish accumulations. Syngnathids prefer lagoons and sheltered bays with sea-grass (Polard, 1984; Howard and Koehn, 1985) and thrive also between brown algae (Browne and Smith, 2007) but not in the open ocean.
Storms and catastrophic flooding events might be the trigger for the offshore transport. This idea is supported by an increased input of sand in the lower part of the section (Kovar, 1982). Furthermore, fluvial influx might be the reason for the scarce occurrence of planktic foraminifers.

2.5.2.3. Autochthonous multi-species vertebrate accumulations

The multi-species fish accumulations point to an epipelagic origin. A relationship between these fish accumulations and intensified upwelling and surface-water productivity is indicated by the planktic and benthic foraminiferal assemblages from the sunfish horizon. Offshore hake prefer the shelf and upper slope from few tens of metres down to several hundred metres. These fish are benthic and undertake diel vertical migrations to prey on small crustaceans, squid and other fish (Cohen et al., 1990). Mackerel are mainly plankton feeders filtering crustaceans out of the water. They are epipelagic, schooling fish and prefer surface waters in shelf environments (Colette and Nauen, 1983). Herring, as one of the most frequent constituents of the Pucking fish fauna, are mainly offshore, pelagic, schooling fishes down to 200 m water depth (Whitehead, 1985). The sunfish *Austromola angerhoferi* might have lived in very similar habitats to its modern relative *Mola mola*, which is a pelagic fish living from surface waters down to several hundred metres depth (Parenti, 2003). Thus it fits very well in the epipelagic pattern represented by the schooling fish – a habitat which is also suitable for the undescribed dolphin. Therefore, these mass-occurrences were formed by "autochthonous" offshore species.
The autochthonous deep water fish fauna is still largely undescribed. Some comments are given by Pfeil (1983). Among sharks, the deep water category is represented by the bramble shark *Echinorhinus pollerspoecki* Pfeil, 1983. Its modern relatives are deep water sharks, living close to the bottom of the shelf (Compagno, 1984). A second representative is the benthic one-finned shark *Heptranchias* sp. which today lives in deep water down to 400-1000 m close to the shelf edge (Serena, 2005). Teleost index taxa of the deep water fauna are lanternfishes (Myctophidae) which are bathypelagic, adapted to lightless depths but display a diel migration to the epipelagic zone (Paxton and Hulley, 1999). Similarly, the hatchetfish *Argyropelecus* is a bathypelagic fish (Quero et al., 1990).

2.5.2.4. Benthic communities

Benthic mass-occurrences are missing entirely. The only autochthonous benthic macrofauna, always low in number, consists of few specialists. The lucinids are adapted to low-oxygen habitats and survive by utilizing sulphide-oxidizing, chemosymbiotic bacteria as symbionts (Taylor and Glover, 2000; Zuschin et al., 2001). *Megaxinus bellardinanus* occurs close to the sunfish skeletons,

indicating hypoxic bottom conditions close to the sunfish fall. This hostile environment may also explain the near absence of gastropods, represented only by two small-sized carnivorous species. The absence of infaunal molluscs and echinoderms, the lack of bioturbation, and the good preservation of the fishes all support the interpretation of a sea bottom close to and sometimes under anoxic conditions.

2.6. Conclusions

The Aquitanian Ebelsberg Formation bears a *Konservat-Lagerstätte* with a variety of macrofossil assemblages. An evaluation of macrofossils recovered from a section near Pucking (Upper Austria) shows that besides the enormous number of specimens these assemblages are bound to specific levels in the rather uniform sediments of the section.

Micropaleontological (foraminifers, dinoflagellates) and geochemical (biomarker, organic carbon, sulfur, carbonate contents, stable isotopes) proxies have been used to reconstruct the paleoceanographic setting. The finely laminated sediments were deposited in the NAFB along the northern shelf of the Central Paratethys. Upwelling and episodically increased coastal runoff provided large amounts of nutrients stimulating primary productivity. All revealed data suggest dysoxic-anoxic bottom waters of an oxygen minimum zone along the outer shelf and upper slope.

The revealed fossil assemblages show specific associations occurring during distinct intervals within the section. Different mechanisms are discussed to explain their origin:

(1) Mass occurrences of pteropods and calcareous nannoplankton occur in several horizons across the section. These accumulations are interpreted as a response to an episodic rise in nutrient availability resulting in blooms of primary productivity. Increased coastal runoff or intensified upwelling activity are considered as the trigger mechanism.

(2) Allochthonous associations of the nautiloid *Aturia* with brown algae indicate a complex transport mechanism. Shells of the offshore-living cephalopods were transported to the coast by surface currents and/or wind currents. Episodic flooding events and storms then mixed the accumulated shells with the algae and drew them offshore again. The latter process also seems to apply to pipefish accumulations observed in the section.

(3) The multi-species vertebrate accumulations of fish and dolphins are considered as parautochthonous as their habitat is in good agreement with the reconstructed paleoenvironment.

(4) Benthic mollusc communities are scarce and of low diversity. They mainly consist of bivalves adapted to anoxic environments and thus are regarded as parautochthonous.

2.7. Acknowledgements

The authors are thankful to Thierry Corrège (University of Bordeaux, France), Martin Head (Brock University, Canada), and an anonymous reviewer for many useful remarks on the manuscript. Dr. Brecht Angerhofer (Buchkirchen, Upper Austria) kindly provided access to the sunfish fossil. This study was financially supported by the Commission for the Paleontological and Stratigraphical

Research of Austria (Austrian Academy of Sciences) and greatly benefited from the cooperation between the universities of Graz and Leoben within the UZAG-framework.

2.8. References

Allison, P., 1988. Konservat-Lagerstätten: cause and classification. Paleobiology 14, 331–344.

Allison, P.A., Briggs, D.E.G., 1993. Exceptional fossil record: distribution of soft-tissue preservation through the Phanerozoic. Geology 21, 527–530.

Almogi-Labin, A., 1982. Stratigraphic and paleoceanographic significance of Late Quaternary pteropods from deep-sea cores in the Gulf of Aqaba (Elat) and northernmost Red Sea. Marine Micropaleontology 7, 53–72.

Almogi-Labin, A., Hemleben, C., Deuser, W.G., 1988. Seasonal variation on the flux of euthecosmatous pteropods collected in deep sediment trap in the Sargasso Sea. Deep-Sea Research 35, 441–464.

Almogi-Labin, A., Luz, B., Duplessy, J.C., 1986. Quaternary paleoceanography, pteropod preservation and stable isotope record of the Red Sea. Palaeogeography, Palaeoclimatology, Palaeoecology 57, 195–211.

Báldi, K., 2006. Paleoceanography and climate of the Badenian (Middle Miocene, 16.4-13.0 Ma) in the Central Paratethys based on foraminifera and stable isotope ($\delta^{18}O$ and $\delta^{13}C$) evidence. International Journal of Earth Sciences 95, 119–142.

Báldi, T., 1986. Mid-Tertiary stratigraphy and paleogeographic evolution of Hungary. Akadémiai Kiadó Budapest, 1–201.

Barakat, A.O., Rullkötter, J., 1997. A comparative study of molecular paleosalinity indicators: chromans, tocopherols and C_{20} isoprenoid thiophenes in Miocene lake sediments (Nördlinger Ries, Southern Germany). Aquatic Geochemistry 3, 169–190.

Berner, R.A., 1984. Sedimentary pyrite formation: An update. Geochimica et Cosmochimica Acta 48, 605–615.

Bernhard, J.M., Sen Gupta, B.K., 1999. Foraminifera of oxygen-depleted environments, in: Sen Gupta, B.K. (Ed.), Modern Foraminifera. Kluwer Academic Press, New York, pp. 201-216.

Biffi, U., Manum, S.B., 1988. Late Eocene-Early Miocene dinoflagellate cyst stratigraphy from the Marche Region (central Italy). Bolletino della Società Paleontologica Italiana 27, 163–212.

Briggs, D.E.G., 2003. The role of decay and mineralization in the preservation of softbodied fossil. Annual Reviews in Earth and Planetary Sciences 31, 275–301.

Brinkhuis, H., Powell, A.J., Zevenboom, D., 1992. High-resolution dinoflagellate cyst stratigraphy of the Oligocene/Miocene transition interval in northwest and central Italy, in: Head, M.J., Wrenn, J.H. (Eds.), Neogene and Quaternary Dinoflagellate Cysts and Acritarchs. American Association of Stratigraphic Palynologists, pp. 219–258.

Browne, R.K., Smith, K., 2007. A new pipefish, *Stigmatopora narinosa* (Syngnathidae) from South Australia. Memoirs of Museum Victoria 64, 1–6.

Cicha, I., Rögl, F., Rupp, C., Ctyroká, J., 1998. Oligocene-Miocene foraminifers of the Central Paratethys. Abhandlungen der Senckenbergischen Naturforschenden Gesellschaft 549, 1–325.

Cohen, D.M., Inada, T., Iwamoto, T., Scialabba, N., 1990. Gadiform fishes of the world (Order Gadiformes). An annotated and illustrated catalogue of cods, hakes, grenadiers and other gadiform fishes known to date. FAO Fishery Synopsis 125/10, 1–442. Food and Agriculture Organization of the United Nations.

Collette, B.B., Nauen, C.E., 1983. Scombrids of the world. An annotated and illustrated catalogue of tunas, mackerels, bonitos, and related species known to date. FAO Fishery Synopsis 125/2, 1–137. Food and Agriculture Organization of the United Nations.

Compagno, L.J.V., 1984. Sharks of the world. An annotated and illustrated catalogue of shark species known to date. FAO Fishery Synopsis 125/4, 1–123. Food and Agriculture Organization of the United Nations.

Dale, B., 1996. Dinoflagellate cyst ecology: modeling and geological applications, in: Jansonius, J., McGregor, D.C. (Eds.), Palynology: Principles and Applications. American Association of Stratigraphic Palynologists Foundation, Dallas, Texas, vol. 3, pp. 1249–1275.

de Verteuil, L., Norris, G., 1996. Miocene dinoflagellate stratigraphy and systematics of Maryland and Virginia. Micropaleontology 42, 1–172.

Deviller, R., de Vernal, A., 2000. Distribution of dinoflagellate cysts in surface sediments of the northern North Atlantic in relation to nutrient content and productivity in surface waters. Marine Geology 166, 103–124.

Didyk, B.M., Simoneit, B.R.T., Brassell, S.C., Eglinton, G., 1978. Organic geochemical indicators of paleoenvironmental conditions of sedimentation. Nature 272, 216–222.

Donovan, S.K., Paul, C.R.C., 1998. The adequacy of the fossil record. Wiley, Chichester.

Espitalié, J., Laporte, J.L., Madec, M., Marquis, F., Leplat, P., Paulet, J., Boutefeu, A., 1977. Méthode rapide de caractérisation des roches mères, de leur potentiel pétrolier et de leur degré d´évolution. Revue de l´ Institut Français du Pérole 32, 23–42.

Fensome, R.A., Williams, G.L., 2004. The Lentin and Williams Index of fossil dinoflagellates 2004 Edition. American Association of Stratigraphic Palynologists, Contributions Series 42, pp. 1–909.

Fensome, R.A., Mac Rae, R.A., Williams, G.L., 2008. DINOFLAJ2, Version 1. American Association of Stratigraphic Palynologists, Data Series 1. Electronic database, http://www.palynology.org/.

Gilmer, R.W., Harbison, G.R., 1986. Morphology and field behaviour of pteropod molluscs: feeding methods in the families Cavoliniidae, Limacinidae and Peraclididae (Gastropoda: Thecosomata). Marine Biology 91, 47–57.

Gooday, A.J., 1993. Deep-sea benthic foraminifera which exploit phytodetritus: characteristic features and controls on distribution. Marine Micropaleontology 22, 187-205.

Gooday, A.J., 2003. Benthic foraminifera (Protista) as tools in deep-water palaeoceanography: Environmental influences on faunal characteristics. Advances in Marine Biology 46, 1–90.

Goossens, H., de Leeuw, J.W., Schenck, P.A., Brassell, S.C., 1984. Tocopherols as likely precursors of pristane in ancient sediments and crude oils. Nature 312, 440–442.

Grantham, P.J., Wakefield, L.L., 1988. Variations in the steranes carbon number distributions of marine source rock derived crude oils through geological time. Organic Geochemistry 12, 61–73.

Green, O.R., 2001. A manual of practical laboratory and field techniques in palaeobiology. Kluwer Academic Publishers, Dordrecht.

Gregorova, R., Schultz, O., Harzhauser, M., Kroh, A., Ćoric, S., 2009. A giant Early Miocene sunfish from the North Alpine Foreland Basin (Austria) and its implication for molid phylogeny. Journal of Vertebrate Paleontology 29, 359–371.

Grunert, P., Soliman, A., Harzhauser, M., Müllegger, S., Piller, W.E., Roetzel, R., Rögl, F., 2010. Upwelling conditions in the Early Miocene Central Paratethys Sea. Geologica Carpathica 61, 129–145.

Gürs, K., Janssen, A.W., 2004. Sea-level related molluscan plankton events (Gastropoda, Euthecosomata) during the Rupelian (Early Oligocene) of the North Sea Basin. Netherlands Journal of Geosciences, Geologie en Mijnbouw 83, 199–208.

Hardenbol, J., Thierry, J., Farley, M.B., Jacquin, T., Graciansky, P.-C., Vail, P.R., 1998. Mesozoic and Cenozoic Sequence Chronostratigraphic Framework of European Basins, in: Graciansky, C.-P., Hardenbol, J., Jacquin, T., Vail, P.R. (Eds.), Mesozoic and Cenozoic sequence stratigraphy of European basins. Society for Sedimentary Geology, Special Publication 60, Tulsa, pp. 3–13.

Harzhauser, M., Mandic, O., 2002. Late Oligocene Gastropods and Bivalves from the Lower and Upper Austrian Molasse Basin, in: Piller, W. E., Rasser, M., (Eds.), The Paleogene of Austria. Österreichische Akademie der Wissenschaften, Schriftenreihe der Erdwissenschaftlichen Kommissionen 14, pp. 671–795.

Hochuli, P.A., 1978. Palynologische Untersuchungen im Oligozän und Untermiozän der Zentralen und Westlichen Paratethys. Beiträge zur Paläontologie von Österreich 4, 1–132.

Howard, R.K., Koehn, J.D., 1985. Population dynamics and feeding ecology of pipefish (Syngnathidae) associated with eelgrass beds of Western Port, Victoria. Australian Journal of Marine and Freshwater Research 36, 361–370.

Kawagata, S., 2001. Tasman Front shifts and associated paleoceanographic changes during the last 250,000 years: foraminiferal evidence from the Lord Howe Rise. Marine Micropaleontology 41, 167–191.

Kovar, J.B., 1982. Eine Blätter-Flora des Egerien (Ober-Oligozän) aus marinen Sedimenten der Zentralen Paratethys im Linzer Raum (Österreich). Beiträge zur Paläontologie von Österreich 9, 1–209.

Krenmayr, H.G., Schnabel, W., 2006. Geologische Karte von Oberösterreich 1:200.000, 1 sheet, 2 additional maps. Geological Survey of Austria, Vienna.

Kroh, A., 2005. Echinoidea neogenica, in: Piller, W.E. (Ed.), Catalogus Fossilium Austriae 2. Österreichische Akademie der Wissenschaften, Wien.

Larkin, K.E., Gooday, A.J., 2009. Foraminiferal faunal responses to monsoon-driven changes in organic matter and oxygen availability at 140 and 300m water depth in the NE Arabian Sea. Deep Sea Research II 56, 403–421.

Li, Q., Radford, S.S., Banner, F.T., 1992. Distribution of microperforate tenuitellid planktonic foraminifers in holes 747A and 749B, Kerguelen Plateau. Proceedings of the Ocean Drilling Program, Scientific Results 120, 569–594.

Li, Q., McGowran, B., 1998. Oceanographic implications of recent planktonic foraminifera along the southern Australian margin. Marine and Freshwater Research 49, 439–445.

Lourens, L., Hilgen, F., Shackleton, N.J., Laskar, J., Wilson, D., 2004. The Neogene Period, in: Gradstein, F.M., Ogg, J.G., Smith, A.G. (Eds.), A Geologic Time Scale 2004. Cambridge University Press, Cambridge, pp. 409–440.

Louwye, S., Laga, P., 2008. Dinoflagellate cyst stratigraphy and palaeoenvironment of the marginal marine Middle and Upper Miocene of the eastern Campine area, northern Belgium (southern North Sea Basin). Geological Journal 43, 75–94

Lukeneder, A., Harzhauser, M., 2002. Shell accumulations of the Nautilidae *Aturia (Aturia) aturi* in the Lower Miocene Paratethys. Abhandlungen der Geologischen Bundesanstalt 57, 459–466.

Maas, M., 2000. Verteilung lebendgefärbter benthischer Foraminiferen in einer intensivierten Sauerstoffminimumzone, Indo-Pacifischer Kontinentalrand, nördliches Arabisches Meer. Meyniana 52, 101–129.

Mackas, D.L., Galbraith, M.D., 2002. Zooplankton distribution and dynamics in a North Pacific eddy of coastal origin: I. Transport and loss of continental margin species. Journal of Oceanography 58, 725–738.

Marret, F., Zonneveld, K.A.F., 2003. Atlas of modern organic-walled dinoflagellate cyst distribution. Review of Palaeobotany and Palynology 125, 1–200.

Meyers, P.A., 2006. Paleoceanographic and paleoclimatic similarities between Mediterranean sapropels and Cretaceous black shales. Palaeogeography, Palaeoclimatology, Palaeoecology 235, 305–320.

Mlíkovský, J., 1987. Eine neue Alkenart (Aves: Alcidae) aus dem Ober-Oligozaen Oesterreichs. Annalen des Naturhistorischen Museums in Wien 88A, 131–147.

Mohan, R., Verma, K., Mergulhao, L-P., Sinha, D.K., Shanvas, S., Guptha, M.V.S., 2006. Seasonal variation of pteropods from the Western Arabian Sea sediment trap. Geo-Marine Letters 26/5, 265–273.

Munsterman, D. K., Brinkhuis, H., 2004. A southern North Sea Miocene dinoflagellate cyst zonation. Netherlands Journal of Geosciences–Geologie en Mijnbouw 83/4, 267–85.

Murray, J., 2001. The niche of benthic foraminifera, critical thresholds and proxies. Marine Micropaleontology 41, 1–7.

Murray, J., 2006. Ecology and Applications of Benthic Foraminifera. Cambridge University Press, Cambridge.

Negri, A., Ferretti, A., Wagner, T., Meyers, P.A., 2009. Organic-carbon-rich sediments through the Phanerozoic: Processes, progress, and perspectives. Palaeogeography, Palaeoclimatology, Palaeoecology 273, 213–217.

Parenti, P., 2003. Family Molidae Bonaparte 1832 – molas and sunfishes. California Academy of Science, Annotated Checklists of Fishes 18, 1–9.

Paxton, J.R., Hulley, P.A., 1999. Myctophidae. Lanternfishes, in: Carpenter, K.E., Niem, V.H. (Eds.), FAO species identification guide for fishery purposes. The living marine resources of the WCP. Vol. 3. Batoid fishes, chimaeras and bony fishes part 1 (Elopidae to Linophrynidae). Food and Agriculture Organization of the United Nations, Rome, pp. 1957–1964.

Peeters, F.J.C., Brummer, G.-J.A., Ganssen, G., 2002. The effect of upwelling on the distribution and stable isotope composition of *Globigerina bulloides* and *Globigerina ruber* (planktic foraminifers) in modern surface waters of the NW Arabian Sea. Global and Planetary Change 34, 269–291.

Peters, K.E., Walters, C.C., Moldowan, J.M., 2005. The Biomarker Guide, Volume 2: Biomarkers and Isotopes in the Petroleum Exploration and Earth History, 2nd ed. Cambridge University Press.

Pfeil, F.H., 1983. Zahnmorphologische Untersuchungen an rezenten und fossilen Haien der Ordnungen Chlamydoselachiformes und Echinorhiniformes. Palaeoichthyologica 1, 1–315.

Piller, W.E., Harzhauser, M., Mandic, O., 2007. Miocene Central Paratethys stratigraphy – current status and future directions. Stratigraphy 4, 151–168.

Polard, D.A., 1984. A review of ecological studies on seagrass-fish communities, with particular reference to recent studies in Australia. Aquatic Botany 18, 33–42.

Quero, J.C., Hureau, J.C., Karrer, C., Post, A., Saldanha, L., 1990. Check-list of the fishes of the eastern tropical Atlantic (CLOFETA) 1, 1–1492. JNICT (Lisbon), SEI (Paris), UNESCO (Paris).

Radke, M., Willsch, H., Welte, D.H., 1980. Preparative hydrocarbon group type determination by automated medium pressure liquid chromatography. Analytical Chemistry 52, 406-411.

Roetzel, R., 1983. Die Faziesentwicklung des Oligozäns in der Molassezone zwischen Krems und Wieselburg (Niederösterreich). Jahrbuch der Geologischen Bundesanstalt 126, 129–179.

Roetzel, R., Ćorić, S., Galović, I., Rögl, F., 2006. Early Miocene (Ottnangian) coastal upwelling conditions along the southeastern scarp of the Bohemian Massif (Parisdorf, Lower Austria, Central Paratethys). Beiträge zur Paläontologie 30, 387–413.

Rögl, F., 1998. Palaeogeographic Considerations for Mediterranean and Paratethys Seaways (Oligocene to Miocene). Annalen des Naturhistorischen Museums in Wien 99A, 279–310.

Rögl, R., Hochuli, P., Muller, C., 1979. Oligocene-Early Miocene stratigraphic correlations in the Molasse Basin of Austria. Annales Geologiques des Pays Helleniques Tome hors series, 1045–1050.

Rohling, E.J., 1994. Review and new aspects concerning the formation of eastern Mediterranean sapropels. Marine Geology 122, 1–28.

Rullkötter, J., 2000. Organic matter: the driving force of early diagenesis, in: Zabel, M. (Ed.), Marine Geochemistry. Springer-Verlag, Berlin, pp. 129–172.

Schenau, S.J., Slomp, C.P., De Lange, G.J., 2000. Phosphogenesis and active phosphorite formation in sediments from the Arabian Sea oxygen minimum zone. Marine Geology 169, 1–20.

Schmid, H. P., Harzhauser, M., Kroh, A., 2001. Hypoxic events on a Middle Miocene carbonate platform of the Central Paratethys (Austria, Badenian, 14 Ma) with contributions by Coric, S., Rögl, F., Schultz, O. Annalen des Naturhistorischen Museums in Wien 102A, 1–50.

Schulz, H.-M., Bechtel, A., Sachsenhofer, R.F., 2005. The birth of the Paratethys during the Early Oligocene: From Tethys to an ancient Black Sea analogue? Global and Planetary Change 49, 163–176.

Schumacher, S., Jorissen, F.J., Dissard, D., Larkin, K.E., Gooday, A.J., 2007. Live (Rose Bengal stained) and dead benthic foraminifera from the oxygen minimum zone of the Pakistan continental margin (Arabian Sea). Marine Micropaleontology 62, 45–73.

Schwark, L., Ferretti, A., Papazzoni, C.A., Trevisani, E., 2009. Organic geochemistry and paleoenvironment of the Early Eocene "Pesciara di Bolca" Konservat-Lagerstätte, Italy. Palaeogeography, Palaeoclimatology, Palaeoecology 273, 272–285.

Schweimanns, M., Felbeck, H., 1985. Significance of the occurrence of chemoautotrophic bacterial endosymbionts in lucinid clams from Bermuda. Marine Ecology Progress Series 24, 113–120.

Seilacher, A., 1970. Begriff und Bedeutung der Fossil-Lagerstätten. Neues Jahrbuch Geologie und Paläontologie, Abhandlungen 1, 34–39.

Serena, F., 2005. Field identification guide to the sharks and rays of the Mediterranean and Black Sea. FAO Species Identification Guide for Fishery Purposes. Food and Agriculture Organization of the United Nations, Rome.

Simoneit, B.R.T., Mazurek, M.A., 1982. Organic matter of the troposphere II. Natural background of biogenic lipid matter in aerosols over rural western US. Atmospheric Environment 16, 2139–2159.

Sinninghe Damsté, J.S., Keely, B.J., Betts, S.E., Baas, M., Maxwell, J.R., de Leeuw, J.W., 1993. Variations in abundances and distributions of isoprenoid chromans and long-chain alkylbenzenes in sediments of the Mulhouse Basin: A molecular sedimentary record of palaeosalinity. Organic Geochemistry 20, 1201–1215.

Spezzaferri, S., Coric, S., Hohenegger, J., Rögl, F., 2002. Basin-scale paleobiogeography and paleoecology: an example from Karpatian (Latest Burdigalian) benthic and planktonic foraminifera and calcareous nannofossils from the Central Paratethys. Geobios, Mémoire spécial 24, 241–256.

Taylor, J.D., Glover, E.A., 2000. Functional anatomy, chemosymbiosis and evolution of the Lucinidae. Geological Society, London, Special Publications 177, 207–225.

Ten Haven, H.L., de Leeuw, J.W., Rullkötter, J., Sinninghe Damste, J.S., 1987. Restricted utility of the pristane / phytane ratio as a palaeoenvironmental indicator. Nature 330, 641–643.

Tissot, B.T., Welte, D.H., 1984. Petroleum Formation and Occurrences. 2nd Edition. Springer Verlag, Berlin.

Toriyama, R., Sato, T., Hamada, T., Komalarjun, P., 1964. *Nautilus pompilius* drifts on the west coast of Thailand. Japanese Journal of Geology and Geography 36, p. 63.

Tsurumi, M., Mackas, D.L., Whitney, F.A., DiBacco, C., Galbraith, M.D., Wong, C.S., 2005. Pteropods, eddies, carbon flux, and climate variability in the Alaska Gyre. Deep-Sea Research 52, 1037–1053.

Volkman, J.K., 1986. A review of sterol markers for marine and terrigenous organic matter. Organic Geochemistry 9, 83–99.

Volkman, J.K., Maxwell, J.R., 1986. Acyclic isoprenoids as biological markers, in: Johns, R.B. (Ed.), Biological Markers in the Sedimentary Record. Elsevier, Amsterdam, pp. 1–42.

Wagner, L.R., 1996. Stratigraphy and hydrocarbons in Upper Austrian Molasse Foredeep (active margin). European Association of Geoscientists and Engineers Special Publication 5, 217–235.

Wagner, L.R., 1998. Tectono-stratigraphy and hydrocarbons in the Molasse Foredeep of Salzburg, Upper and Lower Austria, in: Mascle, A., Puigdefàbregas, C., Luterbacher H.P., Fernàndez, M. (Eds.), Cenozoic Foreland Basins of Western Europe. Geological Society Special Publications 134. Geological Society, London, pp. 339–369.

Ward, P.D., 1987. Natural History of *Nautilus*. Allen & Unwin Press, London.

Whitehead, P.J.P., 1985. Clupeoid fishes of the world. An annotated and illustrated catalogue of the herrings, sardines, pilchards, sprats, shads anchovies and wolf-herrings, part I - Chirocentridae, Clupeidae and Pristigasteridae. FAO Fishery Synopsis, 125/7, 1–303. Food and Agriculture Organization of the United Nations.

Williams, G.L., Brinkhuis, H, Pearce, M.A., Fensome, R.A., Weegink, J.W., 2004. Southern Ocean and global dinoflagellate cyst events compared. Index events for the Late Cretaceous–Neogene. Proceedings of the Ocean Drilling Program, Scientific Results 189, 1–98.

Wuttke, M., 1983. „Weichteil-Erhaltung“ durch lithifizierte Mikroorganismen bei mittel-eozänen Vertebraten aus den Ölschiefern der ‘Grube Messel’ bei Darmstadt. Senckenbergiana Lethaia 65, 509–527.

Zevenboom, D., 1995. Dinoflagellate cysts from the Mediterranean Late Oligocene and Miocene. CIP Gegevens Koninklijke Bibliotheek, Den Haag, 221 p. (Published Ph.D. thesis, State University of Utrecht).

Zuschin, M., Mandic, O., Harzhauser, M., Pervesler, P., 2001. Fossil evidence for chemoautotrophic bacterial symbiosis in the thyasirid bivalve *Thyasira michelottii* from the Middle Miocene (Badenium) of Austria. Historical Biology 15, 223–234.

Appendix 2.1: Tables 2.1-2.6

Tab. 2.1. Distribution and abundance of benthic foraminifers from samples F1-14. Single (s) = 1; rare (r) = 2-9; abundant (a) = ≤ 10.

Species	F1	F2	F3	F4	F5	F6	F7	F8	F9	F10	F11	F12	F13	F14
Ammodiscus tenuissimus		s	r	s	r			a	r		s			
Bathysiphon filiformis		r												
Budashevaella?		r												
Gaudryinopsis austriacus		a						r				r		
Haplophragmoides laminatus	a	a	s	r	s	r	s	a		a		a	a	
Haplophragmoides peripheroexcavatus								r						
Haplophragmoides vasiceki								r				r		
Milliammina sp.										s				
Recurvoides sp.		r					s							
Semivulvulina sp.									s					
Alabamina wolterstorffi													r	
Ammonia discigera						s	r	s	r	r		r	s	
Ammonia pseudobeccarii			s						r					
Ammonia tepida									s					
Ammonia viennensis												s		
Amphicoryna badenensis								s		r	r			
?*Amphicoryna* sp.														s
Amphimorphina haueriana						s	s		r					a
Angulogerina angulosa											r		s	
Angulogerina esuviensis													r	
Angulogerina cf. *muralis*											r			
Asterigerinata planorbis				s										
Aubignyna kiliani				s		s		r	r	r				
Baggina dentata												r		
Biapertorbis alteconicus								r	r		s		s	
Biapertorbis biaperturatus				s		r		r	r	r				
Bolivina beyrichi													r	
Bolivina crenulata	s	r	s	a	a	a	a	a	a	a	r	a	r	a
Bolivina fastigia		s			s	s		s	r	r		r		r
Bolivina grabenensis														r
Bolivina korynoides			s	r	s	a	a	s		a				
Bolivina subalpina														a
Bolivina trunensis	r	r	a	a	a	a	a	a	a	a		a	a	a
Bolivina versatilis													r	
Buccella propinqua			s	s			r							
Bulimina striata														r
Buliminella acicula		r										a		
Cancris primitivus									s					
Cancris turgidus								s				r		
Cassidulina laevigata												s		
Caucasina coprolithoides		r								a			a	a
Caucasina schischkinskayae		a	s	r	s		r	r	r	r		r	a	a
Cibicidoides lopjanicus		s			r		s	r	a			s	r	
Cibicidoides lucidus						r								
Cibicidoides punctatus										s				
Cibicidoides slovenicus													s	
Cibicidoides tenellus		s											r	
Cibicidoides ungerianus								r						

Cibicidoides spp.	s						r		r				r			
Cycloforina ludwigi										s						
Cycloforina sp.				s												
Elphidiella cryptostoma							s									
Elphidiella dollfusi				s		s		r	a	a						
Elphidiella heteropora										s						s
Elphidiella minuta				s		r								s		
Elphidiella roemeri				s												
Elphidiella subcarinata				r			r	s	r							
Elphidiella subnodosa			s	s	s	r	r	r	r	r						
Elphidium crispum									r							
Elphidium felsense									s	s						
Elphidium karpathicum			r		s			r	r		s					
Elphidium cf. *matzenense*					s											
Elphidium cf. *ortenburgense*					s				r							
Elphidium praeforme									r	s						
Eoeponidella ampliportata	s		s	a		a	a	r	r	a		r	r			
?*Epistominella* sp.																s
Escornebovina cuvillieri	r		r		r	r	r	r	a		r	r				
Escornebovina orthorapha			s		s		r	r		r		r				
Escornebovina trochiformis	s			r	s	a	a	r	a	a		r	r			
Escornebovina sp.																s
?*Escornebovina* sp.																s
Fissurina buchneri										s			s			
Fissurina corrosa																s
Fissurina marginata										s						
Fursenkoina acuta				s	s											r
Fursenkoina cf. *mustoni*												r				
Globobulimina pupoides											r					
Globocassidulina subglobosa				s	s		s		r	r		r	r			a
Globulina gibba								r								s
Grigelis pyrula											s					
?*Gyroidina brockerti*				s												
Gyroidinoides parvus										r						r
Gyroidinoides soldanii					s								s			
Hanzawaia boueana			s	r	s			r	r	a			r			
Hanzawaia hovcici																a
Hemirobulina sp.											s					
Heterolepa dutemplei											s					
Laevidentalina inornata	r						r	s			r	s	r			
Laevidentalina intermedia											r					
Laevidentalina reussi											r					
Lagena catenulata										s						
Lagena filicosta										r						
Lagena haidingeri									s							s
Lagena striata										s						
Lenticulina inornata	s		s	r	s	s	r	r	a	a	r					
Lenticulina spp.		r							r			a	r			a
Marginulina subregularis		r										r				r
Marginulina sp.	s															
Melonis pompilioides										s						
Myllostomella advena	*s*		r	a	h	a	a	a	a	a		s	r			a
?*Neoconorbina* sp.									r	r		s				
Neugeborina longiscata								r	s		r					
Nonion commune		r	s	s	s			s	s	a	s	s	r			a
Nonionellina sp.																a
Nuttallides convexus				r			r			r		r				
Parrelloides sp.				r		r										
Planularia moravica																s
Plectofrondicularia sp.												s				a
Porosononion roemeri							r	s	r	a						

?*Porosononion* sp.													s
Pseudoparrella exigua	r		r	s	a	r	r	s	r		r	a	r
Pseudoparrella sp.	r		a	s	r	r	r	r	a		r	a	a
Sigmoilinita sp.								s					r
Siphonodosaria adolphina										s			r
Siphonodosaria cf. *consobrina*													s
Siphonodosaria scripta												s	
Sphaeroidina variabilis													r
?*Stomatorbina* sp.			s										
Trochulina uhligi austriaca						r			s				
Turrilina alsatica						s	r	r	r				
Uvigerina cf. *gracilis*											s		
Uvigerina cf. *rudlingensis*											r		
Valvulineria complanata											s		
Valvulineria palmarealensis									s				r
Valvulineria sp.													s
Virgulopsis tuberculatus		s						s					

Tab. 2.2. Distribution and abundance of planktic foraminifers from samples F1-14. Single (s) = 1; rare (r) = 2-9; abundant (a) = ≤ 10.

Species	F1	F2	F3	F4	F5	F6	F7	F8	F9	F10	F11	F12	F13	F14
Globigerina angulifficinalis				r	s						r			a
Globigerina dubia												r		
Globigerina cf. *falconensis*				s							a			
Globigerina gnaucki					s					r	a	a		a
Globigerina lentiana								s		r	a	a	s	
Globigerina officinalis			s		s				s	a	a	r	a	a
Globigerina ottnangiensis			s								r	a	a	a
Globigerina ouachitaensis											r		r	s
Globigerina praebulloides				s	s		r	s			a	a	a	
Globigerina steiningeri											s	a	r	r
Globigerina sp.														r
Globigerinella cf. *obesa*										r	r			
Globoturborotalita connecta												r		
Globoturborotalita woodi														a
Tenuitella brevispira		r	s	r	s	a	r	r	a	a		a	a	r
Tenuitella clemenciae			s	r	s		r							r
Tenuitella minutissima			s		s	r			r	r		r	r	
Tenuitellinata angustiumbilicata		r	s	r	s	a	r	r	a	a		a	a	
Tenuitellinata pseudoedita				r	s		r		a	a			r	s
Tenuitellinata sp.				a	s	a	a	r	a	a		a	a	s

Tab. 2.3. Frequency of dinoflagellate cysts, acritarchs and other marine microfossils from samples D1 and D2. "x" marks single specimens of taxa documented outside the routine counting.

Species	D1	D2
Dinoflagellate cysts		
Apteodinium spiridoides	0	1
Batiacasphaera sphaerica	1	x
Cleistosphaeridium placacanthum	2	x
Cordosphaeridium cantharellus	24	31
Cordosphaeridium minimum	0	x
Cribroperidinium giuseppei	0	1
Dapsilidinium pseudocolligerum	2	3
Deflandrea phosphoritica	5	5
Distatodinium apenninicum?	0	x
Distatodinium paradoxum	2	x
Glaphyrocysta spp.	25	25
Heteraulacacysta sp.	0	x
Homotryblium tenuispinosum	29	42
Hystrichokolpoma denticulatum	1	x
Hystrichokolpoma cinctum	1	1
Hystrichosphaeropsis obscura	0	x
Hystrichokolpoma rigaudiae	2	1
Lejeunecysta spp.	12	18
Lingulodinium machaerophorum	14	5
Melitasphaeridium choanophorum	0	x
Melitasphaeridium pseudorecurvatum	0	x
Nematosphaeropsis labyrinthus	1	3
Operculodinium israelianum	0	x
Operculodinium spp.	6	6
Polysphaeridium zoharyi	16	23
Reticulatosphaera actinocoronata	5	1
Selenopemphix nephroides	4	2
Selenopemphix quanta	4	16
Spiniferites/Achomosphaera spp.	57	39
Stoveracysta conerae	x	0
Thalassiphora pelagica	8	1
Tuberculodinium vancampoae	5	7
Xandarodinium xanthum	1	1
Round brown cysts (? *Brigantedinium*)	71	60
Cysts indet.	2	8
Total dinoflagellate cysts	300	300
Acritarchs and other marine microfossils		
Paralecaniella indentata	7	19
Cyclopsiella spp.	2	5
Foraminiferal test linning	15	14

Tab. 2.4. Stable isotope values, TOC-, S-, $CaCO_3$-content and TOC/S ratios of samples I1-11. Isotopic values are given relative to VPDB.

Sample	$\delta^{13}C$	$\delta^{18}O$	S	TOC	Carbonate	TOC/S
I1	-0.54	-3.19	1.57	1.61	17	1.0
I2	-0.8	-2.68	1.33	1.6	18	1.2
I3	-0.65	-3.53	1.31	1.69	19	1.3
I4	-0.66	-2.55	1.41	1.81	19	1.3
I5	-0.76	-2.95	1.37	1.67	18	1.2
I6	-0.64	-3.69	1.37	1.47	22	1.1
I7	-0.65	-3.08	1.39	1.55	21	1.1
I8	-0.52	-3.1	1.25	1.55	21	1.2
I9	-0.41	-3.18	1.15	1.48	22	1.3
I10	-0.63	-3.55	1.2	1.59	22	1.3
I11	-0.55	-2.87	1.18	1.65	17	1.4

Tab. 2.5. Bulk organic geochemical parameters.

Sample	TOC	Calcite	S	TOC/S	T_{max}	S1	S2	HI
	%	%	%		°C	mg_{HC}/g_{rock}	mg_{HC}/g_{TOC}	
BIO1	1.76	17.4	1.06	1.67	425	0.24	3.40	200
BIO2	1.72	18.9	1.49	1.15	425	0.22	2.88	180
BIO3	1.77	19.5	1.21	1.46	427	0.23	2.89	193
BIO4	1.90	18.4	1.25	1.52				
BIO5	1.66	17.2	1.42	1.16	425	0.20	2.69	168

Tab. 2.6. Concentration ratios of selected compound groups and biomarkers.

Sample	*n*-C_{15-19}/ *n*-C_{15-33}	*n*-C_{21-25}/ *n*-C_{15-33}	*n*-C_{27-31}/ *n*-C_{15-33}	CPI	Pristane/ Phytane	Steranes (%) C_{27}	C_{28}	C_{29}	Steranes/ Hopanes	diMTTC/ tri-MTTC
BIO1	0.37	0.11	0.39	2.50	0.89	29	16	55	0.94	0.77
BIO2	0.44	0.10	0.35	2.91	1.07	31	12	57	0.89	0.97
BIO3	0.40	0.09	0.42	3.04	1.08	29	13	58	1.00	0.59
BIO4	0.39	0.11	0.36	3.08	1.02	19	21	60	0.95	0.59
BIO5	0.34	0.12	0.39	3.48	1.35	29	13	58	0.97	0.71

Appendix 2.2: Plates 2.1-2.3

Plate 2.1. Compilation of various macrofossils contributing to the mass-accumulations.

1. Undescribed dolphin. (length: 230 cm)

2. Partly disarticulated skeleton of a hake (Merlucciidae*;* length: 140 mm; 2003z0026/0477).

3. Largely complete skeleton of a herring (Clupaeidae; length of head: 60 mm; 2003z0026/0397).

4. Slab with several specimens of pipefish (Syngnathidae; length of largest specimen: 125 mm; 2003z0026/0159).

5. Undescribed lepadid cirripedes attached to driftwood (height: 160 mm; NHM2003z0026/0487).

6. Pteropod bloom consisting of *Limacina* sp. in association with algae (length: c. 150 mm: NHM 1980/25).

7. Pteropod bloom consisting of *Clio* sp. from the near Ebelsberg locality (length: 185 mm; NHM 2003z0026/0926).

8. Brown seaweed *Cystoseirites altoaustriacus* Kovar, 1982 with aerocysts (length: 120 mm).

9. *Aturia* sp. (diameter: 80 mm) in association with phycophyta thalli.

10. Articulated shells of the lucinids bivalve *Megaxinus bellardianus* (Mayer, 1864) (diameter: 52 mm; NHM 2003z0026/01919). These bivalves are frequently found in situ within the sediment.

Plate 2.1. Compilation of various macrofossils contributing to the mass-accumulations.

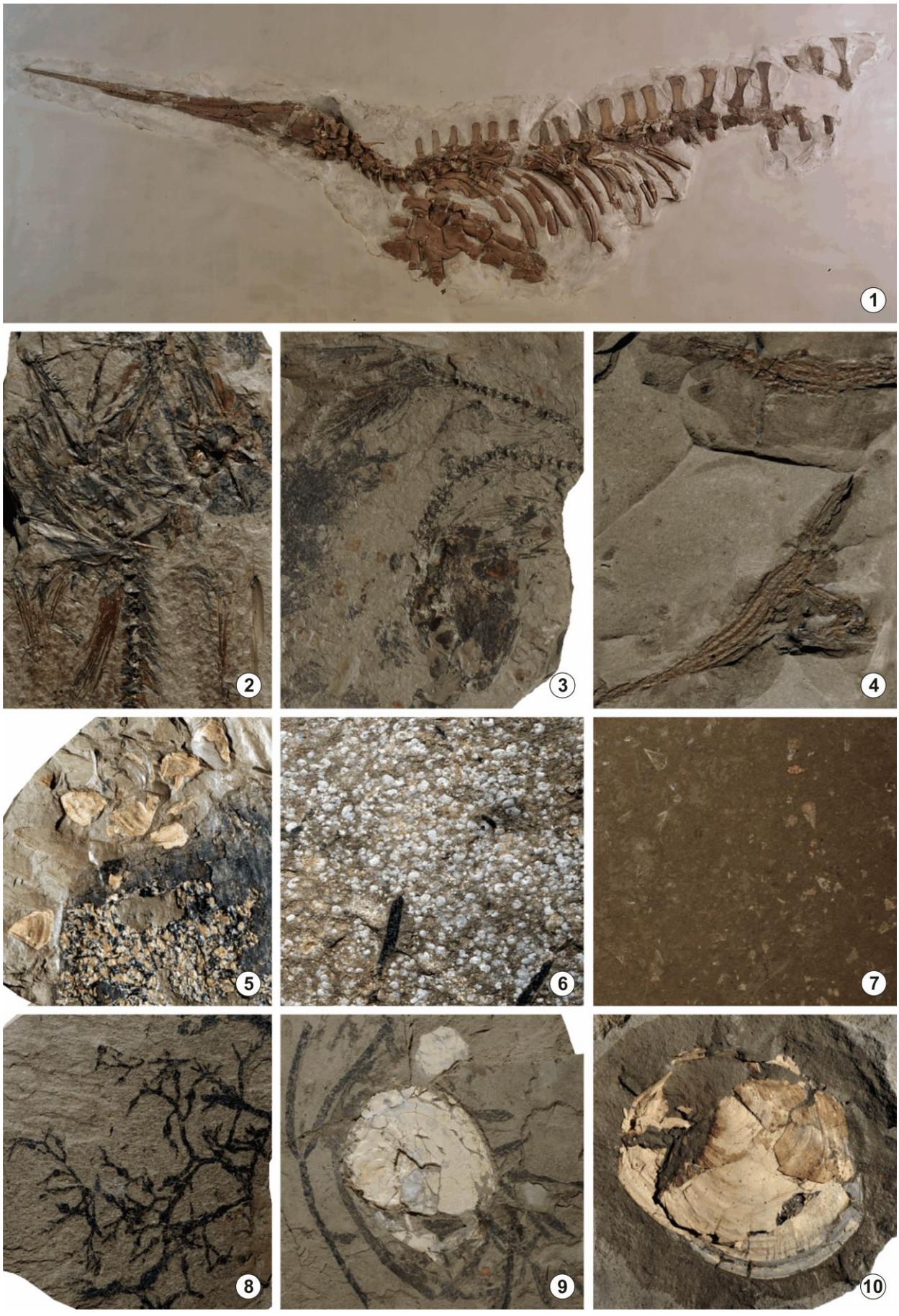

Plate 2.2. Compilation of the most common planktic and benthic foraminifers.

1. *Tenuitella brevispira* (Subbotina, 1960); sample F10
2. *Tenuitellinata angustiumbilicata* (Bolli, 1957); sample F10
3. *Tenuitella minutissima* (Bolli, 1957); sample F9
4. *Globigerina praebulloides* Blow, 1959; sample F11
5. *Globigerina gnaucki* Blow and Banner, 1962; sample F11
6. *Globigerina ottnangiensis* Rögl, 1969; sample F12
7. *Myllostomella advena* (Cushman and Laiming, 1931); sample F9
8. *Haplophragmoides laminatus*; Voloshinova, 1961 ; sample F13
9. *Escornebovina cuvillieri* (Poignant, 1965); spiral view; sample F9
10. *Caucasina schischkinskayae* (Samoylova, 1947); sample F10
11. *Caucasina coprolithoides* (Andreae, 1884); sample F10
12. *Bolivina trunensis* Hofmann, 1967; sample F7
13. *Bolivina korynoides* Hofmann, 1967; sample F7
14. *Bolivina crenulata* Cushman, 1936; sample F7
15. *Bolivina fastigia* Cushman, 1936; sample F9
16. *Pseudoparella exigua* (Brady, 1884); spiral view; sample F7
17. *Pseudoparella exigua* (Brady, 1884); umbilical view; sample F7
18. *Escornebovina trochiformis* (Andreae, 1884); spiral view; sample F7
19. *Escornebovina trochiformis* (Andreae, 1884); umbilical view; sample F7
20. *Eoeponidella ampliportata* Reiser, 1987; sample F7

Plate 2.2. Compilation of the most common planktic and benthic foraminifers.

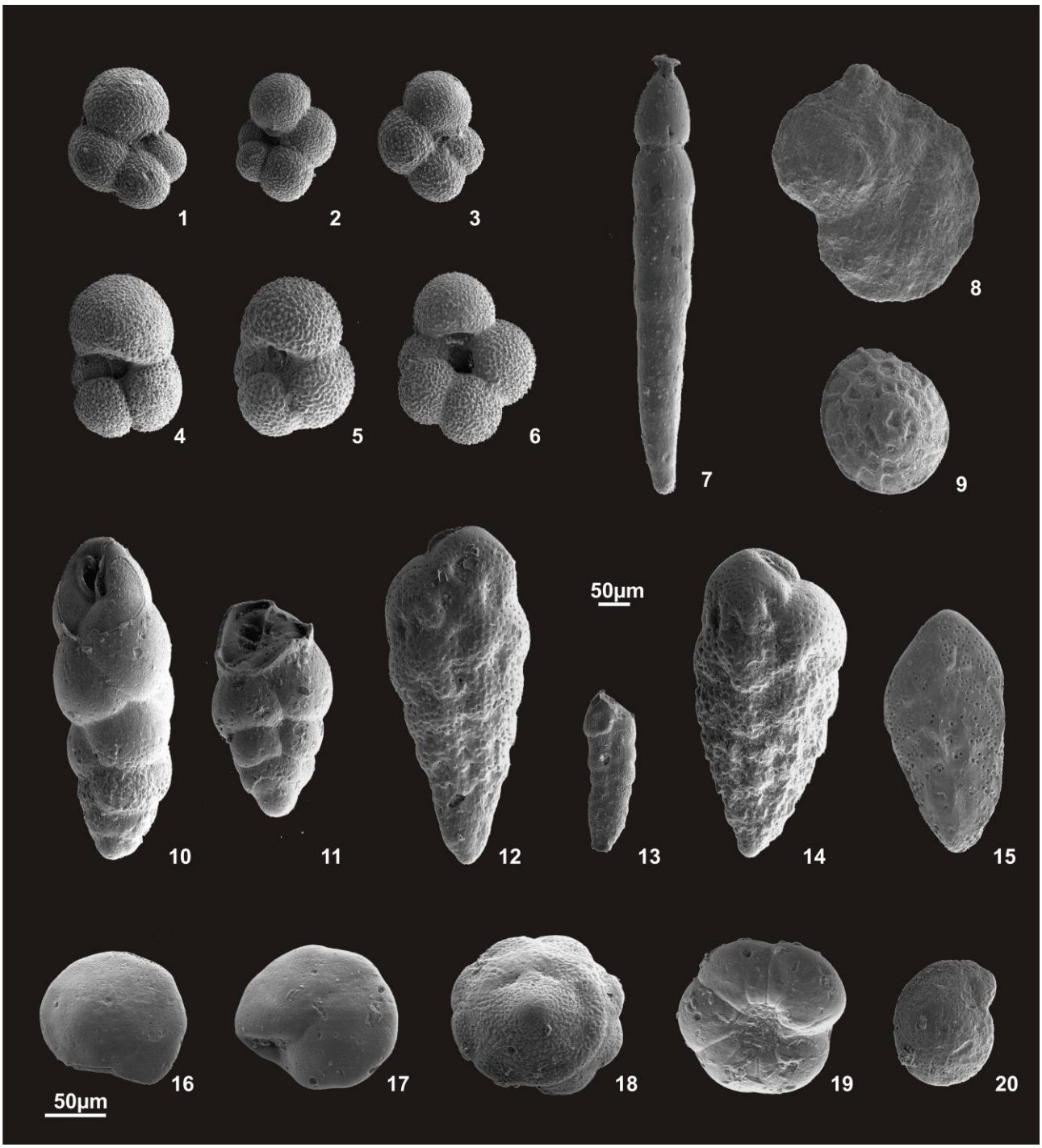

Plate 2.3. Compilation of selected dinoflagellate cysts from samples D1 and D2. Scale bar 20µm.

1. *Distatodinium apenninicum*? Brinkhuis et al., 1992; dorsal view.

2. *Dapsilidinium pseudocolligerum* (Stover, 1977) Bujak *et al.,* 1980; uncertain orientation.

3. *Glaphyrocysta* sp.; ? ventral view .

4. *Nematosphaeropsis labyrinthus* (Ostenfeld) Reid, 1974; uncertain orientation.

5. *Achomosphaera ramulifera* (Deflandre) Evitt, 1963; later view

6. *Cleistosphaeridium placacanthum* (Deflandre and Cookson) Eaton *et al.,* 2001; ?ventral view.

7. *Operculodinium israelianum* (Rossignol) Wall, 1967; uncertain orientation.

8. *Reticulatosphaera actinocoronata* (Benedek) Bujak and Matsuoka, 1986; uncertain orientation.

9. *Cordosphaeridium cantharellus* (Brosius) Gocht, 1969; ?dorsal view.

10. *Polysphaeridium zoharyi* (Rossignol) Bujak, Downie, Eaton and Williams, 1980; uncertain orientation.

11. *Lingulodinium machaerophorum* (Deflandre and Cookson) Wall, 1967; uncertain orientation.

12. *Spiniferites mirabilis* (Rossignol) Sarjeant, 1970; dorsal view.

13. *Apteodinium spiridoides* Benedek, 1972; dorsal view.

14. *Melitasphaeridium pseudorecurvatum* (Morgenroth, 1966) Bujak et al., 1980; left-lateral view.

15, 16. *Deflandrea phosphoritica* Eisenack, 1938; dorsal view, successive foci.

17. *Stoveracysta conerae* Biffi and Manum, 1988; ventral view.
18. *Distatodinium paradoxum* (Brosius) Eaton 1976; uncertain orientation

19, 20. *Hystrichosphaeropsis obscura* Habib, 1972; right lateral view.

Plate 2.3. Compilation of selected dinoflagellate cysts from samples D1 and D2. Scale bar 20µm.

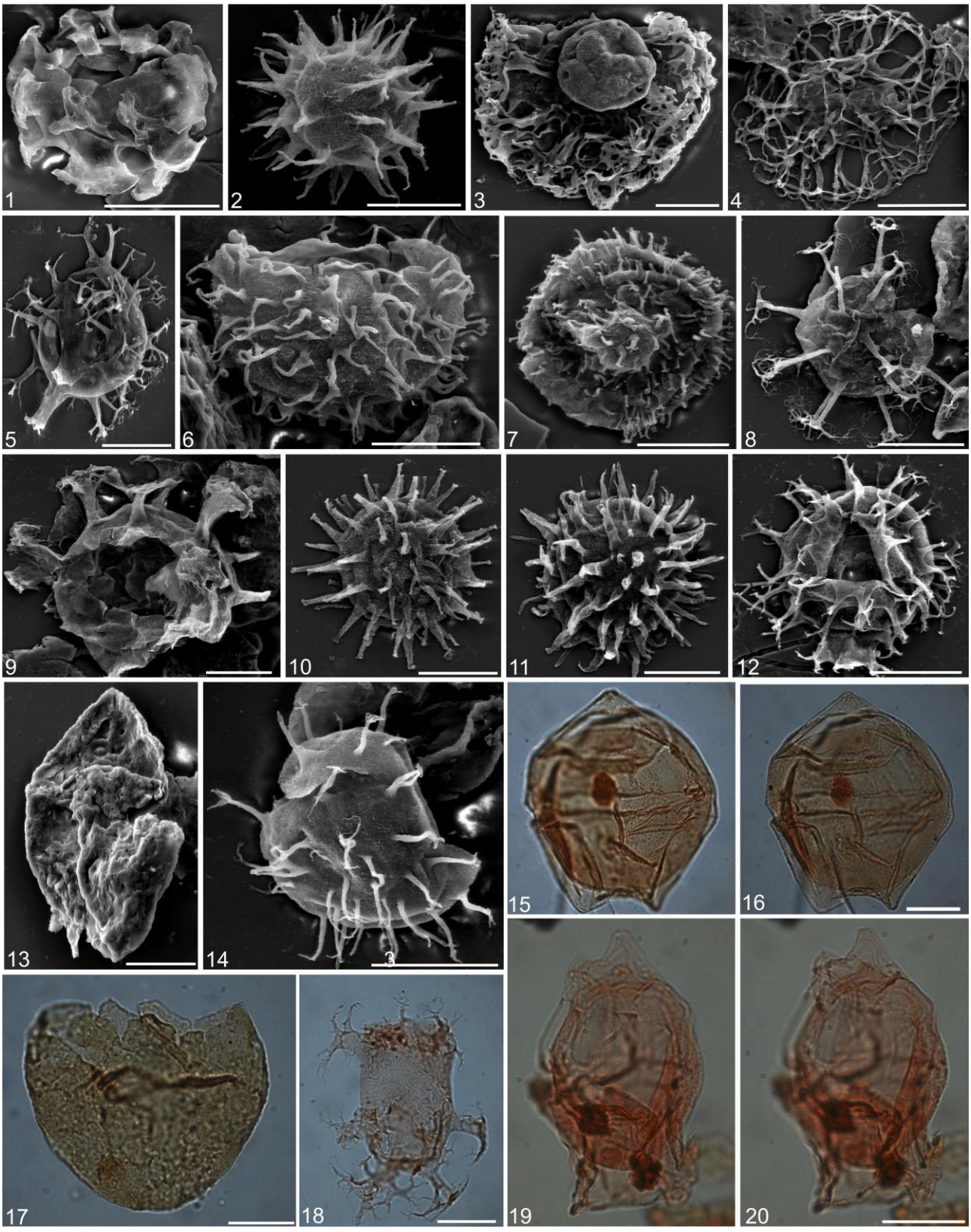

Chapter 3

EARLY BURDIGALIAN UPFILL OF THE PUCHKIRCHEN BASIN (NORTH ALPINE FORELAND BASIN, CENTRAL PARATETHYS): FACIES DEVELOPMENT AND SEQUENCE STRATIGRAPHY

Patrick Grunert[a], Ralph Hinsch[b], Reinhard Sachsenhofer[c], Stjepan Ćorić[d], Mathias Harzhauser[e], Werner E. Piller[a], Hanns Sperl[b]

[a] Institute for Earth Sciences, University of Graz, Heinrichstraße 26, A-8010 Graz, Austria

[b] Rohöl-Aufsuchungs AG, Schwarzenbergplatz 16, A-1015 Vienna, Austria

[c] Department of Applied Geosciences and Geophysics, Montanuniversität Leoben, Peter-Tunner Straße 5, A-8700 Leoben, Austria

[d] Geological Survey of Austria, Neulinggasse 38, A-1030 Vienna, Austria

[e] Natural History Museum Vienna, Geological-Paleontological Department, Burgring 7, A-1014 Vienna, Austria

3.1. Abstract

To improve the prediction of gas and oil bearing strata along the tectonically imbricated southern margin of the Puchkirchen Basin (North Alpine Foreland Basin, Central Paratethys), a better understanding of facies distribution and stratigraphic control of the undisturbed parts of the basin is essential. The present study provides a facies analysis and biostratigraphic evaluation for the pelitic Hall Fm. of the borehole Hochburg 1 in the central part of the Puchkirchen Basin. A statistical evaluation of benthic foraminiferal assemblages together with geochemical proxy records (TOC, sulfur, hydrogen index) reveals a succession of lower Burdigalian depositional environments.

Following a major erosional hiatus, the conglomeratic sands at the base of the section contain reworked Chattian and Aquitanian foraminiferal assemblages that document the reactivation of the basin-axial Puchkirchen Channel System. In the course of the transgression, that is linked to the early Burdigalian rise in eustatic sea-level, the channel gets cut off from its sediment sources on the shelf and a deepening bathyal environment establishes. Agglutinated foraminiferal assemblages with large amounts of *Bathysiphon filiformis* develop that are adapted to an unstable environment with frequent deposition of turbidites. The middle part of the Hall Fm. contains NE prograding prodeltaic sediments that initiate the upfill of the Puchkirchen Basin. High sedimentation rates and increased input of terrestrial-derived organic matter are documented in low TOC/S and HI values and frequent occurrences of *Ammodiscus* spp. and other opportunistic agglutinating foraminifers.

A last major transgression reestablishes a eutrophic and suboxic bathyal environment that is followed by the development of an oxic outer-middle neritic shelf environment.
Based on a comparison of the revealed facies development to existing sequence stratigraphic models for the Puchkirchen Basin three sequences and their corresponding systems tracts can be identified for the lower, middle and upper Hall Fm. Biostratigraphic evidence from benthic foraminifers and calcareous nannoplankton suggests that they correspond to the regional stages of the middle and upper Eggenburgian and lower Ottnangian and to global 3rd-order sequences Bur 1-3.

3.2. Introduction

The Upper Oligocene to Lower Miocene marine deposits of the Puchkirchen Basin in Upper Austria constitute valuable reservoir rocks for the production of biogenic gas in the North Alpine Foreland Basin (Malzer et al., 1993; Wagner, 1998). Current exploration in the basin focuses on its heavily imbricated southern parts along the Alpine thrust front (Hinsch, 2008). In order to predict reservoirs in this area accurately, detailed information on stratigraphy and facies distribution in the undisturbed central and northern part of the basin is essential. Initial facies models derived from subsurface information of several hundred exploration wells and 2D-seismic lines described a deep-marine paleoenvironment mainly controlled by tectonically induced deposition of turbidite fans (Malzer et al., 1993; Wagner, 1996; 1998). Recent studies based on sedimentological core-description, provenance analysis, well-log data and 3D-seimic surveys improved the basic facies models significantly and revealed a variegated depositional environment featuring a long-lived basin-axial channel belt and a succession of prograding delta fans (Linzer, 2001; Kuhlemann and Kempf, 2002; Brügel et al., 2003; De Ruig, 2003; Hubbard et al., 2005; Borowski, 2006; De Ruig and Hubbard, 2006; Hinsch, 2008; Covault et al., 2009; Hubbard et al., 2009). Several attempts have been made to incorporate the observed patterns in facies distribution into a sequence stratigraphic framework for the Puchkirchen Basin (Jin et al., 1995; Zweigel, 1998; Peña, 2007; Hinsch, 2008). The poor bio- and chronostratigraphic control is a major shortcoming of these studies. Age determination is largely based on lithological well-to-well correlation and few attempts have been made to correlate the lithostratigraphic units of the Puchkirchen Basin to the global chronostratigraphic framework (Papp, 1960; Rögl et al., 1979; Grunert et al., 2010a).

In the present study, we introduce quantitative micropaleontology and geochemical analysis as tools to address these issues. Facies analysis based on benthic foraminiferal assemblages and geochemical proxies is applied to the lower Burdigalian Hall Fm. that represents the last deep-marine phase of the Puchkirchen Basin. Trends in facies will be discussed in the context of existing sequence stratigraphic models in order to determine the individual sequence boundaries and systems tracts more precisely. In combination with calcareous nannoplankton biostratigraphy the new data will help to correlate the Hall Fm. more accurately to the international time scale (Lourens et al., 2004). The results will exemplarily document the final sedimentary upfill of the

Puchkirchen Basin and the studied well will serve as a reference site for future studies along the imbricated southern part of the basin.

3.3. Geological Setting

3.3.1. The Puchkirchen Basin

From Late Oligocene and Early Miocene times deep marine sedimentation in the North Alpine Foreland Basin (NAFB) was mainly confined to the Puchkirchen Basin and the southeastern margin of the Bohemian Massif (Wagner, 1998; Kuhlemann and Kempf, 2002; Roetzel et al., 2006; Grunert et al., 2010b, c). The trough of the Puchkirchen Basin extends from Bavaria (SE Germany) to Upper Austria and Salzburg (NE Austria) and parallels the Alpine thrust front with a west-east directed basinal axis (Figs. 3.1, 3.2; Malzer et al., 1993; Kuhlemann and Kempf, 2002). It is confined by the Bohemian Massif to the north and east, by the thrust complexes of the Helvetic Unit, the Rhenodanubian Flysch and the Northern Calcareous Alps to the south, and by the Bavarian shelf to the west (Wenger, 1987; Malzer et al., 1993; Wagner, 1998; Kuhlemann and Kempf, 2002; De Ruig, 2003). Large parts of the southern Puchkirchen Basin have been incorporated in the Alpine thrust sheets as part of the tectonised "Imbricated Molasse" (De Ruig, 2003).

During Chattian to early Burdigalian the Puchkirchen Basin was a deep-marine basin with water depths of 500 to 1500m (Rögl et al., 1979; Wagner, 1998). Vast and moderately inclined shelf and slope areas confined the trough to the north and west, while a steep and tectonically active slope was present in the south close to the Alpine thrust front (Zweigel, 1998; Kuhlemann and Kempf, 2002; De Ruig, 2003). Sediment distribution was mainly triggered by the Puchkirchen Channel System (PCS), an extensive meandering basin-axial channel that was 3 to 5km wide and 10s of

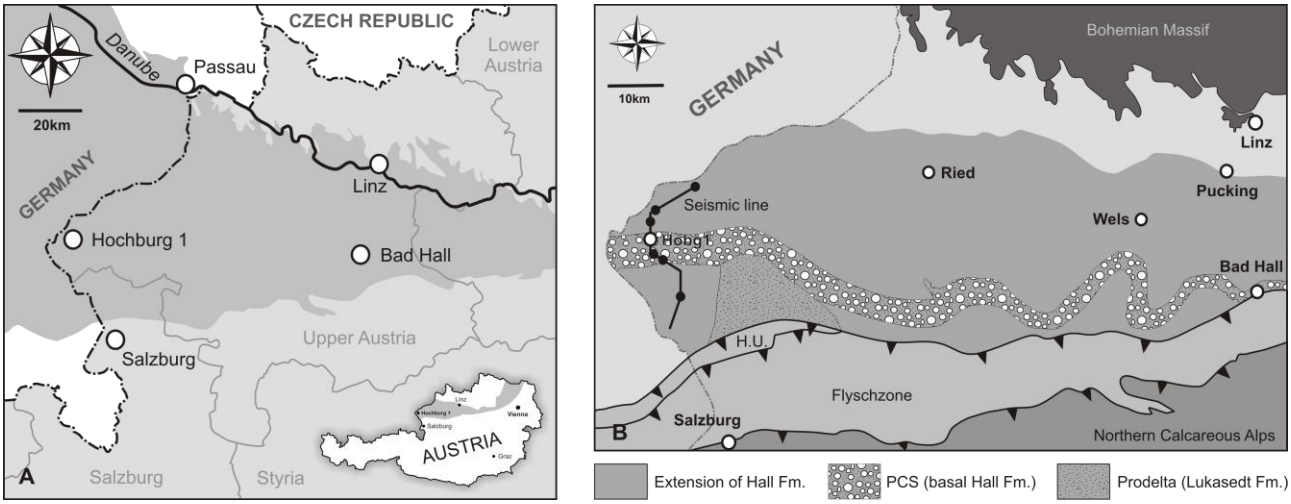

Fig. 3.1. (A) Location of the borehole Hochburg 1 in Upper Austria. The distribution of Oligocene-Miocene marine sediments in the area is indicated in dark grey. (B) Location of the seismic line used for the present study (see Fig. 3.4.) and distribution of the Hall Fm. in the study area based on Wagner (1998). H.U. = Helvetic Unit; PCS = Puchkirchen Channel System.

kilometers long (Figs. 3.1b, 3.2a; De Ruig, 2003; Hubbard et al., 2005; De Ruig and Hubbard, 2006; Hubbard at al., 2009). Several rivers entered the basin from the north, south and west and delivered large amounts of sediment into the basin. Increasing sedimentation rates led to the final upfill of the Puchkirchen Basin by the middle Burdigalian (Fig. 3.2b, c; Zweigel, 1998; Brügel et al., 2003; Borowski, 2006; Hinsch, 2008).

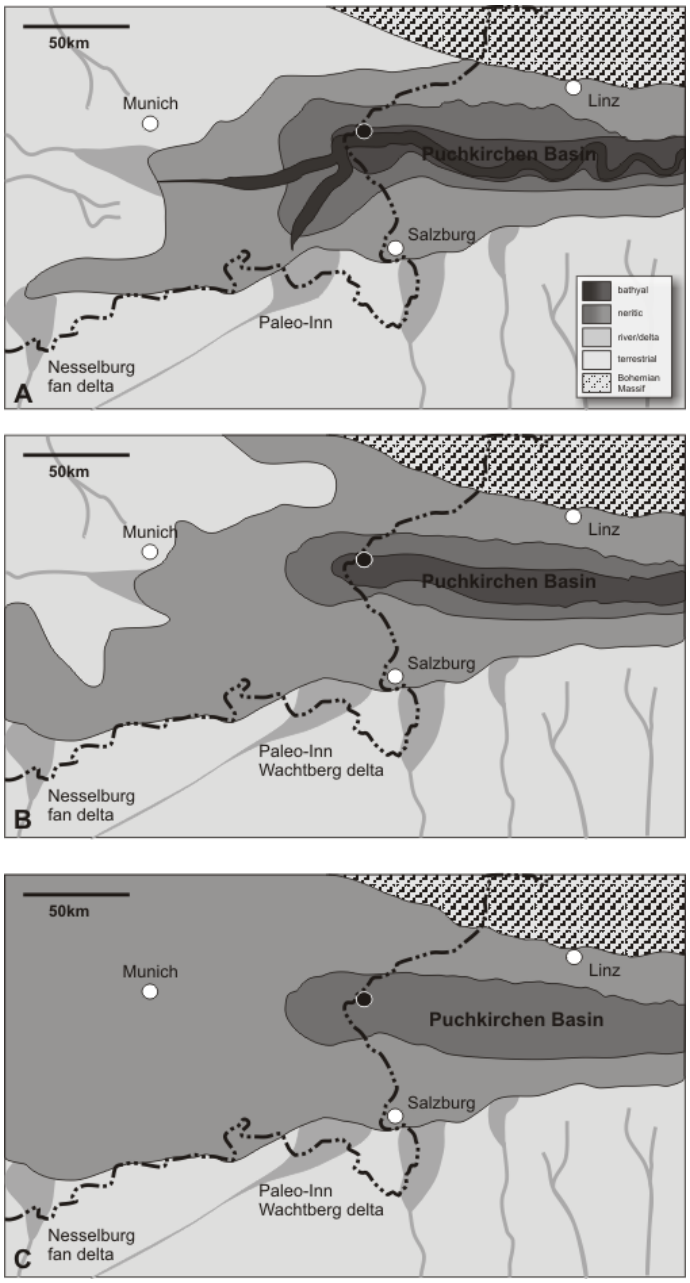

Fig. 3.2. Middle Eggenburgian-early Ottnangian paleogeography of the Puchkirchen Basin based on Wenger (1987), Kuhlemann and Kempf (2002) and Hinsch (2008).

(A) middle Eggenburgian, LST 5 with Puchkirchen Channel System; basal Hall Fm.

(B) middle Eggenburgian, mfs 5; middle Hall Fm.

(C) early Ottnangian, mfs 6; maximum extension of the middle Burdigalian shelf sea after the upfill of the Puchkirchen Basin; uppermost Hall Fm. and Innviertel Group.

3.3.2. The Hall Fm.: sedimentology, microfauna, stratigraphy

The Upper Oligocene and Lower Miocene marine deposits of the Puchkirchen Basin have a thickness of several thousands of meters and comprise the Lower and Upper Puchkirchen Formations, the Hall Fm. and the Innviertel Group (Malzer, 1993; Wagner, 1998). The pelitic Hall Fm. represents the basinal offshore facies of the Puchkirchen Basin during the early Burdigalian (Rögl et al., 1979; Wagner, 1998). It consists of greenish-grey marls with locally thick intercalations of sands and gravel, predominantly in its lower part, and reaches a thickness up to 800m (Bürgl, 1949; Aberer, 1958, 1959; Wagner, 1998). The age of the Hall Fm. has been determined as Burdigalian based on macro- and microfaunal assemblages (Bürgl, 1949; Aberer, 1958, 1959; Braumüller, 1959; Papp, 1960, 1975). Within the regional stratigraphic concept of the Central Paratethys, the Hall Fm. belongs to the Eggenburgian

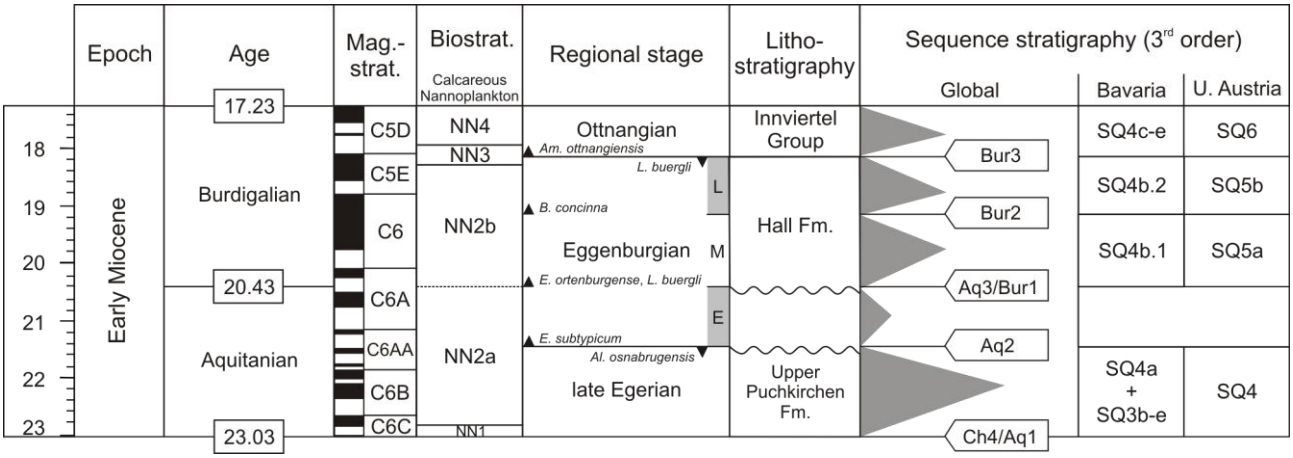

Fig. 3.3. Global and regional stratigraphy of the Aquitanian and early-middle Burdigalian according to Lourens et al. (2004) and Piller et al. (2007). Paratethyan biostratigraphy is based on Wenger (1987), Cicha et al. (1998) and Pippèrr and Reichenbacher (2009). Bavarian sequences are adopted from Peña (2007), Austrian sequences are derived from Hinsch (2008) and herein presented results. See text for discussion of sequence stratigraphic correlation.

stage (Fig. 3.3; Rögl et al., 1979; Cicha et al., 1998; Wagner, 1998).

Based on a distinct turnover in foraminiferal assemblages, the Hall Fm. has been subdivided into a lower and upper portion (Petters, 1936; Bürgl, 1949; Aberer, 1958, 1959; Braumüller, 1959; Cicha et al., 1998; Wagner, 1998). The lower part consists of grey marls, gravel and – locally – mollusc coquinas suggesting a dynamic depositional environment with strong sediment transport and intense reworking (Braumüller, 1959; Küpper and Steininger, 1975; Wagner, 1998). Foraminiferal faunas are typically composed of large agglutinated astrorhizid and lituolid species (Bürgl, 1949; Aberer, 1959). Calcareous tests are rare and mainly consist of *Lenticulina* spp., *Ammonia* spp. and globigerinids (Aberer, 1959; Küpper and Steininger, 1975). The depositional environment is characterized by the terminal PCS that distributed turbiditic mass-flow deposits within the basin (Linzer, 2001; De Ruig, 2003; De Ruig and Hubbard, 2006; Hinsch, 2008; Hubbard et al., 2009).

The upper part of the Hall Fm. consists of yellow-grey sands and clayey marls (Aberer, 1959). Foraminiferal faunas show reduced diversity and are dominated by calcareous forms including *Ammonia beccarii*, *Heterolepa dutemplei*, *Lenticulina inornata*, *Melonis pompilioides* and *Globigerina bulloides* (Aberer, 1959). Sedimentation in the basin was mainly controlled by the progradation of a tidal delta resulting in the upfill of the basin (Zweigel, 1998; Borowski, 2006; Hinsch, 2008).

The Hall Fm. was originally termed “Schlier of Hall” referring to the characteristic sandy clays of the type area close to the town of Bad Hall in Upper Austria (Fig. 3.1; Petters, 1936; Aberer, 1959; Braumüller, 1959). In the course of developing a regional stratigraphic framework for the Central Paratethys Papp (1968) introduced the term Hall Fm. that summarizes the “Schlier of Hall” and coeval deposits in Salzburg and Upper Austria. A more comprehensive concept was developed by Wagner (1998) and Piller et al. (2004) with the Hall Group that unites Eggenburgian formations from different basins and tectonical units in the Austrian part of the NAFB. The Hall, Lindach and

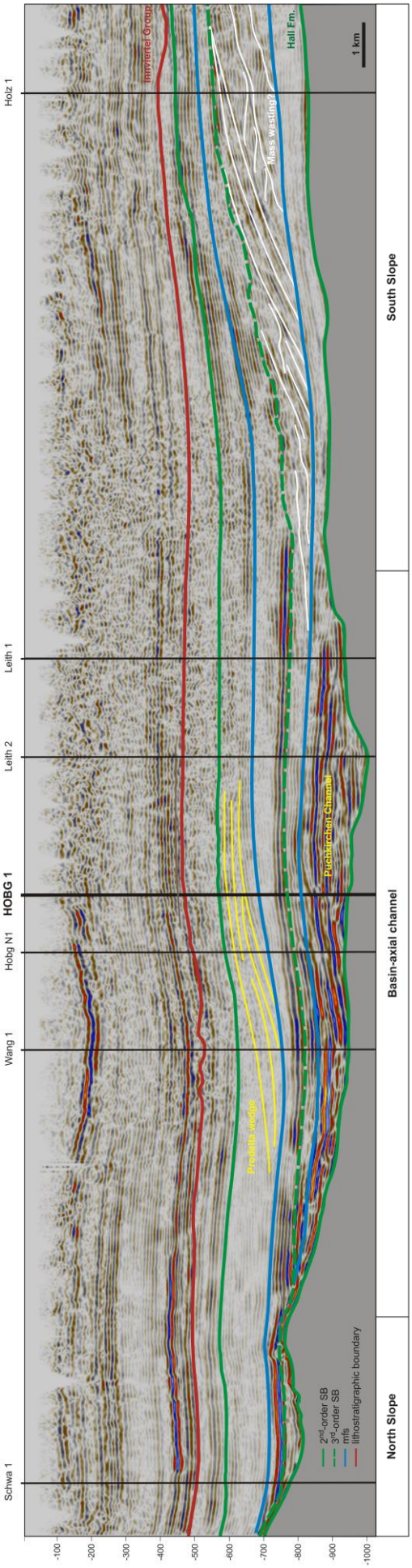

Lukasedt fms. of the Hall Group correspond to the Hall Fm. of Papp (1968). Being aware of the different terminological approaches, the term Hall Fm. will be used in the present paper as defined by Papp (1968) in order to facilitate a comparison with previous studies that mostly refer to this concept.

3.3.3. Borehole Hochburg 1

The sample material of the present study originates from the borehole Hochburg 1 in western Upper Austria that was drilled by Rohöl-Aufsuchungs AG (RAG) in 1983 (Fig. 3.1). A 3400m-thick sequence of Jurassic-Pleistocene sediments was penetrated during drilling. The differentiation of the lithological units by RAG is largely based on the evaluation of well-log data and seismic lines and supported by a qualitative analysis of benthic foraminifers from 26 drill cutting samples. According to RAG, the Hall Fm. has a thickness of 750.8m reaching from 790 to 1540.8m (Figs. 3.4, 3.5). In the logs, several informal units are distinguished: the clayey sands and gravels in the lower part of the Hall Fm. are separated as “Basal Silts” (“Basis Silte”, 1540.8-1323m; Lindach Fm. of Wagner, 1998) from the superimposed silty-sandy clays of the “Hall Series” (“Haller Serie”, 1323 to 790m; Hall Fm. of Wagner, 1998). The interval of the “Gendorf Sands” (“Gendorfer Sande”, 1221 to 1201.8m) marks a distinct package of sands found over large areas in the western Puchkirchen Basin that is used as a prominent seismic reflector.

3.4. Material and Methods

The present study is based on 67 drill cutting samples

Fig. 3.4 (left). Seismic line of the study area. Sequence stratigraphic boundaries and maximum flooding surfaces discussed in the present study are indicated for the Hall Fm. and the lowermost Innviertel Group.

from the Hall Fm. each representing 2m of sediment. Micropaleontological and geochemical analyses were carried out on the same sample where possible. All samples from 790 and 980m as well as individual samples between 990 and 1540m had to be excluded from geochemical analysis due to contamination in the drilling process. In some cases the amount of sediment was not

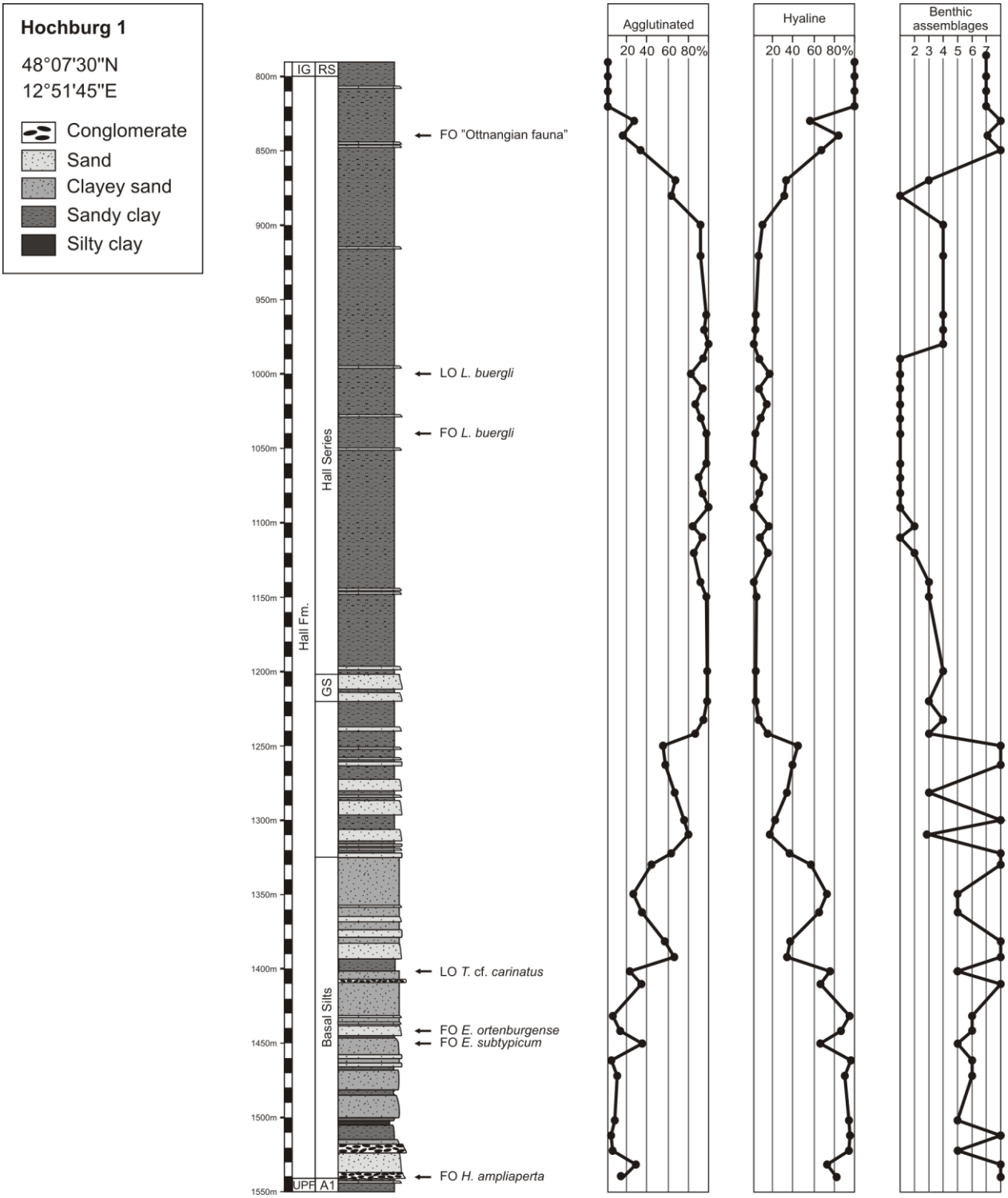

Fig. 3.5. Lithology, lithostratigraphy (including informal units used by RAG; see text) and biostratigraphy, relative abundances of agglutinated and hyaline foraminifers and distribution of benthic foraminiferal assemblages 1-8 in the Hall Fm. UPF = Upper Puchkirchen Fm; A1 = marl at top of the Upper Puchkirchen Fm.; GS = Gendorf Sands; IG = Innviertel Group; RS = Robulusschlier.

sufficient for micropaleontological evaluation and only geochemical measurements were performed.

3.4.1. Micropaleontology

56 samples from the Hall Fm. were used for foraminiferal analysis. 75g of each sample were treated with diluted H_2O_2 for several hours, wet sieved under running tap water and separated into three size-fractions (>250µm, 125-250µm, 63-125µm). At least 200 specimens were counted from size fractions >125µm where possible. Fractions <125µm were not included in the analysis as small specimens show a lower fossilization potential than larger specimens and would bias the results (Kender et al., 2008). Foraminiferal taxonomy follows Wenger (1987) and Cicha et al. (1998).

The morphogroup concept of Kaminski and Gradstein (2005) was applied to agglutinated foraminifers. Introduced by Jones and Charnock (1985) and subsequently refined, the morphogroup concept provides paleoecological information based on the relationship between test morphology and environment (Nagy et al., 1995; van den Akker, 2000; Kaminski and Gradstein, 2005). A list of morphogroups, representative taxa and their palecological implications are given in Tab. 2.1.

Statistical analysis was carried out by using the software PAST (Hammer et al., 2001). Cluster analysis (Ward's Method) and Non-metrical multidimensional scaling (NMDS; Bray-Curtis similarity) were performed on the foraminiferal data to group the samples based on their similarity in composition (Hammer et al., 2001).

A complementary biostratigraphic analysis of nannoplankton assemblages was conducted on 7 samples from the Hall Fm. Smear slides were prepared using standard methods and examined with a light microscope (cross and parallel nicols) with 1000x magnification.

3.4.2. Geochemistry

Powdered bulk sediment from 49 samples of the Hall Fm. was used for geochemical analysis. Contents of sulphur (S) and total organic carbon (TOC) were determined by using a Leco CS-300 analyser. RockEval pyrolysis (Espitalié et al., 1977) was carried out by using a Rock-Eval 2+ instrument. With this method, the amount of hydrocarbons (mgHC/grock) present in the rock sample (S_1) and released from kerogen during gradual heating (S_2) is determined. The S_2 content was normalised against TOC to give the Hydrogen Index ($HI = S_2*100/TOC$).

3.5. Results

3.5.1. Trends in foraminifers

The encountered foraminiferal taxa are listed in Appendix 3.1. A summary of the most important taxa is given in Tab. 3.2 and trends in agglutinated and hyaline foraminifers are shown in Figs. 3.5-3.7. Identification on the species level was often complicated by the preservation of the

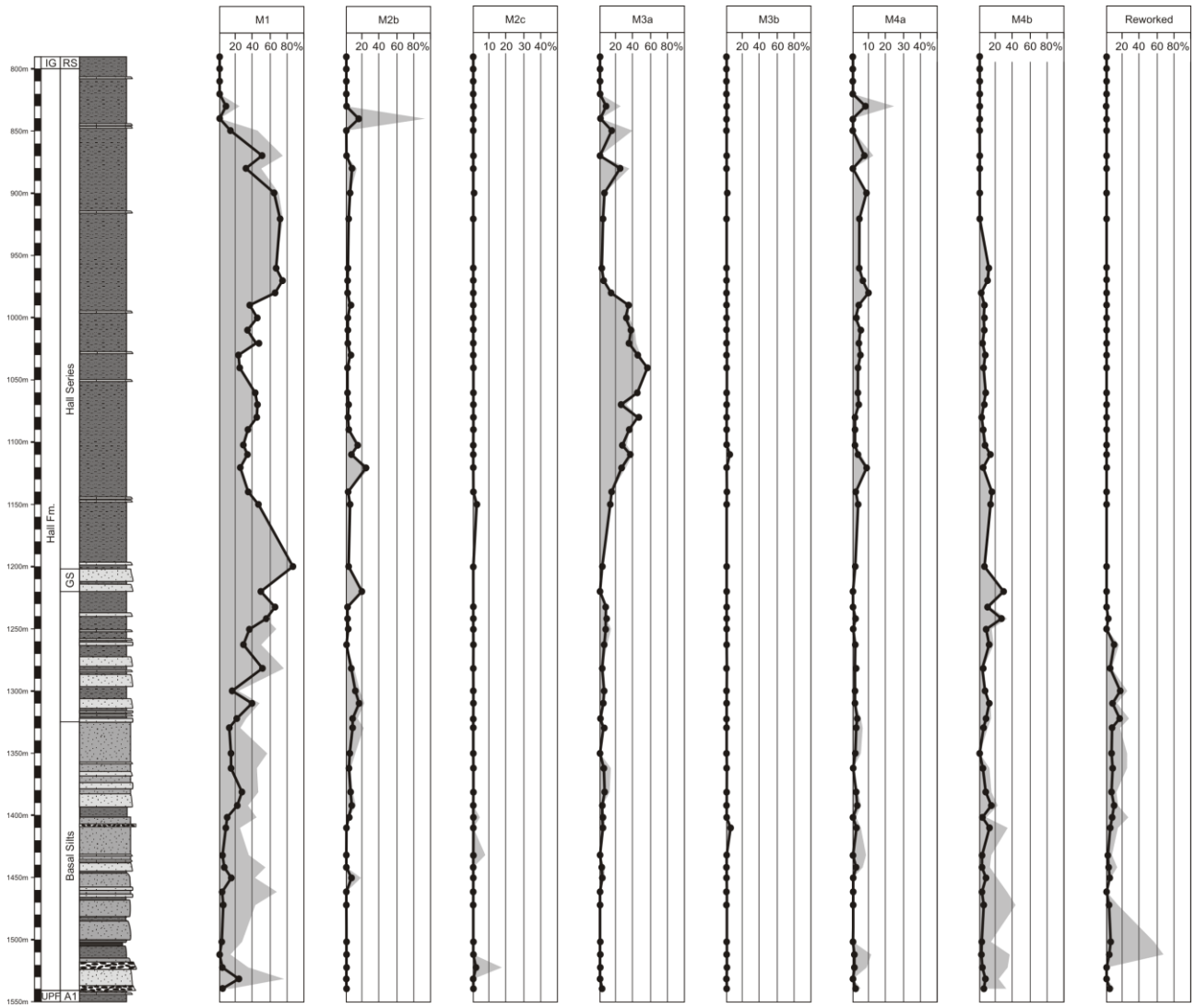

Fig. 3.6. Relative abundances of agglutinated morphogroups in the Hall Fm. The black line shows the abundance for the whole benthic assemblage, the abundance within agglutinated assemblages is indicated in grey.

foraminiferal tests: agglutinated taxa primarily consist of tests with a proteinaceous or mineralized matrix that are heavily compressed. Hyaline and miliolid tests frequently show signs of transport and heavily compressed and broken specimens occur in the lower part of the section.

Agglutinated and hyaline tests dominate the foraminiferal assemblages miliolid taxa occur very rarely (Fig. 3.5). Hyaline taxa show highest abundances in the lower (1540-1330m; A = 65%; σ = 18%) and upper (880-800m; A = 75%; σ = 29%) parts of the section while agglutinated taxa dominate the assemblages with abundances of over 80% from 900 to 1242m.

Within agglutinated foraminifers, M1 is the most abundant morphogroup and almost exclusively represented by *Bathysiphon filiformis* (Fig. 3.6). Percentages are high and increase upwards until a first maximum is reached at 1200m. Above an interval with lower values a second peak occurs between 980 and 900m. Abundance subsequently declines rapidly and M1 vanishes together with the rest of agglutinated foraminifers at 840m. Morphogroup M3a consists of various species of *Ammodiscus*. M3a is rare to absent in the lower part of the Hall Fm. followed by a sudden increase

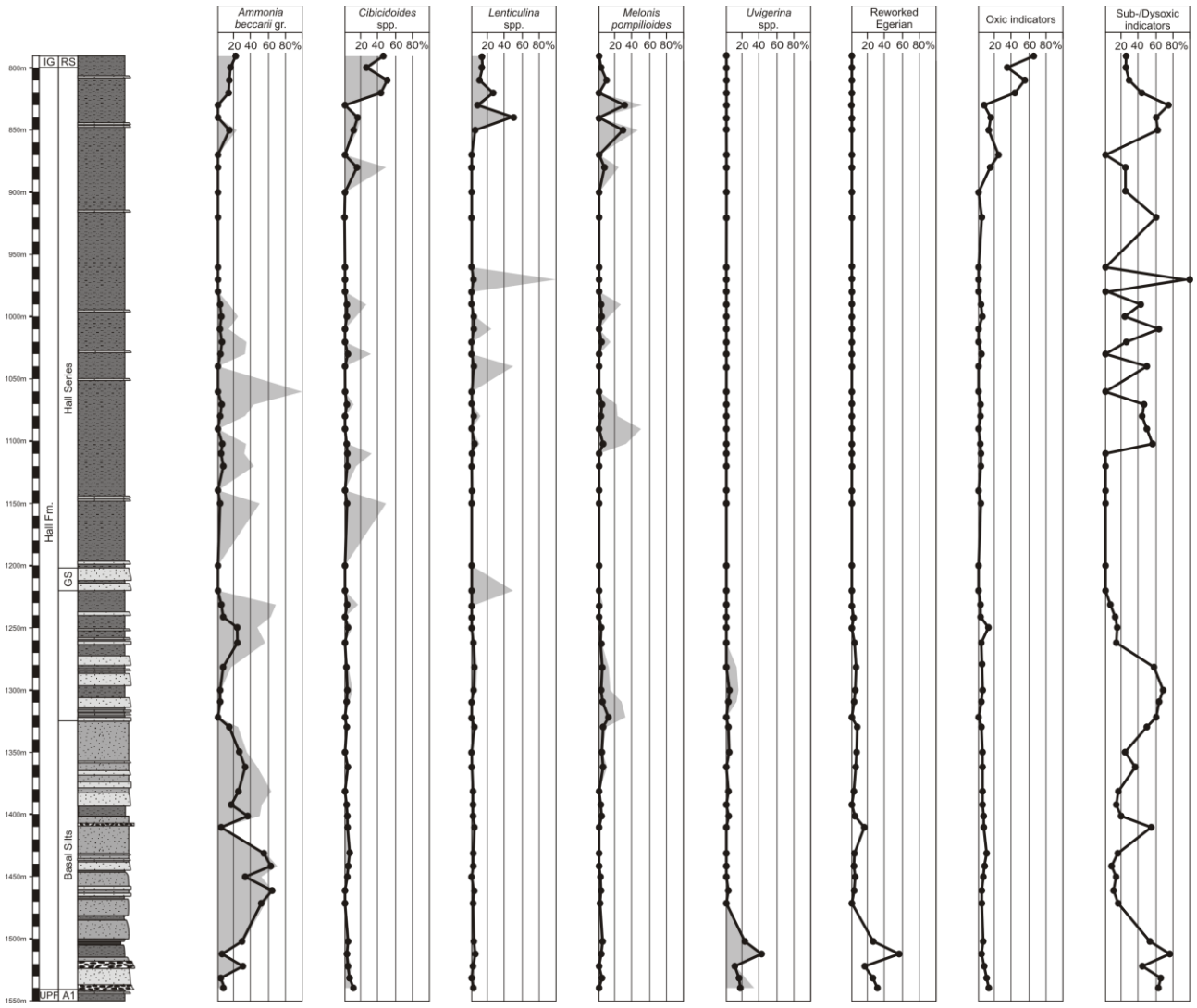

Fig. 3.7. Relative abundances of selected hyaline foraminifers in the Hall Fm. The black line shows the abundance for the whole benthic assemblage, the abundance within hyaline assemblages is indicated in grey. The abundance of reworked foraminiferal tests and index taxa for bottom-water oxygenation refer to the hyaline assemblages.

in abundance between 1120 and 990m. In this interval the abundances of M1 and M3a are inversely correlated (Fig. 3.6). Subsequently, abundance decreases rapidly with an irregular pattern and peaks at 880m, 850m and 830m.

Other agglutinated morphogroups show minor abundances for most parts of the Hall Fm. M2b primarily consists f *Cribrostomoides* spp. and shows elevated abundance in the intervals from 1392 to 1282m and 1120 to 1102m and at 1220m, and 800m depth. M4a is generally rare with increased values from 1442 to 1322m, 1070 to 900m and 1150 to 1110m. M4b is mainly represented by species of *Gaudryinopsis* and shows an overall decreasing trend. Highest abundance occurs between 1540 and 1402m. A second peak occurs between 1242 and 1220m. Abundance subsequently declines with lowest values from 1120 to 990m. The morphogroup vanishes at 920m. Brownish tests of morphogroup M1 are considered reworked (Kender et al., 2005) occurring between 1540 and 1242m with a peak from 1512 to 1502m.

Hyaline taxa show highest abundances in the lower (1540-1250m) and upper (880-800m) parts of the section (Figs. 3.5, 3.7). The samples from the base of the Hall Fm. (1540-1500m) are composed of many suboxic indicators, like the highly abundant *Uvigerina* spp., of which many are reworked Egerian taxa. Subsequent samples up to 1330m are primarily composed of *Ammonia beccarii* gr. and the abundance of oxic and suboxic indicators is low. Assemblages with highly abundant suboxic indicators (e.g., *Melonis pompilioides*, *Lenticulina inornata*) and reworked tests occur from 1322 to 1282m. Increased abundances of *Ammonia beccarii* gr. between 1262 and 1250m herald the interval of very low hyaline abundance between 1242 and 870m. There, hyaline assemblages are characterized by strongly variable abundances of *Ammonia beccarii* gr., *Cibicidoides lopjanicus*, *Lenticulina* spp. and *Melonis pompilioides* and resulting in a very irregular pattern of suboxic indicators. Finally, the hyaline faunas from the top of the Hall Fm. are composed of varying portions of *Ammonia beccarii* gr., *Cibicidoides lopjanicus*, *Heterolepa dutemplei*, *Lenticulina inornata* and *Melonis pompilioides* and show a trend from suboxic towards oxic indicators towards the top.

3.5.2. Benthic foraminiferal assemblages

Cluster analysis and NMDS allow the distinction of eight benthic foraminiferal assemblages (Figs. 3.5, 3.8). Assemblages 1-4 include samples that are dominated by agglutinated forms (A = 89%, σ = 11%) and differences between assemblages mainly occur due to variations in the abundance of morphogroups M1 and M3a.

Assemblage 1 contains samples with equal portions of M1 (A = 27%, σ = 6%) and M3a (A = 27%, σ = 2%) and increased abundances of M2b (A = 16%, σ = 8%).

Assemblage 2 summarizes samples revealing a predominance of M3a (A = 40%, σ = 8%) over M1 (A = 35%, σ = 7%) and slightly increased abundance of M4b (A = 6%, σ = 3%).

Assemblage 3 consists of samples with the highest abundance of M1 of all assemblages (A = 69%, σ = 8%). Morphogroups M3a (A = 5%, σ = 4%), M4a (A = 5%, σ = 4%) and M4b (A = 5%, σ = 5%) show minor and highly variable distribution in the samples.

Assemblage 4 unites samples that show high abundance of M1 (A = 46%, σ = 6%), increased abundance of M4b (A = 14%, σ = 12%) and minor, highly variable occurrences of M2b (A = 8%, σ = 8%) and M3a (A = 5%, σ = 6%).

A predominance of hyaline tests over agglutinated tests (A = 65%, σ = 23%) characterizes assemblages 5-8. Variations between the assemblages are largely caused by varying abundances of *Ammonia beccarii* gr.

Assemblage 5 includes samples with high abundance of *Ammonia beccarii* gr. (A = 32%, σ = 4%) and increased abundance of M1 (A = 10%, σ = 6%). *Uvigerina* spp. (A = 6%, σ = 9%) and reworked agglutinated tests (A = 5%, σ = 3%) show minor abundance.

Assemblage 6 consists of samples dominated by *Ammonia beccarii* gr. (A = 57%, σ = 6%) while no other taxa show significantly increased occurrences.

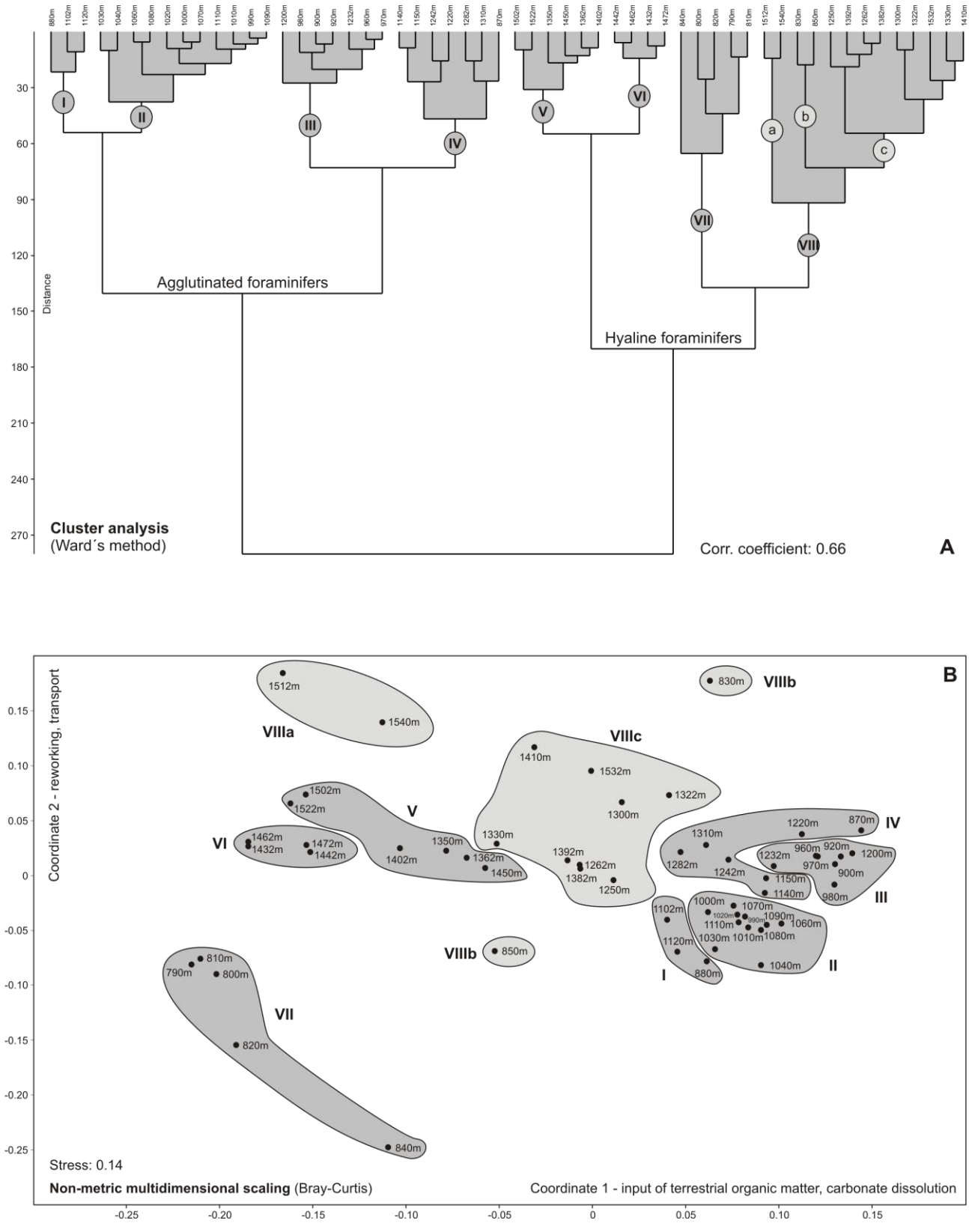

Fig. 3.8. Multivariate statistical analyses of the benthic foraminiferal assemblages. (A) Cluster analysis; (B) Non-metric multidimensional scaling.

Assemblage 7 is characterized by samples with high abundances of *Cibicidoides* spp. (A = 37%, σ = 14%), *Lenticulina inornata* (A = 23%, σ = 17%) and *Ammonia beccarii* gr. (A = 16%, σ = 11%). Agglutinated tests occur very rarely.

Assemblage 8 contains samples with increased abundances of M1 (A = 17%, σ = 11%) and *Ammonia beccarii* gr. (A = 11%, σ = 9%). M4b (A = 7%, σ = 5%), *Melonis pompilioides* (A = 7%, σ = 11%), *Uvigerina* spp. (A = 7%, σ = 14%) and reworked agglutinated taxa (A = 6%, σ = 7%) show minor, strongly varying abundances. NMDS and the high variability within the assemblage suggest that the corresponding cluster is not very robust. Two outliers containing samples from the base (1540m, 1512m) and the top (850m, 830m) of the Hall Fm. suggest an internal subdivision into assemblages 8a-c.

Assemblage 8a inlcudes samples with the highest abundance of *Uvigerina* spp. (A = 36%, σ = 10%). *Ammonia beccarii* gr. (A = 7%, σ = 1%) and *Cibicidoides* spp. (A = 5%, σ = 6%) show minor abundances while agglutinated tests are rare.

Assemblage 8b is composed of samples with the highest abundance of *Melonis pompilioides* (A = 31%, σ = 1%). The agglutinated morphogroups M1 (A = 12%, σ = 5%) and M3a (A = 12%, σ = 5%) show increased abundances, *Ammonia beccarii* gr. (A = 8%, σ = 11%) and *Lenticulina* spp. (A = 6%, σ = 3%) are slightly increased.

Assemblage 8c consists of samples with high abundance of M1 (A = 22%, σ = 9%) and increased occurrences of *Ammonia beccarii* gr. (A = 12%, σ = 10%), M4b (A = 9%, σ = 3%), reworked agglutinated tests (A = 9%, σ = 7%) and M2b (A = 5%, σ = 5%).

The distribution of the assemblages in the Hall Fm. reflects the trends in agglutinated and hyaline tests: the occurrence of the hyaline dominated assemblages 5, 6 and 7 from 1540 to 1330m is followed by the variable abundances of assemblages 3 and 8 between 1322 and 1242m. The latter documents the transition into microfaunas of agglutinated assemblages 1 to 4 that occur from 1232 to 870m. Assemblages 1 and 2 are mainly distributed between 1120 and 990m followed by an interval of assemblage 4 from 980 to 900m. The peak abundance of hyaline taxa is reflected in the abundance of assemblages 7 and 8 at the top of the section.

3.5.3. Geochemistry

Based on the revealed bulk geochemical data, the depth interval between 1540 and 900 m depth is subdivided into three units (Tab. 3.3, Fig. 3.9):

Unit 1 (1540-1390m) is characterized by strongly varying values of TOC (0.23-0.97%), S (0.1-0.8%), TOC/S ratios (1.0-3.3) and HI (16-151 mgHC/gTOC). For samples with low TOC, HI values might be biased by the mineral-matrix effect (Espitalié et al., 1985). Graphs of S_2 (pyrolizable hydrocarbons) versus TOC show that the “true” average HI of organic matter in section 1 is about 160 classifying the organic matter as kerogen type III, derived mainly from landplants (Langford and Blanc-Valleron, 1990).

Unit 2 (1382-1190m) shows TOC values between 0.26 and 0.97% with a subtle increasing trend. The latter is more obvious in the HI values (12-122 mgHC/gTOC). In contrast, sulfur contents (0.1-0.3%) remains rather uniform.

Unit 3 (1160-990m) is characterized by maximum TOC values (up to 1.54%) at its base and a

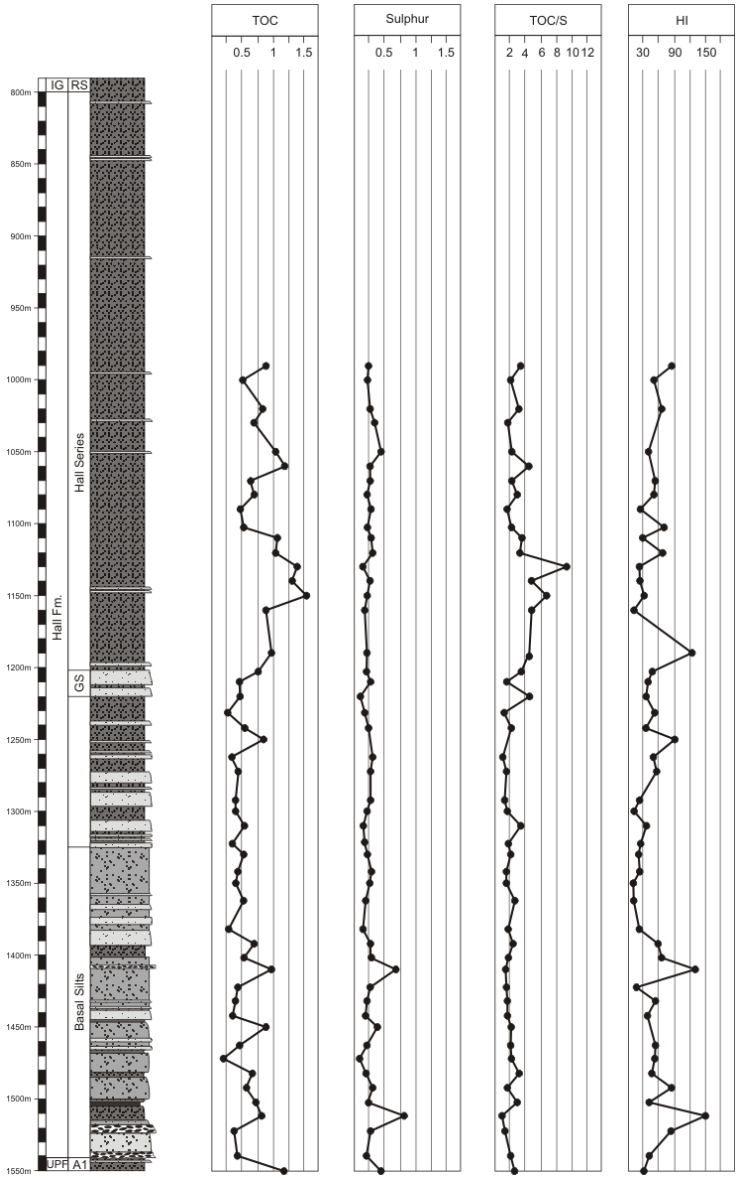

Fig. 3.9. Trends in TOC, sulphur, TOC/S and HI in the Hall Fm.

subsequent decrease in TOC. This trend is contrasted by a parallel increase in HI values increase (13-84 mgHC/gTOC). Sulfur contents shows minor variations (0.15-0.45%), thus TOC/S ratios (1.7-9.3) are controlled by varying TOC values.

3.5.4. Biostratigraphy

The analysed samples from the Hall Formation revealed mostly well-preserved calcareous nannoplankton assemblages that allow a biostratigraphic interpretation (Tab. 3.4; Fig. 3.5). Age determination largely relies on the overall composition of the assemblages due to the absence of the stratigraphically important sphenoliths *S. delphix*, *S. disbelemnos* and *S. belemnos*. An early Burdigalian age is clearly indicated with nannoplankton zones upper NN2 and MNN2b for the basal Hall Fm. based on the continuous occurrence of *Helicosphaera ampliaperta* and rare specimens of *Triquetrorhabdulus* cf. *carinatus* (Fornaciari and Rio, 1996; Lourens et al., 2004). The absence of the latter taxon in the upper part of the Hochburg section (800-1310m, Hall Fm. and Innviertel Group) indicates NN3/MNN3a zone (18.28-17.95Ma). A clear differentiation between upper NN2 and NN3 cannot be drawn.

Benthic foraminiferal assemblages allow a biostratigraphic determination within the framework of the regional stratigraphic concept (Wenger, 1987; Cicha et al., 1998). The occurrences of *Elphidium subtypicum* (FOD 1522m), *E. ortenburgense* (FOD 1442m) and *Lenticulina buergli* (FOD 1040m) suggest a middle-late Eggenburgian age for the interval between 1540 and 850m (Wenger, 1987; Cicha et al., 1998; Rupp and Haunold-Yenke, 2003; Pippèrr and Reichenbacher, 2009). *Uvigerina posthantkeni*, which has also been suggested as an index species for the Eggenburgian, is commonly found at the base of the Hall Fm. In the same interval several index species for the Egerian occur (*Almaena osnabrugensis*, *Bolivina beyrichi beyrichi*, *Bolivina versatilis*,

Fursenkoina halkyardia) and suggest intense reworking. The stratigraphic range of *U. posthantkeni* is under debate as similar occurrences in reworked assemblages of the Hall Fm. and the Innviertel Group have been reported from the study area (Rupp and Haunold-Yenke, 2003). Its stratigraphic value is all the more questionable as Wenger (1987) describes *U. posthantkeni* from Egerian deposits in Bavaria.

An early Ottnangian age is suggested for the uppermost part of the section. The assemblages from 840m and 820 to 800m show strong similarities with the widespread foraminiferal faunas of the lower Ottnangian Innviertel Group (Rupp and Haunold-Yenke, 2003; Rupp et al., 2008; Grunert et al., 2010a). The lower Ottnangian index taxon *Amphicoryna ottnangensis* has not been found (Wenger, 1987).

3.6. Discussion

3.6.1. Depositional environment

While the depositional environment of the PCS is well documented for the basal Hall Fm. (Linzer, 2001; De Ruig, 2003; Hubbard et al., 2005; De Ruig and Hubbard, 2006; Hinsch, 2008; Covault et al., 2009; Hubbard et al., 2009), little is known about the middle and upper parts of the Hall Fm. (Zweigel, 1998; Borowski, 2006; Hinsch, 2008). In the present study the combined records of benthic foraminifers, geochemical proxies and seismic images allow to distinguish six facies types that continuously document paleoenvironmental changes from the base to the top of the Hall Fm.

3.6.1.1. Facies 1: Puchkirchen Channel System (1540-1400m)

Recent studies on the Puchkirchen Basin have documented the Late Oligocene to Early Miocene PCS in great detail (Linzer, 2001; De Ruig, 2003; Hubbard et al., 2005; De Ruig and Hubbard, 2006; Hinsch, 2008; Covault et al., 2009; Hubbard et al., 2009). The basal Hall Fm. represents the youngest and final stage of the meandering, basin-axial channel belt (De Ruig, 2003; Hinsch, 2008; Hubbard et al., 2009). While coarse-grained conglomeratic debris flows and turbidite deposits characterize the channel fill, the overbank deposits consist of fine-grained turbiditic sands (De Ruig, 2003). Two major tributaries of the late PCS have been identified: (1) the Paleo-Inn river entering the basin from the south, and (2) a feeder channel from the Bavarian shelf in the west (Wagner, 1998; Brügel et al., 2003; De Ruig and Hubbard, 2003; Hinsch, 2008).

Seismic images show that the channel was about 4.5km wide in the study area with Hochburg 1 located towards its center (Figs. 3.2, 3.4, 3.10). The interval of channel deposition is situated in the basal 140m of the studied section and reflected in the foraminiferal and geochemical data. The distribution of assemblages 5, 6, 8a and 8c and the strongly irregular geochemical records in this part originate from an alternation of reworked pre-Eggenburgian deposits and Eggenburgian shelf sediments (Figs. 3.5, 3.9).

The data suggest major reworking from the Chattian to lower Aquitanian Upper and Lower

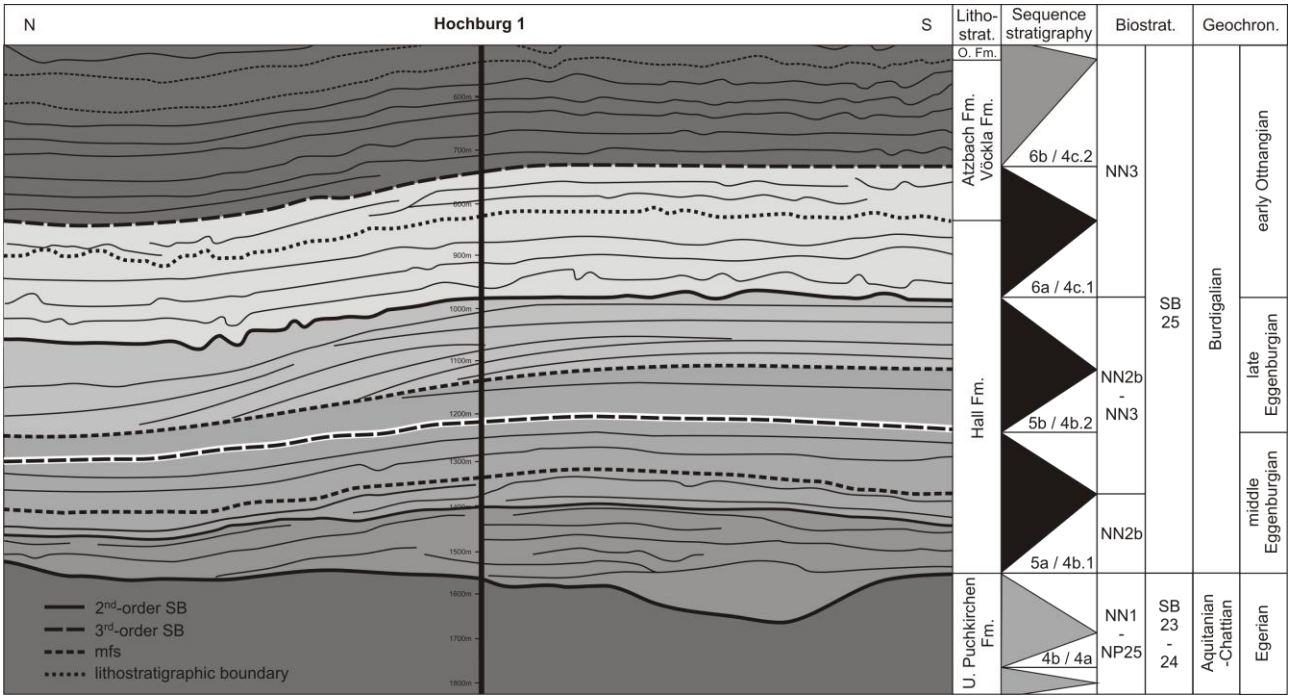

Fig. 3.10. Schematic interpretation of seismic facies along a 4km long N-S directed transect of the seismic line indicated in Fig. 1. Lithostratigraphy is adopted from Papp (1968) and Rupp et al. (2008). Terminology of the identified 3rd-order sequences follows Hinsch (2008) for Upper Austria and Peña (2007) for Bavaria. Biostratigraphy is based on Papp (1960), Rögl et al., (1979), Cicha et al. (1998) and Lourens et al. (2004). See discussion in the text for details on the sequence stratigraphic interpretation.

Puchkirchen fms. for the conglomeratic sands at the base (1540-1490m) and the upper part (1410m) of the channel infill. Foraminiferal assemblages 5 and 8 with astrorhizids, textulariids, buliminds, bolivinids, fursenkoinids and uvigerinids resemble microfossil faunas described from a eutrophic and strongly suboxic paleoenvironment of the organic-rich Upper Puchkirchen and Ebelsberg fms. (Küpper and Steininger, 1975; Wenger, 1987; Cicha et al., 1998; Grunert et al., 2010b). With *Almaena osnabrugensis*, *Bolivina beyrichi beyrichi*, *Bolivina versatilis* and *Fursenkoina halkyardia* the assemblages contain a number of lower and upper Egerian index fossils (Wenger, 1987; Cicha et al., 1998). Strongly varying, and partly high TOC, S and HI values (1512m, 1410m; Fig. 3.9) reflect these episodes of intense reworking. Similar to the foraminiferal assemblages they indicate a eutrophic and suboxic environment characteristic for Aquitanian shales in the basin (Küpper and Steininger, 1975; Cicha et al., 1975; Wagner, 1998; Grunert et al., 2010b). Sediment delivered from the Eggenburgian shelf is mixed with the reworked deposits and indicated by the occurrences of the inner to middle neritic *Ammonia* spp. (Murray, 2006). In contrast, the sandy deposits between 1472 and 1432m and at 1402m are primarily shelf-derived based on the very high abundances of *Ammonia* spp. Low TOC, S and HI values additionally indicate a well-oxygenated shelf environment as a source.

As large parts of the foraminiferal fauna are allochthonous, conditions at the basin floor are mainly inferred from the occurrence of *Bathysiphon filiformis*. This suspension-feeding species is most abundant in eutrophic bathyal areas along the continental shelf where bottom-currents advect

large amounts of nutrients (Gooday et al., 1992, 1997). Together with other extant and fossil species of *Bathysiphon* it has been frequently reported from turbiditic environments and submarine canyons (Miller, 1988, 2005; Koho et al., 2007; De Leo et al., 2010). There they show highest abundances in the upper canyon terraces close to the continental margin during episodes of reduced turbidity currents and minor mass-flow deposition (Koho et al., 2007; De Leo et al., 2010). Episodically increased abundances of *B. filiformis* (1450m, 1410-1402m) might thus reflect phases of benthic recolonization in-between turbidite deposition (Miller, 1988). Its generally low abundance suggests an upper bathyal environment (Jones and Charnock, 1985) that agrees well with estimated water depths of 500m for the coeval turbiditic Lukasedt Fm. (Wagner, 1998).

3.6.1.2. Facies 2: Turbiditic upper bathyal 1 (1392-1330m)

Facies 2 occurs in the upper part of the "Basal Silts" (= Lindach Fm. of Wagner, 1998) in the lower Hall Fm. and contains sandy sediments deposited after the cessation of the PCS. Channel deposition ended when a continuing sea-level rise that flooded the Bavarian shelf cut off the main feeder of the PCS (Hinsch, 2008; Süss et al., 2008). Sedimentation was controlled by turbidites from the southern shelf and slope (Hinsch, 2008).

Turbiditic transport to the basin floor is documented in assemblages 5 and 7c with increased abundances of *Ammonia beccarii* gr. Indicators for reworking are low and mainly consist of brown specimens of *Bathysiphon*. The frequent abundance of *Bathysiphon filiformis* indicates high nutrient flux of shelf-derived organic matter to the sea-floor (Gooday, 1992, 1997; Kaminski et al., 2005; Murray, 2006; Kender et al., 2008). The outer neritic and bathyal morphogroups M1, M2b and M4b suggest an upper bathyal environment (Kaminski and Gradstein, 2005).

Most samples from this interval reveal rather low TOC values and strongly decreased HI values. The very low HI values indicate poor preservation of the organic matter (type IV kerogen; Espitalié et al., 1977). As the very low TOC/S ratios suggest oxygen-depleted conditions, degradation of organic material probably occurred already within the water column. Indications of reworking are limited to the basal part of this interval that is characterized by moderately increased TOC and HI values similar to facies 1.

3.6.1.3. Facies 3: Turbiditic upper bathyal 2 (1322-1250m)

Facies 3 originates from sediments directly above the "Basal Silts" that show an increased portion of silts and clays. Large deltas start to prograde into the basin and a smaller west-east directed deep-water channel ("Gendorf Channel") developed in front of the steep prodelta wedge below the Gendorf Sands (Hinsch, 2008). Common sand packages with internal fining upward cycles reflect episodic turbiditic deposits from the southern slope (Hinsch, 2008; Süss et al., 2008).

The change in sediment input is accompanied by a change in benthic foraminifers. Agglutinated foraminifers dominate for the first time over hyaline forms. Assemblage 3 (which occurs for the

first time) and assemblages 8c suggest an upper bathyal environment with high organic-matter flux based on increased abundances of M1, M2b and M4b (Kaminski and Gradstein, 2005).
TOC values of facies 3 are low and the organic matter is mainly composed of terrestrial-derived organic matter (Espitalié et al., 1977). A subtle increase in HI indicates either improving conditions for organic matter preservation or a slightly increased contribution of autochthonous marine organic material. Low TOC/S ratios suggest continuing oxygen-depleted conditions.
Based on the abundance of *Ammonia beccarii* gr., facies 3 can be subdivided in facies 3a and 3b. In strong contrast to facies 2, *Ammonia beccarii* gr. or other shelf indicators are rare in facies 3a (1322-1300m). Parallel, suboxic hyaline indicators and eutrophic morphogroups M2b and M4b are highly abundant (Kaiho, 1994; Kaminski and Gradstein, 2005). This indicates further deepening and less sediment delivery from the inner and middle shelf. Due to high sea-level sediment gets caught on the shelf and material delivered to the basin floor mainly originates from the slope. Facies 3b (1282-1250m) shows similarities to facies 2 with increased abundance of *A. beccarii* gr. and reduced abundance of suboxic indicators.

3.6.1.4. Facies 4: Eutrophic upper-middle bathyal (1242-1160m, 990-900m)

Facies 4 occurs in two intervals of the middle and upper parts of the Hall Fm. The portion between 1242 and 1160m contains the widespread Gendorf Sands that have been linked to tempestite deposition during a sea-level drop (Strauss, 2008). In this interval, a core is available from 1173 to 1163m that allows detailed insights into the depositional environment (Fig. 3.11). The recovered section consists of alternating clays, silts and sands that are bioturbated (most prominently by echinoid burrows) in many parts. In undisturbed intervals, lenticular and flaser bedding with current ripples in the mm-cm thick sand layers occurs frequently. Reworked mud-clasts are occasionally observed in thick sand packages.
Samples of facies 4 contain foraminiferal assemblages that resemble the Paleogene “flysch-type biofacies” (Kaminski and Gradstein, 2005). This biofacies is dominated by tubular foraminifers of morphogroup M1 and characterizes upper-middle bathyal depositional environments with high sedimentation rates or strong contouritic currents advecting nutrients. High input of organic matter and temporary decreased bottom-water oxygenation are additionally suggested at Hochburg 1 by increased abundances of M1, M2b, M3a, M4a and M4b (van den Akker, 2000; Kaminski et al., 2005). The average TOC/S ratio (3.0) in the interval between 1242 and 1160 supports temporary decreased bottom-water oxygenation (Berner and Raiswell, 1983; Berner, 1984). TOC contents are similar to those in facies 3. Low HI values reflect input of terrestrial organic matter and degradation of marine organic matter due to intense bioturbation (Pratt, 1984).

3.6.1.5. Facies 5: Prograding delta (1150-990m)

Hinsch (2008) describes a NE prograding delta wedge for the upper Hall Fm. that is related to the

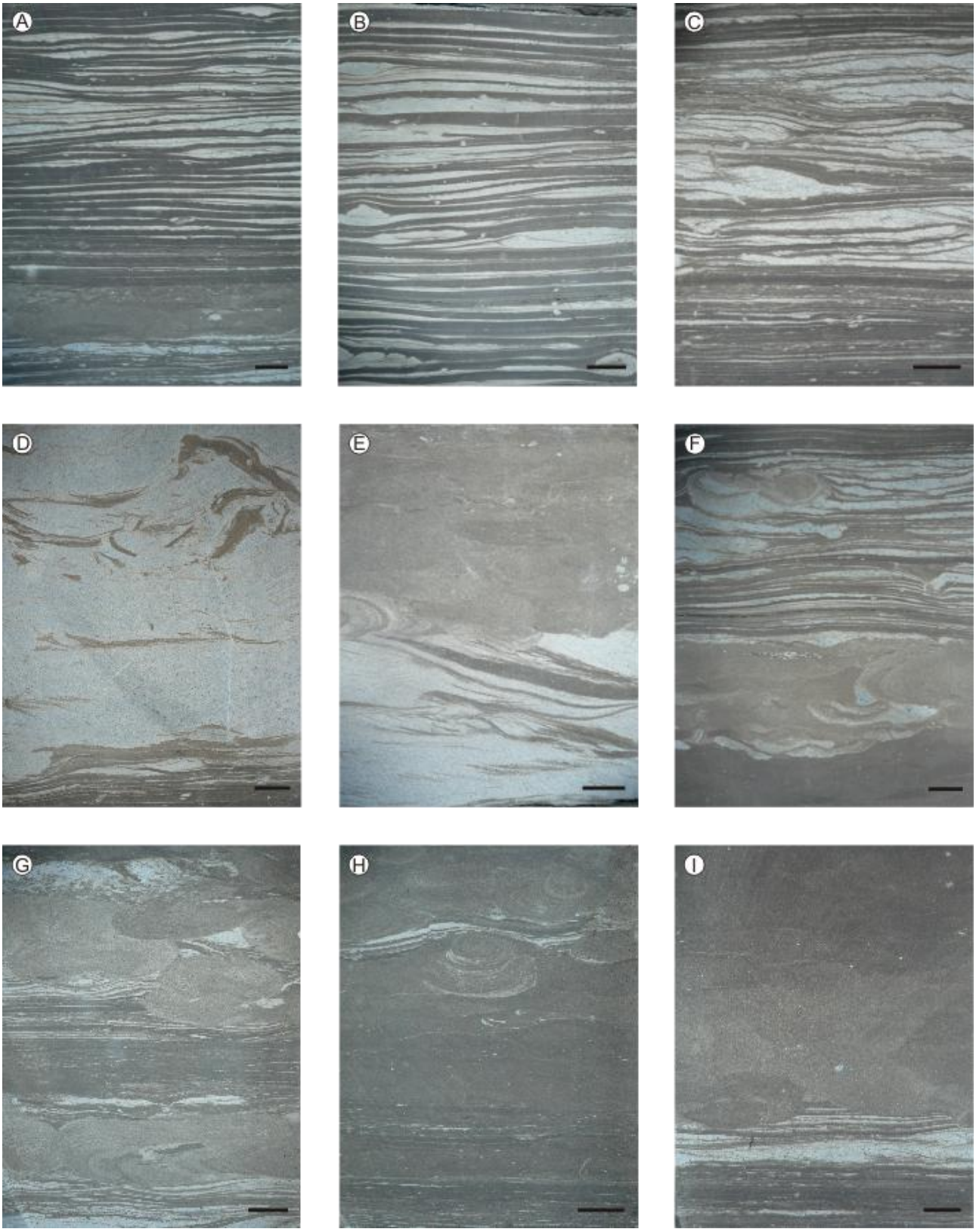

Fig. 3. 11. Representative images of sedimentary structures from the only available core (1173-1163m) out of the Hall Fm. at Hochburg 1. (A-C) Characteristic sandy clays with lenticular and flaser bedding and small-scaled current ripples; (D) reworked mud-clasts in sand matrix; (E-I) bioturbation, mainly cuased by echinoid burrows. Scale bar corresponds to 1cm.

Wachtberg Delta of the Paleo-Salzach river. Generally, the deep-marine trough gets narrowed by the advance of several deltas from the south and north (Zweigel, 1998).

A prodeltaic environment is documented in seismic images as well as in foraminiferal and geochemical proxies. Benthic foraminiferal assemblages are characterized by a nearly absolute dominance of agglutinated foraminifers. Exceptionally high abundances of agglutinated foraminifers have been previously observed in delta fan environments with high sedimentation rates and strong terrestrial input (e.g., Kaminski et al., 1988; Jones, 1999; Kender et al., 2005; Jones, 2006; Kender et al., 2008). Epifaunal, vagile species of morphogroups M2b, M3a and M4a living on the flocculent bottom surface layer together with infaunal morphogroup M4b are all adapted to high organic matter flux and show high abundances in this part of the section (Kaminski et al., 1988; Nagy, 1992; Kaminski et al., 2005). *Bathysiphon filiformis* shows diminished abundances compared to facies 4. Although its occurrence reflects the high organic matter input, *B. filiformis* might have had more difficulties to adapt to the high sedimentation rates than more opportunistic forms like *Ammodiscus* (Bąk, 2000). The strong correlation between high TOC and TOC/S ratios together with low HI values further suggest high input of terrestrial organic matter. Previous studies show that TOC/S ratios >2.8 result from major input of refractory terrestrial organic matter that cannot be metabolized efficiently by sulphate-reducing bacteria (Berner and Raiswell, 1983; Berner, 1984).

The large bathymetric range of morphogroups M3a and M2b and the lowered abundances of M1 suggest a shallowing of the depositional environment towards outer neritic-upper bathyal water depths (Jones and Charnok, 1985; van der Akker et al., 2000). The shallowing trend is most evident in the high abundance of small-sized (<0.25mm) tests of *Ammodiscus* spp. Previous studies indicate that the test-size of ammodiscids correlates with water depth: while large-sized species are mainly described from deep-water settings (e.g., Hart, 1988; Cicha et al., 1998; Govindan, 2004; Kaminski and Gradstein, 2005; Kaminski et al., 2005; Filipescu and Kaminski, 2008), small-sized species seem to occur preferably in delta-influenced shelf settings and even restricted lagoonal environments (e.g., Alve and Nagy, 1984; Nagy and Johanson, 1991; Nagy and Berge, 2008; Nagy et al., 2010).

Upward decreasing TOC values reflect increasing dilution of organic matter by detrital minerals shed by the prograding delta. At the same time, increasing HI values show better preservation of organic matter, probably the combined effect of shorter travel times of organic matter within the shallower water column and more rapid coverage.

3.6.1.6. Facies 6: Outer-middle neritic (850-790m)

The final upfill of the Puchkirchen Basin is documented for the uppermost part of the Hall Fm. (Hinsch, 2008). The development begins with mixed agglutinated and hyaline faunas of assemblage 8b that indicate the transition from the upper bathyal facies 4 into a eutrophic and

suboxic outer neritic environment (Kaiho, 1994; Murray, 2006). The hyaline foraminiferal assemblages with *Ammonia beccarii* gr., *Cibicidoides lopjanicus*, *Lenticulina inornata* and *Melonis pompilioides* from the top of the Hall Fm. resemble the characteristic widespread neritic fauna of the early Ottnangian (e.g., Wenger, 1987; Rupp and Haunold-Yenke, 2003; Pippèrr, 2011). Towards the top, increasing abundances of *Cibicidoides lopjanicus* and *Ammonia beccarii* gr. and a parallel decrease in suboxic indicators suggest a further shallowing towards a well-oxygenated middle neritic environment as described from the superimposed Vöckla Fm. (Faupl and Roetzel, 1987; Krenmayr, 1991; Rupp and Haunold-Yenke, 2003; Rupp and van Husen, 2007; Rupp et al., 2008).

3.6.2. Sequence stratigraphic implications

The facies development of the Hall Fm. in Hochburg 1 together with data from seismic lines crossing Hochburg 1 (Figs. 3.4, 3.10) allow a sequence stratigraphic interpretation that can be compared to the sequence stratigraphic framework for the Puchkirchen Basin (Jin et al., 1995; Zweigel, 1998; Peña, 2007; Hinsch, 2008). Thus the results of Hochburg 1 provide valuable information on the depositional environment and age control that these models derived from seismic surveys lack.

3.6.2.1. Sequence boundaries and systems tracts

Based on a review of sedimentological and seismic data from internal studies by RAG (Borowski, 2006; Strauss, 2008; Süss et al., 2008), Hinsch (2008) proposed a sequence stratigraphic interpretation for the Puchkirchen Basin that includes the 2nd-order sequence SQ 5 comprising the Hall Fm. except its uppermost part. In this model, the lowstand (LST) and transgressive systems tracts (TST) of SQ 5 correspond to the terminal PCS of the basal Hall Fm. The channel shut down as the Bavarian shelf was flooded during the transgression and sediment distribution during the subsequent highstand systems tract (HST) was primarily controlled by deltas prograding from the SW (Brügel et al., 2003; Hinsch, 2008). Turbiditic, tempestitic, tidal, marine and fluvio-marine lithofacies have been described for the HST that document the upfill of the Puchkirchen Basin (Borowski, 2006; Hinsch, 2008).

SQ 5 can be clearly identified at Hochburg 1 between 1540 and 990m. The initial LST deposits are represented by the intensively reworked sediments of facies 1. The drowning of the PCS during subsequent transgression is documented in the deepening bathyal environment of facies 2 to 4. The prograding delta of the Paleo-Salzach river and increasing sedimentation rates during the late HST are particularly well documented in facies 5 from 1150-990m. The maximum flooding surface (mfs) is indicated between 1330 and 1300m. Positioned above the coarse grained basal Hall Fm. and below the onset of the HST this interval is characterized by facies 3a with the absence of *Ammonia beccarii* gr. In contrast, the mfs of SQ 5 has been suggested by Strauss (2008) directly on top of the channel fill based on fish shales found at the borehole Weizberg, c. 2km SE of Hochburg 1. This

horizon is expressed as a thin condensed section with high gamma-ray values in the logs. Log and seismic correlations suggest that this horizon is located between 1400 and 1390m at Hochburg 1. In this interval with increased TOC (up to 0.97%) and HI (up to 134 mgHC/gTOC) values, elevated abundances of M1 and M4b indicate high nutrient-flux and suboxic conditions. The fish shales from Weizberg are not the only record of such deposits from the Eggenburgian. Belead (2007) investigated fish shales within the basal units of the Hall Fm. about c. 30km east of Hochburg 1. The reported TOC values up to 3.5% and HI values up to 280 mgHC/gTOC are similar to those found in the widespread Egerian fish shales and strongly suggest reworking from the Egerian.

Within SQ 5, two 3rd-order sequences have been interpreted from the seismic images that will be named SQ 5a and SQ 5b herein (Hinsch, 2008; Strauss, 2008). They are separated by the Gendorf Sands that are interpreted as tempestitic LST deposits of SQ 5b (Strauss, 2008). More details on the internal subdivision of SQ 5 are available from Bavaria. Based on extensive well-log and seismic data from hydrocarbon exploration Jin et al. (1995), Zweigel (1998) and Penã (2007) suggested one 2nd-order sequence SQ 4 comprising the Eggenburgian and early-middle Ottnangian sediments (= "Upper Marine Molasse") in the Bavarian NAFB. SQ 4 can further be subdivided into several 3rd-order sequences. In this paper, we follow the terminology of the most recent approach by Peña (2007). SQ 4a ("Aquitanian Fish Shales") is excluded from the analysis as it is considered to correspond to the widespread Egerian fish shales (Fig. 3.3). Instead, 3rd-order sequence SQ 4b.1 is regarded as the base of the Eggenburgian deposits and corresponding to SQ 5a in Upper Austria. Marine deposits of the Obing Beds are restricted to the area of the Puchkirchen Basin in the SE and heavily affected by turbiditic sedimentation (Peña, 2007). SQ 4b.2 correponds to SQ 5b and begins with a transgression to the NW. The HST is characterized by delta progradation from the NW and SW (Zweigel, 1998; Peña, 2007).

Inferred from Hinsch (2008) SQ 5a reaches from 1540 to 1222m and SQ 5b from 1222 to 990m at Hochburg 1. Similar to Bavaria SQ 5a is characterized by strong turbiditic deposition and the assemblages show a mixture of agglutinated and calcareous foraminiferal tests. SQ 5b is more clayey and contains almost exclusively agglutinated tests that reflect high sedimentation rates and deltaic influence. However, it is hard to distinguish the two sequences in the bathyal setting suggested for Hochburg 1 and future paleoenvironmental studies will have to focus on the northern shelf and western shelf areas to describe the sequence boundary in greater detail.

The uppermost Hall Fm. and the Innviertel Group have not been included in the sequence stratigraphic evaluation of Hinsch (2008). In Bavaria, 3rd-order sequence SQ 4c and several potential higher-order sequences have been described from upper Eggenburgian to middle Ottnangian deposits (Jin et al., 1995; Peña, 2007; Pippèrr and Reichenbacher, 2010; Pippèrr, 2011). Along the Bavarian shelf, the transgression begins with the lower Ottnangian Untersimbach Beds culminating in the Neuhofen Beds that represent the mfs and HST deposits (Wenger, 1987; Pippèrr and Reichenbacher, 2010; Pippèrr, 2011). Towards the basin center, the Neuhofen Beds directly overlie the Eggenburgian strata that are often characterized by accumulations of *L. buergli*

(Wenger, 1987; Peña, 2007). At Hochburg 1 a similar pattern can be observed within the Hall Fm.: bathyal facies 4 follows directly above the deltaic facies 6 with *L. buergli* and indicates a correlation of the uppermost Hall Fm. and the lower Innviertel Group to SQ 4c in Bavaria. In continuation of Hinsch (2008) the 3rd-order sequence is termed SQ 6 for Austrian study area. Similar to 4th-order sequences SQ 4c.1 and 4c.2 in Bavaria, a further subdivision of SQ 6 into two higher order sequences is indicated by the succession of the marly upper most Hall and Vöckla Fms., sandy Atzbach Fm. and marly Ottnang Fm. in Upper Austria (Peña, 2007; Rupp and van Husen, 2007; Rupp et al., 2008). Consequently, facies 4 and 6 represent TST and HST deposits of SQ 6a.

3.6.2.2. Correlation to global sequence stratigraphy

Paratethyan stratigraphy does not follow the GSSP concept of Hedberg (1976). As a result, the regional stages are defined by holostratotypes that represent a characteristic depositional environment of the particular stage and do not document the stage boundary (Piller et al., 2007). The occurrence of many endemic marker species additionally complicates a correlation to the global stratigraphic record. To overcome these problems Piller et al. (2007) proposed an updated age model for the Central Paratethys based on a correlation of the regional stages to global 3rd-order sequence stratigraphy. For the Puchkirchen Basin, eustatic sea-level has been discussed as the primary agent generating the internal lower Burdigalian sequence boundaries (Zweigel, 1998; Genser, 2007). This is in strong contrast to the situation during Oligocene and early Aquitanian times when the advance of the Alpine thrust front resulted in a complex interplay of tectonics, sedimentary input and eustasy that formed the sequences (Zweigel, 1998; Genser et al., 2007; Hinsch, 2008). For the early Burdigalian, the authors suggest that the basin remained underfilled when thrusting in the eastern Alps ceased followed by viscoelastic relaxation. A minor increase in subsidence during the Ottnangian is related to increased sedimentary input as the topography of the rising Alpine mountains changes (Genser, 2007; Kuhlemann, 2007). Consequently, the new data from bio- and sequence stratigraphy allow to calibrate the Hall Fm. and coeval deposits from Bavaria to the age model of Piller et al. (2007) and to global stratigraphy.

The herein suggested Burdigalian age for the Hall Fm. corresponds well with previous reports by Papp (1960, 1975) who described *Miogypsina intermedia* from the lower part of the Hall Fm. indicating Shallow Benthic Zone 25 (Cahuzac and Poignant, 1997; Lourens et al., 2004). Additional support for a correlation to the Burdigalian comes from macro- and microfossil studies by Aberer and Braumüller (1949) and Aberer (1958). Internal reports of RAG from other drill sites in Upper Austria and Salzburg also confirm upper NN2 for the base of the Hall Fm. As a consequence the beginning of the Hall Fm. and the reactivation of the PCS can be linked to 3rd-order sequence Bur 1 and a major sea-level rise at the base of the Burdigalian that is observed in records from all over the world (Wenger, 1987; Haq, 1988; Abreu and Haddad, 1998; Haq and Al-Quahtani, 2005; Miller et al., 2005; Kominz et al., 2008). Outside the Puchkirchen Basin this transgression that initiated the Burdigalian Seaway is well documented from the Bohemian Massif (Holcová, 2002; Mandic and

Steininger, 2003) and the “Upper Marine Molasse” deposits in Switzerland (Schlunegger et al., 1997).

Reports of nannoplankton zones NN1 and lowermost NN2a for the Upper Puchkirchen Fm. (Rögl et al., 1979) and generally rare occurrences of lower Eggenburgian marine deposits in the study area (Wenger, 1987) indicate a correlation of the erosional hiatus between the Upper Puchkirchen Fm. and the Hall Fm. with 3rd-order sequence Aq 2 (Fig. 3.3; Abreu and Haddad, 1998; Piller et al., 2007).

Biostratigraphy indicates a correlation of SQ 5a and 5b to the middle and upper Eggenburgian, respectively (Wenger, 1987; Pippèrr and Reichenbacher, 2009). Nannoplankton zones upper NN2-NN3 suggest a correspondence of sequence boundary 5b to the global 3rd-order sequence Bur 2 (Rögl et al., 1979; Piller et al., 2007).

The base of SQ 6 can be reliably correlated to 3rd-order sequence Bur 3 based on its lower Ottnangian age and nannoplankton zone NN3 (Rögl et al., 1979; Abreu and Haddad, 1998; Piller et al., 2007). As a consequence, the base of the Ottnangian stage in Upper Austria does not correspond to the base of the Innviertel Group as commonly assumed but is instead located in the uppermost Hall Fm. A similar discrepancy between the lithostratigraphic and chronostratigraphic base of the Ottnangian has been observed by Piller et al. (2007) in the Zogelsdorf Fm. from the Bohemian Massif.

3.7. Conclusions

The results of the present study contribute to ongoing research in order to improve hydrocarbon exploration in the Puchkirchen Basin. Based on benthic foraminiferal assemblages and geochemical proxy records, the herein revealed facies development and biostratigraphic constraints of the pelitic Hall Fm. allow new insights into the early Burdigalian history of the Puchkirchen Basin.

Following the widespread erosion of lower Eggenburgian deposits, a rise in eustatic sea-level during the earliest Burdigalian reactivated the Puchkirchen Channel System. For the corresponding conglomeratic sands at the base of the section, intense reworking of Chattian and Aquitanian sediments is suggested by contain reworked foraminiferal assemblages and strongly varying geochemical records. The channel finally gets cut off from its sediment sources on the shelf in the course of the transgression and a deepening bathyal environment with frequent deposition of turbidites from the southern slope establishes. The revealed agglutinated flysch-type foraminiferal assemblages with large amounts of *Bathysiphon filiformis* are adapted to this unstable environment. Subsequently, a NE prograding delta initiates the sedimentary upfill of the Puchkirchen Basin. High sedimentation rates and increased input of terrestrial-derived organic matter are indicated by the frequent occurrences of *Ammodiscus* and other opportunistic agglutinating foraminifers. A eutrophic and suboxic bathyal environment is re-established during a last major transgression followed by the development of an oxic outer-middle neritic shelf

environment.

The herein presented evidence strongly supports previous studies that suggested a primary control of eustatic sea-level on the Puchkirchen Basin rather than Alpine tectonics during the Burdigalian. The integration of the revealed facies development with available sequence stratigraphic models for the Puchkirchen Basin allows the identification of three 3rd-order sequences and their corresponding systems tracts in the lower, middle and upper Hall Fm. Assemblages of calcareous nannoplankton and benthic foraminifers suggest that they correspond to the regional stages of the middle and upper Eggenburgian and lower Ottnangian and to global 3rd-order sequences Bur 1-3.

3.8. Acknowledgements

The authors would like to thank Ulrich Bieg (RAG), Katarina Borowski (RAG), Steven Hubbard (University of Calgary), Sylvain Richoz (University of Graz) and Fred Rögl (Natural History Museum Vienna) for many helpful comments and discussions. Claudia Puschenjak (University of Graz) and Doris Reischenbacher (University of Leoben) are thanked for performing geochemical measurements, Stefan Pfingstl (University of Graz) for assistance with preparation of the microfossil samples. Wolfgang Mitterlehner (RAG) is thanked for providing access to the core material facility in Pettenbach. This study was financially supported by the Commission for the Paleontological and Stratigraphical Research of Austria (Austrian Academy of Sciences) and Rohöl-Aufsuchungs AG.

3.9. References

Abreu, V.S., Haddad, G.A., 1998. Glacioeustatic fluctuations: the mechanism linking stable isotope events and sequence stratigraphy from the Early Oligocene to Middle Miocene. In: Graciansky, C.-P., Hardenbol, J., Jacquin, T., Vail, P.R. (Eds.), Mesozoic and Cenozoic sequence stratigraphy of European basins. Sedimentary Geology Special Publication, vol. 60. Society for Sedimentary Geology, Tulsa, pp. 245–260.

Aberer, F., 1958. Die Molassezone im westlichen Oberösterreich und in Salzburg. Mitteilungen der Geologischen Gesellschaft in Wien 50, 23–93.

Aberer, F., 1959. Das Miozän der westlichen Molassezone Österreichs mit besonderer Berücksichtigung der Untergrenze und seiner Gliederung. Mitteilungen der Geologischen Gesellschaft in Wien 52, 7–16.

Aberer, F., Braumüller, E., 1949. Die miozäne Molasse am Alpennordrand im Oichten- und Mattigtal nördlich Salzburg. Jahrbuch der Geologischen Bundesanstalt 92, 129–145.

Alve, E., Nagy, J., 1986. Estuarine foraminiferal distribution in Sandebukta, a branch of the Olso fjord. Journal of Foraminiferal Research, 16(4): 261-284.

Bąk, K., 2000. Biostratigraphy of deep-water agglutinated foraminifera in Scaglia Rossa-type deposits of the Pieniny Klippen Belt, Carpathians, Poland. Grzybowski Foundation Special Publication 7, 15–41.

Belead, S.A., 2007. Charakterisierung potentieller Muttergesteine für biogenes Erdgas in der österreichischen Molassezone. Diploma Thesis, Technical University Clausthal, Germany, 98 pp.

Berner, R.A., 1984. Sedimentary pyrite formation: An update. Geochimica et Cosmochimica Acta 48, 605–615.

Berner, R.A., Raiswell, R., 1984. C/S method for distinguishing freshwater from marine sedimentary rocks. Geology 12, 365–368.

Borowski, K., 2006. Lithofacies and depositional environment of the Upper Hall Formation, Alpine Molasse basin, Upper Austria. Diploma Thesis, Technical University Bergakademie Freiberg, Germany. 175 pages.

Braumüller, E., 1959. Der Südrand der Molassezone im Raume von Bad Hall (The Southern Rim of the Molasse Zone in the Bad Hall Area). Erdoel-Zeitschrift 75, 122–130.

Brügel, A., Dunkl, I., Frisch, W., Kuhlemann, J., Balogh, K., 2003. Geochemistry and Geochronology of Gneiss Pebbles from Foreland Molasse Conglomerates: Geodynamic and Paleogeographic Implications for the Oligo-Miocene Evolution of the Eastern Alps. The Journal of Geology 111, 543–563.

Bürgl, H., 1949. Zur Stratigraphie und Tektonik des oberösterreichischen Schliers. Verhandlungen der Geologischen Bundesanstalt 1946, 123–151.

Cahuzac, B., Poignant, A., 1997. Essai de biozonation de l'Oligo-Miocène dans les bassins Européens à l'aide des grands foraminifers néritiques. Bulletin Societe géologique de France 168, 155–169.

Cicha, I., Čtyroká, J., Horváth, M., 1975. Foraminiferen des Egerien. In: Baldí, T., Seneš, J. (Eds.), OM – Egerien. Die Egerer, Pouzdraner, Puchkirchener Schichtengruppe und die Bretkaer Formation. Chronostratigraphie und Neostratotypen, Miozän der Zentralen Paratethys, vol. 5. Verlag der Slowakischen Akademie der Wissenschaften, 233–277.

Cicha, I., Rögl, F., Rupp, C., Ctyroká, J., 1998. Oligocene-Miocene foraminifers of the Central Paratethys. Abhandlungen der Senckenbergischen Naturforschenden Gesellschaft 549, 1–325.

Covault, J.A., Hubbard, S.M., Graham, S.A., Hinsch, R., Linzer, H.-G., 2009. Turbidite-reservoir architecture in complex foredeep-margin and wedge-top depocenters, Tertiary Molasse freoland basin system, Austria. Marine and Petroleum Geology 26, 379–396.

De Leo, F.C., Smith, C.R., Rowden, A.A., Bowden, D.A., Clark, M.R., 2010. Submarine canyons: hotspots of benthic biomass and productivity in the deep sea. Proceedings of the Royal Society B 277, 2783–2792.

De Ruig, M.J., 2003. Deep Marine Sedimentation and Gas Reservoir Distribution in Upper Austria. Oil Gas European Magazine 29, 64–73.

De Ruig, M.J., Hubbard, S.M., 2006. Seismic facies and reservoir characteristics of a deep marine axial channel belt in the Molasse Basin, Puchkirchen Formation, Upper Austria. AAPG Bulletin 90, 735–752.

Espitalié, J., Laporte, J.L., Madec, M., Marquis, F., Leplat, P., Paulet, J., Boutefeu, A., 1977. Méthode rapide de caractérisation des roches mères, de leur potentiel pétrolier et de leur degré d´évolution. Revue de l´ Institut Français du Pérole 32, 23–42.

Espitalié, J., Senga Makadi, K., Trichet, J., 1985. Role of the mineral matrix during kerogen pyrolysis. Organic Geochemistry 6, 365–382.

Faupl, P., Roetzel, R., 1987. Gezeitenbeeinflußte Ablagerungen der Innviertler Gruppe (Ottnangien) in der oberösterreichischen Molassezone. Jahrbuch der Geologischen Bundesanstalt 130, 415–447.

Filipescu, S., Kaminski, M.A., 2008. Paleocene deep-water agglutinated foraminifera in the Transylvanian Basin. In: Kaminski, M. A., Coccioni, R., Marsili, A. (Eds.), Proceedings of the Seventh International Workshop on Agglutinated Foraminifera. Grzybowski Foundation Special Publication, 25–30.

Fornaciari, E., Rio, D., 1996. Latest Oligocene to early middle Miocene quantitative calcareous nannofossil biostratigraphy in the Mediterranean region. Micropaleontology 42, 1–36.

Genser, J., Cloetingh, S.A.P.L., Neubauer, F., 2007. Late orogenic rebound and oblique Alpine convergence: New constraints from subsidence analysis of the Austrian Molasse Basin. Global and Planetary Change 58, 214–223.

Gooday, A.J., Levin, L.A., Thomas, C.L., Hecker, B., 1992. The distribution and ecology of *Bathysiphon filiformis* Sars and *B. major* (protista, foraminiferida) on the continental slope off North Carolina. Journal of Foraminiferal Research 22, 129–146.

Gooday, A.J., Shires, R., Jones, A.R., 1997. Large, deep-sea agglutinated Foraminifera; two differing kinds of organization and their possible ecological significance. Journal of Foraminiferal Research 27, 278–291.

Govindan, A., 2004. Miocene deep water agglutinated foraminifera from offshore Krishna-Godavari Basin, India. Micropaleontology 50, 213-252.

Grunert, P., 2009. Rise and fall of an ancient sea. Initial results from an integrated study on the Central Paratethys. Erstausgabe 2, 157–167.

Grunert, P., Soliman, A., Ćorić, S., Scholger, R., Harzhauser, M., Piller, W. E., 2010a. Stratigraphic re-evaluation of the stratotype for the regional Ottnangian stage (Central Paratethys, middle Burdigalian). Newsletters on Stratigraphy 44, 1–16.

Grunert, P., Harzhauser, M., Rögl, F., Sachsenhofer, R., Gratzer, R., Soliman, A., Piller, W.E., 2010b. Oceanographic conditions as a trigger for the formation of an Early Miocene (Aquitanian) *Konservat-Lagerstätte* in the Central Paratetyhs Sea. Palaeogeography, Palaeoclimatology, Palaeoecology 292, 425–442.

Grunert, P., Soliman, A., Harzhauser, M., Müllegger, S., Piller, W. E., Roetzel, R., Rögl, F., 2010c. Upwelling conditions in the Early Miocene Central Paratethys sea. Geologica Carpathica 61, 129–145.

Hammer, Ø., Harper, D.A.T., Ryan, P.D., 2001. PAST: paleontological statistics software package for education and data analysis. Palaeontologia Electronica 4, 1–9.

Haq, B.U., Hardenbol, J., Vail, P.R., 1988. Mesozoic and Cenozoic chronostratigraphy and cycles of sea-level change. Society of Economic Paleontologists and Mineralogists 42, 71–108.

Haq, B.U., Al-Qahtani, A.M., 2005. Phanerozoic cycles of sea-level change on the Arabian Platform. GeoArabia 10, 127 – 160.

Hart, M.B., 1988. Early Miocene Agglutinated Foraminifera from the Bermuda Abyssal Plain: DSDP Site 603 (NW Atlantic Ocean). Abhandlungen der Geologischen Bundesanstalt 41, 121–131.

Hedberg, H.D., 1976. International Stratigraphic Guide. John Wiley and Sons, New York.

Hinsch, R., 2008. New Insights into the Oligocene to Miocene Geological Evolution of the Molasse Basin of Austria. Oil Gas European Magazine 34, 138–143.

Holcová, K., 2002. Calcareous nannoplankton from the Eggenburgian stratotype and faciostratotypes (Lower Miocene, Central Paratethys). Geologica Carpathica 53, 381–390.

Hubbard, S.M., de Ruig, M.J., Graham, S.A., 2005. Utilizing outcrop analogs to improve subsurface mapping of natural gas-bearing strata in the Puchkirchen Formation, Molasse Basin, Upper Austria. Austrian Journal of Earth Sciences 98, 52–66.

Hubbard, S.M., de Ruig, M.J., Graham, S.A., 2009. Confined channel-levee complex development in an elongate depo-center: Deep-water Tertiary strata of the Austria Molasse basin. Marine and Petroleum Geology 26, 85–112.

Jin, J., Aigner, T., Luterbacher, H.P., Bachmann, G.H., Müller, M., 1995. Sequence stratigraphy and depositional history of the south-eastern German Molasse Basin. Marine and Petroleum Geology 12, 929–940.

Jones, R.W., 1999. Fortis Field (North Sea) revisited: a demonstration of the value of historical micropaleontological data. In: Jones, R.W., Simmons, M.D. (Eds.), Biostratigraphy in production and development geology. Geological Society Special Publication 152, London, 185–200.

Jones, R.W., 2006. Applied Palaeontology. Cambridge University Press, Cambridge.

Jones, R.W., Charnock, M.A., 1985. "Morphogroups" of agglutinating foraminifera. Their life positions and feeding habitats and potential applicability in (paleo)ecological studies. Revue de Paleobiologie 4, 311–320.

Kaiho, K, 1994. Benthic foraminiferal dissolved-oxygen index and dissolved-oxygen levels in the modern ocean. Geology 22, 719–722.

Kaminski, M.A., Gradstein, F.M., 2005. Atlas of Paleogene cosmopolitan deep-water agglutinated foraminifera. London Grzybowski Foundation. Special Publication 10. 547 pages.

Kaminski, M.A., Gradstein, F.M., Berggren, W.A., Geroch, S., Beckmann, J.P., 1988. Flysch-type agglutinated foraminiferal assemblages from Trinidad: taxonomy, stratigraphy and paleobathymetry. Abhandlungen der Geologischen Bundesanstalt 41, 155–228.

Kaminski, M.A., Silye, L., Kender, S., 2005. Miocene deep-water agglutinated foraminifera from ODP hole 909c: Implications from the paleoceanography of the Fram Strait Area, Greenland Sea. Micropaleontology 51, 373–403.

Kender, S., Kaminski, M.A., Cieszkowski, M., 2005. Foraminifera from the Eocene Variegated Shales near Barwinek (Magura Unit, Outer Carpathians), the type locality of Noth (1912) revisited. Annales Societatis Geologorum Poloniae 75, 249–272.

Kender, S., Kaminski, M.A., Jones, R.W., 2008. Early to middle Miocene foraminifera from the deep-sea Congo Fan, offshore Angola. Micropaleontology 54, 477–568.

Koho, K.A., Kouwenhoven, T.J., de Stigter, H.C., van der Zwaan, G.J., 2007. Benthic foraminifera in the Nazaré Canyon, Portuguese continental margin: Sedimentary environments and disturbance. Marine Micropaleontology 66, 27–51.

Kominz, M.A., Browning, J.V., Miller, K.G., Sugarman, P.J., Mizintseva, S., Scotese, C.R., 2008. Late

Cretaceous to Miocene sea-level estimates from the New Jersey and Delaware coastal plain coreholes: an error analysis. Basin Research 20, 211–226.

Krenmayr, H.-G., 1991. Sedimentologische Untersuchungen der Vöcklaschichten (Innviertler Gruppe, Ottnangien) in der oberösterreichischen Molassezone im Gebiet der Vöckla und der Ager. Jahrbuch der Geologischen Bundesanstalt 134, 83–100.

Kuhlemann, J., 2007. Paleogeographic and paleotopographic evolution of the Swiss and Eastern Alps since the Oligocene. Global and Planetary Change 58, 224–236.

Kuhlemann, J., Kempf, O., 2002. Post-Eocene evolution of the North Alpine Foreland Basin and its response to Alpine tectonics. Sedimentary Geology 152, 45–78.

Küpper, I., Steininger, F., 1975. Faziostratotypen der Puchkirchener Schichtengruppe. In: Baldí, T., Seneš, J. (Eds.), OM – Egerien. Die Egerer, Pouzdraner, Puchkirchener Schichtengruppe und die Bretkaer Formation. Chronostratigraphie und Neostratotypen, Miozän der Zentralen Paratethys, vol. 5. Verlag der Slowakischen Akademie der Wissenschaften, 205–220.

Langford, F.F., Blanc-Valleron, M.-M., 1990. Interpreting Rock-Eval Pyrolysis Data Using Graphs of Pyrolizable Hydrocarbons vs. Total Organic Carbon. AAPG Bulletin 74, 799–804.

Linzer, H.-G., 2001. Cyclic channel systems in the Molasse foreland basin of the Eastern Alps – the effects of Late Oligocene foreland thrusting and Early Miocene lateral escape. AAPG Bulletin 85, 118.

Lourens, L., Hilgen, F., Shackleton, N.J., Laskar, J., Wilson, D., 2004. The Neogene Period. In: Gradstein, F.M., Ogg, J.G., Smith, A.G. (Eds.), A Geologic Time Scale 2004. Cambridge University Press, Cambridge, pp. 409–440.

Malzer, O., Rögl, F., Seifert, P., Wagner, L., Wessely, G., Brix, F., 1993. Die Molassezone und deren Untergrund. In: Brix, F., Schultz, O. (Eds.), Erdöl und Erdgas in Österreich. 281-357.

Mandic, O., Steininger, F.F., 2003. Computer-based mollusc stratigraphy - a case study from the Eggenburgian (Early Miocene) type region (NE Austria) - Palaeogeography, Palaeoclimatology, Palaeoecology 197, 263–291.

Miller, K.G., Kominz, M.A., Browning, J.V., Wright, J.D., Mountain, G.S., Katz, M.E., Sugarman, P.J., Cramer, B.S., Christie-Blick, N., Pekar, S.F., 2005. The Phanerozoic record of global sea-level change. Science 310, 1293–1298.

Miller, W., 1988. Giant *Bathysiphon* (Foraminiferida) from Cretaceous turbidites, northern California. Lethaia 21, 363–374.

Miller, W., 2005. A *Bathysiphon* (Foraminifera) 'shell bed' from the Cretaceous of northern California, USA: Example of a parautochthonous macro-skeletal deposit in deep-ocean turbidites. Palaeogeography, Palaeoclimatology, Palaeoecology 260, 342–346.

Murray, J.W., 2006. Ecology and Applications of Benthic Foraminifera. Cambridge University Press, Cambridge.

Nagy, J., 1992. Environmental significance of foraminiferal morphogroups in Jurassic North sea deltas. Palaeogeography, Palaeoclimatology, Palaeoecology 95, 111–134.

Nagy, J., Berge, S.H., 2008. Micropalaeontological evidence of brackish water conditions during deposition of the Knorringfjellet Formation, Late Triassic-Early Jurassic, Spitsbergen. Polar Research 27, 413–427.

Nagy, J., Gradstein, F.M., Kaminski, M.A., Holbourn, A.E.L., 1995. Foraminiferal morphogroups, paleoenvironments and new taxa from Jurassic and Cretaceous strata of Thakkhola, Nepal. In: Kaminski, M.A., Geroch, S., Gasinski, M.A. (Eds.), Proceedings of the Fourth International Workshop on Agglutinated Foraminifera. Grzybowski Foundation, London, 181–209.

Nagy, J., Hess, S., Alve, E., 2010. Environmental significance of foraminiferal assemblages dominated by small-sized *Ammodiscus* and *Trochammina* in Triassic and Jurassic delta-influenced deposits. Earth-Science Reviews 99, 31–49.

Nagy, J., Johansen, H.O., 1991. Delta-influenced foraminiferal assemblages from the Jurassic (Toarcian-Bajocian) of the northern North Sea. Micropaleontology 37, 1–40.

Papp, A., 1960. Das Vorkommen von Miogypsina in Mitteleuropa und dessen Bedeutung für die Tertiärstratigraphie. Mitteilungen der Geologischen Gesellschaft Wien 51, 219.

Papp, A., 1968. Nomenclature of the Neogene of Austria. Verhandlungen der Geologischen Bundesanstalt 1968, 19–27.

Papp, A., 1975. Die Großforaminiferen des Egerien. In: Baldí, T., Seneš, J. (Eds.), OM – Egerien. Die Egerer, Pouzdraner, Puchkirchener Schichtengruppe und die Bretkaer Formation. Chronostratigraphie und Neostratotypen, Miozän der Zentralen Paratethys, vol. 5. Verlag der Slowakischen Akademie der Wissenschaften, 289–307.

Peña, F.A.C., 2007. The Early Miocene Upper Marine Molasse of the German part of the Molasse Basin - a subsurface study. Sequence Stratigraphy, Depositional Environment and Architecture, 3D Basin Modeling. Ph.D. Thesis, Eberhard-Karls-Universität Tübingen, Germany. 133 pages.

Petters, V., 1936. Geologische und mikropaläontologische Untersuchungen der Eurogasco im Schlier Oberösterreichs. Petroleum Zeitschrift 32, 3.

Piller, W.E., Harzhauser, M., Mandic, O., 2007. Miocene Central Paratethys stratigraphy – current status and future directions. Stratigraphy 4, 151–168.

Piller, W.E., Egger, H., Erhart, C., Gross, M., Harzhauser, M., Hubmann, B., van Husen, D., Krenmayr, H.-G., Krystyn, L., Lein, R., Lukeneder, A., Mandl, G., Rögl, F., Roetzel, R., Rupp, C., Schnabel, W., Schönlaub, H.P., Summesberger, H., Wagreich, M., 2004. Die Stratigraphische Tabelle von Österreich 2004 (sedimentäre Schichtfolgen). Österreichische stratigraphische Kommission und Kommission für die paläontologische und stratigraphische Erforschung Österreichs.

Pippèrr, M., 2011. Characterisation of Ottnangian (middle Burdigalian) palaeoenvironments in the North Alpine Foreland Basin using benthic foraminifera—A review of the Upper Marine Molasse of southern Germany. Marine Micropaleontology 79, 80–99.

Pippèrr, M., Reichenbacher, B., 2009. Biostratigraphy and paleoecology of benthic foraminifera from the Eggenburgian "Ortenburger Meeressande" of southeastern Germany (Early Miocene, Paratethys). Neues Jahrbuch für Geologie und Paläontologie Abhandlungen 254, 41–61.

Pippèrr, M., Reichenbacher, B., 2010. Foraminifera from the borehole Altdorf (SE Germany): Proxies for

Ottnangian (early Miocene) palaeoenvironments of the Central Paratethys. Palaeogeography, Palaeoclimatology, Palaeoecology 289, 62–80.

Pratt, L.M., 1984. Influence of paleoenvironmental factors on preservation of organic matter in Middle Cretaceous Greenhorn Formation, Pueblo, Colorado. AAPG Bulletin 68, 1146-1159.

Rögl, F., 1998. Palaeogeographic Considerations for Mediterranean and Paratethys Seaways (Oligocene to Miocene). Annalen des Naturhistorischen Museums in Wien 99A, 279–310.

Rögl, F., Hochuli, P., Mueller, C., 1979. Oligocene-Early Miocene stratigraphic correlations in the Molasse Basin of Austria. Annales Geologiques des Pays Helleniques, Tome hors series, 1045–1050.

Roetzel, R., Ćorić, S., Galović, I., Rögl, F., 2006. Early Miocene (Ottnangian) coastal upwelling conditions along the southeastern scarp of the Bohemian Massif (Parisdorf, Lower Austria, Central Paratethys). Beiträge zur Paläontologie 30, 387–413.

Rupp, C., Haunold-Jenke, Y., 2003. Untermiozäne Foraminiferenfaunen aus dem oberösterreichischen Zentralraum. Jahrbuch der Geologischen Bundesanstalt 143, 227–302.

Rupp, C., Hofmann, T., Jochum, B., Pfleiderer, S., Schedl, A., Schindlbauer, G., Schubert, G., Slapansky, P., Tilch, N., van Husen, D., Wagner, L., Wimmer-Frey, I., 2008. Geologische Karte der Republik Österreich 1:50.000, Blatt 47 Ried im Innkreis. Erläuterungen zu Blatt 47 Ried im Innkreis. Geological Survey of Austria, Vienna.

Rupp, C., van Husen, D., 2007. Zur Geologie des Kartenblattes Ried im Innkreis. In: Egger, H., Rupp, C. (Eds.), Beiträge zur Geologie Oberösterreichs, Arbeitstagung der Geologischen Bundesanstalt 2007. Geological Survey of Austria, Vienna, 73–112.

Schlunegger, F., Leu, W., Matter, A., 1997. Sedimentary Sequences, Seismic Facies, Subsidence Analysis, and Evolution of the Burdigalian Upper Marine Molasse Group, Central Switzerland. AAPG Bulletin 81, 1185–1207.

Strauss, C., 2008. Lithofacies, depositional environment, stratigraphic architecture and hydrocarbon prospectivity of the Hall Fm. within the NW-Austrian Molasse Trough. Unpublished internal report of RAG, 72pp.

Süss, M.P., Strauss, C., Hinsch, R., 2008. Sequence stratigraphy and depositional dynamics of the Puchkirchen basin (Upper Austria). Unpublished internal report of RAG, 28pp.

Van den Akker, T.J.H.A., Kaminski, M.A., Gradstein, F.M., Wood, J., 2000. Campanian to Palaeocene biostratigraphy and paleoenvironments in the Foula Sub-basin, west of the Shetland Islands, UK. Journal of Micropalaeontology 19, 23–43.

Wagner, L.R., 1996. Stratigraphy and hydrocarbons in the Upper Austrian Molasse Foredeep (active margin). In: Wessely, G., Liebl, W. (Eds.), Oil and Gas in Alpidic Thrustbelts and Basins of Central and Eastern Europe. European Association of Geoscientists and Engineers Special Publications 5, pp. 217–235.

Wagner, L.R., 1998. Tectono-stratigraphy and hydrocarbons in the Molasse Foredeep of Salzburg, Upper and Lower Austria. In: Mascle, A., Puigdefábregas, C., Luterbacher, H.P., Fernández, M., (Eds.), Cenozoic Foreland Basins of Western Europe. Geological Society Special Publications 134. Geological Society, London, pp. 339–369.

Wenger, W.F., 1987. Die Foraminiferen des Miozäns der bayerischen Molasse und ihre stratigraphische sowie paläogeographische Auswertung. Zitteliana 16, 173–340.

Zweigel, J., 1998. Eustatic versus tectonic control on foreland basin fill. Contributions to Sedimentary Geology 20. Schweizerbart, Stuttgart.

Appendix 3.1: Tables 3.1-3.4

Tab. 3.1. Characteristics of the herein applied agglutinated morphogroups based on van den Akker et al. (2000) and Kaminski et al. (2005).

Morphogr.	Test shape	Life position	Feeding habitat	Environment	Taxa
M1	Tubular	Erect epifauna	Suspension feeding	Bathyal to abyssal; high sedimentation rates, turbidites, bottom currents	*Bathysiphon* *Psammosiphonella* *Rhizammina*
M2a	Globular	Shallow infauna	Suspension feeding -passive deposit feeding	Bathyal and abyssal	
M2b	Rounded trochospiral and streptospiral, or Planoconvex trochospiral	Surficial epifauna	Active deposit feeding	Shelf to deep marine	*Alveolophragmium* *Budashevaella* *Cribrostomoides*
M2c	Elongate keeled	Surficial epifauna	Active deposit feeding	Shelf to marginal marine	*Spiroplectammina* *Spirorutilus*
M3a	Flattened trochospiral, or Flattened planispiral and streptospiral	Surficial epifauna	Active and passive deposit feeding	Lagoonal to abyssal; floculent bottom layer	*Ammodiscus* *Glomospira* *Siphonaperta*
M3b	Flattened irregular	Surficial epifauna	Passive deposit feeding	Bathyal to abyssal	*Discammina*
M4a	Rounded planispiral	Surficial epifauna - shallow infauna	Active deposit feeding	Inner shelf to upper bathyal	*Cyclammina* *Haplophragmoides* *Reticulophragmium* *Trochammina*
M4b	Elongate subcylindrical, or Elongate tapered	Deep infauna	Active deposit feeding	Inner shelf to upper bathyal; high organic matter flux	*Ammobaculites* *Gaudryinopsis* *Karreriella* *Textularia* *Verneulinulla*

Tab. 3.2. Abundance of the most important foraminiferal taxa (> 5% in at least one sample). The same matrix was used for multivariate statistical analysis.

Sample	M1	M2b	M2c	M3a	M3b	M4a	M4b	Reworked agglutinated foraminifers	*Ammonia beccarii* gr.	*Amphicoryna* spp.	*Bolivina* spp.	*Bulimina/Caucasina* spp.	*Cibicidoides austriacus/ungerianus*	*Cibicidoides lopjanicus*	*Cibicidoides* spp.	*Elphidium* spp.	*?Fissurina* sp.	*Fursenkoina halkyardia*	*Grigelis pyrula*	*Gyroidinoides/Hansenisca* spp.	*Hanzawaia boueana*	*Heterolepa dutemplei*
790m	0	0	0	0	0	0	0	0	**21**	0	0	0	0	**42**	4	4	0	0	0	0	0	**13**
800m	0	0	0	0	0	0	0	0	**17**	0	2	0	0	**29**	**5**	0	0	0	0	**5**	0	2
810m	0	0	0	0	0	0	0	0	**15**	0	0	**5**	0	**50**	0	0	0	0	0	0	0	**5**
820m	0	0	0	0	0	0	0	0	**14**	**14**	0	0	0	**14**	**29**	0	0	0	0	0	0	0
830m	**8**	0	0	**8**	0	**8**	0	0	0	0	0	0	0	0	0	0	0	0	0	0	0	**8**
840m	0	**17**	0	0	0	0	0	0	0	0	0	0	0	0	**17**	0	0	0	0	0	0	0
850m	**15**	0	0	**15**	0	0	0	0	**15**	0	0	0	0	7	4	0	0	0	0	0	0	0
870m	**50**	0	0	0	0	**8**	0	0	0	0	0	0	0	0	0	**8**	0	0	0	0	0	**17**
880m	**33**	**8**	0	**25**	0	0	0	0	0	0	0	0	0	**8**	**8**	0	**8**	0	0	0	0	0
900m	**64**	4	0	4	0	**9**	0	0	0	0	0	0	0	0	0	0	0	0	0	0	0	0
920m	**70**	3	0	3	0	4	0	0	0	4	0	0	0	0	0	1	0	0	0	0	0	1
960m	**67**	2	0	1	0	4	**11**	0	0	0	0	0	0	0	0	0	0	0	0	0	0	0
970m	**71**	0	0	4	0	**6**	**10**	0	0	0	0	0	0	0	0	0	0	0	0	0	0	0
980m	**65**	1	0	**13**	0	**10**	1	0	0	0	0	0	0	0	0	0	0	0	0	0	0	0
990m	**38**	**5**	0	**35**	0	4	**6**	0	1	0	0	0	0	1	1	0	0	0	0	0	0	0
1000m	**36**	1	0	**31**	0	2	**5**	0	4	0	0	0	0	2	0	1	0	0	0	0	0	0
1010m	**33**	1	0	**39**	0	**5**	**6**	0	1	0	0	0	0	0	0	0	0	0	0	0	0	0
1020m	**42**	2	0	**37**	0	4	3	0	**5**	0	0	0	0	0	0	0	0	0	0	0	0	0
1030m	**21**	**5**	0	**46**	0	**5**	**8**	0	3	0	0	0	0	3	0	0	0	0	0	3	0	0
1040m	**24**	1	0	**58**	0	3	**5**	0	0	0	0	0	0	0	0	0	0	0	0	0	0	0
1060m	**41**	1	0	**45**	0	3	**8**	0	0	0	0	0	0	0	0	0	0	0	0	0	0	0
1070m	**42**	3	0	**28**	0	4	**5**	0	4	0	0	0	0	1	0	0	0	0	0	0	0	0
1080m	**42**	2	0	**44**	0	1	1	0	2	0	0	0	0	0	0	1	0	0	0	0	0	0
1090m	**36**	3	0	**36**	0	1	**6**	0	0	0	0	0	0	0	0	0	0	0	0	0	0	0
1102m	**25**	**15**	0	**28**	0	1	**8**	0	**6**	0	0	0	0	1	0	0	0	0	0	0	0	0
1110m	**33**	**7**	0	**37**	2	4	**11**	0	2	0	0	0	0	2	0	0	0	0	0	0	0	0
1120m	**22**	**24**	0	**28**	0	**9**	2	0	**7**	0	0	0	0	0	2	0	0	0	0	0	0	0
1140m	**36**	2	0	**15**	0	2	**16**	0	0	0	0	0	0	0	0	0	0	0	0	0	0	0
1150m	**47**	**5**	1	**11**	0	4	**14**	0	1	0	0	0	0	1	0	0	0	0	0	0	0	0
1200m	**86**	3	0	1	0	1	**6**	0	0	0	0	0	0	0	0	0	0	0	0	0	0	0
1220m	**48**	20	0	0	0	0	**30**	0	0	0	0	0	0	0	0	0	0	0	0	0	0	0
1232m	**63**	1	0	**8**	0	0	**10**	0	4	0	0	0	0	1	0	0	0	0	0	0	0	0
1242m	**48**	1	0	**7**	0	2	**28**	1	**8**	0	0	1	0	0	0	0	0	0	0	0	0	0
1250m	**38**	1	0	**7**	0	0	**9**	0	**22**	1	0	0	0	3	1	3	0	0	0	1	0	0
1262m	**30**	0	0	**5**	0	1	**11**	**10**	**23**	0	0	2	0	0	0	2	0	0	0	1	0	0
1282m	**53**	**7**	0	1	0	1	1	4	**7**	0	0	4	0	0	1	0	0	0	0	1	0	0
1300m	**17**	**12**	0	3	0	1	**7**	**19**	1	0	0	0	2	0	0	1	0	0	0	0	0	1
1310m	**40**	**18**	0	2	0	1	**11**	**9**	1	0	0	0	1	0	0	0	0	0	0	0	0	1
1322m	**21**	**9**	0	0	0	3	**9**	**18**	0	0	0	0	0	0	0	0	0	0	0	**6**	0	0
1330m	**12**	**9**	0	2	0	2	4	**8**	**14**	0	0	**7**	0	0	1	1	0	0	0	3	0	0
1350m	**15**	3	0	0	0	1	0	**7**	**26**	0	0	3	0	0	0	3	0	0	4	3	0	0
1362m	**15**	2	0	4	0	0	4	**9**	**32**	0	0	4	0	3	0	0	0	0	0	0	0	0
1382m	**28**	**6**	0	**6**	0	2	**8**	**7**	**25**	0	0	1	0	0	0	2	0	0	0	0	0	1
1392m	**22**	**8**	0	1	0	3	**14**	**10**	**18**	0	0	0	0	1	0	1	0	0	0	0	0	0
1402m	**10**	1	0	1	0	0	2	**6**	**38**	0	0	1	1	1	0	1	0	0	0	0	0	0
1410m	**9**	0	0	2	2	2	**12**	**5**	3	**5**	**9**	**7**	0	2	0	0	0	0	0	0	0	3
1432m	2	0	0	0	0	0	1	0	**54**	3	0	2	0	2	**6**	1	0	0	0	0	0	0
1442m	**6**	0	0	1	0	1	1	1	**61**	0	0	1	0	1	3	3	0	0	0	0	0	1
1450m	**15**	**7**	0	2	0	0	**8**	2	**33**	0	1	2	0	2	1	3	0	0	0	0	0	0
1462m	2	0	0	0	0	0	1	0	**63**	0	0	1	0	0	0	3	0	0	0	0	0	1
1472m	4	0	0	0	0	0	4	1	**51**	0	0	0	0	0	0	1	0	0	0	0	0	1
1502m	2	0	0	0	0	0	1	4	**30**	0	0	4	0	1	2	1	0	0	0	0	0	2
1512m	0	0	0	0	0	0	0	2	**6**	1	2	3	1	0	1	0	0	**8**	0	0	2	0
1522m	2	0	1	0	0	0	2	0	**31**	1	1	**7**	1	1	2	1	0	0	0	2	2	0
1532m	**23**	0	0	0	0	0	**7**	0	3	3	0	**10**	0	0	**7**	0	0	0	0	0	3	3
1540m	2	0	0	1	0	1	**6**	2	**7**	3	0	2	0	2	**9**	0	0	0	0	0	2	0

Tab. 3.2 (continued).

Sample	*Heterolepa dutemplei*	*Laevidentalina* spp.	Lagenidae indet.	*Lenticulina* spp.	*Melonis pompilioides*	*Myllostomella recta*	*Nonion* spp.	*Oridorsalis umbonatus*	*Porosononion* spp.	*Protelphidium roemeri*	*Pullenia bulloides*	*Sphaeroidina bulloides*	*?Stilostomella* sp.	*Uvigerina* spp.	*Valvulineria* spp.
790m	**13**	0	0	**13**	0	0	0	0	0	0	0	0	0	0	4
800m	2	0	0	**14**	2	0	0	0	**5**	0	0	0	0	0	0
810m	**5**	0	0	**10**	**10**	0	**5**	0	0	0	0	0	0	0	0
820m	0	0	0	**29**	0	0	0	0	0	0	0	0	0	0	0
830m	**8**	0	0	**8**	**31**	0	0	0	0	0	0	0	0	0	**8**
840m	0	0	0	**50**	0	0	0	0	0	0	0	0	0	0	0
850m	0	4	0	4	**30**	0	0	0	0	0	4	0	0	0	0
870m	**17**	0	0	0	0	0	0	0	0	0	0	0	0	0	0
880m	0	0	0	0	8	0	0	0	0	0	0	0	0	0	0
900m	0	2	0	0	0	0	0	0	0	0	0	0	0	0	0
920m	1	0	0	0	0	0	0	0	0	0	0	0	0	0	0
960m	0	0	0	0	0	0	0	0	0	0	0	0	0	0	0
970m	0	0	0	1	0	0	0	0	0	0	0	0	0	0	0
980m	0	0	0	0	0	0	0	0	0	0	0	0	0	0	0
990m	0	0	0	0	1	0	1	0	0	0	0	0	0	0	0
1000m	0	1	0	1	2	0	1	0	0	0	0	0	0	0	0
1010m	0	1	0	1	0	0	1	0	0	0	0	0	1	0	0
1020m	0	0	0	0	2	0	1	0	0	0	1	0	0	0	0
1030m	0	0	0	0	0	0	0	0	0	0	0	0	0	0	0
1040m	0	1	0	1	0	0	0	0	0	0	0	0	0	0	0
1060m	0	0	0	0	0	0	0	0	0	0	0	0	0	0	0
1070m	0	1	2	0	2	0	0	0	0	0	0	0	0	0	0
1080m	0	0	0	1	1	0	1	0	0	0	0	0	0	0	0
1090m	0	0	0	0	0	0	0	0	0	0	0	0	0	0	0
1102m	0	0	2	2	**5**	0	0	0	0	0	1	0	0	0	0
1110m	0	0	0	0	0	0	0	0	0	0	0	0	0	0	0
1120m	0	0	0	0	0	0	0	0	0	0	0	0	0	0	0
1140m	0	0	0	0	0	0	0	0	0	0	0	0	0	0	0
1150m	0	0	0	0	0	0	0	0	0	0	0	0	0	0	0
1200m	0	0	0	0	0	0	0	0	0	0	0	0	0	0	0
1220m	0	0	0	0	0	0	0	0	0	0	0	0	0	0	0
1232m	0	0	0	0	0	0	0	0	0	0	0	0	0	0	0
1242m	0	0	0	0	0	0	1	1	0	0	0	0	0	0	0
1250m	0	1	0	0	2	0	3	3	0	0	0	0	0	0	0
1262m	0	0	0	2	1	0	2	0	0	1	0	0	0	0	0
1282m	0	1	0	3	4	0	1	0	0	0	0	0	0	0	0
1300m	1	1	0	1	3	0	0	1	0	0	2	1	1	3	0
1310m	1	0	0	0	**5**	0	0	0	0	0	1	0	0	2	0
1322m	0	0	0	0	**12**	0	3	0	0	0	0	0	0	0	0
1330m	0	2	0	4	**5**	0	2	0	0	0	3	0	0	1	0
1350m	0	1	0	0	3	0	4	1	1	1	0	0	0	3	0
1362m	0	2	0	0	**6**	0	4	0	0	1	2	0	**5**	0	0
1382m	1	2	0	1	0	0	0	0	0	0	1	0	1	1	1
1392m	0	1	0	1	1	0	0	1	1	1	1	0	1	0	0
1402m	0	3	0	1	3	0	1	2	0	1	1	0	0	1	0
1410m	3	2	0	2	0	0	2	2	0	0	2	2	**5**	0	2
1432m	0	0	0	1	0	0	2	0	0	2	0	1	3	0	0
1442m	1	2	0	1	0	0	1	0	1	0	0	0	3	0	1
1450m	0	1	0	0	2	0	0	0	1	0	0	0	0	0	0
1462m	1	0	0	2	3	0	4	0	1	1	0	0	0	1	0
1472m	1	4	0	1	1	0	1	1	3	0	1	0	0	0	0
1502m	2	3	0	2	4	0	3	0	1	1	1	0	2	**22**	0
1512m	0	1	0	**5**	1	0	1	0	0	0	0	0	2	**43**	0
1522m	0	4	0	1	0	0	2	0	1	0	0	0	0	**11**	1
1532m	3	0	0	0	3	3	0	0	0	0	3	0	0	**17**	0
1540m	0	2	0	2	0	0	0	0	2	0	1	2	1	**29**	0

Tab. 3.3. TOC, S, TOC/S and HI values from the lower and middle Hall Fm.

Depth	Informal Unit	TOC	S	TOC/S	HI
990m	Hall Series	0.86	0.25	3.4	84
1000m	Hall Series	0.51	0.24	2.1	51
1020m	Hall Series	0.82	0.26	3.2	64
1030m	Hall Series	0.68	0.35	1.9	
1050m	Hall Series	1.03	0.45	2.3	43
1060m	Hall Series	1.18	0.26	4.5	
1070m	Hall Series	0.62	0.27	2.3	56
1080m	Hall Series	0.68	0.23	3.0	53
1090m	Hall Series	0.49	0.29	1.7	28
1102m	Hall Series	0.53	0.24	2.2	70
1110m	Hall Series	1.05	0.29	3.6	30
1120m	Hall Series	1.02	0.31	3.3	67
1130m	Hall Series	1.39	0.15	9.3	24
1140m	Hall Series	1.28	0.26	4.9	26
1150m	Hall Series	1.54	0.23	6.7	31
1160m	Hall Series	0.89	0.18	4.9	13
1190m	Hall Series	0.97	0.22	4.4	122
1202m	Gendorf Sands	0.75	0.21	3.6	47
1210m	Gendorf Sands	0.47	0.28	1.7	43
1220m	Gendorf Sands	0.49	0.11	4.5	35
1232m	Hall Series	0.26	0.18	1.4	54
1242m	Hall Series	0.54	0.25	2.2	35
1250m	Hall Series	0.79			90
1262m	Hall Series	0.32	0.3	1.1	50
1272m	Hall Series	0.44	0.27	1.6	59
1292m	Hall Series	0.39	0.28	1.4	38
1300m	Hall Series	0.39	0.23	1.7	13
1310m	Hall Series	0.54	0.16	3.4	35
1322m	Hall Series	0.34	0.18	1.9	24
1330m	Basal Hall Silts	0.52	0.24	2.2	19
1342m	Basal Hall Silts	0.45	0.29	1.6	22
1350m	Basal Hall Silts	0.41	0.26	1.6	12
1362m	Basal Hall Silts	0.52	0.19	2.7	13
1382m	Basal Hall Silts	0.29	0.15	1.9	21
1392m	Basal Hall Silts	0.67	0.27	2.5	60
1402m	Basal Hall Silts	0.52	0.27	1.9	71
1410m	Basal Hall Silts	0.97	0.65	1.5	128
1422m	Basal Hall Silts	0.43	0.27	1.6	16
1432m	Basal Hall Silts	0.39	0.22	1.8	56
1442m	Basal Hall Silts	0.35	0.2	1.8	40
1450m	Basal Hall Silts	0.86	0.39	2.2	
1462m	Basal Hall Silts	0.48	0.23	2.1	54
1472m	Basal Hall Silts	0.23	0.1	2.3	52
1482m	Basal Hall Silts	0.66	0.2	3.3	47
1492m	Basal Hall Silts	0.55	0.31	1.8	84
1502m	Basal Hall Silts	0.72	0.24	3.0	44
1512m	Basal Hall Silts	0.78	0.79	1.0	151
1522m	Basal Hall Silts	0.37	0.27	1.4	84
1540m	Basal Hall Silts	0.41	0.2	2.1	44

Tab. 3.4. Nannoplankton species identified from selected samples of the Hall Fm.

Sample	*Braarudosphaera bigelowii*	*Coccolithus miopelagicus*	*Coccolithus pelagicus*	*Cricolithus Jonesii*	*Cyclicargolithus floridanus*	*Helicosphaera ampliaperta*	*Helicosphaera ampliaperta (small)*	*Helicosphaera carteri*	*Helicosphaera euphratis*	*Helicosphaera scissura*	*Helicosphaera scissura (small)*	*Pontosphaera multipora*	*Reticulofenestra bisecta*	*Reticulofenestra excavata*	*Reticulofenestra gelida*	*Reticulofenestra lockeri*	*Reticulofenestra minuta*	*Reticulofenestra pseudoumbilica*	*Reticulofenestra* sp.	*Sphenolithus dissimilis*	*Sphenolithus heteromorphus*	*Sphenolithus morjformis*	*Triquetrorhabdulus* cf. *carinatus*	*Thoracosphaera saxea*	*Thoracosphaera sp.*	*Zyghrablithus bijugatus*
800m			f	x	x	x	x	x			x	x	x	f	f	x	f					x				x
900m			c		x	x	x					x	x	f	x	x	x	x								
1200m			c	x			x	x				x	x	x								x				
1310m			x																							
1402m	x	x	x		x	x	f		x	x		x	x	x			x	x		x			x	x		
1450m			c	x				x								x										
1512m A			c		x		x	x				x		x	x	x		x							x	
1512m B		x	c		x			x				x	x		cf.			x	x				x			x
1512m C			x		x	x	x	x		x		x	x	x		x	x	x	x	x		x				
1540m			c		x	x	x	f	x	x		x			cf.	x		x	f		cf.	x				

Appendix 3.2. Absolute abundances of benthic foraminifers in the Hall Fm. at Hochburg 1.

Sample	*?Alveolophragmium* sp.	*?Ammobaculites sp.*	*Ammodiscus miocenicus*	*Ammodiscus* cf. *miocenicus*	*Ammodiscus* cf. *tenuissimus*	*Ammodiscus peruvianus*	*Ammodiscus* sp.	*?Ammodiscus* sp.	*Bathysiphon filiformis*	*Bathysiphon filiformis* (brown)	*Bathysiphon* sp.1	*?Bathysiphon* sp.	*Bigenerina agglutinans*	*Budashevaella multicamerata*	*Budashevaella* cf. *wilsoni*	*?Budashevaella* sp.	*Cribrostomoides moravica*	*Cribrostomoides subglobosus*	*Cribrostomoides* spp.	*?Cribrostomoides* sp.	*Cyclammina praecancellata*
800m																					
810m																					
820m																					
830m					1				1												
840m																					
850m			1				3		4												
870m									4												
880m			1			1		1	3												
900m							2		29												
920m							2		49												
960m							3		199		1								6	1	
970m			1		4	1		2	136					1							1
980m			1		6	3	1		51												1
990m	1		41			8		1	54							2			4		2
1000m			53			9	2		70			1								3	1
1010m			40			8	6		43							1				1	2
1020m			32		1	7			46					1							
1030m			12			4	2		8										1		1
1040m			26			20	42		35										1		2
1060m			25			19	81		112		1									2	
1070m		1	2			12	38		79										4		1
1080m			3		2	7	57		67										2	1	
1090m			15			22	132	1	168									1	8	3	
1102m			10			4	38		46										28		
1110m			1			1	15		15										3		1
1120m			1			4	8		10									2	5		
1140m			13			6	55	1	176			3							7		2
1150m							10		42									2	1		
1200m							1		77					1					1	1	
1232m						1	21		182									2			
1242m						3	7		63												
1250m			2			1	4		44							1					
1262m						1	6		39	13											
1282m		1					1		40	3						1			3		
1300m						2	11		57	70		3					1	17	13	3	
1310m	1					1	1		34	9		2						3	4	1	
1322m									7	6									1		1
1330m							2		14	10				1	1			2	1	1	
1350m									11	5											
1362m							4		15	9									1		
1382m				2		2	5		44	10						2			4	1	
1392m		1	1			1			29	15	1			2		1		1			1
1402m							3		19	13						1			1		1
1410m						1			5	3											
1432m									4	1											
1442m								1	9	2											
1450m							1	1	14	2		1		1				3		3	
1462m																					
1472m									2	1		1									
1490m									7	1											
1502m									2	4											
1512m									2	7											
1522m									4												
1532m									3			1									
1540m								1	2	2		1	2								

Appendix 3.2 (continued).

Sample	*Cyclammina* sp.	*Discammina* cf. *compressa*	*Gaudryinopsis beregoviensis*	*Gaudryinopsis* spp.	*?Gaudryinopsis* spp.	*Glomospira serpens*	*Haplophragmoides vasiceki vasiceki*	*Haplophragmoides* sp.	*?Haplophragmoides* sp.	*Karreriella* cf. *gaudryinoides*	*Karreriella* cf. *hantkeniana*	*Karreriella* spp.	*?Karreriella* spp.	*?Psammosiphonella cylindrica*	*Reticulophragmium acutidorsatum*	*Reticulophragmium* cf. *rotundidorsatum*	*Reticulophragmium* spp.	*?Reticulophragmium* spp.	*?Rhizammina* sp.	*Siphonaperta* cf. *criborosa*	*Spiroplectammina pectinata*
800m																					
810m																					
820m																					
830m																					
840m																					
850m																					
870m							1														
880m																					
900m	1														2		1				
920m															1		2				
960m			5	19			1		1						3			1			
970m			4	12											3	4	1		1		
980m									1						1	1		1			
990m			6						2								2				
1000m			1	5					2							1					
1010m				7	1										1	1		1			
1020m				2												4					
1030m				3				1													
1040m			1	5											1						
1060m				21					2						1	1	1				
1070m	1		6	3											2		2				
1080m			1	1											1	1					
1090m			11	17				2							2		1				
1102m				8												2					
1110m				5											1						
1120m				1												2		1			
1140m				72											1	3	2				
1150m			2	9				1										2			1
1200m				5														1			
1232m				14	3																
1242m				5			1								1						
1250m				7		1															
1262m	1			13																	
1282m															1						
1300m			8	8					1						2						
1310m				5													1		1		
1322m				3																	
1330m				5				1									2				
1350m															1						
1362m				3						1											
1382m				8				1	1			1				1				1	
1392m				1	1										1		2	1			
1402m												2							1		
1410m		1		4														1			
1432m											2			1			1				
1442m																					
1450m				2									1								
1462m												1									
1472m			1	1																	
1490m																					
1502m																					
1512m			1		4													2			
1522m																		1			1
1532m																					
1540m													3					1			

Appendix 3.2 (continued).

Sample	*Spirorutilus carinatus*	*Textularia gramen*	*Textularia pala*	*Textularia* spp.	*?Textularia* sp.	*?Textularia* spp. (black)	*Textulariidae indet.*	*?Textulariidae indet.*	*Trochammina* sp.	*?Verneuilinulla* sp.	M1 indet.	M2b indet.	M3a indet.	M3b indet.	M4a indet.	M4b indet.	Agglutinated indet.	*?Cycloforina* sp.	*Pyrgo simplex*	*Sigmoilopsis* cf. *ottnangensis*
800m																				
810m																				
820m																				
830m															1		1			
840m												1								
850m																	1			
870m											2						1			
880m											1	1								
900m											1	2					5			
920m											4	2					10			
960m			1												7	7	39			
970m			5								8				3		12			
980m			1								3	1			3		8			
990m																2	12			
1000m			2								5					2	14		1	
1010m											3				2		15			
1020m			1									1								
1030m												1					3			
1040m											1	1			2	1	13			
1060m															3		8			
1070m												1			2		16			
1080m																	6			
1090m			2														80			
1102m			1		2						1					5	12			
1110m														1						
1120m									1			4								
1140m			10									1					149			
1150m			1								2	2			1	1	14			
1200m																	2			
1232m																13	39			
1242m			6		1							1				25				
1250m			1													2	1			
1262m			1		1												3			1
1282m					1							1								
1300m			1								3	11				9	65			
1310m			1	1							1	8				3				1
1322m												2					1			
1330m												5					7			
1350m												2							1	
1362m												1								
1382m		1		2							1	2	1			1	5			2
1392m			1				14			1	3	8				2	9			
1402m	1									1						1	1		1	
1410m							2									1	2			
1432m	1																3			
1442m								1							1	1	2			
1450m			1				1				1					3	3			
1462m											2									
1472m							1													
1490m																				
1502m																1				
1512m						2														
1522m	1			1												3		1		
1532m											3					2				
1540m																2	7			

Appendix 3.2 (continued).

Sample	*Sigmoilopsis* sp.	*Sigmoilinita tenuis*	*?Sigmoilinita* sp.	*Siphonaperta* sp.	*?Spirolocculina* sp.	*Miliolidae indet.*	*Alabamina tangentialis*	*Almaena osnabrugensis*	*Ammonia beccharii* gr.	*Amphicoryna danuviensis*	*Amphicoryna* sp.	*Amphimorphina haueriana*	*Amphistegina* sp.	*Asterigerinata planorbis*	*Bolivina* cf. *antiqua*	*Bolivina beyrichi beyrichi*	*Bolivina* cf. *budensis*	*Bolivina dilatata dilatata*	*Bolivina hebes*	*Bolivina vaceki vaceki*
800m							2		7									1		
810m									3											
820m									1		1									
830m		1																		
840m																				
850m									4											
870m																				
880m																				
900m																				
920m	1									3										
960m					1															
970m					3															
980m																				
990m									1											
1000m									9											
1010m									1											
1020m									5											
1030m									1											
1040m																				
1060m			1						1											
1070m							1		8											
1080m									3											
1090m																				
1102m						1			11											
1110m									1											
1120m									3											
1140m																				
1150m									1											
1200m																				
1232m									11											
1242m									11											
1250m									25		1									
1262m									31											
1282m									5					1						
1300m		2			1				3											
1310m									1											
1322m																				
1330m									17					1						
1350m									19											
1362m		1							31											
1382m									40											
1392m		1							26					1						
1402m									77											
1410m									2	3								2		
1432m									135	8										
1442m		1				1			97											
1450m									35									1		
1462m									71											
1472m									35											
1490m									3											
1502m									30									2		
1512m				1				1	29	4		1		1		1	2		2	3
1522m									71	2					1			1		
1532m									1	1										
1540m						1			9	4			1	1						

Appendix 3.2 (continued).

Sample	*Boltvina versatilis*	*Boltvina* cf. *versatilis*	*Bulimina coprolithoides*	*Bulimina elongata*	*Bulimina* cf. *insignis*	*Bulimina striata mexicana*	*Bulimina striata striata*	*Bulimina subulata*	*Bulimina* spp.	*?Caneris* sp.	*Caucasina cylindrica*	*Caucasina schischkinskayae*	*Cibicidoides austriacus*	*Cibicidoides dalmatinus*	*Cibicidoides lobatulus*	*Cibicidoides lopjanicus*	*Cibicidoides* cf. *lopjanicus*	*Cibicidoides* cf. *oligocenicus*	*Cibicidoides* cf. *pachyderma*	*Cibicidoides pseudoungerianus*	*Cibicidoides ungerianus/ornatus*
800m																12					
810m								1								6	4				
820m																1					
830m																					
840m																					
850m																1				1	
870m																					
880m																	1				
900m																					
920m																					
960m																					
970m																					
980m																					
990m																				1	
1000m															1		2			2	
1010m																					
1020m																					
1030m																1					
1040m																					
1060m																					
1070m																				2	
1080m																					
1090m																					
1102m																				1	
1110m																1					
1120m																					
1140m																					
1150m																				1	
1200m																					
1232m																1				2	
1242m							1														
1250m																		1		3	
1262m							2														
1282m			1				1		1												
1300m													5			1					2
1310m																					1
1322m																					
1330m			5	3																	
1350m							1		1												
1362m				2		1						1				1				2	
1382m				1																	
1392m																				1	
1402m							1		2								2		1		2
1410m	1	2							2			2								1	
1432m									2		1	2			1	9			1	4	
1442m									2							3					
1450m				1			1									3					
1462m				1																	
1472m																					
1490m							1					1									
1502m			2		1				1											1	
1512m	1			5			6		1		1	1		1					4		4
1522m	1			4			5		4		3						1		1	1	3
1532m								1				2									
1540m									2	1					1	1			6	2	

Appendix 3.2 (continued).

Sample	*Cibicidoides* spp.	*?Cibicidoides* spp.	*Dentalina* sp.	*Dentalinoides aproximata*	*Elphidiella heteropora*	*Elphidiella* spp.	*?Elphidiella* sp.	*Elphidium fichtelianum*	*Elphidium glabratum*	*Elphidium ortenburgense*	*Elphdium reussi*	*Elphidium* cf. *reussi*	*Elphidium subtypicum*	*Elphidium* cf. *subumbilicatum*	*Elphidium* spp.	*?Fissurina* sp.	*Fursenkoina acuta*	*Fursenkoina halkyardia*	*Fursenkoina* spp.	*?Fursenkoina* spp.	*Globocassidulina oblonga*
800m	2																				
810m																					
820m	2																				
830m																					
840m	1																				
850m	1																				
870m										1											
880m	1															1					
900m																					
920m								1													
960m																					
970m																					
980m																					
990m	1																				
1000m									1				1								
1010m																					
1020m																					
1030m																					
1040m																					
1060m																					
1070m																					
1080m															1						
1090m										1											
1102m																					
1110m																					
1120m	1																				
1140m																					
1150m																					
1200m																					
1232m																					
1242m																					
1250m	1						1				1		1		2						
1262m									1	2											
1282m	1																				
1300m			3							1		1									
1310m																					
1322m																					
1330m	1				1										1						
1350m											1				1						
1362m						1															
1382m					1						1		1		1						
1392m							1				2										
1402m										1	2										
1410m																					
1432m	6									1	1										
1442m		2								2	1				2						
1450m											1		1		1						
1462m						1					2				1						
1472m															1						
1490m	1																				
1502m	2														1						
1512m	2			1	1						1				1			44	6		2
1522m	3				1	1					1			1	1		1			1	2
1532m	1	1																			
1540m	2	1			1															1	

Appendix 3.2 (continued).

Sample	*Grigelis pyrula*	*Guttulina uvula*	*Gyroidinoides mamillatus*	*Gyroidinoides parvus*	*Gyroidinoides* spp.	*Hansenisca soldanii*	*Hanzawaia boueana*	*?Hanzawaia sp.*	*Heterolepa dutemplei*	*?Heterolepa dutemplei*	*Laevidentalina boueana*	*Laevidentalina* spp.	*Lagena gracilicosta*	*Lagena* spp.	*?Lagenidae* indet.	*Lapugyina* sp.	*Lenticulina buergli*	*Lenticulina inornata* gr.	*Lenticulina* spp.	*Melonis pompilioides*	*Melonis* spp.
800m					1	1			1									6		1	
810m									1									2		2	
820m																		2			
830m									1									1		4	
840m																		2	1		
850m												1						1		8	
870m									2												
880m																				1	
900m												1									
920m									1												
960m																					
970m																			2		
980m																					
990m																				2	
1000m						1						2					1		1	4	
1010m												1							2		
1020m																				2	
1030m			1																		
1040m												1					1				
1060m																					
1070m												1			3					4	
1080m																			1	2	
1090m																				1	
1102m															3				3	10	
1110m																					
1120m																					
1140m																					
1150m																					
1200m																					
1232m																					1
1242m																					
1250m						1						1	1							2	
1262m		1				1													2	1	
1282m				1								1	1					2		3	
1300m						1			1	2		2	1					5		10	
1310m										1						1				5	
1322m				2																4	
1330m					1	3						2						5		6	
1350m	3				1	1						1								2	
1362m												2								5	1
1382m										2		4						1			
1392m												1						1		1	
1402m												6			1			3		6	
1410m									2			1						1			
1432m									1			1						3		1	
1442m									1			3						1			
1450m												1								2	
1462m									1									2		3	
1472m									1			3						1		1	
1490m						1															
1502m									2			3						2		3	1
1512m				2			7	1	1		2	4		1				28		5	
1522m				3	1		5		1			10		1				3			1
1532m							1		1										1	1	
1540m							2					2						2			

Appendix 3.2 (continued).

Sample	*Myllostomella recta*	*Naugeborina longiscata*	*Nonion commune*	*Nonion* spp.	*Nonionella liebusi*	*Nonionidae* indet.	*Oridorsalis umbonatus*	*?Pappina* sp.	*Pararotalia* sp.	*Porosononion granosum*	*Porosononion* sp.	*Praeglobobulimina pyrrula*	*Praeglobobulimina* spp.	*Protelphidium roemeri*	*Pullenia bulloides*	*Pyrgo simplex*	*Sphaeroidina bulloides*	*Stilostomella* spp.	*Uvigerina* cf. *brunnensis*	*Uvigerina* cf. *hantkeni*	*Uvigerina multistriata*
800m										2											
810m			1																		
820m																					
830m																					
840m																					
850m															1						
870m																					
880m																					
900m																					
920m																					
960m																					
970m																					
980m																					
990m			1																		
1000m			2			1															
1010m			1															1			
1020m				1											1						
1030m																					
1040m																					
1060m																					
1070m																					
1080m			1																		
1090m																					
1102m															1						
1110m																					
1120m																					
1140m																					
1150m																					
1200m																					
1232m																					
1242m			1				1														
1250m				3			3		1												
1262m			2											1							
1282m			1									1									
1300m							2								9		2	5		1	
1310m															1						
1322m					1																
1330m						3									4						
1350m				3			1		1	1		1		1					1		
1362m			4									1		1	2			5			
1382m															2	1		1			
1392m							1			2			1	2	1			1			
1402m			2			1	4					1	1	2	2			1			
1410m			1				1								1		1	3			
1432m			4	1						1				4			3	8			
1442m						1				1								4			
1450m										1											
1462m			1	2		1					1			1					1		
1472m				1		1	1			2			1		1						
1490m				1																	
1502m				3						1				1	1			2			2
1512m	1		6			1		5			1		1		1			8			2
1522m		1	4					1	3	3			2					1			
1532m	1														1						
1540m										2		1			1		3	1			

Appendix 3.2 (continued).

Sample	*Uvigerina parviformis*	*Uvigerina posthantkeni*	*Uvigerina* cf. *posthantkeni*	*Uvigerina rudlingensis*	*Uvigerina semiornata*	*Uvigerina* spp.	*Vaginulinopsis pedum*	*Valvulineria complanata*	*?Valvulineria complanata*	*Valvulineria petrolei*	*Hyalin indet.*
800m											6
810m											
820m											
830m										1	1
840m											1
850m											
870m											1
880m											
900m											3
920m											
960m											2
970m											
980m											
990m											1
1000m											9
1010m											2
1020m											5
1030m											
1040m											
1060m											
1070m											
1080m											1
1090m											
1102m											2
1110m											1
1120m											3
1140m											
1150m											
1200m											1
1232m											1
1242m											4
1250m											3
1262m											9
1282m						3					4
1300m			6		2	3					16
1310m			2								5
1322m											6
1330m			1								15
1350m						1					11
1362m											3
1382m						1		1			7
1392m											8
1402m				2							35
1410m								1			11
1432m											40
1442m								1			18
1450m											20
1462m											21
1472m											13
1490m											
1502m			2			18					14
1512m		25			1	195	2		1		75
1522m	2		9			13		2			40
1532m	2					3					4
1540m			6			29					17

Chapter 4

FACIES DEVELOPMENT ALONG THE TIDE-INFLUENCED SHELF OF THE BURDIGALIAN SEAWAY: AN EXAMPLE FROM THE OTTNANGIAN STRATOTYPE (EARLY MIOCENE, MIDDLE BURDIGALIAN)

Patrick Grunert[a], Ali Soliman[a], Stjepan Ćorić[b], Reinhard Roetzel[b], Mathias Harzhauser[c], Werner E. Piller[a]

[a] Institute for Earth Sciences, University of Graz, Heinrichstraße 26, A-8010 Graz, Austria

[b] Geological Survey of Austria, Neulinggasse 38, A-1030 Vienna, Austria

[c] Natural History Museum Vienna, Geological-Paleontological Department, Burgring 7, A-1014 Vienna, Austria

Abstract

Herein, we report quantitative micropaleontological (benthic foraminifers, dinoflagellate cysts, calcareous nannoplankton), sedimentological (grain-size analysis) and geophysical (background gamma radiation) analyses from Ottnang-Schanze, the stratotype for the regional Ottnangian stage (Central Paratethys; Lower Miocene, middle Burdigalian). The revealed trends in bathymetry, primary productivity, bottom-water oxygenation and water energy allow exemplary insights into the paleoenvironment of the terminal Burdigalian Seaway. Several facies of a eutrophic environment with suboxic bottom-waters are distinguished that reflect a transition from an outer neritic to upper bathyal towards a middle neritic setting under the influence of storm events and currents.

A comparison with available data from Upper Austria and Bavaria consistently shows the regressive trend during the late early Ottnangian. In Upper Austria, the deep-water facies from the lower part of the stratotype represents the most distal sediments. The upper part together with localities closer to the northern coast records inner to middle neritic environments that are heavily affected by tidal currents. The facies distribution results from the progradation of a tide-influenced environment along the northern shelf of the North Alpine Foreland Basin, heralding the closure of the Burdigalian Seaway. The available age estimate for the stratotype constrains the onset of the regressive phase to 18 Ma.

4.1. Introduction

The North Alpine Foreland Basin (NAFB) represents one of the major sedimentary basins of the Central Paratethys Sea from Oligocene to Early Miocene (Lemcke, 1988; Rögl, 1998a; Wagner, 1998; Kuhlemann and Kempf, 2002). Via the Rhône Basin in the West it acted as the marine

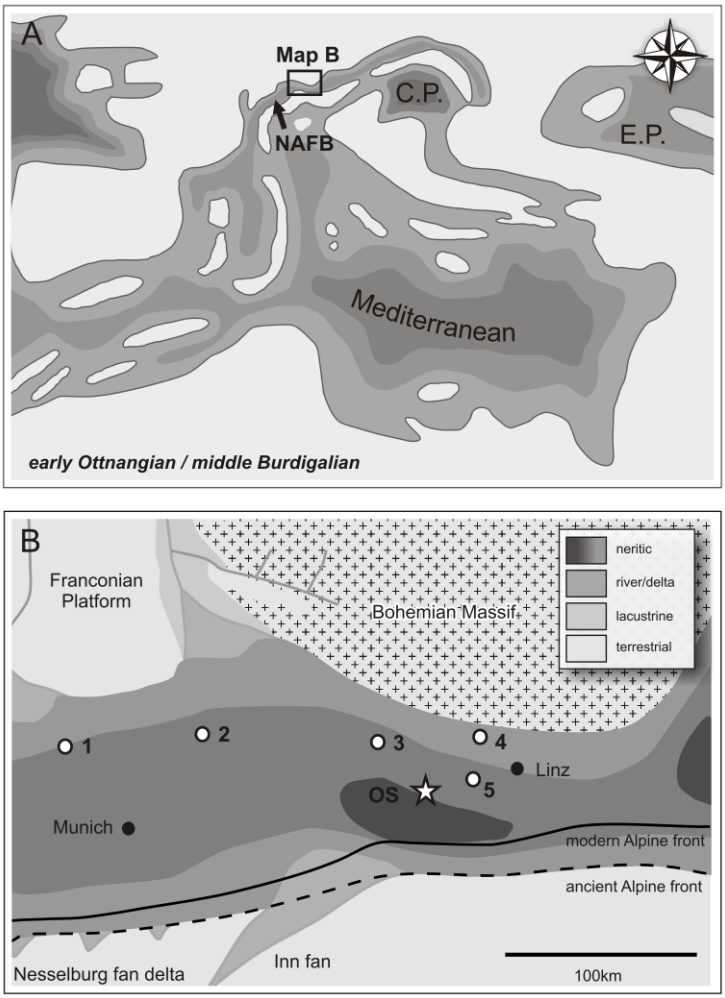

Fig. 4.1. Early Ottnangian (middle Burdigalian) paleogeography of (A) the Central Paratethys and Mediterranean seas and (B) the study area in the North Alpine Foreland Basin (NAFB). The maps follow Rögl (1998a), Kuhlemann and Kempf (2002) and Harzhauser and Piller (2007). OS = stratotype Ottnang-Schanze. 1-5 = early Ottnangian localities in Upper Austria and eastern Bavaria that are compared to the stratotype: 1 = drill-sites Schrobenhausen and Stockhausen, Neuhofen Beds (Pippèrr, 2011); 2 = drill-site Altdorf, Neuhofen Beds (Pippèrr & Reichenbacher, 2010); 3 = outcrops Höhenmühle, Neuhofen and Oberschwärzenbach, Neuhofen Beds (Pippèrr & Reichenbacher, 2010; Pippèrr, 2011); 4 = S margin of Bohemian Massif, Atzbach Fm. (Faupl and Roetzel, 1987); 5 = Wels area, Atzbach and Ottnang Fms. (Rupp and Haunold-Jenke, 2003).

gateway between the Western Mediterranean/Atlantic realm and the Central Paratethys (Fig. 4.1a; Rögl, 1998a; Kuhlemann and Kempf, 2002). The connection was only interrupted during late Chattian and Aquitanian, when the gateway was temporarily blocked and freshwater environments developed in the west (Berger, 1996). A major transgression re-established basin-wide marine conditions during the early Burdigalian, initiating a wave of faunal immigration from the Atlantic and Mediterranean into the Central Paratethys (Vavra, 1979; Berger, 1996; Schlunegger et al., 1997; Rögl, 1998a; Kroh and Harzhauser, 1999; Mandic and Steininger, 2003; Kroh and Menkveld-Gfellner, 2006). This newly established gateway is commonly referred to as the Burdigalian Seaway (Allen et al., 1985). In contrast to the wide and deep-marine Oligocene foreland basin, the Burdigalian Seaway was a strait with extensive shelf areas narrowed by the advancing Alpine thrust front. Deep-water environments were limited to the remnants of the up-filled Puchkirchen Basin and the easternmost part of the NAFB along the steep escarpment of the Bohemian Massif (Wenger, 1987; Rögl, 1998a; Wagner, 1998; Kuhlemann and Kempf, 2002; Rupp and Haunold-Jenke, 2003; Roetzel et al., 2006; Grunert et al., 2010a). The narrowing of the basin resulted in amplified currents that are linked to increased tides. The widespread tidal deposits along the northern shelf have become a prominent example for sedimentation under meso- and macrotidal control and complex interacting current patterns have been discussed in a number of

sedimentological and modelling studies (Homewood and Allen, 1981; Allen and Homewood, 1984; Allen et al., 1985; Faupl and Roetzel, 1987; 1990; Keller, 1989; Tessier and Gigot, 1989; Lesueur et al., 1990; Krenmayr, 1991; Schaad et al., 1992; Martel et al., 1994; Sztanó, 1994; 1995; Sztanó and De Boer, 1995; Uchmann and Krenmayr, 1995; 2004; Krenmayr et al., 1996; Salvermoser, 1999; Bieg, 2005; Heimann et al., 2009; Grunert et al., 2010a). Marine sedimentation in the NAFB finally ceased due to its constant upfill during the middle Burdigalian, marking the onset of a major paleogeographic reorganisation of the Central Paratethys (Berger, 1996; Rögl, 1998a; Harzhauser and Piller, 2007).

In the present study, we provide a detailed facies analysis of the section Ottnang-Schanze which represents the stratotype for the regional Ottnangian stage (Lower Miocene, middle Burdigalian; Figs. 4.2, 4.3). Since its initial description in the 19th century and the designation as holostratotype by Rögl et al. (1973) only few data on the section have been published (e.g., Rupp et al., 1991; Rupp and van Husen, 2007; Rupp et al., 2008). The facies of the outcrop is commonly summarized as a euhaline sublittoral environment (Rögl et al., 1973; Zorn, 1995; Janz and Vennemann, 2005; Rupp and van Husen, 2007; Rupp et al., 2008). However, this interpretation is based on a small number of samples and no information on their relative position within the outcrop is given in any publication. The lack of detailed paleoenvironmental information is all the more surprising as the

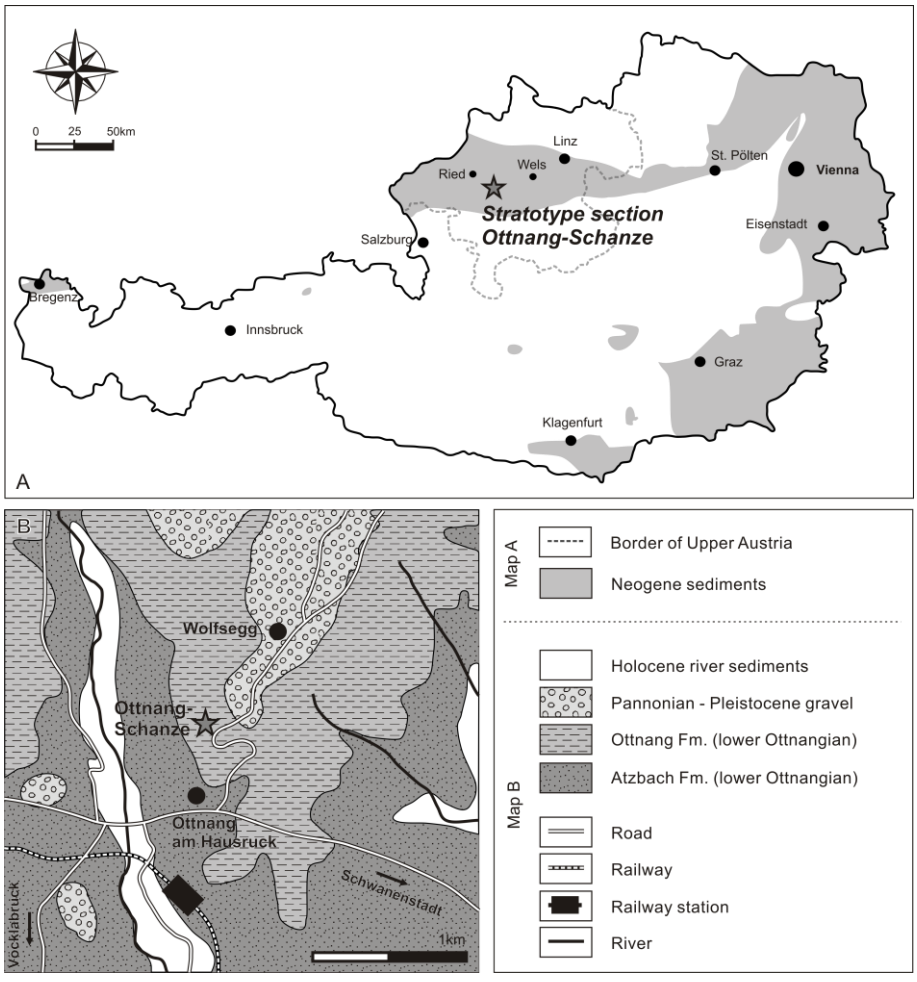

Fig. 4.2. (A) Location of the stratotype section in the Austrian part of the NAFB. (B) Geography and geology of the study area based on Krenmayr and Schnabel (2006) and Rupp et al. (2008).

lithology of the section indicates various depositional environments (Fig. 4.3; Grunert et al., 2010b).

The herein presented analyses of microfossil assemblages (benthic foraminifers, dinoflagellate cysts, calcareous nannoplankton), grain-size and background gamma radiation is based on new sample material and allows a detailed evaluation of the paleoenvironment. Facies types will be discussed with respect to the paleoecological key-parameters water depth, water energy, nutrient availability, primary productivity and bottom water oxygenation, and the revealed facies development will exemplarily document the dynamic paleoenvironment of the terminal Burdigalian Seaway.

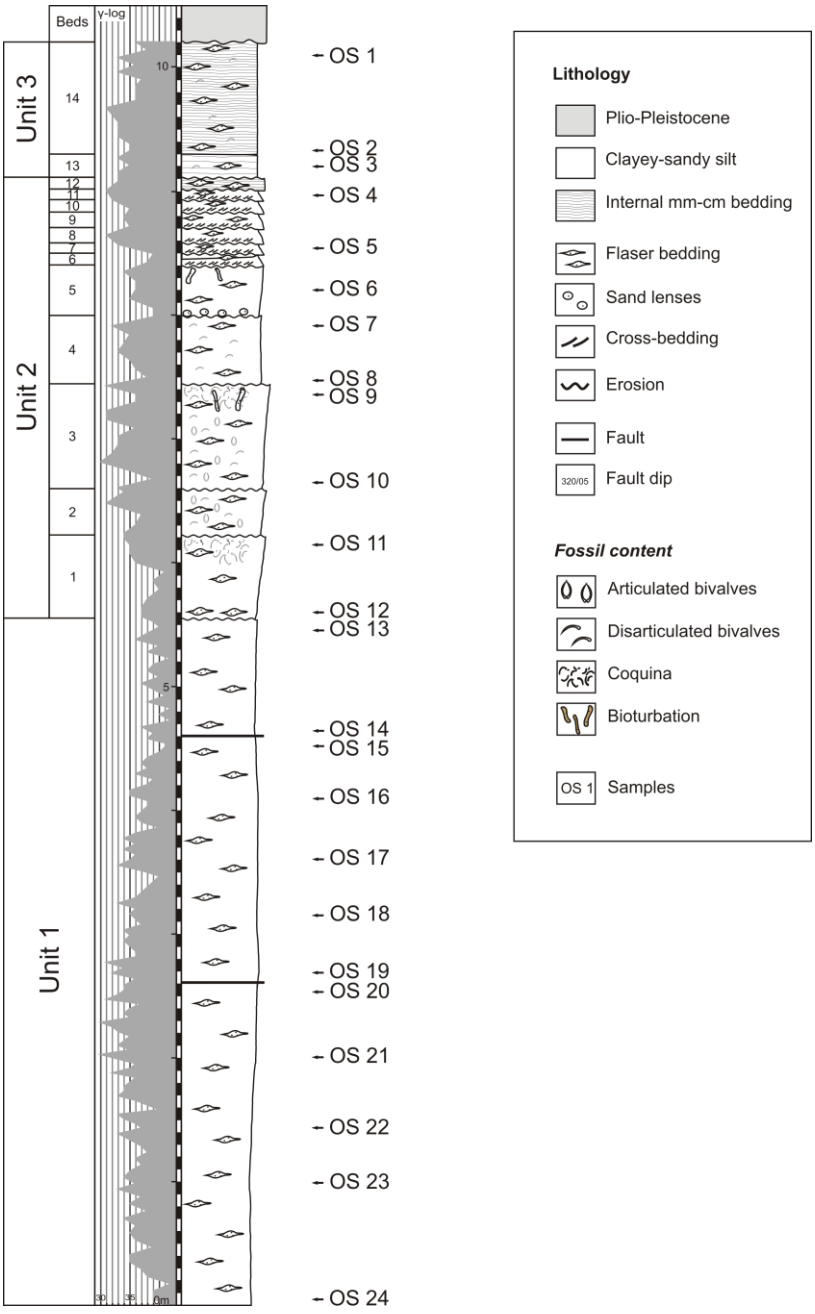

Fig. 4.3. Lithological units, background gamma radiation and lithology of the stratotype Ottnang-Schanze.

4.2. Regional setting

The studied section Ottnang-Schanze has been chosen as the stratotype for the regional Ottnangian stage by Rögl et al. (1973). The regional stratigraphic concept for the Central Paratethys originates from its complex paleogeographic history that is reflected in distinct biogeographic patterns (for details see e.g., Harzhauser and Piller, 2007). The concept paralleling global Oligocene-Miocene stratigraphy has been established over 40 years ago mainly on the basis of endemic fossil assemblages and has been applied to the Central Paratethys since then (Cicha et al., 1967; Steininger and Seneš, 1971; Baldí and Seneš, 1975; Papp et al., 1973, 1974, 1978, 1985; Stevanović et al., 1990). For each of the regional stages a holostratotype and several faciostratotypes have been

selected (Piller et al., 2007). As they represent characteristic facies of regional importance these sections do not follow the GSSP concept of the International Commission for Stratigraphy introduced by Hedberg (1976). More recently, larger data-sets and new stratigraphic approaches allow an improved calibration of the regional stages to the international chronostratigraphic framework (e.g., Rögl, 1998a; Piller et al., 2007; Lirer et al., 2009; de Leeuw et al., 2010; Grunert et al., 2010b; Vasiliev et al., 2010). According to Piller et al. (2007), the Ottnangian corresponds to the middle Burdigalian Bur 3-cycle (Abreu and Haddad, 1998; Fig. 4.4).

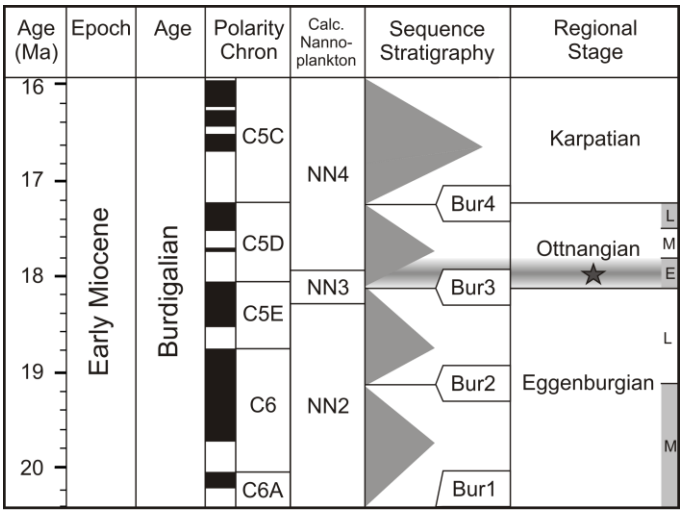

Fig. 4.4 Global and regional stratigraphy of the Burdigalian according to Piller et al. (2007). Correlation of the stratotype with the international time-scale (Lourens et al., 2004) is based on Grunert et al. (2010b).

The study area is located in the NAFB of Upper Austria (Fig. 4.2). The Ottnangian sediments in the region are summarized in the Innviertel Group (Papp and Cicha, 1973; Rupp et al., 2008). While the lower and middle Ottnangian silts and sands originate from fully marine transgressive and highstand phases, the brackish-fluvial *Oncophora* Beds represent the regressive facies of the upper Ottnangian. The sediments of the stratotype section belong to the lower Ottnangian Ottnang Formation that summarizes the pelitic basinal deposits in the area (Rupp et al., 2008; Grunert et al., 2010b). The average thickness of the Ottnang Fm. is reported with 80-100m and shows considerable lateral variations (Bürgl, 1949; Aberer, 1958; Kaltbeitzer, 1988; Wagner, 1998). The Ottnang Fm. overlies the Atzbach Fm., the Kletzenmarkt-Glaukonit Fm. and the Plesching Fm. and partly interfingers with these units. It is followed up by the middle Ottnangian Ried and Reith Fms. and the Enzenkirchen Sands (Rupp and van Husen, 2007; Rupp et al., 2008). Detailed information on the geological setting can be found on the Austrian geological maps ÖK 200 “Upper Austria” (Krenmayr and Schnabel, 2006) and ÖK 47 “Ried im Innkreis” (Rupp et al., 2008).

The section Ottnang-Schanze is located in the Vöcklabruck district, c. 700 m SSW Wolfsegg and 500 m N of the village Ottnang in Upper Austria (Fig. 4.2). It is part of an abandoned clay pit near a memorial to the Peasant Wars (called “Schanze”) and has been declared a natural heritage site and geotop (Rögl et al., 1973; Reiter, 1989).

At the outcrop and its surroundings the Ottnang Fm. overlies the Atzbach Fm. The contact between the two formations is not exposed at the outcrop but the Atzbach Fm. has been reported from the close-by village of Nieder-Ottnang (Rögl et al., 1973, p. 142; Roetzel and Rupp, 1991). Based on geological maps and information from drill-sites in the vicinity of the stratotype, most of the

Innviertel Group in the study area is made up by the Vöckla and Atzbach Fms. (Aberer, 1958; Schläger, 1988; personal communication R. Hinsch, RAG). The Ottnang Fm. is represented with a thickness of 40-60 m. Its top is eroded and covered by late Miocene and Pleistocene deposits (Rögl et al., 1973; Schläger, 1988; Rupp et al., 2008).

The age of the section and the Ottnang Fm. in general has been discussed since the 19th century (see Rögl et al., 1973; Rupp et al., 2008; Grunert et al., 2010b for summaries). Recently, Grunert et al. (2010b) presented a conclusive calibration of the stratotype to an absolute age of 18.06-17.95 Ma by using a combination of bio- and magnetostratigraphy.

4.3. Material and methods

4.3.1. Lithology

A detailed lithological log of the succession and 24 samples (OS 1-24) were taken in 2007 (Fig. 4.3). Grain-size analysis of the sample material was conducted by wet sieving and using a Sedigraph for grain-sizes <0.063mm at the Geological Survey of Austria. Background gamma radiation was measured with a portable scintillation counter (Heger-Breitband-Gammasonde).

4.3.2. Micropaleontology

All 24 samples were included in micropaleontological analyses. For foraminiferal analysis, 100g of each sample were treated with diluted H_2O_2 for several hours and wet sieved under running tap water. Dried samples were split using a splitting device described in Rupp (1986) and at least 200 specimens were counted from size fractions >150µm. Foraminiferal species have been identified based on Wenger (1987), Cicha et al. (1998) and Rupp and Haunold-Jenke (2003). For paleoenvironmental analyses, benthic foraminifers were grouped according to their bathymetric distribution, microhabitat, oxygen dependency and organic matter flux (Tabs. 4.1, 4.2).

For dinoflagellate cyst analysis, a standard palynological technique for the extraction of organic-walled microfossils from sediments has been applied with slight modifications following Green (2001). 20-30g of sediment were treated with 100ml of HCl (35%) and then macerated in 30-50ml of cold concentrated HF (48%) overnight to remove any carbonates and silicates. Before sieving (mesh-sizes: 125µm, 20µm), the residues were treated for 30 seconds in an ultrasonic bath and stained with red Safranin "O". Two slides of each sample were prepared by using glycerine jelly as a mounting media and sealed with nail varnish. Dinoflagellate cysts were determined and documented using a Zeiss microscope (Axioplan 2) fitted with a Leica digital camera. 250 dinoflagellate cysts were counted in every sample; the remainder of the slide(s) was then scanned for rare specimens. Taxonomy follows Fensome et al. (1993; 2008). The observed taxa are listed in Tab. 4.3.

Smear slides for nannoplankton investigations were prepared using standard methods and examined with a light microscope (cross and parallel nicols) with 1000x magnification. At least 300 specimens were counted from each sample. A further 100 view squares were checked for

paleoecologically important nannoplankton taxa. The encountered taxa are listed in Tab. 4.4.
Statistical analysis was carried out by using the software PAST (Hammer et al., 2001). Diversity of the individual microfossil groups is expressed by the total number of taxa (S) and the Fisher alpha index (α), the distribution of species within an assemblage is reflected by dominance (D) and equitability (J) (Hammer and Harper, 2006). Cluster analysis (Ward's Method) and non-metric multidimensional scaling (NMDS; Bray-Curtis similarity) were applied to the combined data-sets of all three microfossil groups to define distinct microfossil assemblages (Hammer et al., 2001). Rare taxa (<2% in all samples) and undetermined specimens were excluded from statistical analysis.

4.4. Results

4.4.1. Lithology

The exposed section is 10.2m thick and disturbed by two tectonic faults (Fig. 4.3). Sedimentation shows distinct changes allowing to subdivide the section into three lithological units:
Unit 1 (0-5.5m) shows rather homogeneous greenish-brown sediments of clayey silts and clayey-sandy silts with sand-lenses and flaser bedding. The sand lenses have a lateral extrusion of up to 30 cm and often contain plant debris. Sediments show no bedding and are heavily bioturbated.
Unit 2 (5.5-9.1m) shows an overall coarsening upward trend and is subdivided into 12 beds separated by erosional surfaces. The succession starts with clayey-sandy silts and flaser bedding similar to Unit 1 and soon passes into mollusc-rich pelitic sediments. Each bed shows internal gradation: beds 1-5 reflect coarsening-upward cycles and beds 6-12 fining-upward cycles. Beds with coarsening-upward cycles show indistinct dm-layering and articulated bivalves at the base, passing into bioturbated sediments with bivalve coquinas. Fining-upward cycles (max. thickness: 10 cm) start with ripple-cross-bedded silty sands passing into sandy silts.
Unit 3 (9.1-10.2m) shows two beds with an increased thickness of clayey-sandy silts compared to beds 6-12 with a distinct lamination, flaser-bedding, and disarticulated bivalve shells enriched in sand-lenses.
Gamma logging and grain-size analysis both reflect the three lithologic units recognized in the outcrop during field-work (Tabs. 4.5, 4.6; Figs. 4.3, 4.5). Unit 1 shows clayey silts at the base (OS 24-OS 22), followed by clayey-sandy silts (OS 21-OS 13). The mean grain-size distribution reveals a slight increase (coarsening upward) from the base up to OS 16, caused by an increase in the fine-sand fractions. In the uppermost part of Unit 1 (OS 15-OS 13) an increasing pelitic component is observed. This trend is also reflected by the gamma log trend. The mean grain-size of Unit 1 ranges between 6.4 and 7.2 Phi (A = 6.8 Phi, σ = 0.3).
Unit 2 starts with clayey-sandy silts comparable with Unit 1 (OS 12) which then turn into clayey sand-silts (OS11-OS 8, OS 5). The latter are continuously interrupted by slightly finer clayey-sandy silts (OS 7, OS 6, OS 4). The coarsening trend is also documented in a lowered mean grain-size value of 6.2 Phi (σ = 0.4). Skewness of these sediments is strongly positive (0.6-1.1) indicating the

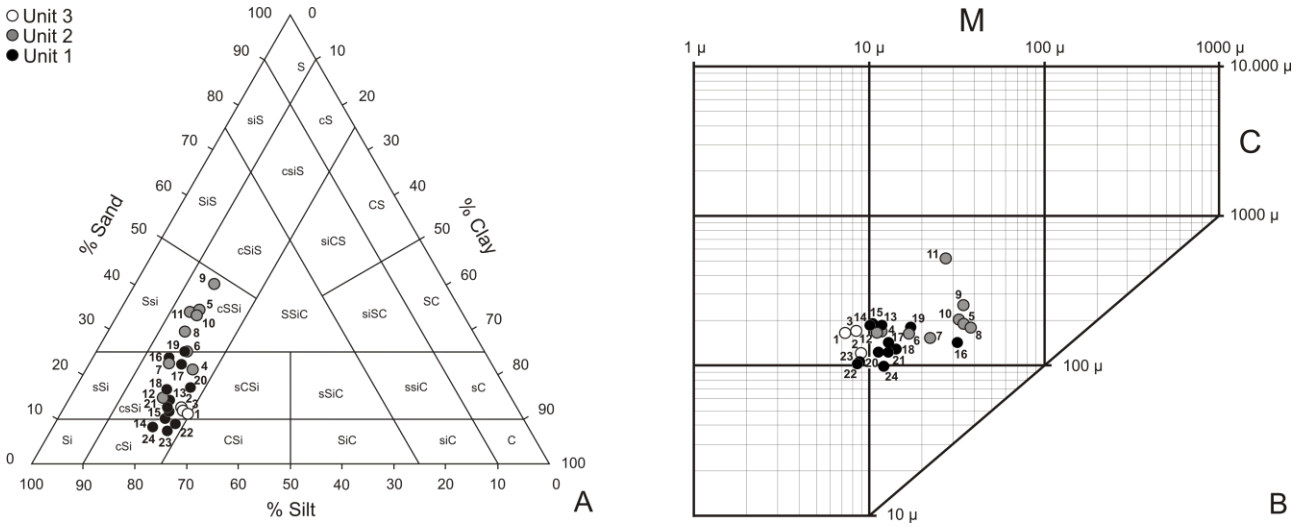

Fig. 4.5. (A) Nomenclature of sediments from the stratotype samples based on grain-size analysis following Füchtbauer (1959) and Müller (1961). (B) CM-diagram for the samples from the stratotype (Passega, 1957).

dominance of the coarser grain sizes in these samples. Also gamma log values are distinctively lower than in Unit 1 reflecting higher sand content.

The clayey-sandy silts of Unit 3 (OS 3-OS 1) show increasing silt- and clay-content with mean values above 7 Phi. Gamma log values show only a small difference to Unit 2 which may be caused by the extensive flaser bedding in this part of the section.

In the CM-diagram (Passega, 1957, 1964; Passega and Byramjee, 1969), in which C is the one-percentile and M is the median of the grain-size distribution, the majority of the samples plots in segment RS that indicates transport in uniform suspension (Fig. 4.5b). Besides a prominent silt-content, sediments from Ottnang-Schanze are characterized by high portions of fine sand and considerable clay-portions. According to Passega (1977) such sediments were deposited by currents where bottom turbulence is not competent to support suspended particles coarser than fine sand. These currents may also include interflows and surface currents. Variation in the CM-diagram mainly occurs along M indicating highest bottom turbulence for samples OS 16, OS 11-8 and OS 5.

4.4.2. Microfossil abundance and diversity

4.4.2.1. Benthic foraminifers

Altogether 117 benthic foraminiferal taxa have been identified (Tab. 4.1). Those with hyaline tests are dominating the samples (A = 85%, σ = 10%; Fig. 4.6). Miliolids show a mean abundance of 10% (σ = 4%) mostly represented by *Sigmoilinita tenuis* and *Sigmoilopsis ottnangensis*. Agglutinated

Fig. 4.6 (right)**.** Trends in benthic foraminiferal assemblages. IN = inner neritic species, ON-B = outer neritic-bathyal species, INF = infaunal species, EPI = epifaunal species, DIF = deep-infaunal species, OX = oxyphilic species, S-DOX = sub- and dysoxic indicators, DOX = dysoxic indicators.

Oxygen
%OX
%S-DOX
%DOx
Food
Oxygen
%EPI
%INF
% epifaunal without Lenticulina
%DIF
Nutrients
Water depth
%ON-B
%IN
Equitability
Dominance
Fisher alpha
No. Species
Test material
Agglutinated
Hyaline
Miliolid
OS 1
OS 2
OS 3
OS 4
OS 5
OS 6
OS 7
OS 8
OS 9
OS 10
OS 11
OS 12
OS 13
OS 14
OS 15
OS 16
OS 17
OS 18
OS 19
OS 20
OS 21
OS 22
OS 23
OS 24
Facies
Beds
Unit 3
Unit 2
Unit 1
0m

taxa occur rarely (A = 6%, σ = 7%) with the exception of samples OS 17 and OS 11-10 (A = 22%, σ = 5%) which show peaks of *Spiroplectammina pectinata*.

The total number of taxa per sample varies between 18 and 42 with an average number of 25 for Unit 1 (σ = 8), 30 for Unit 2 (σ = 7) and 29 for Unit 3 (σ = 12). Within Unit 1, values slowly drop after initially increased numbers in its lower part (OS 24-19), only interrupted by a positive peak in OS 14. Unit 2 shows two patterns of increasing numbers with distinct peaks in OS 9 and OS 4. Unit 3 starts with highest numbers of all samples in OS 3 and drops to lower numbers at the top. Accordingly, Fisher alpha diversity values show similar trends in a range between 3.8 and 13. Unit 1 has an average diversity of 9.9 (σ = 2.5) with highest values in its lower part (OS 24-17) and lower numbers with a positive peak in OS 14 at the top. Unit 2 reveals a lower average value of 6.1 (σ = 2) and peaks in OS 12, OS 9 and OS 4. Finally, Unit 3 has an average diversity of 6.9 (σ = 2.5) with a positive peak in OS 3. Dominance is generally low in the samples of Unit 1 (A = 0.09, σ = 0.02) with a trend towards higher values in Units 2 and 3 ($A_{Unit\ 2}$ = 0.15, $\sigma_{Unit\ 2}$ = 0.07; $A_{Unit\ 3}$ = 0.21, $\sigma_{Unit\ 3}$ = 0.12). Conversely, equitability is high for Unit 1 (A = 0.86, σ = 0.03) and changes towards lower values in Units 2 and 3 ($A_{Unit\ 2}$ = 0.72, $\sigma_{Unit\ 2}$ = 0.09; $A_{Unit\ 3}$ = 0.68, $\sigma_{Unit\ 3}$ = 0.16) with a positive peak in OS 2.

Foraminiferal taxa characteristic for outer neritic-upper bathyal settings show high abundances in Unit 1 and the lower part of Unit 2 (OS 24-12; A = 32%, σ = 12%) and a sharp decrease in samples OS 11-1 (A = 8%, σ = 4%). Conversely, inner neritic taxa mainly occur in samples OS 7-1 (A = 12%, σ = 8%) from Units 2 and 3 while they are very rare (A = 2%, σ = 2%) in Unit 1 and the lower part of Unit 2 (OS 24-8).

Indicators for elevated nutrient flux show highest abundances in Units 2 and 3 (OS 10-1; A = 17%, σ = 5%) mainly related to the abundance of *Caucasina* spp. While samples OS 18-11 show very low values (A = 2%, σ = 3%), the lower part of Unit 1 revealed average values of 8% (σ = 2%) due to the occurences of *Praeglobobulimina* spp. and *Caucasina* spp. (OS 24-19)

Epi- and infaunal taxa are distributed almost equally in most samples of Unit 1 and lowermost Unit 2 (OS 24-12; A_{epi} = 41%, σ_{epi} = 8%; A_{inf} = 39%, σ_{inf} = 7%). Deep infaunal taxa occur in samples OS 16-13 (A = 4%, σ = 2%) and OS 24-21 (A = 8%, σ = 1%). Units 2 and 3 show a general increase in epifaunal taxa (A_{epi} = 53%, σ_{epi} = 6%; A_{inf} = 25%, σ_{inf} = 8%) and absence of deep infaunal taxa. The high abundance of epifaunal taxa primarily results from an average increase of 20% in the abundance of *L. inornata* in the upper part of the section. Peak abundances of epifaunal taxa are documented for OS 11-8, OS 4, OS 3 and OS 1.

Index taxa for sub- and dysoxic bottom waters dominate foraminiferal assemblages throughout the section (A = 78%, σ = 7%). Suboxic taxa dominate over dysoxic taxa, the later being restricted to samples OS 24-21 and OS 16-13 of Unit 1. The abundance of oxyphilic taxa is very low (A = 6%, σ = 4%) with peaks in samples OS 18, OS 15 and OS 10-11.

4.4.2.2. Dinoflagellate cysts

64 taxa of dinoflagellate cysts have been identified (Tab. 4.3). Most taxa show low abundances with

less than 5%, only *Apteodinium* spp., *Achomosphaera/Spiniferites* spp., *Exochosphaeridium insigne*, *Lingulodinium machaerophorum*, *Operculodinium centrocarpum*, *Spiniferites* spp. and round brown cysts occur commonly.

The total number of taxa (A = 31, σ = 4) as well as diversity values (A = 9.1; σ = 1.5) show no clear trends (Fig. 4.7). Dominance is low with lower values for Unit 1 and the lower part of Unit 2 (OS 24-10; A = 0.14, σ = 0.04) than for the upper part of Unit 2 and Unit 3 (OS 9-1; A = 0.3, σ = 0.07).

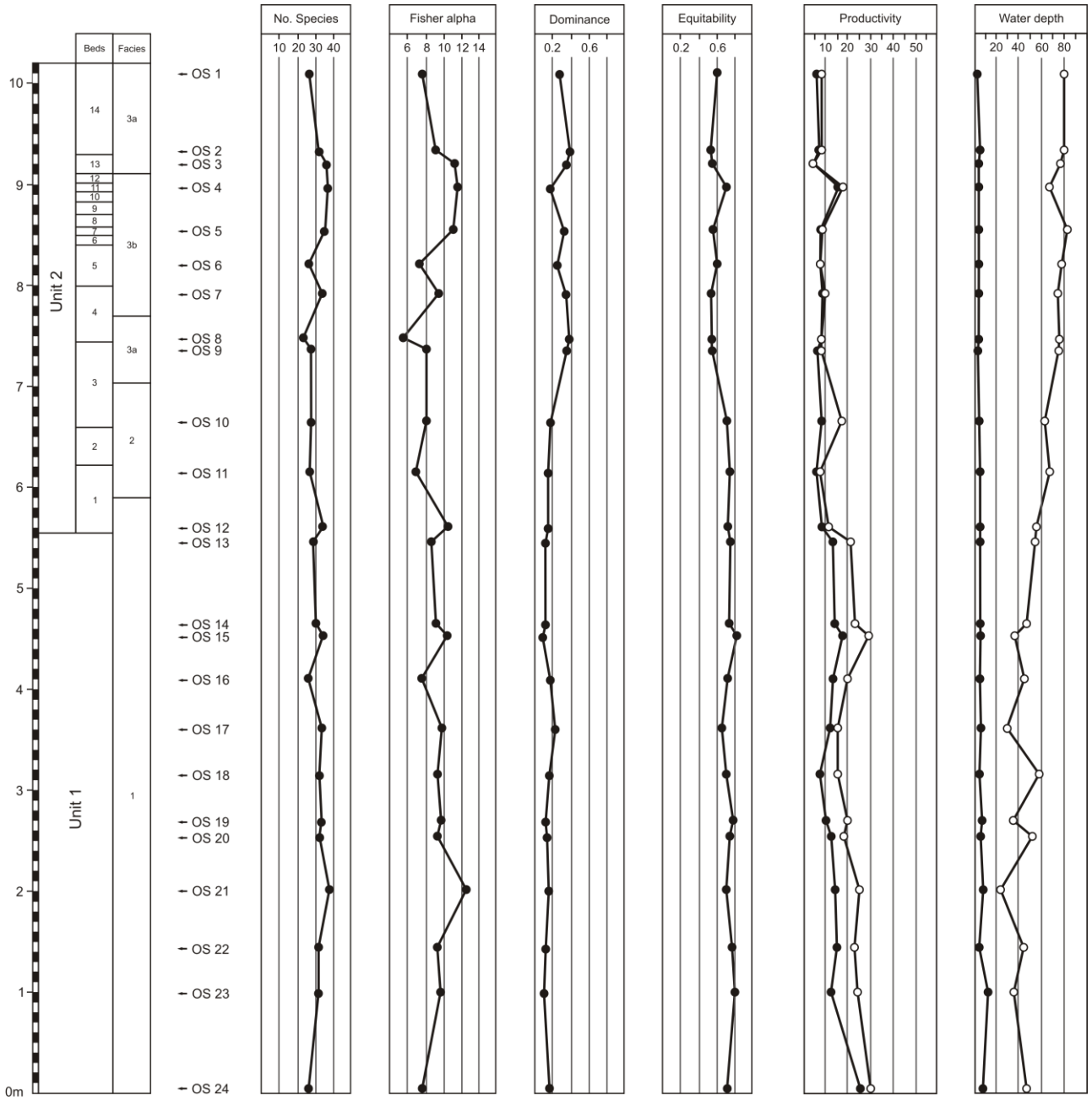

Fig. 4.7. Trends in dinoflagellate cyst assemblages. Coastal taxa include *Apteodinium* spp., *Cleistosphaeridium* spp., *Cribroperidinium* spp., *Exochosphaeridium insigne*, *Glaphyrocysta* spp., *Homotryblium tenuispinosum*, *Operculodinium* spp., *Polysphaeridium zoharyi* and *Tuberculodinium vancompae* (Marret and Zonneveld, 2003; Pross and Brinkhuis, 2005; de Vernal and Marret, 2007). *Impagidinium* spp., *Nematosphaeropsis* spp. and *Reticulatosphaera actinocoronata* are considered oceanic taxa (Pross and Brinhuis, 2005; de Vernal and Marret, 2007).

Accordingly, equitability shows high values in Unit 1 and the lower part of Unit 2 (OS 24-10; A = 0.74, σ = 0.05) and lower values in samples OS 9-1 (A = 0.57, σ = 0.04).

The abundance of oceanic dinoflagellate cysts is low (A = 4%, σ = 2%) and shows highest abundances in the lower part of Unit 1 (OS 24-19; Fig. 4.7). Dinoflagellate cysts associated with coastal environments show a high abundance throughout the samples with an increasing trend from Unit 1 (A = 43%, σ = 10%) to Units 2 and 3 (A = 73%, σ = 8%).

High abundances of indicators for surface water productivity (heterotrophic protoperidinoid cysts, autotrophic *L. machaerophorum*) are documented for Unit 1 (A = 22%, σ = 5%) with highest abundances in samples OS 24-21 and OS 15-13. For Units 2 and 3 a sudden drop of productivity indicators is documented (A = 10%, σ = 4%) mainly related to diminishing numbers of *L. machaerophorum*.

4.4.2.3. Calcareous nannoplankton

A total of 43 autochthonous, 27 Paleogene and 27 Cretaceous nannoplankton taxa have been

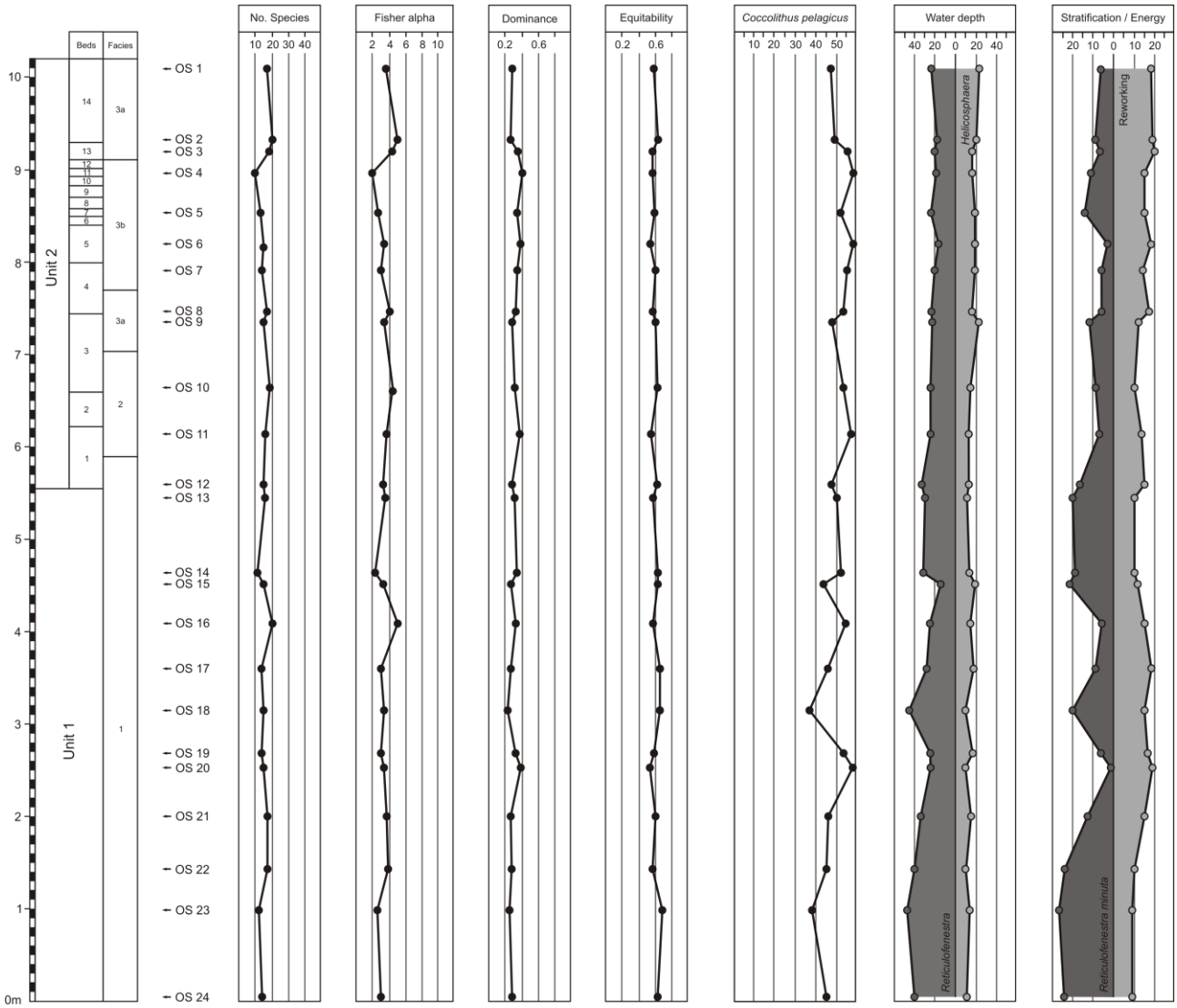

Fig. 4.8. Trends in calcareous nannoplankton assemblages.

determined. They are well preserved and occur commonly throughout the section.

The autochthonous assemblages are dominated by *Coccolithus pelagicus* with mean abundances of 50% (σ = 6%) throughout the section. Its abundance increases slightly from the bottom to the top of the section ($A_{Unit\ 1}$ = 47%, $\sigma_{Unit\ 1}$ = 6%; $A_{Unit\ 2}$ = 55%, $\sigma_{Unit\ 2}$ = 4%; $A_{Unit\ 3}$ = 51%, $\sigma_{Unit\ 3}$ = 5%) reaching highest values in samples OS 8-4 and OS 3 (Fig. 4.8). Besides *C. pelagicus*, only few taxa (*Helicosphaera ampliaperta, Cyclicargolithus floridianus* and reticulofenestrids) occur frequently. Other nannoplankton taxa like the stratigraphically important group of sphenoliths are very scarce or missing.

Reticulofenestrids are mainly represented by *Reticulofenestra excavata* and *R. minuta* (A = 12%, σ = 6%). Values of *R. minuta* show two peaks, one at the base of Unit 1 (OS 24-22; A = 25%, σ = 2%) and one the top of Unit 1 and the base of Unit 2 (OS 14-12; A = 19%, σ = 2%). In Units 2 and 3 values drop (A = 9%, σ = 4%). *R. excavata* shows highest abundances in the lower portion of Unit 1 (OS 24-16; A = 16%, σ = 3%) and then passes into lower values for the rest of the section. Helicosphaerids are mainly represented by *Helicosphaera ampliaperta* which increases in abundance from the bottom to the top of the section ($A_{Unit\ 1}$ = 11%, $\sigma_{Unit\ 1}$ = 4%; $A_{Unit\ 2}$ = 14%, $\sigma_{Unit\ 2}$ = 3%; $A_{Unit\ 3}$ = 15%, $\sigma_{Unit\ 3}$ = 4%).

The total number of autochthonous species varies between 10 and 20 (A = 15, σ = 3) showing highest numbers in Unit 3 (OS 3-1; Fig. 4.8). Diversity is low and varies between 2.0 and 4.7 (A = 3.4, σ = 0.7) with highest values in Unit 3. Variations in dominance (A = 0.31, σ = 0.04) and equitability (A = 0.59, σ = 0.04) are minimal and without trends.

Reworked coccoliths are predominantly composed of Cretaceous taxa (dominated by *Watznaueria barnesae*) and to a lesser degree of Paleogene taxa. They occur frequently (A = 14%, σ = 4%) with highest abundances in two intervals in Units 2 and 3 (OS 8-1) and in the middle part of Unit 1 (OS 21-16).

4.4.3. Microfossil assemblages

Cluster analysis and non-metric multidimensional scaling performed on the combined data-sets of the studied microfossil groups allow the identification of four microfossil assemblages (Tab. 4.7; Fig. 4.9). Within each microfossil group the abundances of only a few taxa are responsible for the differences between the assemblages: (1) the ratio between outer neritic to upper bathyal and inner to middle neritic foraminifers, (2) the ratio between the dinoflagellate cysts *Apteodinium* spp., *Achomosphaera*/*Spiniferites* spp. and *Polysphaeridium zoharyi*, and (3) the ratio between helicospherids and reticulofenestrids in the calcareous nannoplankton.

Assemblage 1 (OS 24-12) corresponds to Unit 1 and lowermost Unit 2. It is mainly composed of infaunal, outer neritic to upper bathyal foraminiferal species (*Amphicoryna ottnangensis*, *Laevidentalina* spp., *Lenticulina* spp., *Gyroidinoides* spp., *Oridorsalis umbonatus*, *Valvulineria complanata)*. Dinoflagellate cysts show approximately equal portions of *Apteodinium* spp. and *Achomosphaera*/*Spiniferites* spp. and elevated abundances of *L. machaerophorum* and

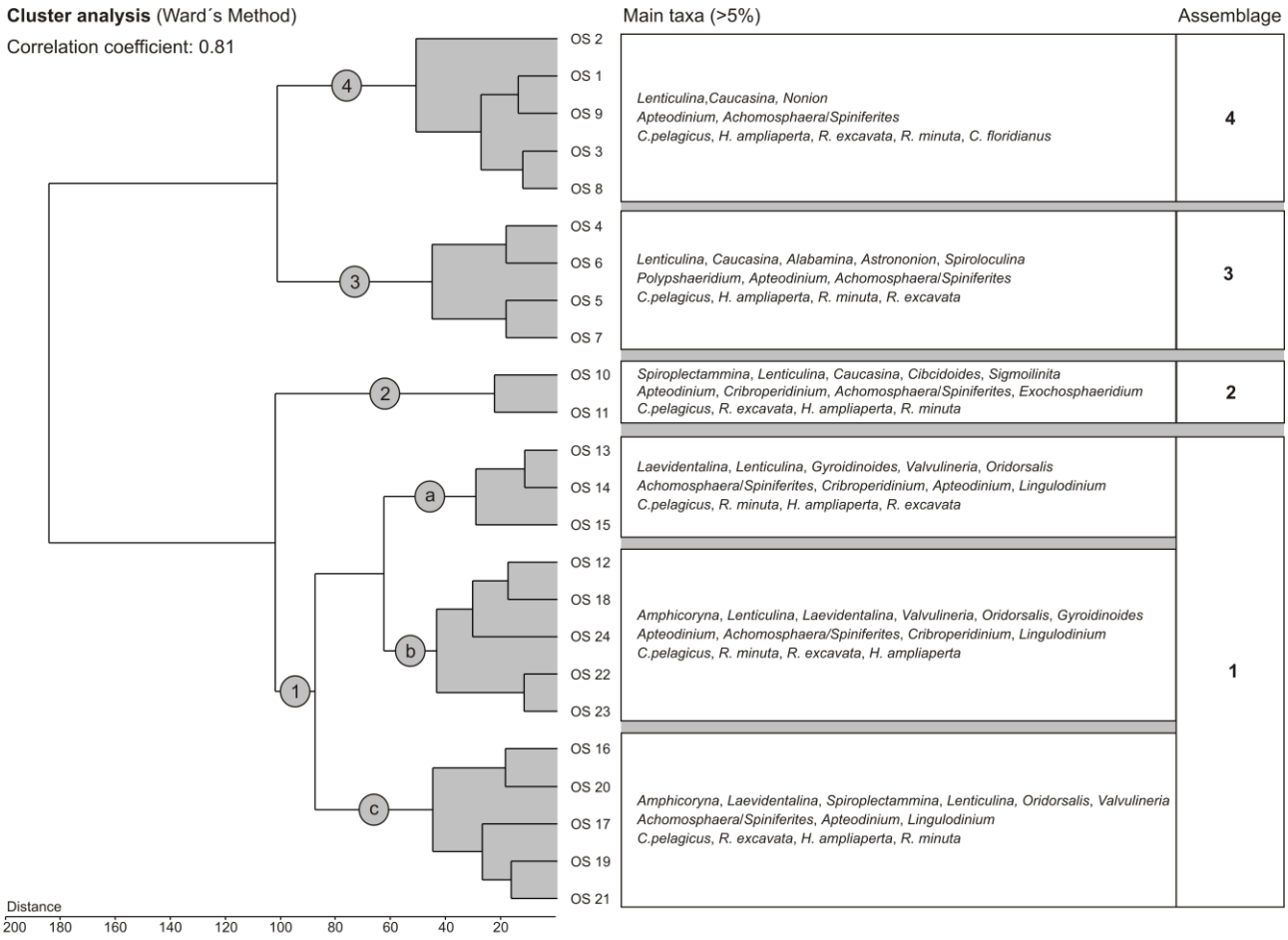
Cluster analysis (Ward´s Method)
Correlation coefficient: 0.81
Main taxa (>5%)
Assemblage
OS 2
OS 1
OS 9
OS 3
OS 8
Lenticulina,Caucasina, Nonion
Apteodinium, Achomosphaera/Spiniferites
C.pelagicus, H. ampliaperta, R. excavata, R. minuta, C. floridianus
4
OS 4
OS 6
OS 5
OS 7
Lenticulina, Caucasina, Alabamina, Astrononion, Spiroloculina
Polypshaeridium, Apteodinium, Achomosphaera/Spiniferites
C.pelagicus, H. ampliaperta, R. minuta, R. excavata
3
OS 10
OS 11
Spiroplectammina, Lenticulina, Caucasina, Cibcidoides, Sigmoilinita
Apteodinium, Cribroperidinium, Achomosphaera/Spiniferites, Exochosphaeridium
C.pelagicus, R. excavata, H. ampliaperta, R. minuta
2
OS 13
OS 14
OS 15
Laevidentalina, Lenticulina, Gyroidinoides, Valvulineria, Oridorsalis
Achomosphaera/Spiniferites, Cribroperidinium, Apteodinium, Lingulodinium
C.pelagicus, R. minuta, H. ampliaperta, R. excavata
OS 12
OS 18
OS 24
OS 22
OS 23
Amphicoryna, Lenticulina, Laevidentalina, Valvulineria, Oridorsalis, Gyroidinoides
Apteodinium, Achomosphaera/Spiniferites, Cribroperidinium, Lingulodinium
C.pelagicus, R. minuta, R. excavata, H. ampliaperta
1
OS 16
OS 20
OS 17
OS 19
OS 21
Amphicoryna, Laevidentalina, Spiroplectammina, Lenticulina, Oridorsalis, Valvulineria
Achomosphaera/Spiniferites, Apteodinium, Lingulodinium
C.pelagicus, R. excavata, H. ampliaperta, R. minuta
1
4
3
2
a
b
c
Distance
200 180 160 140 120 100 80 60 40 20

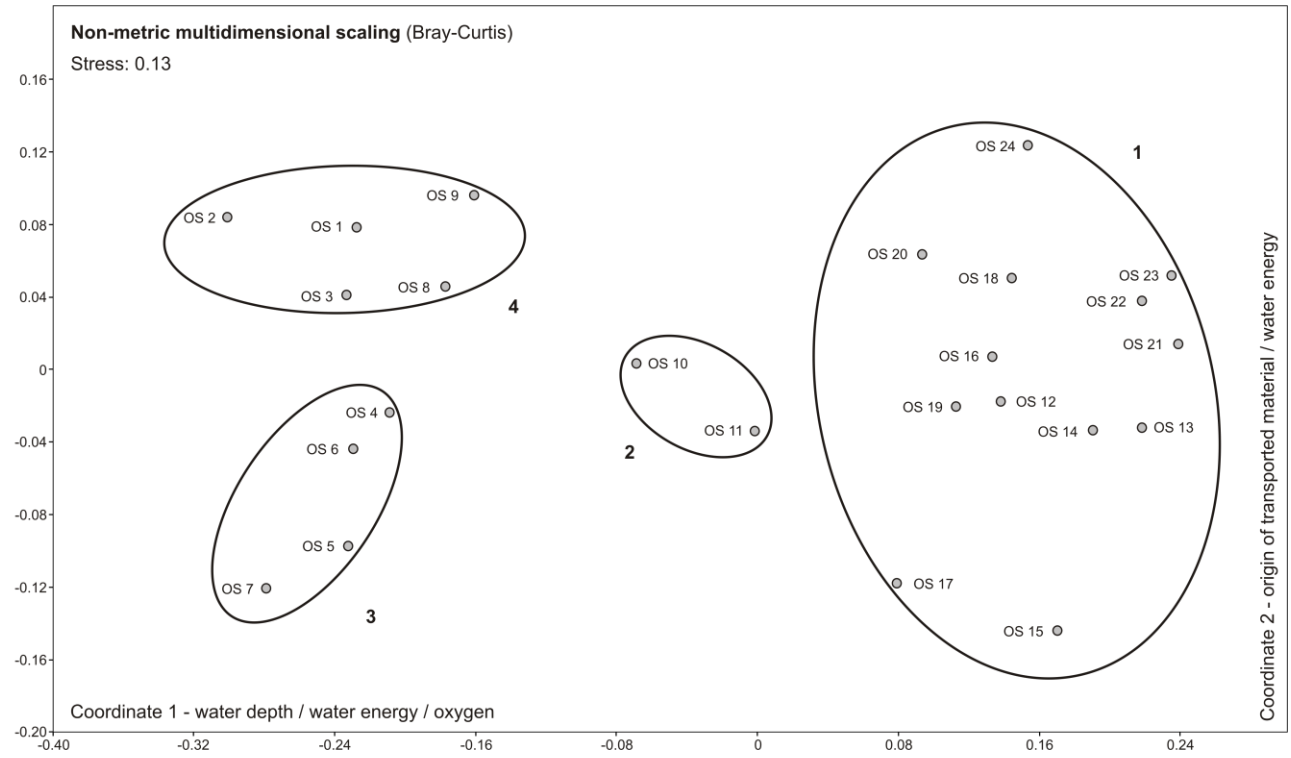
Non-metric multidimensional scaling (Bray-Curtis)
Stress: 0.13
OS 2
OS 1
OS 9
OS 3
OS 8
4
OS 4
OS 6
OS 5
OS 7
3
OS 10
OS 11
2
OS 24
1
OS 20
OS 18
OS 23
OS 22
OS 21
OS 16
OS 19
OS 12
OS 14
OS 13
OS 17
OS 15
0.16
0.12
0.08
0.04
0
-0.04
-0.08
-0.12
-0.16
-0.20
-0.40 -0.32 -0.24 -0.16 -0.08 0 0.08 0.16 0.24
Coordinate 1 - water depth / water energy / oxygen
Coordinate 2 - origin of transported material / water energy

Cribroperidinium spp. Coccoliths are characterized by highest abundances of reticulofenestrids and lowest abundances of helicosphaerids of all assemblages.

In contrast to assemblages 2-4, cluster analysis suggests three subclusters (1a-c) for assemblage 1 that are mainly determined by changes in the abundance of *A. ottnangensis*, *Cribroperidinium* spp., *E. insigne*, *Reticulofenestra excavata* and *R. minuta*. However, the bulk of microfossil taxa are equally distributed in clusters 1a-c and the results from NMDS indicate that their internal organisation is not very robust. Consequently, the assemblages of all three subclusters are considered parts of one assemblage.

Assemblage 2 (OS 11-10) from the lower part of Unit 2 (beds 1-3) shows a composition intermediate between assemblages 1 and 3-4. Foraminifers reveal highest abundance of *S. pectinata* of all samples together with increased occurrences of *L. inornata*, *Caucasina* spp., *Cibicidoides* spp. and *S. tenuis*. Except for *L. inornata*, taxa characteristic for Assemblage 1 occur in very low numbers with *A. ottnangensis* as the most common. Dinoflagellate cysts show affinities to assemblages 3-4 with high abundances of *Apteodinium* spp. and significantly decreased abundances of *Achomosphaera/Spiniferites* spp. and *L. machaerophorum* while increased abundances of *Cribroperidinium* spp. and *E. insigne* indicate relations to assemblage 1. Reticulofenestrids decrease markedly in their abundance while helicosphaerids show a slight increase.

Assemblage 3 (OS 7-4) comprises samples from the upper portion of bed 4 up to bed 12 of Unit 2. *L. inornata* and *Caucasina* spp. dominate the foraminiferal assemblages and *Alabamina tangentialis*, *Astrononion perfossum* and *Spiroloculina* spp. occur frequently. Unusually high abundance of *P. zoharyi* together with *Apteodinium* spp. and low occurrences of *Achomosphaera/Spiniferites* spp. characterize dinoflagellate cysts. The ratio between reticulofenestrids and helicosphaerids is approximately even.

Assemblage 4 (OS 9-8, 3-1) summarizes the upper part of bed 3 and the lower portion of bed 4 of Unit 2 and Unit 3. Foraminifers are dominated by *L. inornata* and *Caucasina* spp. with minor abundance of *Nonion commune*. Amongst dinoflagellate cysts, *Apteodinium* spp. show highest abundance of all samples while *Achomosphaera/Spiniferites* spp. reveal very low abundance. Reticulofenestrids and helicosphaerids are evenly distributed.

4.5. Discussion

Paleogeographic reconstructions indicate that the sediments of the stratotype were deposited

Fig. 4.9 (left). Statistical analyses based on foraminiferal, dinoflagellate cyst and calcareous nannoplankton assemblages. (A) Cluster analysis with indication of the main taxa characterizing each of the revealed clusters and the inferred assemblages 1-4. (B) Non-metric multidimensional scaling with position of assemblages 1-4. Gradients of environmental parameters determining the distribution of the samples along each of the coordinates are indicated.

towards the centre of the NAFB, c. 50-60km off the northern coastline along the Bohemian Massif (Fig. 4.1b; Kuhlemann and Kempf, 2002). Consequently, the paleoenvironment was described as a tranquil sublittoral shelf in previous studies (Rögl et al., 1973; Wagner, 1998; Kuhlemann and Kempf, 2002; Rupp et al., 2008). Based on the new results that indicate a more diverse depositional environment for the stratotype, several types of facies will be discussed in the following. The improved facies model will then be compared to previous studies from Upper Austria and eastern Bavaria in order to put it in the context of the overall development along the shelf of the terminal Burdigalian Seaway.

4.5.1. Facies development

4.5.1.1. Facies 1: Outer neritic to bathyal "Schlier of Ottnang"

Lithology: Unit 1, Unit 2 / bed 1
Samples: OS 24-12
Fossil assemblage: 1

Facies 1 represents the characteristic "Schlier of Ottnang"-facies which has been frequently described from the studied outcrop as well as from the Ottnang Fm. in general (Reuss, 1864; Petters, 1936; Bürgl, 1949; Aberer, 1958; Rögl et al., 1973; Hochuli, 1978; Rupp and van Husen, 2007; Rupp et al., 2008). The foraminiferal assemblages with *Laevidentalina* spp., *Oridorsalis umbonatus*, *Gyroidinoides* spp. and *Valvulineria complanata* are characteristic for an outer neritic to bathyal setting of 100-250m (e.g., Poag, 1981; Wenger, 1987; Leckie and Olson, 2003; Murray, 2006). The accessory benthic foraminifers *Amphicoryna ottnangensis*, *Cibicidoides* spp., *Nonion commune*, *Spiroplectammina pectinata* and *Sigmoilopsis ottnangensis* support this interpretation (Wenger, 1987; Leckie and Olson, 2003; Murray, 2006; Frieling et al., 2009; Pippèrr and Reichenbacher, 2010). Diversity values between 5.2-13 range well within those reported for benthic foraminifers from normal marine shelf and deep-water assemblages (Murray, 2006). The occurrences of the dinoflagellate cysts *Nematosphaeropsis* spp., *Reticulatosphaera actinocoronata* and *Impagidinium* spp. as well as increased dinoflagellate diversity additionally indicate an outer neritic-bathyal environment (Dale, 1996; Vink et al., 2000; Pross and Brinkhuis, 2005; de Vernal and Marret, 2007).
A eutrophic environment with high surface water productivity is suggested by all studied biota. Amongst dinoflagellate cysts, increased abundance of heterotrophic protoperidinoid taxa and the autotrophic *L. machaerophorum* documents fairly productive surface waters (Marret and Zonneveld, 2003). Eutrophic surface waters stimulating high primary productivity are also indicated by high abundances of *Coccolithus pelagicus* and *Reticulofenestra minuta*. The latter has been reported to thrive along eutrophic continental margins with increased continental runoff and river input (Haq, 1980; Aubry, 1992; Flores et al., 2005; Wade and Bown, 2006). Further indications for increased primary productivity are documented in literature by Rögl et al. (1973)

and Bachmann (1973) who report high amounts of diatoms, radiolarians and silicoflagellates. Bachmann (1973), points out that many of the silicoflagellates are similar to those of a contemporaneous upwelling site in the Lower Austrian NAFB (Roetzel et al., 2006; Grunert et al., 2010b). For the Upper Austrian study area, riverine input via the Wachtberg delta has been suggested as the primary source of nutrients during the Ottnangian (Faupl and Roetzel, 1987; Brügel et al., 2003).

Increased organic matter flux to the sea-floor is clearly documented in benthic foraminifers which are largely composed of infaunal species adapted to sub- and dysoxic environments. Food availability and oxygenation of bottom waters are antagonistic key-parameters that determine the distribution of benthic foraminifers ("TROX" and "TROX-2" models; Jorissen et al., 1995; van der Zwaan et al., 1999). The high food availability of eutrophic environments usually results in low oxygenated bottom waters due to microbial degradation of organic matter and foraminiferal assemblages are dominated by infaunal species. At Ottnang-Schanze, the abundances of infaunal foraminifers as well as index species for lowered oxic conditions suggest a eutrophic, suboxic environment for Facies 1. The poorly oxygenated environment is also reflected in the composition of the mollusc fauna with high amounts of chemosymbiont bearing lucinids and infaunal echinoids like *Brissopsis ottnangensis* (Rögl et al., 1973; Kroh, 2007; Rupp and van Husen, 2007). Extant relatives of the later are known to withstand suboxic conditions (Thompson et al., 1985; Smallwood et al., 1999; Levin, 2003).

Sedimentary structures have been obscured by bioturbation and direct evidence for current activity is missing. In most samples the elevated abundance of *R. minuta* suggests a minor influence of currents as blooms of small reticulofenestrids have been described as indicators for a well stratified water column (Ćorić and Hohenegger, 2008). A temporary increase in current strength might be indicated for the middle part of Unit 1 (OS 20-16) where *R. minuta* is less abundant and reworked nannoplankton taxa as well as coastal dinoflagellate cysts become more prominent. This assumption is supported by a higher sand content in samples OS 20-16 similar to OS 11-8 and OS 5 from Unit 2 (Fig. 4.5). Noteworthy, the parallel disappearance of dysoxic foraminiferal index taxa and a decrease in *L. machaerophorum* indicate lowered surface water productivity and better oxygenated, yet suboxic bottom-waters and document subtle changes within the outer neritic – upper bathyal environment of Facies 1.

4.5.2.2. Facies 2: Tide- and storm-influenced outer – middle neritic

Lithology: Unit 2, beds 1-3
Samples: OS 11, 10
Fossil assemblage: 2

Facies 2 marks the beginning of a shallowing trend from an outer neritic to upper bathyal towards a middle neritic environment. Increasing sand content, heavy flaser and wavy bedding, cross bedding, bivalve coquinas, commonly occurring plant debris and erosional surfaces document an

agitated shelf environment under the strong influence of storm events and currents (Johnson and Baldwin, 1996; Reading and Collinson, 1996; Dashtgard et al., in press). The characteristic outer neritic – bathyal foraminiferal communities of Facies 1 are replaced by middle – outer neritic *Spiroplectammina-Lenticulina-Caucasina* assemblages (Wenger, 1987; Leckie and Olson, 2003; Murray, 2006). A shallowing is also suggested by increased abundances of the coastal dinoflagellate cysts of *Apteodinium* spp. and *Cribroperidinium* spp. (Pross and Brinkhuis, 2005).
Based on the low diverse foraminiferal assemblages with *S. pectinata*, *L. inornata* and *Caucasina* spp. bottom-waters remained suboxic due to the constantly high flux of organic matter (Kaiho, 1994; Bernhard and Sen Gupta, 2002; Murray, 2006). Besides the above mentioned foraminiferal taxa the samples are characterized by high abundances of the miliolids *S. tenuis* and *S. ottnangensis*. The fossil and extant records suggest that the abundance of these species is controlled rather by food supply and oxygen conditions than water depth. Accordingly, increased abundances of *S. pectinata* and *S. ottnangensis* in the NAFB have been reported from the outer neritic to bathyal Neuhofen Beds (Wenger, 1987; Pippèrr and Reichenbacher, 2010; Pippèrr, 2011) as well as from marginal inner neritic paleoenvironments (Frieling et al., 2009). *S. ottnangensis* is an endemic species of the Burdigalian Central Paratethys (Wenger, 1987; Cicha et al., 1998) and often compared to the extant *S. schlumbergeri* from the Adriatic Sea. Jorissen (1987) showed a positive correlation of *S. schlumbergeri* with organic matter input.

4.5.2.3. Facies 3: Current-influenced middle neritic

Lithology: Unit 2, Unit 3
Samples: OS 9-1
Fossil assemblages: 3, 4

The abundance of inner neritic benthic foraminifers in Facies 3 clearly increases (e.g., *Ammonia* spp., *Astrononion perfossum*, *Elphidium* spp., *Quinqueloculina* sp., *Spiroloculina* spp.) while outer neritic – bathyal taxa, most noteably *Gyroidinoides* spp., *O. umbonatus* and *V. complanata*, vanish. This trend coincides with an increased sand content and most likely reflects a shallowing towards a middle neritic environment and increased current-driven sediment transport from the inner shelf. The bathymetric and hydrodynamic changes are further documented in the high abundances of the coastal dinoflagellate cysts *Apteodinium* spp. and *Polysphaeridium zoharyi*, decreasing abundances of *Reticulofenestra minuta* and increased reworking of calcareous nannoplankton (Marret and Zonneveld, 2003; Pross and Brinkhuis, 2005; Ćorić and Hohenegger, 2008). Furthermore, an evaluation of diatom assemblages from samples OS 9-7, 4 and 1 revealed assemblages mainly composed of the shallow marine taxa *Paralia sulcata*, *Actinocyclus* spp., *Coscinodiscus* spp. and *Sceptroneis* sp. (pers. comment I. Galović; Fenner, 1991; Zong, 1997; McQuoid and Nordberg, 2003a, b; Gebühr et al., 2009).
Eutrophic conditions together with elevated surface water productivity prevailed as strong currents delivered high amounts of nutrients from the Wachtberg delta to the study area (Faupl and Roetzel,

1987). Increased nutrient input is reflected by the dominance of *C. pelagicus* and the increasing abundance of *H. ampliaperta*. Dinoflagellate cyst assemblages show an average drop of 12% in productivity proxies. This is mainly caused by the vanishing of *L. machaerophorum* whereas the abundance of heterotrophic protoperidinoids remains constant. *L. machaerophorum* is the cyst of the autotrophic dinoflagellate *L. polyedrum* which might be outcompeted by siliceous phytoplankton thriving on the increased input of nutrients from the hinterland. Planktic diatoms and silicoflagellates are reported frequently from this part of the section (Bachmann, 1973; Rögl et al., 1973) and large centric valves of diatoms were commonly observed in samples from Units 2 and 3. Together with input of nutrients stimulating phytoplankton growth, food supply for the benthic communities remained high and suboxic index taxa persist. Detritivore *Caucasina* spp. and *F. acuta*, as well as *S. tenuis* and *S. ottnangensis*, taxa that are adapted to high organic matter flux, frequently show increased abundances (Jorissen, 1987; Spezzaferri et al., 2002; Murray, 2006).
Within Facies 3, two different depositional subenvironments (Facies 3a, b) can be distinguished from microfossil assemblages and grain-size analysis. These reflect different levels of water energy and transport and varying sources of transported material within the middle neritic environment.

Facies 3a

Lithology: Unit 2, beds 3-4, 13-14
Samples: OS 9-8, 3-1
Fossil assemblage: 4

A middle neritic environment is suggested for Facies 3a by the high occurrences of *L. inornata* and *Caucasina* spp. together with commonly occurring *N. commune* and *A. tangentialis* (Murray, 1984; Liu et al., 1997; Leckie and Olson, 2003; Murray, 2006; Frieling et al., 2009). Highest abundances of *Apteodinium* spp. in all assemblages and the presence of species of *Cleistosphaeridium*, *Cribroperidinium* and *Operculodinium* document increased transport from the inner shelf as a consequence of increased current strength (Brinkhuis, 1994; Marret and Zonneveld, 2003).
While all samples of Facies 3a show great similarities in microfossil abundance, grain-size analysis reveals increased amounts in silt and clay for samples OS 1-3 clearly separating them from OS 8-9 (Fig. 4.5). This change is accompanied by a different set of sedimentary structures in Unit 3 including commonly occurring lamination and small-sized mollusc coquinas in sand lenses besides still heavy flaser bedding. We suggest that the latter features indicate at least temporarily decreased water energy and transport.

Facies 3b

Lithology: Unit 2, beds 4-12
Samples: OS 7-4
Fossil assemblage: 3

The most prominent feature that distinguishes Facies 3b from the other revealed facies types is the high abundance of *Polysphaeridium zoharyi* in the dinoflagellate assemblages and the increased abundance of *Spiroloculina* spp. in the foraminiferal assemblages. Today, *P. zoharyi* is known from mesotrophic inner neritic near-shore associations and littoral embayments, often associated with the presence of mangrove swamps (Williams and Bujak, 1977; Marret and Zonneveld, 2003). Its ability to tolerate strong salinity fluctuations has been documented from estuarine environments with increased freshwater influx (e.g., Rossignol, 1962; Edwards, 1998; Marret and Zonneveld, 2003; de Vernal and Marret, 2007) as well as high saline lagoonal environments (Wall and Warren, 1969; Wall et al., 1977; Morzadec-Kerfourn, 1979, 1983; Bradford and Wall, 1984; McMinn, 1990; Edwards and Andrle, 1992). From the Central Paratethys, increased abundances of *P. zoharyi* have been reported from a middle Ottnangian restricted near-shore environment (Jiménez-Moreno et al., 2006).

Species of *Spiroloculina* are commonly described from marine-hypersaline environments with a maximum water-depth of 40m (e.g., Graham and Militante, 1959; Kumar and Manivannan, 2001; Wang and Chappell, 2001; Gandhi and Rajamanickam, 2004; Murray, 2006; Izuka and Resig, 2008). Langer and Lipps (2003) report assemblages composed of thin-shelled *S. attenuata, Ammonia* spp. and *Elphidium striatopunctatum* from bay inlets of the Madang Lagoon in Papua New Guinea and relate its distribution to high fresh-water runoff, organic input and low-oxygen conditions. In many cases these shallow-water environments are influenced by strong current activity (e.g. Gandhi and Rajamanickam, 2004; Gargouri-Ben Ayed et al., 2007). In contrast, the commonly occurring hyaline foraminiferal species *A. tangentialis*, *A. perfossum*, *Caucasina* spp., *F. acuta*, *N. commune* and *L. inornata* are known from fully marine middle neritic environments (e.g., Murray, 1984; Liu et al., 1997; Leckie and Olson, 2003; Murray, 2006). Furthermore, recent and past brackish environments are usually dominated by species of *Ammonia*, *Elphidium* and increased amounts of miliolids and agglutinated taxa (Poag, 1981; Rögl, 1998b; Leckie and Olson, 2003; Culver and Buzas, 2002; Murray, 2006). In our samples these taxa make up only a minor amount of the assemblages and tests of *Quinqueloculina* are often abraded and heavily damaged indicating transport and mixed assemblages. We suggest that Facies 3b documents highest current energy of the section with a potential estuarine source for the transported material.

4.5.3. Facies development of the terminal Burdigalian Seaway

The revealed facies development suggests a prograding sublittoral environment during the late early Ottnangian in the study area. However, at the stratotype the Ottnang Fm. is only represented with its middle to upper part with the top eroded. Including available data of a wider area allows to discuss the revealed bathymetric trend in the context of the overall development of the Burdigalian Seaway during the early Ottnangian:

In the area of Upper Austria, most studies focus on the tide-influenced shelf deposits from which sand waves and tidal channels have been reported along the northern coastline of the Burdigalian

Seaway from the lower Ottnangian Atzbach Fm. (Aberer, 1958; Faupl and Roetzel, 1987, 1990; Krenmayr, 1991; Uchmann and Krenmayr, 1995; Krenmayr et al., 1996; Rupp and van Husen, 2007; Rupp et al., 2008). A meso- and macrotidal setting with current velocities of 0.5m/sec and complex patterns of tidal currents have been suggested in several studies (Faupl and Roetzel, 1987, 1990; Bieg, 2005). Accordingly, benthic foraminiferal assemblages from a study area located c. 30km NE from Ottnang-Schanze near the city of Wels (Fig 2a) document a high energy environment with strong current transport from the inner shelf for the Atzbach Fm. (Petters, 1936; Aberer, 1958; Rupp and Haunold-Jenke, 2003; Rupp et al., 2008). The well-sorted assemblages mainly contain species of *Cibicidoides*, known to occur attached to coarse grained material in high energetic environments (Schönfeld et al., 1997; Murray, 2006), and inner to middle neritic taxa such as *Ammonia*, *Elphidium*, *Lobatula* and *Nonion* (Wenger, 1987; Rupp and Haunold-Jenke, 2003). The Ottnang Fm. as represented by the stratotype is overlying and partly interfingering with these deposits and is regarded as the outer neritic equivalent to the sands of the Atzbach Fm. (Rögl et al., 1973; Roetzel and Rupp, 1991; Krenmayr et al., 2006; Rupp and van Husen, 2007; Rupp et al., 2008). The present study shows however that several facies types can be distinguished along the sublittoral shelf. Different facies types within the Ottnang Fm. have been indicated but not discussed by Rupp and Haunold-Jenke (2003) from the Wels area. There, the faunal composition with high abundances of *Cibicidoides*, *Lobatula*, *Elphidium* and other inner to middle neritic taxa reveals strong similarities with the Atzbach Fm. Given the location of the Wels study area closer to the northern coast and the considerably low abundances of middle to outer neritic foraminifers, a more proximal setting shallower than Facies 3 is indicated for both, the Atzbach and Ottnang Fms.

A bathymetric trend similar to that from the stratotype has been reconstructed from foraminiferal assemblages for the Neuhofen Beds that represent synchronous pelitic deposits in eastern Bavaria (Wenger, 1987; Doppler et al., 2005; Pippèrr and Reichenbacher, 2010; Pippèrr, 2011). While the lower part of the Neuhofen Beds suggests a middle to outer neritic environment with high organic matter flux and suboxic bottom waters, the upper part suggests a shallowing of the environment with higher diversity and better oxygenated bottom waters (Pippèrr and Reichenbacher, 2010; Pippèrr, 2011). The later authors link these trends to the systems tracts of a sequence stratigraphic framework indicating a transgressive phase during the earliest Ottnangian and a maximum flooding surface with a subsequent highstand systems tract during the late early Ottnangian (Zweigel, 1998; Pippèrr, 2011).

The comparison of the data from Upper Austria and eastern Bavaria consistently show a shallowing trend during the late early Ottnangian reflected in different facies types of the prograding northern shelf of the terminal Burdigalian Seaway. In Upper Austria, the lower part of the stratotype represents the most distal sediments deposited during a basin-wide transgression. Its upper part together with more northwards positioned localities represent an inner to middle neritic environment under the influence of storm events and strong currents, the later most likely related to intensified tidal conditions. The present results confirm the interpretation of Pippèrr (2011) that

the maximum marine transgression occurred during early Ottnangian and the available age estimate for the stratotype constrains the maximum flooding surface to c. 18 Ma (Grunert et al., 2010b).

4.6. Conclusions

In the present study, new quantitative micropaleontological, sedimentological and geophysical data are evaluated from the section Ottnang-Schanze, the stratotype for the regional Ottnangian stage (Central Paratethys; Lower Miocene, middle Burdigalian). Assemblages of benthic foraminifers, dinoflagellate cysts, calcareous nannoplankton, grain-size distribution and background gamma radiation reveal trends in bathymetry, primary productivity, bottom-water oxygenation and water energy that indicate a more diverse paleoenvironment than previously suggested. Several facies of a eutrophic environment with suboxic bottom-waters are distinguished that document a transition from an outer neritic to upper bathyal towards a middle neritic environment under the influence of storm events and tidal currents.

Previous studies in eastern Bavaria have shown a regressive trend during late early Ottnangian. A comparison of microfossil data from the stratotype and other localities in Upper Austria indicates that the outer neritic to upper bathyal facies from the lower part of the stratotype represents the most distal sediments. The upper part together with localities situated closer to the northern coast record inner to middle neritic environments under strong influence of tidal currents. The revealed facies distribution results from the progradation of the tide-influenced northern shelf of the North Alpine Foreland Basin, heralding the closure of the Burdigalian Seaway and the final regression of the sea towards the East. The available age dating for the stratotype constrains the onset of the regressive phase to 18 Ma.

4.7. Acknowledgements

The authors would like to thank Ines Galović (Croatian Geological Survey, Zagreb), Ralph Hinsch (Rohöl-Aufsuchungs AG, Vienna), Fred Rögl (Natural History Museum Vienna), Christian Rupp (Geological Survey of Austria, Vienna) and Robert Scholger (University of Leoben) for many helpful comments and discussions. Anton Englert and Franz Topka (Natural History Museum Vienna) are acknowledged for assistance with the field-work. Peter Pohn (Wolfsegg) kindly provided access to the outcrop. This study was financially supported by the Commission for the Paleontological and Stratigraphical Research of Austria (Austrian Academy of Sciences).

4.8. References

Aberer, F., 1958. Die Molassezone im westlichen Oberösterreich und in Salzburg. Mitteilungen der Geologischen Gesellschaft in Wien 50, 23–93.

Abreu, V.S., Haddad, G.A., 1998. Glacioeustatic fluctuations: the mechanism linking stable isotope events and sequence stratigraphy from the Early Oligocene to Middle Miocene. In: Graciansky, C.-P., Hardenbol, J., Jacquin, T., Vail, P.R. (Eds.), Mesozoic and Cenozoic sequence stratigraphy of European basins. Sedimentary Geology Special Publication, vol. 60. Society for Sedimentary Geology, Tulsa, pp. 245–260.

Ainsworth, R.B., Flint, S.S., Howell, J., 2008. Predicting coastal depositional style: influence of basin morphology and accommodation/sediment supply regime within a sequence stratigraphic framework. Recent Advances in Shallow-Marine Stratigraphy. In: Hampson, G.J., Stell, R.J., Burgess, P.B., Dalrymple, R.W. (Eds.), Recent Advances in Models of Siliciclastic Shallow-Marine Stratigraphy: Introduction and Perspectives. Society for Sedimentary Geology Special Publication, vol. 90. Society for Sedimentary Geology, Tulsa, pp. 237–263.

Allen, P.A., Homewood, P., 1984. Evolution and mechanics of a Miocene tidal sandwave. Sedimentology 31, 63–81.

Allen, P.A., Mange-Rajetzky, M., Matter, A., Homewood, P., 1985. Dynamic palaeogeography of open Burdigalian sea-way, Swiss Molasse Basin. Eclogae Geologicae Helveticae 79, 351–381.

Aubry, M., 1992. Late Paleogene calcareous nannoplankton evolution: a tale of climatic deterioration. In: Prothero, D.R., Berggren, W.A. (Eds.), Eocene-Oligocene Climatic and Biotic Evolution. Princeton University Press, Princeton, pp. 272–309.

Bachmann, A., 1973. Die Silicoflagellaten aus dem Stratotypus des Ottnangien. In: Papp, A., Rögl, F., Seneš, J. (Eds.), Miozän M2 – Ottnangien. Die Innviertler, Salgotarjaner, Bantapusztaer Schichtengruppe und die Rzehakia Formation. Chronostratigraphie und Neostratotypen, Miozän der Zentralen Paratethys, vol. 3. Verlag der Slowakischen Akademie der Wissenschaften, Bratislava, 275–295.

Báldi, K., 2006. Paleoceanography and climate of the Badenian (Middle Miocene, 16.4–13.0 Ma) in the Central Paratethys based on foraminifera and stable isotope ($\delta^{18}O$ and $\delta^{13}C$) evidence. International Journal of Earth Science 95, 119–142.

Baldí, T., Seneš, J., 1975. OM – Egerien. Die Egerer, Pouzdraner, Puchkirchener Schichtengruppe und die Bretkaer Formation. Chronostratigraphie und Neostratotypen, Miozän der Zentralen Paratethys, vol. 5. Verlag der Slowakischen Akademie der Wissenschaften, Bratislava.

Barmawidjaja, D.J., Jorissen, F.J., Puskaric, S., Van der Zwaan, G.J., 1992. Microhabitat selection by benthic foraminifera in the northern Adriatic Sea. Journal of Foraminiferal Research 22, 297–317.

Bernhard, J.M., Sen Gupta, B.K., 2002. Foraminifera of Oxygen-Depleted Environments. In: Sen Gupta, B.K. (Ed.), Modern Foraminifera. Kluwer Academic Publishers, Dordrecht-Boston-London, pp. 201–216.

Berger, J.-P., 1996. Cartes paléogéographiques-palinspastiques du bassin molassique suisse (Oligocène inférieur – Miocène moyen). Neues Jahrbuch für Geologie und Paläontologie 202, 1–44.

Bieg, U., 2005. Palaeooceanographic modelling in global and regional scale: An example from the Burdigalian Seaway. Ph.D. Thesis, Eberhard-Karls-Universität Tübingen, Germany.

Bradford, M.R., Wall, D.A., 1984. The distribution of Recent organic-walled dinoflagellate cysts in the Persian Gulf, Gulf of Oman, and northwestern Arabian Sea. Palaeontographica B 192, 1–84.

Brinkhuis, H., 1994. Late Eocene to Early Oligocene dinoflagellate cysts from the Priabonian type-area

(Northeast Italy): biostratigraphy and paleoenvironmental interpretation. Palaeogeography, Palaeoclimatology, Palaeoecology 107, 121–163.

Brügel, A., Dunkl, I., Frisch, W., Kuhlemann, J., Balogh, K., 2003. Geochemistry and Geochronology of Gneiss Pebbles from Foreland Molasse Conglomerates: Geodynamic and Paleogeographic Implications for the Oligo-Miocene Evolution of the Eastern Alps. The Journal of Geology 111, 543–563.

Bürgl, H., 1949. Zur Stratigraphie und Tektonik des oberösterreichischen Schliers. Verhandlungen der Geologischen Bundesanstalt 1946, 123–151.

Cicha, I., Rögl, F., Rupp, C., Ctyroká, J., 1998. Oligocene-Miocene foraminifers of the Central Paratethys. Abhandlungen der Senckenbergischen Naturforschenden Gesellschaft 549, 1–325.

Cicha, I., Seneš, J., Tejkal, J., 1967. M3 (Karpatien). Die Karpatische Serie und ihr Stratotypus. Chronostratigraphie und Neostratotypen, Miozän der Zentralen Paratethys, vol. 1. Verlag der Slowakischen Akademie der Wissenschaften, Bratislava.

Ćorić, S., Hohenegger, J., 2008. Quantitative analyses of calcareous nannoplankton assemblages from the Baden-Sooss section (Middle Miocene of Vienna Basin, Austria). Geologica Carpathica 59, 447–460.

Corliss, B.H., 1991. Morphology and microhabitat preferences of benthic foraminifera from the northwest Atlantic Ocean. Marine Micropaleontology 17, 195–236.

Culver, S.J. and Buzas, M.A., 2002. Biogeography of Neritic Benthic Foraminifera. In: Sen Gupta, B.K. (Ed.), Modern Foraminifera. Kluwer Academic Publishers, Dordrecht-Boston-London, pp. 92–102.

Dale, B., 1996. Dinoflagellate cyst ecology: modeling and geological applications. In: Jansonius, J., McGregor, D.C. (Eds.), Palynology: Principles and Applications. American Association of Stratigraphic Palynologists Foundation Books, vol. 3. American Association of Stratigraphic Palynologists, Dallas, pp. 1249–1275.

Dalrymple, R.W., Choi, K., 2007. Morphologic and facies trends through the fluvial-marine transition in tide-dominated depositional systems: A schematic framework for environmental and sequence-stratigraphic interpretation. Earth-Science Reviews 81, 135–174.

Dashtgard, S.E., Gingras, M.K., MacEachern, J.A., 2009. Tidally modulated shorefaces. Journal of Sedimentary Research 79, 793–807.

Dashtgard, S.E., MacEachern, J.A., Frey, S.E., Gingras, M.K., in press. Tidal effects on the shoreface: Towards a conceptual framework. Sedimentary Geology, doi:10.1016/j.sedgeo.2010.09.006.

De Leeuw, A., Bukowski, K., Krijgsman, W., Kuiper, K.F., 2010. Age of the Badenian salinity crisis. Impact of Miocene climate variability on the circum-mediterranean region. Geology 38, 715–718.

Den Dulk, M., Reichardt, G.J., Van Heyst, S., Zachariasse, W.J., Van der Zwaan, G.J., 2000. Benthic foraminifera as proxies of organicmatter flux and bottomwater oxygenation? A case history from the northern Arabian Sea. Palaeogeography, Palaeoclimatology, Palaeoecology 161, 337–359.

Doppler, G., Heissig, K., Reichenbacher, B., 2005. Die Gliederung des Tertiärs im süddeutschen Molassebecken. Newsletters on Stratigraphy 41, 359–375.

Edwards, L.E., Andrle, V.A.S., 1992. Distribution of selected dinoflagellate cysts in modern marine

sediments. In: Head, M.J., Wrenn, J.H. (Eds.), Neogene and Quaternary dinoflagellate cysts and acritarchs. American Association of Stratigraphic Palynologists, Dallas, pp. 259–288.

Edwards, L.E., 1998. Modern and near modern dinocysts from Florida Bay. Abstracts from the Sixth International Conference on Modern and Fossil Dinoflagellates, 37.

Faupl, P., Roetzel, R., 1987. Gezeitenbeeinflußte Ablagerungen der Innviertler Gruppe (Ottnangien) in der oberösterreichischen Molassezone. Jahrbuch der Geologischen Bundesanstalt 130, 415–447.

Faupl, P., Roetzel, R., 1990. Die Phosphoritsande und Fossilreichen Grobsande: Gezeitenbeeinflußte Ablagerungen der Innviertler Gruppe (Ottnangien) in der oberösterreichischen Molasse. Jahrbuch der Geologischen Bundesanstalt 133, 157–180.

Fenner, J., 1991. Taxonomy, stratigraphy, and paleooceanographic implications of Paleocene diatoms. Proceedings ODP Scientific Results 114, 123–154.

Fensome, R.A., MacRae, R.A., Williams, G.L., 2008. DINOFLAJ2, Version 1. American Association of Stratigraphic Palynologists Data Series, vol. 1. American Association of Stratigraphic Palynologists, Dallas.

Fensome, R.A, Taylor, F.J.R., Norris, G., Sarjeant, W.A.S., Wharton, D.I., Williams, G.L., 1993. A classification of living and fossil dinoflagellates. Micropaleontology Special Publication 7, 1–351.

Flores, J.A., Sierro, F.R., Filippelli, M.R., Bárcena, M.A., Pérez-Folgado, M., Vásquez, A., Utrilla, R., 2005. Surface water dynamics and phytoplankton communities during deposition od cyclic late Messinian sapropel sequences in the Western Mediterranean. Marine Micropaleontology 56, 50–79.

Frey, S.E., Dashtgard, S.E., in press. Sedimentology, ichnology, and hydrodynamics of strait-margin, sand-and-gravel beaches and shorefaces: Juan de Fuca strait, British Columbia, Canada. Sedimentology.

Frieling, D., Pippèrr, M., Schneider, S., Reichenbacher, B., 2009. Sedimentology and stratigraphy at the rocky coast of the upper Burdigalian Molasse Sea: a case study from Gurlarn near Passau (SE Germany). Facies 55, 47–62.

Füchtbauer, H., 1959. Zur Nomenklatur der Sedimentgesteine. Erdöl und Kohle 12, 605–613.

Gandhi, M.S., Rajamanickam, G.V., 2004. Distribution of certain ecological parameters and foraminiferal distribution in the depositional environment of Palk Strait, east coast of India. Indian Journal of Marine Sciences 33, 287–295.

Gargouri-Ben Ayed, Z., Souissi, R., Souissi, M., Abdeljaouad, S., Zouari, K., 2007. Sedimentary dynamics and ecological state of Nakta tidal flat (littoral), South of Sfax, Gulf of Gabès, Tunisia. Chinese Journal of Geochemistry 26, 244–251.

Gebühr, C., Wiltshire, K.H., Aberle, N., Beusekom, J.E.E., van and Gerdts, G., 2009. Influence of nutrients, temperature, light and salinity on the occurence of *Paralia sulcata* at Helgoland Roads, North Sea. Aquatic Biology 7, 185–197.

Graham, J.J., Militante, P.J., 1959. Recent foraminifera from the Puerto Galera, northern Mindoro, Philippines. Stanford University Publications, Stanford.

Green, O.R., 2001. A manual of practical laboratory and field techniques in palaeobiology. Kluwer Academic

Publishers, Dordrecht-Boston-London.

Grunert, P., Soliman, A., Harzhauser, M., Müllegger, S., Piller, W. E., Roetzel, R., Rögl, F., 2010a. Upwelling conditions in the Early Miocene Central Paratethys sea. Geologica Carpathica 61, 129–145.

Grunert, P., Soliman, A., Ćorić, S., Scholger, R., Harzhauser, M., Piller, W. E., 2010b. Stratigraphic re-evaluation of the stratotype for the regional Ottnangian stage (Central Paratethys, middle Burdigalian). Newsletters on Stratigraphy 44, 1–16.

Hammer, Ø., Harper, D.A.T., 2006. Paleontological Data Analysis. Blackwell Publishing, Oxford.

Hammer, Ø., Harper, D.A.T., Ryan, P.D., 2001. PAST: paleontological statistics software package for education and data analysis. Palaeontologia Electronica 4, 1–9.

Haq, B.U., 1980. Miocene biogeographic history of calcareous nannoplankton and paleoceanography of the Atlantic Ocean. Marine Micropaleontology 7, 119–194.

Harzhauser, M., Piller, W. E., 2007. Benchmark data of a changing sea. Palaeogeography, Palaeobiogeography and Events in the Central Paratethys during the Miocene. Palaeogeography, Palaeoclimatology, Palaeoecology 253, 8–31.

Hedberg, H.D., 1976. International Stratigraphic Guide. John Wiley and Sons, New York.

Heimann, F.U.M., Schmid, D.U., Pippèrr, M., Reichenbacher, B., 2009. Re-interpreting the Baltringer Horizont as a subtidal channel facies: implications for a new understanding of the Upper Marine Molasse "Cycles" (Early Miocene). Neues Jahrbuch für Geologie und Paläontologie, Abhandlungen 254, 135–149.

Hochuli, P.A., 1978. Palynologische Untersuchungen im Oligozän und Untermiozän der Zentralen und Westlichen Paratethys. Beiträge zur Paläontologie von Österreich 4, 1–132.

Hohenegger, J., 2005. Estimation of environmental paleogradient values based on presence/absence data: a case study using benthic foraminifera for paleodepth estimation. Palaeogeography, Palaeoclimatology, Palaeoecology 217, 115–130.

Homewood, P., Allen, P.A., 1981. Wave-, tide-, and current-controlled sandbodies of Miocene Molasse, Western Switzerland. AAPG Bulletin 65, 2534–2545.

Izuka, S.K., Resig, J.M., 2008. Evidence for Late Pliocene-Early Pleistocene marine environments in the deep subsurface of the Lihue Basin, Kauai, Hawaii. Palaios 23, 442–451.

Janz, H., Vennemann, T. W., 2005. Isotopic composition (O, C, Sr, and Nd) and trace element ratios (Sr/Ca, Mg/Ca) of Miocene marine and brackish ostracods from North Alpine Foreland deposits (Germany and Austria) as indicators for palaeoclimate. Palaeogeography, Palaeoclimatology, Palaeoecology 225, 216–247.

Jiménez-Moreno, G., Head, M.J., Harzhauser, M., 2006. Early and Middle Miocene dionflagellate cyst stratigraphy of the Central Paratethys, Central Europe. Journal of Micropalaeontology 25, 113–139.

Johnson, H.D., Baldwin, C.T., 1996. Shallow clastic seas. In: Reading, H.G. (Ed.), Sedimentary Environments: Processes, Facies and Stratigraphy. 3rd edition. Blackwell Science, Oxford, 232–280.

Jones, R.W., 1994. The Challenger Foraminifera. Oxford University Press, Oxford.

Jorissen, F.J., 1987. The distribution of benthic foraminifera in the Adriatic Sea. Marine Micropaleontology 12, 21–48.

Jorissen, F.J., Stigter, H.C. De, Widmark, J.G.V., 1995. A conceptual model explaining benthic foraminiferal microhabitats. Marine Micropaleontoloy 26, 3–15.

Kaiho, K., 1994. Benthic foraminiferal dissolved-oxygen index and dissolved-oxygen levels in the modern ocean. Geology 22, 719–722.

Kaltbeitzer, J., 1988. Geologische, sedimentpetrologische und hydrogeologische Untersuchungen im Hausruckgebiet östlich von Eberschwang. Master thesis, Ludwig-Maximilians-Universität, Munich, Germany.

Keller, B., 1989. Fazies und Stratigraphie der Oberen Meeresmolasse (unteres Miozän) zwischen Napf und Bodensee. Ph.D. Thesis, University of Bern, Switzerland.

Kouwenhoven, T.J., van der Zwaan, G.J., 2006. A reconstruction of late Miocene Mediterranean circulation patterns using benthic foraminifera. Palaeogeography, Palaeoclimatology, Palaeoecology 238, 373–385.

Krenmayr, H.-G., 1991. Sedimentologische Untersuchungen der Vöcklaschichten (Innviertler Gruppe, Ottnangien) in der oberösterreichischen Molassezone im Gebiet der Vöckla und der Ager. Jahrbuch der Geologischen Bundesanstalt 134, 83–100.

Krenmayr, H.-G., Roetzel, R., Rupp, C., 1996. Stop 2: Puchkirchen-Berg. In: Krenmayr, H.-G., Roetzel, R. (Eds.), Exkursionsführer, 11. Sedimentologentreffen, Exkursion B2, Oligozäne und miozäne Becken- und Gezeitensedimente in der Molassezone Oberösterreichs. Berichte der Geologischen Bundesanstalt 33, 1–43.

Krenmayr, H.G., Schnabel, W., 2006. Geologische Karte von Oberösterreich 1:200.000, 1 sheet, 2 additional maps. Geological Survey of Austria, Vienna.

Kroh, A., Harzhauser, M., 1999. An Echinoderm Fauna from the Lower Miocene of Austria: Paleoecology and Implications for Central Paratethys Paleobiogeography. Annalen des Naturhistorischen Museums Wien 101A, 145–191.

Kroh, A., Menkveld-Gfeller, U., 2006. Echinoids from the Belpberg Beds (Obere Meeresmolasse, Middle Burdigalian) in the area of Bern (Switzerland). Eclogae Geologicae Helvetiae 99, 193–203.

Kroh, A., 2007. Climate Changes in the early to Middle Miocene of the Central Paratethys and the Origin of its Echinoderm Fauna. Palaeogeography, Palaeoclimatology, Palaeoecology 253, 169–207.

Kuhlemann, J., Kempf, O., 2002. Post-Eocene evolution of the North Alpine Foreland Basin and its response to Alpine tectonics. Sedimentary Geology 152, 45–78.

Kumar, V., Manivannan, V., 2001. Benthic foraminiferal responses to bottom water characteristics in the Palk Bay, off Rameswaram, southeast coast of India. Indian Journal of Marine Sciences 30, 173–179.

Langer, M.R., Lipps, J.H., 2003. Foraminiferal distribution and diversity, Madang Reef and Lagoon, Papua New Guinea. Coral Reefs 22, 143–154.

Leckie, R.M., Olson, H.C., 2003. Foraminifera as proxies for sea-level change on siliciclastic margins. In: Olson, H.C., Leckie, R.M. (Eds.), Micropaleontologic Proxies for Sea-Level Change and Stratigraphic

Discontinuities, Society for Sedimentary Geology Special Publication, vol. 75. Society for Sedimentary Geology, Tulsa, pp. 5–19.

Lemcke, K., 1988. Geologie von Bayern I. Das bayerische Alpnevorland vor der Eiszeit. Schweizerbart, Stuttgart.

Lesueur, J.-P., Rubino, J.-L., Giraudmaillet, M., 1990. Organisation et structures internes des dépôts tidaux du Miocène rhodanien. Bulletin de la Societe Geologique de France 6, 49–65.

Levin, L.A., 2003. Oxygen minimum zone benthos: adaptation and community response to hypoxia. Oceanography and Marine Biology 41, 1–45.

Lirer, F., Harzhauser, M., Pelosi, N., Piller, W.E., Schmid, H.P., Sprovieri, M., 2009. Astronomically forced teleconnection between Paratethyan and Mediterranean sediments during the Middle and Late Miocene. Palaeogeography, Palaeoclimatology, Palaeoecology 275, 1–13.

Lourens, L., Hilgen, F., Shackleton, N.J., Laskar, J., Wilson, D., 2004. The Neogene Period. In: Gradstein, F.M., Ogg, J.G., Smith, A.G. (Eds.), A Geologic Time Scale 2004. Cambridge University Press, Cambridge, pp. 409–440.

Liu, C., Browning, J.V., Miller, K.G., Olsson, R.K., 1997. Paleocene benthic foraminiferal biofacies and sequence stratigraphy, Island Beach borehole, New Jersey. In: Miller, K.G., Snyder, S.W. (Eds.), Proceedings of the Ocean Drilling Program, Scientific Results 150, 267–275.

Mandic, O., Steininger, F.F., 2003. Computer-based mollusc stratigraphy – a case study from the Eggenburgian (Lower Miocene) type region (NE Austria). Palaeogeography, Palaeoclimatology, Palaeoecology 197, 263–291.

Marret, F., Zonneveld, K.A.F., 2003. Atlas of modern organic-walled dinoflagellate cyst distribution. Review of Palaeobotany and Palynology 125, 1–200.

Martel, A.T., Allen, P.A., Slingerland, R., 1994. Use of tidal-circulation modeling of paleogeographical studies: An example from the Tertiary of the Alpine perimeter. Geology 22, 925–928.

Martins, V., Dubert, J., Jouanneau, J.M., Weber, O., da Silva, E.F., Patinha, C., Dias, J.M.A., Rocha, F., 2007. A multiproxy approach of the Holocene evolution of shelf-slope circulation on the NW Iberian Continental Shelf. Marine Geology 239, 1–18.

McMinn, A., 1990. Recent dinoflagellate cyst distribution in eastern Australia. Review of Paleobotany and Palynology 65, 305–310.

McQuoid, M.R., Nordberg, K., 2003a. Environmental influence on the diatom and silicoflagellate assemblages in Koljö Fjord (Sweden) over the last two centuries. Estuaries 26, 927–937.

McQuoid, M.R., Nordberg, K., 2003b. The diatom *Paralia sulcata* as an environmental indicator species in coastal sediments. Estuarine, Coastal and Shelf Science 56, 339–354.

Morzadec-Kerfourn, M.-T., 1979. Indicateurs écologiques du domaine littoral: végétation et plancton organique. Océanis 5, 207–213.

Morzadec-Kerfourn, M.-T., 1983. Interêt de dinoflagellés pour l'établissement de reconstruction paléogéographique: exemple du Golfe de Gabes (Tunésie). Cahiers de Micropaléontologie 4, 15–22.

Müller, G., 1961. Das Sand-Silt-Ton Verhältnis in rezenten marinen Sedimenten. Neues Jahrbuch für Mineralogie, Monatshefte, 148–163.

Murray, J.W., 1984. Paleogene and Neogene benthic foraminifers from Rockall Plateau. Initial Reports of the Deep Sea Drilling Project 81, 503–534.

Murray, J.W., 2006. Ecology and Applications of Benthic Foraminifera. Cambridge University Press, Cambridge.

Nichols, G., 1999. Shallow seas. In: Nichols, G. (Ed.), Sedimentology and Stratigraphy. Blackwell Science, Oxford, pp. 180–193.

Okada, H., McIntyre, A., 1979. Seasonal distribution of modern Coccolithophores in the Western North Atlantic Ocean. Marine Biology 54, 319–328.

Papp, A., Marinescu, F., Seneš, J., 1974. M5 – Sarmatien (sensu E. Suess, 1866). Die Sarmatische Schichtengruppe und ihr Stratotypus. Chronostratigraphie und Neostratotypen, Miozän der Zentralen Paratethys, vol. 4. Verlag der Slowakischen Akademie der Wissenschaften, Bratislava.

Papp, A., Rögl, F., Seneš, J., 1973. Miozän M2 – Ottnangien. Die Innviertler, Salgotarjaner, Bantapusztaer Schichtengruppe und die Rzehakia Formation. Chronostratigraphie und Neostratotypen, Miozän der Zentralen Paratethys, vol. 3. Verlag der Slowakischen Akademie der Wissenschaften, Bratislava.

Papp, A., Cicha, I., 1973. Die Entwicklung der Innviertler Schichtengruppe – $M2_{a\text{-}c(d)}$ – und ihrer Äquivalente in Österreich und anschließenden Gebieten. In: Papp, A., Rögl, F., Seneš, J. (Eds.), Miozän M2 – Ottnangien. Die Innviertler, Salgotarjaner, Bantapusztaer Schichtengruppe und die Rzehakia Formation. Chronostratigraphie und Neostratotypen, Miozän der Zentralen Paratethys, vol. 3., 54–78. Verlag der Slowakischen Akademie der Wissenschaften, Bratislava.

Papp, A., Cicha, I., Seneš, J., Steininger, F., 1978. M4 – Badenien (Moravien, Wielicien, Kosovien). Chronostratigraphie und Neostratotypen, Miozän der Zentralen Paratethys, vol. 6. Verlag der Slowakischen Akademie der Wissenschaften, Bratislava.

Papp, A., Jámbor, Á., Steininger, F.F., 1985. M6 – Pannonien (Slavonien und Serbien). Chronostratigraphie und Neostratotypen, Miozän der Zentralen Paratethys, vol. 7. Verlag der Slowakischen Akademie der Wissenschaften, Bratislava.

Passega, R., 1957. Texture as characteristic of clastic deposition. Bulletin of the American Association of Petroleum Geologists 41, 1952–1984.

Passega, R., 1964. Grain size representation by CM patterns as a geological tool. *Journal of* Sedimentary Petrology 34, 830–847.

Passega, R., 1977. Significance of CM diagrams of sediments deposited by suspension. Sedimentology 24, 723–733.

Passega, R., Byramjee, R., 1969. Grain-size image of clastic deposits. Sedimentology 13, 233–252.

Petters, V., 1936. Geologische und mikropaläontologische Untersuchungen der Eurogasco im Schlier Oberösterreichs. Petroleum Zeitschrift 32, 3.

Pezelj, Đ., Sremac, J., Sokač, A., 2007. Palaeoecology of the Late Badenian foraminifera and ostracoda from

the SW Central Paratethys (Medvednica Mt., Croatia). Geologia Croatica 60, 139–150.

Piller, W.E., Harzhauser, M., Mandic, O., 2007. Miocene Central Paratethys stratigraphy – current status and future directions. Stratigraphy 4, 151–168.

Pippèrr, M., Reichenbacher, B., 2010. Foraminifera from the borehole Altdorf (SE Germany): Proxies for Ottnangian (early Miocene) palaeoenvironments of the Central Paratethys. Palaeogeography, Palaeoclimatology, Palaeoecology 289, 62–80.

Poag, C.W., 1981. Ecologic Atlas of Benthic Foraminifera of the Gulf of Mexico. Woods Hole: Marine Science International, 174 pp.

Pross, J., Brinkhuis, H., 2005. Organic-walled dinoflagellate cysts as paleoenvironmental indicators in the Paleogene; a synopsis of concepts. Paläontologische Zeitschrift 79, 53–59.

Reading, H.G., Collinson, J.D., 1996. Clastic coasts. In: Reading, H.G. (Ed.), Sedimentary Environments: Processes, Facies and Stratigraphy. 3rd edition. Blackwell Science, Oxford, pp. 154–231.

Reiter, E., 1989. Das Naturdenkmal „Ottnangien“ zwischen Wolfsegg und Ottnang am Hausruck. Oberösterreichische Heimatblätter 43, 262–270.

Reolid, M., Rodríguez-Tovar, F.J., Nagy, J., Olóriz, F., 2008. Benthic foraminiferal morphogroups of mid to outer shelf environments of the Late Jurassic (Prebetic Zone, southern Spain): characterization of biofacies and environmental significance. Palaeogeography, Palaeoclimatology, Palaeoecology 261, 280–299.

Reuss, A.E., 1864. Die Foraminiferen des Schliers von Ottnang. Verhandlungen der Geologischen Reichsanstalt 1864, 20–21.

Roetzel, R., Rupp, C., 1991. Ottnang, Sandgrube Fischer. In: Roetzel, R., Nagel, D. (Eds.), Exkursionen im Tertiär Österreichs. Österreichische Paläontologische Gesellschaft, Vienna, pp. 36–38.

Roetzel, R., Ćorić, S., Galović, I., Rögl, F., 2006. Early Miocene (Ottnangian) coastal upwelling conditions along the southeastern scarp of the Bohemian Massif (Parisdorf, Lower Austria, Central Paratethys). Beiträge zur Paläontologie 30, 387–413.

Rögl, F., Schultz, O., Hölzl, O., 1973. Holostratotypus und Faziostratotypen der Innviertler Schichtengruppe. In: Papp, A., Rögl, F., Seneš, J. (Eds.), Miozän M2 – Ottnangien. Die Innviertler, Salgotarjaner, Bantapusztaer Schichtengruppe und die Rzehakia Formation. Chronostratigraphie und Neostratotypen, Miozän der Zentralen Paratethys, vol. 3. Verlag der Slowakischen Akademie der Wissenschaften, Bratislava, 140–196.

Rögl, F., 1998a. Palaeogeographic Considerations for Mediterranean and Paratethys Seaways (Oligocene to Miocene). Annalen des Naturhistorischen Museums in Wien 99A, 279–310.

Rögl, F., 1998b. Foraminiferenfauna aus dem Karpat (Unter-Miozän) des Korneuburger Beckens. Beiträge zur Paläontologie Österreichs 23, 123–174.

Rögl, F., Spezzaferri, S., 2003. Foraminiferal paleoecology and biostratigraphy of the Mühlbach section (Gaindorf Formation, Lower Badenian), Lower Austria. Annalen des Naturhistorischen Museums in Wien 104A, 23–75.

Rossignol, M., 1962. Analyse pollinique de sédiments marins Quaternaires en Israël. II. Sédiments pléistocènes. Pollen Spores 4, 121–148.

Rupp, C., 1986. Paläoökologie der Foraminiferen in der Sandschalerzone (Badenien, Miozän) des Wiener Beckens. Beiträge zur Paläontologie Österreichs 12, 1–180.

Rupp, C., Roetzel, R., Stojaspal, F., 1991. Ottnang-Schanze. In: Roetzel, R. and Nagel, D. (Eds.), Exkursionen im Tertiär Österreichs. Österreichische Paläontologische Gesellschaft, Vienna, 38–41.

Rupp, C., Haunold-Jenke, Y., 2003. Untermiozäne Foraminiferenfaunen aus dem oberösterreichischen Zentralraum. Jahrbuch der Geologischen Bundesanstalt 143, 227–302.

Rupp, C., Hofmann, T., Jochum, B., Pfleiderer, S., Schedl, A., Schindlbauer, G., Schubert, G., Slapansky, P., Tilch, N., Husen, D. van, Wagner, L., Wimmer-Frey, I., 2008. Geologische Karte der Republik Österreich 1:50.000, Blatt 47 Ried im Innkreis. Erläuterungen zu Blatt 47 Ried im Innkreis. Geological Survey of Austria, Vienna.

Rupp, C., Husen, D. van, 2007. Zur Geologie des Kartenblattes Ried im Innkreis. In: Egger, H., Rupp, C. (Eds.), Beiträge zur Geologie Oberösterreichs, Arbeitstagung der Geologischen Bundesanstalt 2007. Geological Survey of Austria, Vienna, 73–112.

Salvermoser, S., 1999. Zur Sedimentologie gezeitenbeeinflußter Sande in der Oberen Meeresmolasse und Süßbrackwassermolasse (Ottnangium) von Niederbayern und Oberösterreich. Münchner Geologische Hefte A 26, 1–179.

Schaad, W., Keller, B., Matter, A., 1992. Die Obere Meeresmolasse (OMM) am Pfänder: Beispiel eines Gilbert-Deltakomplexes. Eclogae Geologicae Helveticae 85, 145–168.

Schläger, A., 1988. Geologische Aufnahme des Hausruckgebietes nördlich von Ottnang/Oberösterreich. Master thesis, Ludwig-Maximilians-Universität, Munich, Germany.

Schlunegger, F., Leu, W., Matter, A., 1997. Sedimentary Sequences, Seismic Facies, Subsidence Analysis, and Evolution of the Burdigalian Upper Marine Molasse Group, Central Switzerland. AAPG Bulletin 81, 1185–1207.

Schönfeld, J., 1997. The Impact of Mediterranean Outflow Water (MOW) on Benhic foraminiferal assemblages and surface sediments at the southern Portuguese continental margin. Marine Micropaleontology 29, 211–236.

Spezzaferri, S., Ćorić, S., Hohenegger, J., Rögl, F., 2002. Basin-scale paleobiogeography and paleoecology: an example from Karpatian (Latest Burdigalian) benthic and planktonic foraminifera and calcareous nannofossils from the Central Paratethys. Geobios 35, 241–256.

Spezzaferri, S., Tamburini, F., 2007. Paleodepth variations on the Eratosthenes Seamount (Eastern Mediterranean: sea-level changes or subsidence? eEarth Discussions 2, 115–132.

Smallwood, B.J., Wolff, G.A., Bett, B.J., Smith, C.R., Gage, J.D., Patience, A., Hoover, D., 1999. Megafauna can control the quality of organic matter in marine sediments. Naturwissenschaften 86, 320–324.

Steininger, F., Seneš, J., 1971. M1 – Eggenburgien. Die Eggenburger Schichtengruppe und ihr Stratotypus. Chronostratigraphie und Neostratotypen, Miozän der Zentralen Paratethys, vol. 2. Verlag der

Slowakischen Akademie der Wissenschaften, Bratislava.

Stevanović, P., Nevesskaja, L.A., Marinescu, F., Sokac, A., Jámbor, A., 1990. Pl1 – Pontien (sensu F. Le Play, N.P. Barbot, N. I. Andrusov). Chronostratigraphie und Neostratotypen, Neogen der Westlichen ("Zentralen") Paratethys, vol. 8. Verlag der Slowakischen Akademie der Wissenschaften, Bratislava.

Sztanó, O., 1994. The tide-influenced Petervasara Sandstone, early Miocene, northern Hungary: sedimentology, paleogeography and basin development. Geologica ultraiectina 120, 1–155.

Sztanó, O., 1995. Palaeogeographic significance of tidal deposits: an example from an early Miocene Paratethys embayment, Northern Hungary. Palaeogeography Palaeoclimatology Palaeoecology 113, 173–187.

Sztanó, O., de Boer, P.L., 1995. Amplification of tidal motions in the Early Miocene North Hungarian Bay. Sedimentology 42, 665–682.

Tessier, B., Gigot, P., 1989. A vertical record of different tidal cyclicities: an example from the Miocene Marine Molasse of Digne (Haute Provence, France). Sedimentology 36, 767–776.

Thompson, J.B., Mullins, H.T., Newton, C.R., Vercoutere, T., 1985. Alternative biofacies model for dysaerobic communities. Lethaia 18, 167–179.

Uchmann, A., Krenmayr, H.-G., 1995. Trace fossils from Lower Miocene (Ottnangian) molasse deposits of Upper Austria. Paläontologische Zeitschrift 69, 503–524.

Uchmann, A. and Krenmayr, H.-G., 2004. Trace fossils, Ichnofabrics and Sedimentary Facies in the Shallow Marine Lower Miocene Molasse of Upper Austria. Jahrbuch der Geologischen Bundesanstalt 144, 233–251.

Van der Zwann, G.J., Duijnstee, I.A.P., den Dulk, M., Ernst, S.R., Jannik, N.T., Kouwenhoven, T.J., 1999. Benthic foraminifers: proxies or problems? A review of paleocological concepts. Earth Science Reviews 46, 213–236.

Van Hinsbergen, D.J.J., Kouwenhoven, T.J., van der Zwaan, G.J., 2005. Paleobathymetry in the backstripping procedure: correction for oxygenation effects on depth estimates. Palaeogeography, Palaeoclimatology, Palaeoecology 221, 245–265.

Vasiliev, I., de Leeuw, A., Filipescu, S., Krijgsman, W., Kuiper, K., Stoica, M., Briceag, A., 2010. The age of the Sarmatian-Pannonian transition in the Transylvanian Basin (Central Paratethys). Palaeogeography Palaeoclimatology Palaeoecology 297, 54–69.

Vavra, N., 1979. Die Bryozoenfauna des österreichischen Tertiärs. Neues Jahrbuch für Geologie und Paläontologie, Abhandlungen 157, 366–392.

De Vernal, A., Marret, F., 2007. Organic-walled dinoflagellate cysts: Tracers of sea-surface conditions. In: Hillaire-Marcel, C., Vernal, A. (Eds.), Proxies in late Cenozoic paleoceanography. Developments in Marine Geology, vol. 1. Elsevier, Amsterdam, pp. 371–408.

Vink, A., Zonneveld, K.A.F., Willems, H., 2000. Organic-walled dinoflagellate cysts in western equatorial Atlantic surface sediments: distributions and their relation to environment. Review of Palaeobotany and Palynology 112, 247–286.

Wade, B.S., Bown, P.R., 2006. Calcareous nannofossils in extreme environments: the Messinian Salinity Crisis, Polemi Basin, Cyprus. Palaeogeography 233, 271–286.

Wagner, L., 1998. Tectono-stratigraphy and hydrocarbons in the Molasse Foredeep of Salzburg, Upper and Lower Austria. In: Mascle, A., Puigdefábregas, C., Luterbach, H.P., Fernández, M., (Eds.), Cenozoic Foreland Basins of Western Europe. Geological Society Special Publications, vol. 134. Geological Society, London, pp. 339–369.

Wall, D., Warren, J.S., 1969. Dinoflagellates in Red Sea piston cores. In: Degens, E.T., Ross, D.A. (Eds.), Hot Brines and Recent Heavy Metal Deposits in the Red Sea. Springer, Berlin, pp. 317–327.

Wall, D., Dale, B., Lohmann, G.P., Smith, W.K., 1977. The environmental and climatic distribution of dinoflagellate cysts in Modern marine sediments from regions in the North and South Atlantic Oceans and adjacent seas. Marine Micropaleontology 2, 121–200.

Wang, P., Chappell, J., 2001. Foraminifera as Holocene environmental indicators in the South Alligator River, Northern Australia. Quaternary International 83-85, 47–62.

Wenger, W.F., 1987. Die Foraminiferen des Miozäns der bayerischen Molasse und ihre stratigraphische sowie paläogeographische Auswertung. Zitteliana 16, 173–340.

Williams, G.L., Bujak, J.P., 1977. Distribution patterns of some North Atlantic Cenozoic dinoflagellate cysts. Marine Micropalaeontology 2, 223–233.

Zong, Y., 1997. Mid and late Holocene sea level changes in Roudsea marsh, northwest England: a diatom biostratigraphical investigation. The Holocene 7, 311–323.

Zorn, I., 1995. Preliminary report on the ostracodes from the Ottnangian (Early Miocene) of Upper Austria. Proceedings of the 12th International Symposium on Ostracoda, Prague, Czech Republic, pp. 237–243.

Zweigel, J. (1998). Eustatic versus tectonic control on foreland basin fill. Contributions to Sedimentary Geology 20. Schweizerbart, Stuttgart.

Appendix 4.1.: Tables 4.1-4.3

Tab. 4.1. Benthic foraminifers from the stratotype.

	OS 1	OS 2	OS 3	OS 4	OS 5	OS 6	OS 7	OS 8
Alabamina tangentialis (CLODIUS)	12	10	47	68	224	36	88	64
Ammonia beccharii (LINNÉ) gr.	8	16	23	34	32	20	8	0
Amphicoryna ottnangensis (TOULA)	4	4	7	4	16	13	40	1
?*Amphicoryna* sp.	0	0	0	0	0	0	0	0
Astacolus crepidulus (FICHTEL & MOLL)	0	0	0	0	8	0	0	0
Asteringerinata planorbis (D'ORBIGNY)	0	0	0	0	0	0	0	0
Astrononion perfossum (CLODIUS)	16	0	16	34	88	112	64	80
Astrononion cf. *perfossum* (CLODIUS)	0	0	0	0	0	0	8	0
Aubignyna cf. *brixi* RÖGL	4	0	0	0	0	0	0	0
?*Aubignyna* sp.	0	0	1	0	0	0	0	0
?*Biapertorbis biaperturatus* POKORNY	0	0	1	0	0	0	0	0
Bolivina concinna (KNIPSCHEER & MARTIN)	0	0	0	0	0	0	0	0
Bolivina cf. *budensis* (HANTKEN)	0	0	1	0	0	0	0	0
Bulimina elongata D'ORBIGNY	0	4	0	0	0	0	8	0
Bulimina sp.	0	0	0	0	0	0	0	0
Caucasina cylindrica ZAPLETALOVA	84	38	141	116	336	172	192	176
Caucasina subulata (CUSHMAN & PARKER)	4	0	0	0	0	0	0	0
Chilostomella ovoidea REUSS	0	0	0	0	0	0	0	0
Chilostomella sp.	0	0	0	0	0	0	0	0
?*Chilostomella* sp.	0	0	0	0	0	4	0	0
Cibicidoides austriacus (D'ORBIGNY)	1	0	1	0	0	0	0	3
Cibicidoides lopjanicus (MYATLYUK)	0	8	34	2	0	0	0	1
Cibicidoides ornatus (CICHA & ZAPLETALOVA)	0	0	0	0	8	0	0	0
Cibicidoides pseudoungerianus (CUSHMAN)	12	0	0	8	24	24	8	8
Cibicidoides ungerianus ungerianus (D'ORBIGNY)	0	0	0	0	0	0	0	0
Cibicidoides spp.	4	0	1	6	0	4	24	9
Dentalina cf. *acuta* D'ORBIGNY	0	0	0	0	0	0	0	0
Dentalina sp.	0	0	0	0	0	0	0	0
?*Dentalinoides aproximata* (REUSS)	0	0	0	0	0	0	0	0
?*Elphidiella* sp.	0	0	1	0	0	0	0	0
Elphidium angulatum (EGGER)	0	0	1	0	0	0	0	0
Elphidium crispum (LINNÉ)	0	0	0	0	8	0	0	8
Elphidium fichtelianum (D'ORBIGNY)	0	2	0	0	0	0	0	0
Elphidium glabratum CUSHMAN	0	0	0	0	0	0	0	0
Elphidium hauerinum (D'ORBIGNY)	0	0	5	0	0	4	0	0
Elphidium karpaticum MYATLYUK	0	0	0	0	0	0	0	0
Elphidium matzenense PAPP	0	0	1	0	0	0	0	0
Elphidium ortenburgense (EGGER)	0	0	3	0	0	4	8	0
Elphidium reussi MARKS	0	0	0	4	0	0	0	0
Elphidium rugulosum CUSHMAN & WICKENDEN	0	0	0	2	0	0	0	0
Elphidium subtypicum PAPP	0	0	0	2	0	0	0	0
Elphidium spp.	0	0	0	4	0	4	0	0
Elphidiidea indet.	4	4	0	0	8	0	0	0
Fursenkoina acuta (D'ORBIGNY)	12	6	19	16	72	68	88	72
Glandulina ovula D'ORBIGNY	0	0	0	2	0	0	0	0
?*Glandulina* sp.	0	0	0	0	0	0	0	0
Globocassidulina oblonga (REUSS)	0	0	0	0	8	4	16	0
Globocassidulina cf. *globosa* (HANTKEN)	0	0	0	0	0	0	0	0
Globulina gibba D'ORBIGNY	0	0	2	0	0	0	0	0
Gyroidinoides octocameratus (CUSHMAN & HANNA)	0	0	0	0	0	0	0	0
Gyroidinoides cf. *octocameratus* (CUSHMAN & HANNA)	0	0	0	0	0	0	0	0
Gyroidinoides parvus (CUSHMAN & RENZ)	0	0	0	4	0	0	0	0
Hansenisca soldanii (D'ORBIGNY)	0	0	0	0	0	0	0	0
Hanzawaia boueana (D'ORBIGNY)	4	10	10	16	24	12	16	0
Hanzawaia cf. *boueana* (D'ORBIGNY)	0	2	0	0	0	0	0	0
Hemirobulina glabra (D'ORBIGNY)	0	0	0	0	0	0	0	8
Hemirobulina cf. *pediformis* (BORNEMANN)	0	0	0	0	0	0	0	0
Heterolepa dutemplei (D'ORBIGNY)	4	2	2	2	0	0	1	9
Laevidentalina cf. *boueana* (D'ORBIGNY)	0	0	0	2	8	0	0	0
Laevidentalina communis (D'ORBIGNY)	4	2	5	4	32	0	0	0
Laevidentalina elegans (D'ORBIGNY)	0	0	0	0	8	0	0	0
Laevidentalina sp.	0	0	0	0	0	4	0	0
Lagena gracilicosta REUSS	0	0	5	2	0	0	0	0

Tab. 4.1 (continued).

	OS 1	OS 2	OS 3	OS 4	OS 5	OS 6	OS 7	OS 8
Lagena striata (D'ORBIGNY)	0	0	1	4	8	0	0	8
Lagena sp.	0	2	0	0	0	0	0	0
?*Lagena* sp.	0	0	0	0	0	0	0	0
Lenticulina calcar (LINNÉ)	0	0	0	0	0	0	0	0
Lenticulina inornata (D'ORBIGNY)	309	11	274	133	350	156	275	539
Lenticulina gibba (D'ORBIGNY)	1	0	0	0	0	0	0	0
Lobatula lobatula (WALKER & JACOB)	4	6	5	6	16	12	8	0
?*Lobatula lobatula* (WALKER & JACOB)	0	0	0	0	0	0	0	0
Marginulina hirsuta D'ORBIGNY	0	0	0	0	0	0	0	0
Marginulina wengeri RUPP & HAUNOLD-YENKE	0	0	0	0	0	0	0	0
Melonis pompilioides (FICHTEL & MOLL)	0	0	4	2	0	0	0	0
Melonis sp.	0	0	0	0	0	0	0	0
Myllostomella advena (CUSHMAN & LAIMING)	0	0	0	0	0	0	0	0
Myllostomella recta (PALMER & BERMUDEZ)	0	0	0	0	0	0	0	0
Nonion commune (D'ORBIGNY)	14	28	35	34	96	44	24	49
Nonionidae indet.	0	0	0	0	8	0	0	0
Oridorsalis umbonatus (REUSS)	0	0	0	4	0	0	0	0
?*Porosononion* sp.	4	0	0	0	0	0	0	8
Praeglobobulimina pyrula-pupoides gr.	0	0	0	0	0	0	0	0
Praeglobobulimina sp.	0	0	0	0	0	0	0	0
?*Protelphidium roemeri* (CUSHMAN)	0	0	0	0	0	0	0	0
Pullenia bulloides (D'ORBIGNY)	0	2	2	2	0	0	0	0
Pullenia quinqueloba (REUSS)	0	0	1	0	0	0	0	0
Pullenia sp.	0	0	2	2	0	0	0	0
Quadrimorphina petrolei (ANDREAE)	0	0	0	0	0	0	0	0
Saracenaria arcuata (D'ORBIGNY)	0	0	0	2	0	0	0	0
?*Stilostomellidae* indet.	0	0	0	0	0	0	0	0
Vaginulinopsis cf. *hauerina* (D'ORBIGNY)	0	0	0	0	0	0	0	0
Vaginulinopsis sp.	0	0	1	0	0	0	0	0
Valvulineria complanata (D'ORBIGNY)	0	0	2	4	0	0	0	0
Hyaline indet.	20	8	27	62	48	28	26	48
Cycloforina cf. *ludwigi* (REUSS)	0	0	0	0	0	0	0	0
?*Cycloforina* sp.	0	0	0	6	0	4	0	8
Pyrgo cf. *lucernula* SCHWAGER	0	0	0	0	0	0	0	0
Pyrgo lunula (D'ORBIGNY)	0	0	1	2	8	0	0	0
Pyrgo simplex (D'ORBIGNY)	0	0	2	2	0	0	0	0
Quinqueloculina buchiana D'ORBIGNY	0	0	0	0	11	4	0	7
Quinqueloculina cf. *buchiana* D'ORBIGNY	0	0	0	0	32	0	0	0
Quinqueloculina sp.	0	0	0	0	1	0	0	0
Sigmoilinita tenuis (CZIJZEK)	0	0	0	4	16	0	0	32
Sigmoilopsis ottnangensis CICHA, CTYROKA & ZAPLETALOVA	10	0	1	0	3	20	21	79
Sigmoilopsis cf. *ottnangensis* CICHA, CTYROKA & ZAPLETALOVA	0	0	0	0	0	0	0	0
Spiroloculina canalilucuta D'ORBIGNY	0	0	1	0	0	0	0	0
Spiroloculina lamposa HUSSEY	12	14	15	94	56	44	24	8
Spiroloculina sp.	0	0	1	0	0	0	0	0
Miliolidae indet.	0	0	1	0	0	0	0	0
Martinotiella communis (D'ORBIGNY)	0	0	0	0	0	0	0	0
Spiroplectamina pectinata (REUSS)	2	0	8	4	74	28	8	38
Textularia gramen D'ORBIGNY	0	0	0	2	0	0	0	0
Textularia cf. *gramen* D'ORBIGNY	0	0	0	0	0	0	0	1
Textularia sp.	0	0	0	0	8	0	0	1
Hyaline	529	165	681	587	1430	725	902	1091
Miliolid	22	14	22	108	127	72	45	134
Agglutinated	2	0	8	6	82	28	8	40
Total	553	179	711	701	1639	825	955	1265
Number of taxa	24	20	42	39	31	24	21	26
Diversity (Fisher alpha)	5.1	5.8	9.8	8.9	5.4	4.6	3.8	4.6
Dominance	0.34	0.10	0.20	0.11	0.12	0.12	0.15	0.22
Equitability	0.56	0.86	0.61	0.73	0.75	0.79	0.76	0.65
Inner neritic taxa (%)	5	25	9	22	7	11	6	1
Outer neritic-bathyal taxa (%)	3	8	8	13	17	5	9	5
Epifauna (%)	66	31	51	44	39	38	41	59
Infauna (%)	20	32	28	23	30	33	36	21

Tab. 4.1 (continued).

	OS 1	OS 2	OS 3	OS 4	OS 5	OS 6	OS 7	OS 8
Deep infauna (%)	0	0	0	0	0	0	0	0
Oxic indicators (%)	4	7	7	5	3	4	4	5
Suboxic indicators (%)	86	66	82	65	82	81	87	87
Dysoxic indicators (%)	0	0	0	0	0	0	0	0
High nutrient-flux ndicators (%)	16	23	20	17	21	21	21	14

Tab. 4.1 (continued).

	OS 9	OS 10	OS 11	OS 12	OS 13	OS 14	OS 15	OS 16
Alabamina tangentialis (CLODIUS)	44	24	16	0	0	2	0	0
Ammonia beccharii (LINNÉ) gr.	4	16	0	0	0	0	0	3
Amphicoryna ottnangensis (TOULA)	10	148	125	40	5	7	0	4
?*Amphicoryna* sp.	0	0	0	0	0	0	0	0
Astacolus crepidulus (FICHTEL & MOLL)	0	0	0	6	0	2	0	0
Asteringerinata planorbis (D'ORBIGNY)	1	0	0	0	0	0	0	0
Astrononion perfossum (CLODIUS)	27	56	0	0	0	0	0	1
Astrononion cf. *perfossum* (CLODIUS)	0	0	0	0	0	0	0	0
Aubignyna cf. *brixi* RÖGL	0	0	0	0	0	0	0	0
?*Aubignyna* sp.	0	0	0	0	0	0	0	0
?*Biapertorbis biaperturatus* POKORNY	0	0	0	0	0	0	0	0
Bolivina concinna (KNIPSCHEER & MARTIN)	1	0	0	0	0	0	0	0
Bolivina cf. *budensis* (HANTKEN)	0	0	0	0	0	0	0	0
Bulimina elongata D'ORBIGNY	0	8	16	0	0	0	0	0
Bulimina sp.	1	0	0	0	0	0	0	0
Caucasina cylindrica ZAPLETALOVA	52	328	80	0	0	0	0	0
Caucasina subulata (CUSHMAN & PARKER)	0	0	0	0	0	0	0	0
Chilostomella ovoidea REUSS	0	0	0	0	0	0	0	0
Chilostomella sp.	0	0	0	0	0	1	1	0
?*Chilostomella* sp.	0	0	0	0	0	0	0	0
Cibicidoides austriacus (D'ORBIGNY)	1	4	1	0	0	0	0	0
Cibicidoides lopjanicus (MYATLYUK)	2	0	9	0	0	0	0	0
Cibicidoides ornatus (CICHA & ZAPLETALOVA)	1	0	0	2	0	1	0	2
Cibicidoides pseudoungerianus (CUSHMAN)	20	128	80	0	4	3	0	1
Cibicidoides ungerianus ungerianus (D'ORBIGNY)	0	0	0	0	0	2	2	0
Cibicidoides spp.	1	0	0	0	0	0	0	0
Dentalina cf. *acuta* D'ORBIGNY	0	0	0	0	0	0	0	0
Dentalina sp.	0	0	4	0	0	6	0	0
?*Dentalinoides aproximata* (REUSS)	0	0	0	0	4	0	0	0
?*Elphidiella* sp.	1	0	0	0	0	0	0	0
Elphidium angulatum (EGGER)	0	0	0	0	0	0	0	0
Elphidium crispum (LINNÉ)	0	0	0	0	0	0	0	0
Elphidium fichtelianum (D'ORBIGNY)	0	0	0	0	0	0	0	0
Elphidium glabratum CUSHMAN	1	0	0	0	0	0	0	0
Elphidium hauerinum (D'ORBIGNY)	0	0	0	0	0	0	0	0
Elphidium karpaticum MYATLYUK	0	0	0	1	0	0	0	0
Elphidium matzenense PAPP	0	0	0	0	0	0	0	0
Elphidium ortenburgense (EGGER)	0	0	0	0	0	0	0	0
Elphidium reussi MARKS	1	0	0	0	0	0	0	0
Elphidium rugulosum CUSHMAN & WICKENDEN	0	0	0	0	0	0	0	0
Elphidium subtypicum PAPP	0	0	0	0	0	0	0	0
Elphidium spp.	1	0	0	0	0	0	0	0
Elphidiidea indet.	0	0	0	0	0	0	0	0
Fursenkoina acuta (D'ORBIGNY)	16	56	32	0	0	0	0	1
Glandulina ovula D'ORBIGNY	1	0	0	0	0	0	0	0
?*Glandulina* sp.	0	0	0	0	0	0	0	0
Globocassidulina oblonga (REUSS)	1	0	0	1	4	0	0	0
Globocassidulina cf. *globosa* (HANTKEN)	0	0	0	1	0	0	0	0
Globulina gibba D'ORBIGNY	1	0	1	2	0	0	0	0
Gyroidinoides octocameratus (CUSHMAN & HANNA)	0	0	0	1	0	0	0	0
Gyroidinoides cf. *octocameratus* (CUSHMAN & HANNA)	0	0	32	0	0	0	0	0
Gyroidinoides parvus (CUSHMAN & RENZ)	0	24	0	26	24	16	0	2
Hansenisca soldanii (D'ORBIGNY)	0	0	0	0	0	0	0	0
Hanzawaia boueana (D'ORBIGNY)	10	24	0	0	0	0	0	0
Hanzawaia cf. *boueana* (D'ORBIGNY)	0	0	0	0	0	0	0	0
Hemirobulina glabra (D'ORBIGNY)	0	0	0	0	0	0	0	0
Hemirobulina cf. *pediformis* (BORNEMANN)	0	0	0	0	0	5	0	0
Heterolepa dutemplei (D'ORBIGNY)	4	0	1	0	0	1	1	0
Laevidentalina cf. *boueana* (D'ORBIGNY)	0	8	0	32	20	17	4	15
Laevidentalina communis (D'ORBIGNY)	5	8	32	4	8	2	1	0
Laevidentalina elegans (D'ORBIGNY)	5	0	0	0	0	1	0	0
Laevidentalina sp.	0	0	0	0	0	1	0	0
Lagena gracilicosta REUSS	0	0	0	2	4	2	0	0
Lagena striata (D'ORBIGNY)	0	0	0	0	0	0	0	0
Lagena sp.	0	0	0	0	0	0	0	0
?*Lagena* sp.	0	3	4	1	0	1	0	0
Lenticulina calcar (LINNÉ)	0	0	0	0	0	0	0	0
Lenticulina inornata (D'ORBIGNY)	542	407	241	19	11	14	6	5

Tab. 4.1 (continued).

	OS 9	OS 10	OS 11	OS 12	OS 13	OS 14	OS 15	OS 16
Lenticulina gibba (D'ORBIGNY)	0	0	0	0	2	0	0	0
Lobatula lobatula (WALKER & JACOB)	2	16	0	0	0	0	0	0
?*Lobatula lobatula* (WALKER & JACOB)	0	0	0	0	0	0	0	1
Marginulina hirsuta D'ORBIGNY	0	0	0	0	1	0	0	0
Marginulina wengeri RUPP & HAUNOLD-YENKE	0	8	0	0	0	0	0	0
Melonis pompilioides (FICHTEL & MOLL)	1	8	0	0	0	0	0	0
Melonis sp.	0	0	0	0	0	0	0	0
Myllostomella advena (CUSHMAN & LAIMING)	0	0	0	3	0	1	0	0
Myllostomella recta (PALMER & BERMUDEZ)	0	0	0	0	0	0	0	0
Nonion commune (D'ORBIGNY)	23	118	7	9	4	2	3	4
Nonionidae indet.	0	0	0	0	0	0	0	0
Oridorsalis umbonatus (REUSS)	1	8	48	10	16	9	1	5
?*Porosononion* sp.	0	0	0	0	0	0	0	0
Praeglobobulimina pyrula-pupoides gr.	0	0	0	0	9	4	0	0
Praeglobobulimina sp.	0	0	0	0	0	0	0	1
?*Protelphidium roemeri* (CUSHMAN)	0	0	0	0	0	0	0	0
Pullenia bulloides (D'ORBIGNY)	0	0	0	0	0	0	0	0
Pullenia quinqueloba (REUSS)	0	0	0	0	0	0	0	0
Pullenia sp.	0	0	0	0	0	0	0	0
Quadrimorphina petrolei (ANDREAE)	0	8	0	0	0	0	0	0
Saracenaria arcuata (D'ORBIGNY)	0	0	0	3	0	0	0	0
?*Stilostomellidae* indet.	0	0	0	0	0	0	0	0
Vaginulinopsis cf. *hauerina* (D'ORBIGNY)	0	0	0	0	0	0	0	0
Vaginulinopsis sp.	0	0	0	0	0	0	0	0
Valvulineria complanata (D'ORBIGNY)	1	8	0	11	16	16	0	10
Hyaline indet.	15	80	97	21	12	22	3	11
Cycloforina cf. *ludwigi* (REUSS)	0	3	0	0	0	0	0	1
?*Cycloforina* sp.	0	16	0	0	0	0	0	0
Pyrgo cf. *lucernula* SCHWAGER	0	0	16	0	0	0	0	0
Pyrgo lunula (D'ORBIGNY)	1	8	0	0	0	0	0	0
Pyrgo simplex (D'ORBIGNY)	0	0	0	0	0	0	0	0
Quinqueloculina buchiana D'ORBIGNY	15	19	19	1	0	6	0	3
Quinqueloculina cf. *buchiana* D'ORBIGNY	0	1	0	1	0	0	0	0
Quinqueloculina sp.	1	0	1	0	0	1	0	0
Sigmoilinita tenuis (CZIJZEK)	6	136	96	1	0	0	0	0
Sigmoilopsis ottnangensis CICHA, CTYROKA & ZAPLETALOVA	63	102	93	5	14	5	1	0
Sigmoilopsis cf. *ottnangensis* CICHA, CTYROKA & ZAPLETALOVA	0	1	0	0	0	0	0	0
Spiroloculina canalilucuta D'ORBIGNY	0	0	0	0	0	0	0	0
Spiroloculina lamposa HUSSEY	7	88	0	6	0	3	0	0
Spiroloculina sp.	0	0	0	0	0	0	0	0
Miliolidae indet.	2	0	18	0	4	2	0	0
Martinotiella communis (D'ORBIGNY)	0	0	0	0	0	0	0	0
Spiroplectamina pectinata (REUSS)	90	461	415	2	0	3	1	3
Textularia gramen D'ORBIGNY	0	2	0	1	0	0	0	0
Textularia cf. *gramen* D'ORBIGNY	1	0	0	0	0	0	0	0
Textularia sp.	0	0	1	0	0	0	0	0
Hyaline	797	1496	826	195	144	138	22	66
Miliolid	95	374	243	14	18	17	1	4
Agglutinated	91	463	416	3	0	3	1	3
Total	983	2333	1485	212	162	158	24	73
Number of taxa	41	35	25	27	18	30	11	18
Diversity (Fisher alpha)	8.6	5.8	4.5	8.2	5.2	11.0	7.9	7.6
Dominance	0.32	0.11	0.13	0.10	0.08	0.07	0.14	0.11
Equitability	0.51	0.73	0.75	0.80	0.91	0.86	0.90	0.87
Inner neritic taxa (%)	2	5	0	3	0	2	0	4
Outer neritic-bathyal taxa (%)	6	4	9	41	52	41	29	44
Epifauna (%)	79	62	71	36	44	41	50	32
Infauna (%)	10	25	20	46	41	41	25	42
Deep infauna (%)	0	0	0	0	6	3	4	1
Oxic indicators (%)	4	11	13	3	2	4	13	4
Suboxic indicators (%)	91	77	77	78	82	70	75	70
Dysoxic indicators (%)	0	0	0	0	6	3	4	1
High nutrient-flux ndicators (%)	5	15	6	0	6	3	0	1

Tab. 4.1 (continued).

	OS 17	OS 18	OS 19	OS 20	OS 21	OS 22	OS 23	OS 24
Alabamina tangentialis (CLODIUS)	1	1	0	2	0	3	3	0
Ammonia beccharii (LINNÉ) gr.	0	1	2	1	3	0	1	1
Amphicoryna ottnangensis (TOULA)	8	12	15	23	30	13	20	28
?*Amphicoryna* sp.	0	0	0	1	0	0	1	0
Astacolus crepidulus (FICHTEL & MOLL)	0	0	1	0	1	0	0	0
Asteringerinata planorbis (D'ORBIGNY)	0	0	0	0	0	0	0	0
Astrononion perfossum (CLODIUS)	0	2	1	7	0	0	0	0
Astrononion cf. *perfossum* (CLODIUS)	0	0	0	3	1	0	0	0
Aubignyna cf. *brixi* RÖGL	0	0	0	0	0	0	0	0
?*Aubignyna* sp.	0	0	0	0	0	0	0	0
?*Biapertorbis biaperturatus* POKORNY	0	0	0	0	0	0	0	0
Bolivina concinna (KNIPSCHEER & MARTIN)	0	0	0	0	0	0	0	0
Bolivina cf. *budensis* (HANTKEN)	0	0	0	0	0	0	0	0
Bulimina elongata D'ORBIGNY	0	0	1	0	1	1	0	0
Bulimina sp.	0	0	0	0	0	0	0	0
Caucasina cylindrica ZAPLETALOVA	0	1	6	6	2	0	1	0
Caucasina subulata (CUSHMAN & PARKER)	0	0	2	0	1	0	0	0
Chilostomella ovoidea REUSS	0	0	0	0	2	0	2	0
Chilostomella sp.	0	0	0	0	0	0	0	0
?*Chilostomella* sp.	0	0	0	0	0	0	0	0
Cibicidoides austriacus (D'ORBIGNY)	0	0	0	2	1	0	0	0
Cibicidoides lopjanicus (MYATLYUK)	0	0	1	0	0	0	0	0
Cibicidoides ornatus (CICHA & ZAPLETALOVA)	0	0	0	0	2	0	1	1
Cibicidoides pseudoungerianus (CUSHMAN)	1	2	0	4	0	4	2	0
Cibicidoides ungerianus ungerianus (D'ORBIGNY)	0	0	0	0	1	3	1	1
Cibicidoides spp.	0	0	0	1	0	0	2	0
Dentalina cf. *acuta* D'ORBIGNY	0	0	0	0	1	0	4	0
Dentalina sp.	0	0	1	0	0	1	0	0
?*Dentalinoides aproximata* (REUSS)	0	0	0	0	0	0	0	0
?*Elphidiella* sp.	0	0	0	0	0	0	0	0
Elphidium angulatum (EGGER)	0	0	0	0	0	0	0	0
Elphidium crispum (LINNÉ)	0	0	0	0	0	0	0	0
Elphidium fichtelianum (D'ORBIGNY)	0	0	0	0	0	0	0	0
Elphidium glabratum CUSHMAN	0	0	0	0	0	0	0	0
Elphidium hauerinum (D'ORBIGNY)	0	0	0	0	0	0	0	0
Elphidium karpaticum MYATLYUK	0	0	0	0	0	0	0	0
Elphidium matzenense PAPP	0	0	0	0	0	0	0	0
Elphidium ortenburgense (EGGER)	0	0	0	0	0	0	0	0
Elphidium reussi MARKS	0	0	0	0	0	0	0	0
Elphidium rugulosum CUSHMAN & WICKENDEN	0	0	0	0	0	0	0	0
Elphidium subtypicum PAPP	0	0	0	0	1	0	0	0
Elphidium spp.	0	1	0	1	0	0	0	0
Elphidiidea indet.	0	0	0	0	0	0	0	0
Fursenkoina acuta (D'ORBIGNY)	1	1	0	2	1	0	0	0
Glandulina ovula D'ORBIGNY	0	0	0	0	0	0	0	0
?*Glandulina* sp.	0	0	0	0	0	0	1	0
Globocassidulina oblonga (REUSS)	1	2	0	0	0	0	0	0
Globocassidulina cf. *globosa* (HANTKEN)	0	0	0	0	0	0	0	0
Globulina gibba D'ORBIGNY	0	0	1	0	0	1	1	0
Gyroidinoides octocameratus (CUSHMAN & HANNA)	0	0	0	0	0	0	0	0
Gyroidinoides cf. *octocameratus* (CUSHMAN & HANNA)	0	0	0	0	0	0	0	0
Gyroidinoides parvus (CUSHMAN & RENZ)	1	4	5	19	11	9	16	0
Hansenisca soldanii (D'ORBIGNY)	0	0	0	1	0	0	0	0
Hanzawaia boueana (D'ORBIGNY)	0	0	1	1	1	1	1	0
Hanzawaia cf. *boueana* (D'ORBIGNY)	0	0	0	0	0	0	0	0
Hemirobulina glabra (D'ORBIGNY)	0	0	0	0	0	0	0	0
Hemirobulina cf. *pediformis* (BORNEMANN)	0	0	0	0	0	0	0	0
Heterolepa dutemplei (D'ORBIGNY)	1	0	0	0	1	1	1	0
Laevidentalina cf. *boueana* (D'ORBIGNY)	1	10	6	15	12	9	0	1
Laevidentalina communis (D'ORBIGNY)	0	1	2	2	3	6	1	0
Laevidentalina elegans (D'ORBIGNY)	0	0	0	0	0	0	0	0
Laevidentalina sp.	0	0	0	0	0	0	0	0
Lagena gracilicosta REUSS	1	0	1	0	1	1	0	1
Lagena striata (D'ORBIGNY)	0	0	1	1	0	0	0	1
Lagena sp.	0	0	1	0	0	0	0	0
?*Lagena* sp.	0	1	0	0	0	0	0	0
Lenticulina calcar (LINNÉ)	0	0	0	0	0	0	0	1
Lenticulina inornata (D'ORBIGNY)	5	9	8	4	13	18	31	8

Tab. 4.1 (continued).

	OS 17	OS 18	OS 19	OS 20	OS 21	OS 22	OS 23	OS 24
Lenticulina gibba (D'ORBIGNY)	0	0	0	1	2	0	0	0
Lobatula lobatula (WALKER & JACOB)	1	1	0	2	0	0	0	0
?*Lobatula lobatula* (WALKER & JACOB)	0	0	0	0	0	0	0	0
Marginulina hirsuta D'ORBIGNY	0	0	0	0	4	7	13	6
Marginulina wengeri RUPP & HAUNOLD-YENKE	0	0	0	0	0	1	0	0
Melonis pompilioides (FICHTEL & MOLL)	0	0	1	0	0	0	1	0
Melonis sp.	0	0	0	2	2	3	0	0
Myllostomella advena (CUSHMAN & LAIMING)	0	0	0	0	0	0	0	1
Myllostomella recta (PALMER & BERMUDEZ)	0	0	0	1	0	0	0	0
Nonion commune (D'ORBIGNY)	3	1	2	12	15	7	8	9
Nonionidae indet.	0	1	0	0	0	0	1	0
Oridorsalis umbonatus (REUSS)	1	5	10	9	21	22	17	10
?*Porosononion* sp.	0	0	0	0	0	0	0	0
Praeglobobulimina pyrula-pupoides gr.	0	0	0	1	16	19	14	9
Praeglobobulimina sp.	0	0	0	0	0	0	0	0
?*Protelphidium roemeri* (CUSHMAN)	0	0	0	0	3	0	0	0
Pullenia bulloides (D'ORBIGNY)	0	0	0	0	0	0	0	0
Pullenia quinqueloba (REUSS)	0	0	0	0	0	0	0	0
Pullenia sp.	0	0	0	0	0	0	0	0
Quadrimorphina petrolei (ANDREAE)	0	0	0	1	0	0	0	0
Saracenaria arcuata (D'ORBIGNY)	0	0	0	0	0	1	0	0
?*Stilostomellidae* indet.	0	0	0	0	0	0	1	0
Vaginulinopsis cf. *hauerina* (D'ORBIGNY)	0	0	0	0	0	0	1	0
Vaginulinopsis sp.	0	0	0	0	0	0	0	0
Valvulineria complanata (D'ORBIGNY)	0	2	2	18	26	29	25	7
Hyaline indet.	3	8	10	31	25	19	16	19
Cycloforina cf. *ludwigi* (REUSS)	1	1	0	0	0	0	0	0
?*Cycloforina* sp.	0	0	0	0	0	0	0	0
Pyrgo cf. *lucernula* SCHWAGER	0	0	0	0	0	0	0	0
Pyrgo lunula (D'ORBIGNY)	0	0	0	0	0	0	0	0
Pyrgo simplex (D'ORBIGNY)	0	0	0	1	0	0	0	0
Quinqueloculina buchiana D'ORBIGNY	0	0	1	0	0	0	10	0
Quinqueloculina cf. *buchiana* D'ORBIGNY	0	0	0	0	0	5	0	0
Quinqueloculina sp.	0	1	1	0	8	1	0	1
Sigmoilinita tenuis (CZIJZEK)	2	7	2	7	3	4	6	1
Sigmoilopsis ottnangensis CICHA, CTYROKA & ZAPLETALOVA	2	6	5	15	7	14	14	3
Sigmoilopsis cf. *ottnangensis* CICHA, CTYROKA & ZAPLETALOVA	0	0	0	0	0	0	0	0
Spiroloculina canalilucuta D'ORBIGNY	0	0	0	0	0	0	0	0
Spiroloculina lamposa HUSSEY	0	0	0	1	0	0	1	0
Spiroloculina sp.	0	0	0	0	0	0	0	0
Miliolidae indet.	1	0	0	0	0	0	0	0
Martinotiella communis (D'ORBIGNY)	0	0	0	0	3	0	0	0
Spiroplectamina pectinata (REUSS)	8	4	9	15	5	7	11	3
Textularia gramen D'ORBIGNY	0	0	0	0	0	0	0	0
Textularia cf. *gramen* D'ORBIGNY	0	0	0	0	0	0	0	0
Textularia sp.	0	0	0	0	0	0	0	0
Hyaline	29	66	81	174	204	179	187	104
Miliolid	6	15	9	24	18	24	31	5
Agglutinated	8	4	9	15	8	7	11	3
Total	43	85	99	213	230	210	229	112
Number of taxa	19	25	28	34	35	28	33	20
Diversity (Fisher alpha)	13.0	11.9	13.0	11.4	11.5	8.7	10.6	7.1
Dominance	0.10	0.08	0.07	0.07	0.07	0.07	0.07	0.13
Equitability	0.88	0.87	0.87	0.83	0.83	0.86	0.83	0.80
Inner neritic taxa (%)	0	2	3	2	2	0	1	1
Outer neritic-bathyal taxa (%)	9	27	25	31	34	38	28	16
Epifauna (%)	53	48	43	39	35	42	50	26
Infauna (%)	28	35	39	34	44	43	37	48
Deep infauna (%)	0	0	0	0	8	9	7	8
Oxic indicators (%)	9	12	4	7	5	6	6	3
Suboxic indicators (%)	74	71	81	76	76	78	75	73
Dysoxic indicators (%)	0	0	0	0	8	9	7	8
High nutrient-flux ndicators (%)	0	1	10	4	10	11	7	8

Tab.4.2. Bathymetric distribution (IN = inner neritic, MN = middle neritic, ON = outer neritic, B = bathyal), microhabitat (E = epifaunal, I = infaunal, DI = deep infaunal), oxygen dependency (O = oxic, S = suboxic, D = dysoxic) and dependence on high organic matter flux (H = high OM flux) for benthic foraminifers from the stratotype.

References: 1 Kaiho (1994), 2 Hohenegger (2005), 3 Rögl & Spezzaferri (2003), 4 Murray (2006), 5 Barmawidjaja et al. (1992), 6 Bernhard & Sen Gupta (2002), 7 Pipperr & Reichenbacher (2010), 8 Reolid et al. (2008), 9 Jones (1994), 10 Pezelj et al. (2007), 11 Kouwenhoven & Van der Zwaan (2006), 12 Den Dulk et al. (2000), 13 Van Hinsbergen et al. (2005), 14 Spezzaferri et al. (2002), 15 Spezzaferri & Tamburini (2007), 16 Martins et al. (2007), 17 Baldi (2006), 18 Corliss et al. (1991), 19 Roetzel et al. (2006), 20 Leckie & Olson (2003), 21 Grunert et al. (2010a), 22 Wenger (1987).

	Depth	Habitat	Oxygen	Productivity	References
Alabamina tangentialis	ON-B	E/I	S		1.2
Ammonia spp.	IN	E/SI	O/S		3,4,5,6
Amphicoryna spp.	MN-B	I	S		1,2,7,8
Astacolus crepidulus	IN				9
Asterigerinata spp.	IN-MN	E	O		4,10
Astrononion spp.	IN-B	E/I	S		4,6,11,12
Aubignyna spp.	IN	?I			4
Biapertorbis biaperturatus	ON-B	E	?S		7,8
Bolivina spp.	IN-B	I/DI	D		4,5,13
Bulimina elongata	IN-B	I	S/D	H	4,13,14
Caucasina spp.	IN-B	I	S/D		4,13,14
Chilostomella spp.	ON-B	DI	D		4,6
Cibicidoides spp.	MN-B	E	O		1,2,3,7
Dentalina spp.	IN-B	I	S/D		1,2,4,6,15
Elphidiella spp.	IN-ON	?I			4
Elphidium spp. (keeled)	IN	E	O		3,4,16
Elphidium spp. (non-keeled)	IN	I	O		4
Fursenkoina acuta	IN-B	I	S/D		4,7,14,17
Glandulina spp.	MN-B	I	S		9,10
Globocassidulina spp.	MN-B	I	O/S		4,6
Globulina gibba	IN-B		O		2,22
Gyroidinoides spp.	B	E	S		18,19
Hansenisca soldanii	B	E	S		9,10,18
Hanzawaia boueana	IN	E	S		4,11,12
Hemirobulina spp.	IN-B	?I			20
Heterolepa dutemplei	IN-B	E	O		2,4,17
Laevidentalina spp.	ON-B	I	S/D		2,8
Lagena spp.	IN-B	I	S		1,2,8,11
Lenticulina spp.	MN-B	E	S		1,3,8,11,17
Lobatula lobatula	IN-MN	E	O		2,15,22
Marginulina spp.	IN-B	?I	?O		8,19
Melonis spp.	MN-B	I	S/D	H	1,4,15
Myllostomella advena	MN-B	I	S/D		19,21
Myllostomella recta	MN-B	I	S/D		19,21
Nonion commune	MN-B	I/E	S		2,3,15
Oridorsalis umbonatus	B	E	S		1,4,10
Porosononion spp.	IN-MN				2
Praeglobobulimina spp.	MN-B	DI	D	H	1,2,3,4,16
Protelphidium roemeri	?IN-ON				22
Pullenia spp.	ON-B	I	S		1,4,11,12
Pyrgo spp.	IN-B	E	O/S		1,4
Quadrimorphina petrolei	B	I	S		1,4,22
Saracenaria arcuata	ON-B	I			2,8
Vaginulinopsis spp.	MN-B	I			2,8,9
Valvulineria complanata	ON-B	I	S		1,4,6

Tab. 4.2 (continued).

	Depth	Habitat	Oxygen	Productivity	References
Cycloforina spp.		E			
Pyrgo spp.	IN-B	E			4
Quinqueloculina spp.	IN-ON	E	O/S		4
Sigmoilinita tenuis	MN-B	E	O		10,22
Sigmoilopsis ottnangensis	MN-B	E	?S		7,22
Spiroloculina spp.	IN	E	O/S		4,6
Martinotiella communis	ON-B	E	O		10,15
Spiroplectamina pectinata	MN-B	E	S		7,22
Textularia spp.	IN-B	E	O/S		4,10

Tab. 4.3. Dinoflagellate cysts from the stratotype.

	OS 1	OS 2	OS 3	OS 4	OS 5	OS 6	OS 7	OS 8
Apteodinium spiridoides BENEDEK	30	168	149	100	70	98	35	152
Achomosphaera/Spiniferites spp.	21	12	19	18	9	21	18	19
Apteodinium australiense (DEFLANDRE & COOKSON) WILLIAMS	0	0	0	0	1	0	0	0
Apteodinium spp.	132	12	10	5	0	1	1	3
Batiacasphaera sphaerica STOVER	2	0	0	0	0	0	0	0
Cerebrocysta poulsenii DE VERTEUIL & NORRIS	0	0	0	0	0	0	0	0
Cleistosphaeridium placacanthum/ancyreum	7	0	4	3	20	25	6	15
Cordosphaeridium cantharellus (BROSIUS) GOCHT	0	1	1	0	0	1	0	0
Cousteaudinium aubryae DE VERTEUIL & NORRIS	0	0	1	0	0	0	0	0
Cribroperidinium giuseppei (MORGENROTH) HELENES	4	1	4	1	1	0	2	6
Cribroperidinium tenuitabulatum (GERLACH) HELENES	1	2	1	4	3	1	0	3
Dapsilidinium pseudocolligerum/pastielsii	0	1	4	5	2	1	3	3
Deflandrea phosphoritica EISENACK	0	0	0	0	0	0	0	0
"Distatodinium cavatum" ZEVENBOOM & SANTARELLI	1	0	0	0	0	0	0	0
Distatodinium paradoxum (BROSIUS) EATON	0	2	8	2	2	2	7	0
Exochosphaeridium insigne DE VERTEUIL & NORRIS	3	7	14	6	5	7	3	10
Glaphyrocysta reticulosa (GERLACH) STOVER & EVITT s.l.	4	5	2	3	1	0	1	0
Glaphyrocysta spp.	13	14	4	16	1	0	1	0
Heteraulacacysta sp. A COSTA & DOWNIE	0	0	0	0	1	0	0	0
Homotryblium tenuispinosum DAVEY & WILLIAMS	0	1	0	0	0	0	1	0
Hystrichokolpoma cinctum KLUMPP	0	0	0	1	0	0	1	1
Hystrichokolpoma denticulatum MATSUOKA	0	1	1	1	1	0	1	0
Hystrichokolpoma rigaudiae DEFLANDRE & COOKSON	0	2	3	1	1	1	0	0
Hystrichokolpoma truncatum BIFFI & MANUM	1	1	0	0	0	0	0	0
Hystrichokolpoma spp.	0	4	0	2	3	3	0	3
Hystrichosphaeropsis obscura HABIB	0	0	1	0	0	0	1	0
Impagidinium paradoxum (WALL) STOVER & EVITT	0	0	1	1	0	0	1	0
Lejeunecysta brassensis BIFFI & GRIGNANI	0	0	0	1	0	0	0	0
Lejeunecysta communis BIFFI & GRIGNANI	0	0	0	1	2	1	0	0
Lejeunecysta convexa MATSUOKA & BUJAK	0	0	1	0	1	1	1	1
Lejeunecysta diversiforma (BRADFORD) ARTZNER & DÖRHÖFER	1	0	2	2	1	0	2	3
Lejeunecysta spp.	0	4	1	6	2	3	1	1
Lingulodinium machaerophorum (DEFLANDRE & COOKSON) WALL	6	1	1	5	1	1	1	2
Melitasphaeridium choanophorum (DEFLANDRE & COOKSON) HARLAND & HILL	0	0	1	1	1	1	1	0
Membranilarnacia? picena BIFFI & MANUM	1	0	1	1	0	0	0	0
Membranophoridium sp.	1	0	1	1	0	0	0	0
Nematosphaeropsis downieii BROWN	1	1	1	1	0	1	1	1
Nematosphaeropsis labyrinthus (OSTENFELD) REID	0	0	0	0	0	0	0	0
Operculodinium centrocarpum (DEFLANDRE & COOKSON) WALL	5	3	9	7	2	5	1	3
Operculodinium piaseckii STRAUSS & LUND	0	0	1	0	0	0	0	0
Palaeocystodinium miocaenicum STRAUSS, LUND & LUND-CHRISTENSEN	0	0	0	0	0	0	0	0
Palaeocystodinium powellii STRAUSS, LUND & LUND-CHRISTENSEN	0	0	0	1	0	0	0	0
Pentadinium laticinctum GERLACH	1	1	1	1	1	0	0	1
Polysphaeridium zoharyi (ROSSIGNOL) BUJAK	9	4	10	34	110	67	141	0
Reticulatosphaera actinocoronata (BENEDEK) MATSUOKA & BUJAK	0	2	2	0	2	3	5	2
Rounded brown cysts	8	7	2	25	6	7	10	12
Selenopemphix armageddonensis DE VERTEUIL & NORRIS	0	0	0	0	0	1	0	0
Selenopemphix brevispinosa HEAD, MORRIS & MUDIE	1	0	1	1	0	1	2	0
Selenopemphix nephroides BENEDEK	3	6	2	4	1	1	3	1
Selenopemphix quanta (BRADFORD) MATSUOKA	1	0	0	0	0	0	1	0
Spiniferites pseudofurcatus (KLUMPP) SARJEANT	0	5	0	1	1	1	2	9
Spiniferites solidago DE VERTEUIL & NORRIS	0	1	1	0	0	0	0	0
Sumatradinium druggii LENTIN, FENSOME & WILLIAMS	0	0	0	0	1	0	1	0
Sumatradinium hispidum (DRUGG) LENTIN & WILLIAMS	0	1	0	0	2	1	1	0
Sumatradinium soucouyantiae DE VERTEUIL & NORRIS	2	2	1	2	1	1	2	1
Tectatodinium pellitum WALL	0	0	0	0	0	0	0	0
Thalassiphora pelagica (EISENACK) EISENACK & GOCHT	1	1	0	0	1	0	0	0
Trinovantedinium spp.	0	0	0	0	1	0	0	0
Tuberculodinium vancampoae (ROSSIGNOL) WALL	1	1	1	1	1	0	0	0
Xandarodinium xanthum REID	0	0	0	1	1	0	0	0
Protoperidinium cysts indet.	0	0	0	0	0	0	0	0
Dinoflagellate cysts indet.	0	0	0	0	0	0	0	0
Reworked dinocysts	0	0	0	1	0	0	0	0
Total	261	274	267	267	260	257	258	252

Tab. 4.3 (continued).

	OS 1	**OS 2**	**OS 3**	**OS 4**	**OS 5**	**OS 6**	**OS 7**	**OS 8**
Number of taxa	27	31	36	37	35	27	32	22
Diversity (Fisher alpha)	7.6	9.0	11.2	11.7	10.9	7.6	9.6	5.8
Dominance	0.28	0.39	0.33	0.18	0.26	0.23	0.33	0.38
Equitability	0.60	0.53	0.56	0.68	0.56	0.60	0.54	0.55
Coastal taxa (%)	80	80	78	67	83	79	74	76
Restricted marine taxa (%)	4	3	6	15	43	26	56	1
Offshore taxa (%)	1	4	3	3	3	3	3	3
Protoperidinoid species (%)	6	7	4	16	7	7	9	8
Protoperidinoids + *L. machaerophorum* (%)	8	8	4	18	8	7	10	8

Tab. 4.3 (continued).

	OS 9	OS 10	OS 11	OS 12	OS 13	OS 14	OS 15	OS 16
Apteodinium spiridoides BENEDEK	146	97	70	65	49	42	27	59
Achomosphaera/Spiniferites spp.	21	30	31	58	39	53	47	62
Apteodinium australiense (DEFLANDRE & COOKSON) WILLIAMS	0	0	0	0	0	0	0	0
Apteodinium spp.	0	0	1	0	1	1	2	2
Batiacasphaera sphaerica STOVER	0	2	0	0	0	0	0	0
Cerebrocysta poulsenii DE VERTEUIL & NORRIS	0	0	0	0	0	0	0	0
Cleistosphaeridium placacanthum/ancyreum	7	6	9	9	14	11	12	4
Cordosphaeridium cantharellus (BROSIUS) GOCHT	0	0	0	0	0	0	1	0
Cousteaudinium aubryae DE VERTEUIL & NORRIS	0	0	0	0	0	0	0	0
Cribroperidinium giuseppei (MORGENROTH) HELENES	6	9	38	5	39	35	27	7
Cribroperidinium tenuitabulatum (GERLACH) HELENES	6	4	35	27	8	12	9	3
Dapsilidinium pseudocolligerum/pastielsii	1	0	5	4	2	6	2	3
Deflandrea phosphoritica EISENACK	0	0	0	0	0	0	0	0
"Distatodinium cavatum" ZEVENBOOM & SANTARELLI	0	0	0	0	0	0	0	0
Distatodinium paradoxum (BROSIUS) EATON	1	1	1	0	0	3	0	0
Exochosphaeridium insigne DE VERTEUIL & NORRIS	8	36	12	15	11	3	8	8
Glaphyrocysta reticulosa (GERLACH) STOVER & EVITT s.l.	1	0	0	1	0	1	0	0
Glaphyrocysta spp.	1	1	0	1	1	2	1	0
Heteraulacacysta sp. A COSTA & DOWNIE	0	1	1	4	7	0	4	0
Homotryblium tenuispinosum DAVEY & WILLIAMS	0	0	1	1	0	0	0	0
Hystrichokolpoma cinctum KLUMPP	0	0	0	0	1	0	0	0
Hystrichokolpoma denticulatum MATSUOKA	1	1	0	4	1	0	0	0
Hystrichokolpoma rigaudiae DEFLANDRE & COOKSON	0	1	3	1	0	1	1	0
Hystrichokolpoma truncatum BIFFI & MANUM	0	0	0	0	0	0	0	0
Hystrichokolpoma spp.	0	4	1	1	3	3	1	1
Hystrichosphaeropsis obscura HABIB	1	0	2	1	0	1	0	0
Impagidinium paradoxum (WALL) STOVER & EVITT	0	0	1	0	0	0	0	0
Lejeunecysta brassensis BIFFI & GRIGNANI	1	0	0	0	1	3	1	1
Lejeunecysta communis BIFFI & GRIGNANI	0	0	0	1	0	0	1	0
Lejeunecysta convexa MATSUOKA & BUJAK	1	1	0	0	0	0	0	0
Lejeunecysta diversiforma (BRADFORD) ARTZNER & DÖRHÖFER	1	1	0	0	0	0	1	0
Lejeunecysta spp.	3	7	3	1	7	5	14	6
Lingulodinium machaerophorum (DEFLANDRE & COOKSON) WALL	2	13	5	5	23	26	27	19
Melitasphaeridium choanophorum (DEFLANDRE & COOKSON) HARLAND & HILL	2	0	2	0	0	1	1	0
Membranilarnacia? picena BIFFI & MANUM	0	0	0	0	0	0	0	0
Membranophoridium sp.	0	0	0	0	0	0	0	0
Nematosphaeropsis downieii BROWN	1	1	1	1	4	2	5	4
Nematosphaeropsis labyrinthus (OSTENFELD) REID	1	0	0	0	0	0	0	0
Operculodinium centrocarpum (DEFLANDRE & COOKSON) WALL	16	2	4	8	7	8	6	10
Operculodinium piaseckii STRAUSS & LUND	0	0	0	0	0	0	0	1
Palaeocystodinium miocaenicum STRAUSS, LUND & LUND-CHRISTENSEN	0	0	0	0	0	0	1	0
Palaeocystodinium powellii STRAUSS, LUND & LUND-CHRISTENSEN	1	0	0	0	0	0	0	0
Pentadinium laticinctum GERLACH	0	0	1	0	1	0	0	0
Polysphaeridium zoharyi (ROSSIGNOL) BUJAK	1	4	1	5	5	3	1	3
Reticulatosphaera actinocoronata (BENEDEK) MATSUOKA & BUJAK	1	1	4	3	1	3	5	3
Rounded brown cysts	12	7	7	12	11	13	8	3
Selenopemphix armageddonensis DE VERTEUIL & NORRIS	1	0	0	1	1	1	3	3
Selenopemphix brevispinosa HEAD, MORRIS & MUDIE	0	1	0	0	0	0	0	0
Selenopemphix nephroides BENEDEK	0	4	3	1	6	1	7	2
Selenopemphix quanta (BRADFORD) MATSUOKA	0	0	0	4	0	3	0	0
Spiniferites pseudofurcatus (KLUMPP) SARJEANT	11	9	7	7	5	2	14	4
Spiniferites solidago DE VERTEUIL & NORRIS	0	0	0	0	0	0	0	0
Sumatradinium druggii LENTIN, FENSOME & WILLIAMS	0	0	0	0	1	0	0	0
Sumatradinium hispidum (DRUGG) LENTIN & WILLIAMS	0	4	0	1	0	3	0	1
Sumatradinium soucouyantiae DE VERTEUIL & NORRIS	0	5	2	2	2	3	8	4
Tectatodinium pellitum WALL	0	0	0	1	0	0	0	0
Thalassiphora pelagica (EISENACK) EISENACK & GOCHT	0	0	0	0	0	0	0	0
Trinovantedinium spp.	0	0	0	0	1	0	1	4
Tuberculodinium vancampoae (ROSSIGNOL) WALL	2	0	0	1	1	0	2	0
Xandarodinium xanthum REID	0	0	0	1	0	1	2	2
Protoperidinium cysts indet.	0	0	0	0	0	0	1	0
Dinoflagellate cysts indet.	0	0	0	1	0	0	0	0
Reworked dinocysts	0	1	0	0	0	0	0	1
Total	257	254	251	253	253	252	251	220

Tab. 4.3 (continued).

	OS 9	OS 10	OS 11	OS 12	OS 13	OS 14	OS 15	OS 16
Number of taxa	28	28	27	33	29	30	33	26
Diversity (Fisher alpha)	8.0	8.0	7.7	10.1	8.5	8.9	10.2	7.7
Dominance	0.34	0.19	0.14	0.14	0.11	0.11	0.09	0.17
Equitability	0.55	0.69	0.73	0.72	0.78	0.77	0.81	0.72
Coastal taxa (%)	75	63	68	55	54	47	38	44
Restricted marine taxa (%)	2	2	3	4	3	4	2	3
Offshore taxa (%)	2	3	4	4	4	4	5	4
Protoperidinoid species (%)	7	12	6	9	12	13	18	12
Protoperidinoids + *L. machaerophorum* (%)	8	17	8	11	21	23	29	20

Tab. 4.3 (continued).

	OS 17	OS 18	OS 19	OS 20	OS 21	OS 22	OS 23	OS 24
Apteodinium spiridoides BENEDEK	38	83	30	71	29	45	28	91
Achomosphaera/Spiniferites spp.	108	43	67	42	92	59	51	34
Apteodinium australiense (DEFLANDRE & COOKSON) WILLIAMS	0	0	0	0	0	0	0	0
Apteodinium spp.	2	3	10	2	0	3	8	1
Batiacasphaera sphaerica STOVER	0	0	1	1	0	0	0	0
Cerebrocysta poulsenii DE VERTEUIL & NORRIS	0	1	1	0	0	0	0	0
Cleistosphaeridium placacanthum/ancyreum	16	9	14	6	10	19	8	4
Cordosphaeridium cantharellus (BROSIUS) GOCHT	1	0	0	0	1	3	0	0
Cousteaudinium aubryae DE VERTEUIL & NORRIS	0	0	0	0	0	0	0	0
Cribroperidinium giuseppei (MORGENROTH) HELENES	1	18	12	6	6	5	9	6
Cribroperidinium tenuitabulatum (GERLACH) HELENES	1	13	0	3	1	5	1	4
Dapsilidinium pseudocolligerum/pastielsii	3	5	6	1	5	4	7	0
Deflandrea phosphoritica EISENACK	0	0	0	0	1	2	0	0
"Distatodinium cavatum" ZEVENBOOM & SANTARELLI	0	0	0	0	0	0	0	0
Distatodinium paradoxum (BROSIUS) EATON	1	1	3	1	1	0	1	0
Exochosphaeridium insigne DE VERTEUIL & NORRIS	10	11	10	24	6	15	16	5
Glaphyrocysta reticulosa (GERLACH) STOVER & EVITT s.l.	1	0	0	0	0	0	0	0
Glaphyrocysta spp.	3	0	1	1	1	1	0	1
Heteraulacacysta sp. A COSTA & DOWNIE	1	2	1	6	1	5	2	0
Homotryblium tenuispinosum DAVEY & WILLIAMS	1	0	0	0	1	1	0	0
Hystrichokolpoma cinctum KLUMPP	0	0	0	0	0	1	0	0
Hystrichokolpoma denticulatum MATSUOKA	0	0	0	0	0	0	0	0
Hystrichokolpoma rigaudiae DEFLANDRE & COOKSON	1	0	0	1	2	0	2	1
Hystrichokolpoma truncatum BIFFI & MANUM	0	0	0	0	0	0	0	1
Hystrichokolpoma spp.	2	2	3	0	1	1	5	1
Hystrichosphaeropsis obscura HABIB	0	1	0	2	0	1	0	1
Impagidinium paradoxum (WALL) STOVER & EVITT	0	0	0	0	0	0	0	0
Lejeunecysta brassensis BIFFI & GRIGNANI	1	0	1	2	0	0	1	0
Lejeunecysta communis BIFFI & GRIGNANI	0	0	0	0	2	1	0	0
Lejeunecysta convexa MATSUOKA & BUJAK	1	1	1	0	1	1	1	0
Lejeunecysta diversiforma (BRADFORD) ARTZNER & DÖRHÖFER	1	1	0	0	2	0	0	2
Lejeunecysta spp.	8	1	3	5	9	6	4	13
Lingulodinium machaerophorum (DEFLANDRE & COOKSON) WALL	11	19	24	18	30	18	27	11
Melitasphaeridium choanophorum (DEFLANDRE & COOKSON) HARLAND & HILL	1	1	3	0	4	0	2	0
Membranilarnacia? picena BIFFI & MANUM	0	0	0	0	0	0	0	0
Membranophoridium sp.	0	0	0	0	0	0	0	0
Nematosphaeropsis downieii BROWN	1	2	4	5	7	3	11	13
Nematosphaeropsis labyrinthus (OSTENFELD) REID	0	0	0	0	0	0	0	0
Operculodinium centrocarpum (DEFLANDRE & COOKSON) WALL	3	10	8	12	2	9	9	8
Operculodinium piaseckii STRAUSS & LUND	0	0	1	0	0	0	0	0
Palaeocystodinium miocaenicum STRAUSS, LUND & LUND-CHRISTENSEN	0	1	0	3	2	0	0	0
Palaeocystodinium powellii STRAUSS, LUND & LUND-CHRISTENSEN	1	0	0	2	1	3	0	1
Pentadinium laticinctum GERLACH	0	0	0	0	0	0	0	0
Polysphaeridium zoharyi (ROSSIGNOL) BUJAK	0	1	4	4	3	7	2	0
Reticulatosphaera actinocoronata (BENEDEK) MATSUOKA & BUJAK	8	3	7	4	9	2	6	2
Rounded brown cysts	8	9	7	5	7	8	4	17
Selenopemphix armageddonensis DE VERTEUIL & NORRIS	2	0	3	6	5	4	8	9
Selenopemphix brevispinosa HEAD, MORRIS & MUDIE	0	0	0	0	0	0	1	1
Selenopemphix nephroides BENEDEK	3	1	3	9	2	11	4	19
Selenopemphix quanta (BRADFORD) MATSUOKA	1	0	1	0	1	0	1	1
Spiniferites pseudofurcatus (KLUMPP) SARJEANT	12	3	15	1	2	1	2	1
Spiniferites solidago DE VERTEUIL & NORRIS	0	0	0	0	0	0	0	0
Sumatradinium druggii LENTIN, FENSOME & WILLIAMS	0	0	0	0	0	0	0	0
Sumatradinium hispidum (DRUGG) LENTIN & WILLIAMS	0	2	0	0	0	0	0	0
Sumatradinium soucouyantiae DE VERTEUIL & NORRIS	2	2	3	3	2	7	0	2
Tectatodinium pellitum WALL	0	0	0	1	0	0	0	0
Thalassiphora pelagica (EISENACK) EISENACK & GOCHT	0	0	0	0	0	0	0	0
Trinovantedinium spp.	0	0	3	0	1	1	2	1
Tuberculodinium vancampoae (ROSSIGNOL) WALL	0	1	1	2	1	0	1	0
Xandarodinium xanthum REID	0	1	1	0	1	0	1	0
Protoperidinium cysts indet.	0	0	0	0	0	0	0	0
Dinoflagellate cysts indet.	0	0	0	0	3	0	0	0
Reworked dinocysts	0	1	0	1	1	0	1	0
Total	254	252	252	250	256	252	226	251

Tab. 4.3 (continued).

	OS 17	OS 18	OS 19	OS 20	OS 21	OS 22	OS 23	OS 24
Number of taxa	32	31	32	31	38	31	31	27
Diversity (Fisher alpha)	9.7	9.3	9.7	9.3	12.3	9.3	9.7	7.7
Dominance	0.22	0.16	0.11	0.13	0.16	0.11	0.10	0.17
Equitability	0.65	0.70	0.79	0.75	0.70	0.79	0.80	0.71
Coastal taxa (%)	30	59	36	52	23	44	36	48
Restricted marine taxa (%)	2	3	4	3	4	6	4	0
Offshore taxa (%)	5	3	6	4	7	3	11	7
Protoperidinoid species (%)	11	7	10	12	13	15	12	26
Protoperidinoids + *L. machaerophorum* (%)	15	15	20	19	25	23	24	30

Tab 4.4. Calcareous nannoplankton from the stratotype.

Autochthonous species	**OS 1**	**OS 2**	**OS 3**	**OS 4**	**OS 5**	**OS 6**	**OS 7**	**OS 8**
Braarudosphaera bigelowii (GRAN & BRAARUD) DEFLANDRE	0	0	0	0	0	1	0	1
Calcidiscus sp.	0	0	0	0	0	0	0	0
Coccolithus miopelagicus BUKRY	0	1	0	0	0	0	0	0
Coccolithus pelagicus (WALLICH) SCHILLER	150	158	175	190	170	190	170	150
Coronocyclus nitescens (KAMPTNER) BRAMLETTE & WILCOXON	0	1	0	0	0	0	0	0
Coronosphaera mediterranea (LOHMAN) GAARDER	3	0	0	0	1	0	0	1
Cyclicargolithus floridanus (ROTH & HAY) BUKRY	17	32	19	16	18	10	15	13
Cricolithus jonesii (COHEN)	0	1	0	0	1	0	2	0
Discoaster deflandrei BRAMLETTE & RIEDEL	0	0	0	0	0	0	0	1
Discoaster sp.	0	0	0	0	0	0	0	0
Helicosphaera ampliaperta BRAMLETTE & WILCOXON	61	52	33	50	54	55	48	43
Helicosphaera minuta MÜLLER	0	4	0	0	0	0	0	0
Helicosphaera carteri (WALLICH) KAMPTNER	3	1	3	0	0	2	2	1
Helicosphaera euphratis HAQ	0	0	1	0	0	0	0	0
Helicosphaera intermedia MARTINI	0	0	0	0	0	1	0	0
Helicosphaera scissura MILLER	2	5	12	2	7	5	10	5
Helicosphaera sellii (BUKRY & BRAMLETTE) JAFAR & MARTINI	0	2	1	0	0	0	0	0
Helicosphaera sp.	0	0	1	0	0	0	0	0
Holodiscolithus macroporus (DEFLANDRE & FERT) ROTH	0	0	0	0	0	0	0	0
Lithostromoation sp.	0	1	0	0	0	0	0	0
Pontosphaera multipora (KAMPTNER) ROTH	0	0	1	0	0	0	0	1
Pontosphaera sp.	0	0	1	0	0	0	0	0
Reticulofenestra bisecta (HAY) ROTH	2	7	6	3	4	4	1	4
Reticulofenestra excavata LEHOTAYOVA	38	21	33	20	18	32	34	37
Reticulofenestra gelida (GEITZENAUER) WISE	0	0	0	2	1	3	3	5
Reticulofenestra haqii BACKMAN	2	0	0	0	0	0	0	0
Reticulofenestra lockeri MÜLLER	0	1	0	0	0	0	0	1
Reticulofenestra minuta ROTH	22	28	21	35	47	12	20	17
Reticulofenestra pseudoumbilica (GARTNER) GARTNER	7	3	0	0	4	6	4	1
Reticulofenestra sp.	2	4	1	1	0	1	0	2
Sphenolithus cf. *belemnos* BRAMLETTE & WILCOXON	0	0	0	0	0	0	0	0
Sphenolithus capricornutus BUKRY & PERCIVAL	0	0	1	0	0	0	0	0
Sphenolithus conicus BUKRY	0	0	0	0	0	0	0	0
Sphenolithus disbelemnos FORNACIARI & RIO	1	0	1	0	1	1	0	0
Sphenolithus dissimilis BUKRY & PERCIVAL	0	0	0	0	0	0	0	0
Sphenolithus moriformis (BRONNIMANN & STRADNER) BRAMLETTE & WILCOXON	2	1	2	1	0	0	0	1
Sphenolithus procerus MAIORANO & MONECHI	0	0	0	0	0	0	0	0
Sphenolithus cf. *tintinnabulum* MAIORANO & MONECHI	1	0	0	0	0	0	0	0
Sphenolithus sp.	1	2	0	0	0	1	0	0
Thoracosphaera heimii (LOHMANN) KAMPTNER	0	0	0	0	0	0	0	0
Thoracosphaera saxea STRADNER	1	1	0	0	1	0	1	0
Umbilicosphaera sp.	0	1	0	0	0	0	1	0
Total autochthonous species	315	325	312	320	327	324	311	283
Number of taxa	17	20	18	10	13	15	14	17
Diversity (Fisher alpha)	3.8	4.7	4.2	2.0	2.7	3.3	3.0	4.0
Dominance	0.29	0.27	0.34	0.40	0.33	0.39	0.34	0.33
Equitability	0.59	0.62	0.57	0.57	0.59	0.53	0.60	0.57
Reworked from Paleogene								
Blackites sp.	0	0	0	0	0	0	0	0
Chiasmolithus sp.	0	1	0	0	0	1	1	2
Cribrocentrum reticulatum (GARTNER & SMITH) PERCH-NIELSEN	0	1	0	1	0	1	0	0
Cruciplacolithus sp.	0	0	0	0	0	0	0	0
Cyclicargolithus abisectus (MÜLLER) WISE	0	0	0	0	0	0	0	0
Cyclicargoithus luminis (SULLIVAN) BUKRY	0	0	0	0	0	0	0	0
Discoaster lodoensis BRAMLETTE & RIEDEL	0	0	0	0	0	0	0	0
Discoaster taninodifer BRAMLETTE & RIEDEL	0	0	0	1	0	0	0	0
Discoaster barbardiensis TAN	0	0	0	0	0	0	0	0
Discoaster saipanensis BRAMLETTE & RIEDEL	0	0	0	0	0	0	1	0
Discoaster sp.	0	1	0	0	0	0	0	0
Ericsonia formosa (KAMPTNER) HAQ	4	1	1	1	2	0	1	0
Ericsonia robusta (BRAMLETTE & SULLIVAN) EDWARDS & PERCH-NIELSEN	0	1	1	0	0	0	0	0
Heliolithus kleinpellii SULLIVAN	0	0	0	0	0	0	0	0
Lanternithus minutus STRADNER	0	0	0	3	3	0	1	0
Tribrachiatus orthostylus (BRAMLETTE & RIEDEL) SHAMREI	0	0	0	0	0	0	0	1
Pemma sp.	0	0	0	0	0	0	0	0

Tab 4.4 (continued).

	OS 1	OS 2	OS 3	OS 4	OS 5	OS 6	OS 7	OS 8
Pontosphaera duocava (BRAMLETTE & SULLIVAN) ROMEIN	1	0	0	0	0	0	0	0
Pontosphaera exilis (BRAMLETTE & SULLIVAN) ROMEIN	1	0	0	0	0	1	0	0
Prinsius martinii (PERCH-NIELSEN) HAQ	0	0	0	1	2	1	0	0
Reticulofenestra dictyoda (DEFLANDRE & FERT) STRADNER	1	1	7	0	0	0	4	2
Reticulofenestra hillae BUKRY & PERCIVAL	0	0	0	0	0	0	1	0
Reticulofenestra stavensis (LEVIN & JOERGER) VAROL	0	1	1	3	1	0	0	1
Reticulofenestra umbilica (LEVIN) MARTINI & RITZKOWSKI	0	0	1	0	0	1	0	1
Toweius sp.	0	8	5	1	0	0	0	2
Zygrhablithus bijugatus (DEFLANDRE) DEFLANDRE	0	0	2	1	1	2	0	3
Reworked from Cretaceous								
Arkhangelskiella cymbiformis VEKSHINA	0	0	2	0	0	4	1	2
Arkhangelskiella maastrichtiana BURNETT	0	0	1	0	0	0	0	2
Biscutum ellipticum (GÓRKA) GRÜN	0	0	0	0	0	0	0	1
Broinsonia parca parca (STRADNER) BUKRY	1	0	1	1	0	0	0	0
Calculites ovalis (STRADNER) PRINS & SISSINGH	0	0	0	0	0	1	0	0
Cribrosphaerella ehrenbergii (ARKHANGELSKY) DEFLANDRE	0	0	0	0	0	0	0	1
Cyclagelosphaera reinhardtii (PERCH-NIELSEN) ROMEIN	1	0	0	1	1	4	1	0
Eiffellithus gorkae REINHARDT	2	3	2	1	0	2	0	0
Eiffellithus turriiseiffelii (DEFLANDRE) REINHARDT	0	0	1	0	0	0	0	0
Lucianorhabdus cayuxii DEFLANDRE	0	0	0	0	0	0	0	0
Microrhabdulus belgicus HAY & TOWE	0	0	0	0	0	0	0	0
Microrhabdulus decoratus DEFLANDRE	2	0	1	0	0	0	0	0
Micula decussata VEKSHINA	5	4	4	5	4	11	2	2
Nannoconus steinmannii KAMPTNER	0	0	0	0	0	0	0	0
Placozygus fibuliformis (REINHARDT) HOFFMANN	0	0	0	2	0	0	0	1
Prediscosphaera cretacea (ARKHANGELSKY) GARTNER	2	3	5	1	1	0	1	0
*Prolatipatela multicarinata G*ARTNER	0	0	0	0	0	0	0	0
Quadrum trifidum (STRADNER) PRINS & PERCH-NIELSEN	0	0	0	0	0	0	0	0
Reinhardtites levis PRINS & SISSINGH	0	0	0	0	0	1	0	0
Retecapsa crenulata (BRAMLETTE & MARTINI) GRÜN	1	0	0	3	1	2	0	0
Watznaueria barnesae (BLACK) PERCH-NIELSEN	40	40	31	27	37	30	34	34
Watznaueria biporta BUKRY	0	0	0	0	0	0	0	0
Watznaueria britannica (STRADNER) REINHARDT	5	1	6	1	1	5	2	0
Watznaueria fossacincta (BLACK) BOWN	4	4	1	1	0	1	0	0
Watznaueria manivitae BUKRY	0	0	0	0	0	1	0	0
Zeugrhabdotus diplogramus (DEFLANDRE) BURNETT	0	0	0	1	2	0	0	0
Zeugrhabdotus sp.	1	3	5	1	0	0	1	0
Total reworked	71	74	78	57	56	69	51	56
Total reworked Paleogene	7	16	18	12	9	7	9	13
Total reworked Cretaceous	64	58	60	45	47	62	42	43
Total	386	399	390	377	383	393	362	339

Tab 4.4 (continued).

Autochthonous species	**OS 9**	**OS 10**	**OS 11**	**OS 12**	**OS 13**	**OS 14**	**OS 15**	**OS 16**
Braarudosphaera bigelowii (GRAN & BRAARUD) DEFLANDRE	0	2	0	1	1	0	2	2
Calcidiscus sp.	0	0	0	0	1	1	0	0
Coccolithus miopelagicus BUKRY	0	1	0	0	0	0	0	1
Coccolithus pelagicus (WALLICH) SCHILLER	147	155	167	160	164	170	140	170
Coronocyclus nitescens (KAMPTNER) BRAMLETTE & WILCOXON	0	0	0	0	0	0	0	0
Coronosphaera mediterranea (LOHMAN) GAARDER	0	0	1	3	0	0	2	1
Cyclicargolithus floridanus (ROTH & HAY) BUKRY	23	16	11	23	24	12	12	12
Cricolithus jonesii (COHEN)	0	2	1	0	0	0	0	1
Discoaster deflandrei BRAMLETTE & RIEDEL	1	0	0	0	0	0	0	0
Discoaster sp.	1	0	0	0	0	0	0	0
Helicosphaera ampliaperta BRAMLETTE & WILCOXON	56	30	28	36	28	39	59	35
Helicosphaera minuta MÜLLER	1	0	0	0	0	0	0	0
Helicosphaera carteri (WALLICH) KAMPTNER	3	0	2	1	2	0	0	0
Helicosphaera euphratis HAQ	0	0	0	0	0	0	0	0
Helicosphaera intermedia MARTINI	0	0	0	0	0	0	0	0
Helicosphaera scissura MILLER	4	7	5	4	5	4	3	9
Helicosphaera sellii (BUKRY & BRAMLETTE) JAFAR & MARTINI	0	0	0	0	0	0	0	0
Helicosphaera sp.	0	0	0	0	0	0	0	0
Holodiscolithus macroporus (DEFLANDRE & FERT) ROTH	0	1	0	0	0	0	0	0
Lithostromoation sp.	0	0	0	0	0	0	0	0
Pontosphaera multipora (KAMPTNER) ROTH	0	0	0	0	1	0	0	0
Pontosphaera sp.	0	0	0	0	0	0	0	0
Reticulofenestra bisecta (HAY) ROTH	0	8	7	6	1	2	5	2
Reticulofenestra excavata LEHOTAYOVA	20	31	35	39	30	34	25	45
Reticulofenestra gelida (GEITZENAUER) WISE	6	0	3	0	1	3	0	5
Reticulofenestra haqii BACKMAN	1	0	0	1	0	0	4	0
Reticulofenestra lockeri MÜLLER	0	0	0	0	0	0	0	0
Reticulofenestra minuta ROTH	35	26	20	55	66	63	68	20
Reticulofenestra pseudoumbilica (GARTNER) GARTNER	4	4	2	1	1	2	2	7
Reticulofenestra sp.	1	2	2	4	0	0	1	1
Sphenolithus cf. *belemnos* BRAMLETTE & WILCOXON	0	0	0	1	0	0	0	0
Sphenolithus capricornutus BUKRY & PERCIVAL	0	0	0	0	0	0	0	1
Sphenolithus conicus BUKRY	0	0	0	0	1	0	0	0
Sphenolithus disbelemnos FORNACIARI & RIO	0	1	0	0	0	0	1	1
Sphenolithus dissimilis BUKRY & PERCIVAL	0	0	1	0	0	0	0	0
Sphenolithus moriformis (BRONNIMANN & STRADNER) BRAMLETTE & WILCOXON	0	2	0	0	1	0	0	1
Sphenolithus procerus MAIORANO & MONECHI	0	0	0	0	0	0	0	0
Sphenolithus cf. *tintinnabulum* MAIORANO & MONECHI	0	0	0	0	0	0	0	0
Sphenolithus sp.	0	0	1	0	0	0	1	1
Thoracosphaera heimii (LOHMANN) KAMPTNER	0	1	0	0	0	1	0	1
Thoracosphaera saxea STRADNER	0	2	0	1	0	0	0	0
Umbilicosphaera sp.	1	0	0	0	0	0	1	0
Total autochthonous species	304	291	286	336	327	331	326	316
Number of taxa	15	18	16	15	16	11	15	20
Diversity (Fisher alpha)	3.3	4.2	3.7	3.2	3.5	2.2	3.2	4.7
Dominance	0.29	0.31	0.37	0.28	0.31	0.33	0.27	0.32
Equitability	0.60	0.61	0.55	0.61	0.57	0.61	0.61	0.57
Reworked from Paleogene								
Blackites sp.	0	0	0	0	0	0	0	0
Chiasmolithus sp.	0	1	0	0	1	0	0	0
Cribrocentrum reticulatum (GARTNER & SMITH) PERCH-NIELSEN	1	0	0	0	0	0	0	0
Cruciplacolithus sp.	0	0	0	0	1	0	0	1
Cyclicargolithus abisectus (MÜLLER) WISE	0	0	0	0	0	0	0	0
Cyclicargoithus luminis (SULLIVAN) BUKRY	0	1	0	0	0	0	0	0
Discoaster lodoensis BRAMLETTE & RIEDEL	0	0	0	0	0	0	0	1
Discoaster taninodifer BRAMLETTE & RIEDEL	0	0	0	0	0	0	0	0
Discoaster barbardiensis TAN	0	0	0	0	0	2	0	0
Discoaster saipanensis BRAMLETTE & RIEDEL	0	0	0	0	0	0	0	0
Discoaster sp.	0	0	0	0	0	0	0	0
Ericsonia formosa (KAMPTNER) HAQ	0	2	0	2	0	2	1	0
Ericsonia robusta (BRAMLETTE & SULLIVAN) EDWARDS & PERCH-NIELSEN	0	0	0	0	0	0	0	0
Heliolithus kleinpellii SULLIVAN	0	0	0	0	1	0	0	0
Lanternithus minutus STRADNER	0	0	0	1	0	0	2	2
Tribrachiatus orthostylus (BRAMLETTE & RIEDEL) SHAMREI	0	0	0	0	0	0	0	0
Pemma sp.	0	1	0	0	0	0	0	0

Tab 4.4 (continued).

	OS 9	OS 10	OS 11	OS 12	OS 13	OS 14	OS 15	OS 16
Pontosphaera duocava (BRAMLETTE & SULLIVAN) ROMEIN	0	0	0	0	0	0	0	0
Pontosphaera exilis (BRAMLETTE & SULLIVAN) ROMEIN	0	0	0	0	0	0	1	0
Prinsius martinii (PERCH-NIELSEN) HAQ	0	0	0	0	0	0	0	0
Reticulofenestra dictyoda (DEFLANDRE & FERT) STRADNER	0	0	0	0	0	1	0	1
Reticulofenestra hillae BUKRY & PERCIVAL	0	0	0	0	1	0	0	0
Reticulofenestra stavensis (LEVIN & JOERGER) VAROL	0	0	0	3	0	0	1	0
Reticulofenestra umbilica (LEVIN) MARTINI & RITZKOWSKI	0	0	0	1	0	0	0	1
Toweius sp.	1	2	0	6	5	1	2	3
Zygrhablithus bijugatus (DEFLANDRE) DEFLANDRE	2	1	0	0	1	0	1	1
Reworked from Cretaceous								
Arkhangelskiella cymbiformis VEKSHINA	1	1	1	1	1	2	1	1
Arkhangelskiella maastrichtiana BURNETT	0	0	0	0	1	0	0	0
Biscutum ellipticum (GÓRKA) GRÜN	0	0	0	0	1	0	0	0
Broinsonia parca parca (STRADNER) BUKRY	0	0	0	0	0	0	0	0
Calculites ovalis (STRADNER) PRINS & SISSINGH	1	0	0	0	0	0	1	0
Cribrosphaerella ehrenbergii (ARKHANGELSKY) DEFLANDRE	1	0	0	0	0	0	0	0
Cyclagelosphaera reinhardtii (PERCH-NIELSEN) ROMEIN	4	0	0	1	0	1	1	0
Eiffellithus gorkae REINHARDT	0	0	1	1	0	0	2	1
Eiffellithus turriiseiffelii (DEFLANDRE) REINHARDT	0	0	0	0	0	0	0	0
Lucianorhabdus cayuxii DEFLANDRE	0	0	0	0	0	0	0	0
Microrhabdulus belgicus HAY & TOWE	0	0	0	0	1	0	0	0
Microrhabdulus decoratus DEFLANDRE	1	0	0	2	0	0	0	0
Micula decussata VEKSHINA	2	1	4	2	3	3	2	0
Nannoconus steinmannii KAMPTNER	0	0	0	0	0	0	0	0
Placozygus fibuliformis (REINHARDT) HOFFMANN	0	0	0	0	0	0	0	0
Prediscosphaera cretacea (ARKHANGELSKY) GARTNER	2	1	0	1	1	2	0	0
Prolatipatela multicarinata GARTNER	0	0	0	0	0	1	0	0
Quadrum trifidum (STRADNER) PRINS & PERCH-NIELSEN	0	0	0	0	0	0	0	0
Reinhardtites levis PRINS & SISSINGH	0	0	1	0	0	0	0	0
Retecapsa crenulata (BRAMLETTE & MARTINI) GRÜN	0	0	0	2	0	0	0	1
Watznaueria barnesae (BLACK) PERCH-NIELSEN	19	19	31	23	17	17	19	37
Watznaueria biporta BUKRY	1	0	0	0	0	0	0	1
Watznaueria britannica (STRADNER) REINHARDT	3	3	3	5	1	1	3	3
Watznaueria fossacincta (BLACK) BOWN	0	0	0	5	1	3	1	0
Watznaueria manivitae BUKRY	0	0	0	0	0	0	0	0
Zeugrhabdotus diplogramus (DEFLANDRE) BURNETT	2	0	0	0	0	0	2	1
Zeugrhabdotus sp.	1	0	1	2	0	0	0	0
Total reworked	42	33	42	58	37	36	40	55
Total reworked Paleogene	4	8	0	13	10	6	8	10
Total reworked Cretaceous	38	25	42	45	27	30	32	45
Total	346	324	328	394	364	367	366	371

Tab 4.4 (continued).

Autochthonous species	**OS 17**	**OS 18**	**OS 19**	**OS 20**	**OS 21**	**OS 22**	**OS 23**	**OS 24**
Braarudosphaera bigelowii (GRAN & BRAARUD) DEFLANDRE	2	0	0	0	0	3	3	1
Calcidiscus sp.	0	0	0	0	0	0	0	0
Coccolithus miopelagicus BUKRY	0	0	0	3	1	0	0	0
Coccolithus pelagicus (WALLICH) SCHILLER	150	120	165	190	150	138	120	134
Coronocyclus nitescens (KAMPTNER) BRAMLETTE & WILCOXON	0	0	0	0	1	0	0	0
Coronosphaera mediterranea (LOHMAN) GAARDER	0	0	0	0	0	0	0	0
Cyclicargolithus floridanus (ROTH & HAY) BUKRY	20	16	17	18	12	10	11	9
Cricolithus jonesii (COHEN)	0	7	0	1	0	1	0	2
Discoaster deflandrei BRAMLETTE & RIEDEL	0	0	0	0	0	0	0	0
Discoaster sp.	0	0	0	0	1	1	0	0
Helicosphaera ampliaperta BRAMLETTE & WILCOXON	52	26	46	28	38	20	29	26
Helicosphaera minuta MÜLLER	0	0	0	0	0	0	0	0
Helicosphaera carteri (WALLICH) KAMPTNER	3	1	1	0	5	0	3	1
Helicosphaera euphratis HAQ	0	2	0	1	1	0	0	0
Helicosphaera intermedia MARTINI	0	0	0	0	0	0	0	0
Helicosphaera scissura MILLER	4	4	5	3	6	10	10	7
Helicosphaera sellii (BUKRY & BRAMLETTE) JAFAR & MARTINI	0	0	0	0	0	0	0	0
Helicosphaera sp.	0	0	0	0	0	2	0	0
Holodiscolithus macroporus (DEFLANDRE & FERT) ROTH	0	0	0	0	0	0	0	0
Lithostromoation sp.	0	0	0	1	0	0	0	0
Pontosphaera multipora (KAMPTNER) ROTH	1	0	0	0	0	1	0	0
Pontosphaera sp.	0	0	0	0	0	0	0	0
Reticulofenestra bisecta (HAY) ROTH	6	2	6	2	5	0	4	4
Reticulofenestra excavata LEHOTAYOVA	46	69	43	55	56	47	45	42
Reticulofenestra gelida (GEITZENAUER) WISE	3	4	2	5	0	1	0	0
Reticulofenestra haqii BACKMAN	1	0	1	1	0	0	3	0
Reticulofenestra lockeri MÜLLER	0	1	0	0	0	1	0	1
Reticulofenestra minuta ROTH	26	65	18	3	44	76	84	71
Reticulofenestra pseudoumbilica (GARTNER) GARTNER	6	0	6	11	4	1	4	1
Reticulofenestra sp.	3	4	2	0	1	1	0	2
Sphenolithus cf. *belemnos* BRAMLETTE & WILCOXON	0	0	0	0	0	0	0	0
Sphenolithus capricornutus BUKRY & PERCIVAL	0	0	0	0	0	0	0	0
Sphenolithus conicus BUKRY	0	0	0	0	0	0	0	0
Sphenolithus disbelemnos FORNACIARI & RIO	0	0	0	0	0	0	0	0
Sphenolithus dissimilis BUKRY & PERCIVAL	0	0	0	0	0	0	0	0
Sphenolithus moriformis (BRONNIMANN & STRADNER) BRAMLETTE & WILCOXON	0	1	1	0	1	0	0	0
Sphenolithus procerus MAIORANO & MONECHI	0	0	0	0	1	0	0	0
Sphenolithus cf. *tintinnabulum* MAIORANO & MONECHI	0	0	0	0	0	0	0	0
Sphenolithus sp.	0	0	0	0	0	0	0	0
Thoracosphaera heimii (LOHMANN) KAMPTNER	0	0	0	0	0	0	0	1
Thoracosphaera saxea STRADNER	0	1	1	2	0	1	0	0
Umbilicosphaera sp.	0	1	0	0	1	1	0	0
Total autochthonous species	323	323	314	324	328	314	316	301
Number of taxa	14	15	14	15	17	17	12	14
Diversity (Fisher alpha)	3.0	3.3	3.0	3.3	3.8	3.9	2.5	3.0
Dominance	0.27	0.23	0.32	0.39	0.27	0.28	0.25	0.28
Equitability	0.65	0.65	0.59	0.53	0.60	0.57	0.68	0.62
Reworked from Paleogene								
Blackites sp.	1	0	0	0	0	0	0	0
Chiasmolithus sp.	0	0	0	0	0	0	0	1
Cribrocentrum reticulatum (GARTNER & SMITH) PERCH-NIELSEN	0	0	0	0	0	0	0	0
Cruciplacolithus sp.	1	0	0	0	0	0	0	0
Cyclicargolithus abisectus (MÜLLER) WISE	0	1	0	0	0	0	0	0
Cyclicargoithus luminis (SULLIVAN) BUKRY	0	0	0	0	0	0	0	0
Discoaster lodoensis BRAMLETTE & RIEDEL	0	0	0	0	0	0	0	0
Discoaster taninodifer BRAMLETTE & RIEDEL	0	0	0	0	0	0	0	0
Discoaster barbardiensis TAN	0	0	0	0	0	0	0	0
Discoaster saipanensis BRAMLETTE & RIEDEL	0	0	0	0	0	0	0	0
Discoaster sp.	0	0	0	0	0	0	0	0
Ericsonia formosa (KAMPTNER) HAQ	1	2	4	1	1	0	0	0
Ericsonia robusta (BRAMLETTE & SULLIVAN) EDWARDS & PERCH-NIELSEN	0	2	1	0	0	0	0	0
Heliolithus kleinpellii SULLIVAN	0	0	0	0	0	0	0	0
Lanternithus minutus STRADNER	0	1	1	0	1	0	0	0
Tribrachiatus orthostylus (BRAMLETTE & RIEDEL) SHAMREI	0	0	0	0	0	0	0	0
Pemma sp.	0	0	0	0	0	0	0	0

Tab 4.4 (continued).

	OS 17	OS 18	OS 19	OS 20	OS 21	OS 22	OS 23	OS 24
Pontosphaera duocava (BRAMLETTE & SULLIVAN) ROMEIN	1	0	0	0	0	0	0	0
Pontosphaera exilis (BRAMLETTE & SULLIVAN) ROMEIN	0	0	0	0	1	0	0	0
Prinsius martinii (PERCH-NIELSEN) HAQ	2	0	1	0	0	0	0	0
Reticulofenestra dictyoda (DEFLANDRE & FERT) STRADNER	1	1	1	4	0	1	0	4
Reticulofenestra hillae BUKRY & PERCIVAL	0	0	1	0	0	0	0	0
Reticulofenestra stavensis (LEVIN & JOERGER) VAROL	0	1	0	3	1	0	0	0
Reticulofenestra umbilica (LEVIN) MARTINI & RITZKOWSKI	0	0	0	0	0	0	0	1
Toweius sp.	2	0	0	2	1	0	3	2
Zygrhablithus bijugatus (DEFLANDRE) DEFLANDRE	1	0	0	0	0	1	1	1
Reworked from Cretaceous								
Arkhangelskiella cymbiformis VEKSHINA	2	2	0	2	3	3	0	0
Arkhangelskiella maastrichtiana BURNETT	0	0	0	0	0	0	0	0
Biscutum ellipticum (GÓRKA) GRÜN	0	0	0	0	0	0	0	0
Broinsonia parca parca (STRADNER) BUKRY	0	0	0	0	1	0	0	1
Calculites ovalis (STRADNER) PRINS & SISSINGH	0	1	0	0	1	0	0	0
Cribrosphaerella ehrenbergii (ARKHANGELSKY) DEFLANDRE	0	3	1	2	1	0	0	0
Cyclagelosphaera reinhardtii (PERCH-NIELSEN) ROMEIN	2	3	2	2	0	0	2	0
Eiffellithus gorkae REINHARDT	2	0	1	0	0	0	0	1
Eiffellithus turriiseiffelii (DEFLANDRE) REINHARDT	0	0	0	1	0	0	0	0
Lucianorhabdus cayuxii DEFLANDRE	0	0	0	0	0	1	0	0
Microrhabdulus belgicus HAY & TOWE	0	0	0	0	0	0	0	0
Microrhabdulus decoratus DEFLANDRE	2	0	0	0	0	0	0	0
Micula decussata VEKSHINA	4	1	9	5	2	6	1	1
Nannoconus steinmannii KAMPTNER	0	1	0	0	0	0	0	0
Placozygus fibuliformis (REINHARDT) HOFFMANN	1	0	0	0	0	0	1	0
Prediscosphaera cretacea (ARKHANGELSKY) GARTNER	1	4	2	1	1	1	3	0
Prolatipatela multicarinata GARTNER	0	0	0	0	0	0	0	0
Quadrum trifidum (STRADNER) PRINS & PERCH-NIELSEN	0	0	0	0	1	0	0	0
Reinhardtites levis PRINS & SISSINGH	0	0	0	0	0	0	0	0
Retecapsa crenulata (BRAMLETTE & MARTINI) GRÜN	3	1	0	2	1	0	1	0
Watznaueria barnesae (BLACK) PERCH-NIELSEN	36	22	30	41	32	15	14	16
Watznaueria biporta BUKRY	0	0	0	0	0	0	0	0
Watznaueria britannica (STRADNER) REINHARDT	4	10	4	3	4	3	5	1
Watznaueria fossacincta (BLACK) BOWN	3	1	1	5	3	0	1	0
Watznaueria manivitae BUKRY	0	0	0	0	1	1	0	0
Zeugrhabdotus diplogramus (DEFLANDRE) BURNETT	0	0	0	0	1	0	0	0
Zeugrhabdotus sp.	1	0	0	2	0	0	0	0
Total reworked	71	58	59	76	57	33	32	30
Total reworked Paleogene	10	9	9	10	5	3	4	10
Total reworked Cretaceous	61	49	50	66	52	30	28	20
Total	394	381	373	400	385	347	348	331

Tab 4.5. Granulometric data of the stratotype. Nomenclature follows Füchtbauer (1959) and Müller (1961). Proportions of sand, silt and clay in weight percent.

Sample	Nomenclature	sand	c. sand	m. sand	f. sand	silt	c. silt	m. silt	f. silt	clay
OS 1	clayey-sandy silt	**11.2**	0.0	0.6	10.5	**64.1**	16.2	25.9	22.0	**24.6**
OS 2	clayey-sandy silt	**12.6**	0.0	0.2	12.4	**64.7**	20.9	24.3	19.5	**22.7**
OS 3	clayey-sandy silt	**11.9**	0.1	0.6	11.2	**64.8**	20.6	23.7	20.6	**23.2**
OS 4	clayey-sandy silt	**21.0**	0.2	0.6	20.3	**58.2**	20.0	21.1	17.2	**20.7**
OS 5	clayey sand-silt	**34.4**	0.1	0.8	33.5	**50.3**	22.2	14.4	13.7	**15.3**
OS 6	clayey-sandy silt	**25.0**	0.1	0.6	24.3	**57.5**	22.8	18.7	16.0	**17.5**
OS 7	clayey-sandy silt	**22.4**	0.1	0.4	21.9	**62.2**	29.2	18.6	14.5	**15.4**
OS 8	clayey sand-silt	**29.4**	0.1	0.6	28.7	**55.6**	27.8	14.3	13.6	**14.9**
OS 9	clayey sand-silt	**40.0**	0.1	1.5	38.4	**44.7**	16.3	15.3	13.2	**15.3**
OS 10	clayey sand-silt	**33.1**	0.1	0.9	32.1	**51.5**	21.4	15.1	15.0	**15.4**
OS 11	clayey sand-silt	**33.8**	0.7	2.0	31.1	**52.5**	20.0	17.7	14.8	**13.7**
OS 12	clayey-sandy silt	**14.8**	0.2	0.7	13.9	**67.3**	24.5	22.7	20.1	**18.0**
OS 13	clayey-sandy silt	**14.2**	0.1	0.7	13.4	**66.2**	27.5	20.0	18.7	**19.6**
OS 14	clayey-sandy silt	**10.1**	0.1	0.7	9.3	**69.1**	28.8	20.7	19.5	**20.8**
OS 15	clayey-sandy silt	**11.7**	0.2	0.8	10.7	**67.5**	26.1	22.4	18.9	**20.8**
OS 16	clayey-sandy silt	**23.6**	0.1	0.4	23.1	**61.6**	31.5	15.6	14.5	**14.8**
OS 17	clayey-sandy silt	**22.1**	0.1	0.5	21.6	**59.9**	22.5	19.5	17.9	**17.9**
OS 18	clayey-sandy silt	**16.6**	0.0	0.2	16.4	**65.5**	29.2	18.6	17.6	**17.9**
OS 19	clayey-sandy silt	**25.0**	0.3	0.6	24.1	**57.8**	23.1	18.4	16.3	**17.2**
OS 20	clayey-sandy silt	**17.0**	0.0	0.2	16.7	**60.8**	24.3	19.1	17.4	**22.3**
OS 21	clayey-sandy silt	**12.6**	0.0	0.5	12.1	**67.4**	31.1	18.8	17.6	**20.0**
OS 22	clayey silt	**8.9**	0.0	0.4	8.5	**67.7**	26.3	20.8	20.5	**23.4**
OS 23	clayey silt	**7.3**	0.1	0.3	6.9	**70.1**	27.5	22.1	20.5	**22.6**
OS 24	clayey silt	**8.2**	0.0	0.2	8.0	**72.5**	33.7	20.8	18.0	**19.3**

Tab 4.6. Statistic moments (mean: first moment in Phi; standard deviation (Stand.dev): second moment in Phi; skewness: third moment) of the stratotype samples. Sorting is derived from standard deviation (Friedman, 1962).

Sample	Sorting	Mean (Phi)	σ (Phi)	Skewness
OS 1	extreme badly sorted	7.41	2.83	0.58
OS 2	extreme badly sorted	7.14	2.78	0.72
OS 3	extreme badly sorted	7.22	2.83	0.66
OS 4	extreme badly sorted	6.82	2.90	0.80
OS 5	extreme badly sorted	5.99	2.84	1.06
OS 6	extreme badly sorted	6.42	2.80	0.90
OS 7	extreme badly sorted	6.23	2.68	1.05
OS 8	extreme badly sorted	5.99	2.81	1.10
OS 9	extreme badly sorted	5.98	2.87	1.10
OS 10	extreme badly sorted	6.04	2.79	0.97
OS 11	extreme badly sorted	5.83	2.63	0.68
OS 12	very badly sorted	6.71	2.55	0.62
OS 13	extreme badly sorted	6.80	2.81	0.83
OS 14	extreme badly sorted	6.95	2.76	0.79
OS 15	extreme badly sorted	6.95	2.78	0.76
OS 16	extreme badly sorted	6.14	2.67	1.13
OS 17	extreme badly sorted	6.58	2.81	0.86
OS 18	extreme badly sorted	6.59	2.76	0.94
OS 19	extreme badly sorted	6.38	2.78	0.86
OS 20	extreme badly sorted	6.90	2.92	0.78
OS 21	extreme badly sorted	6.78	2.80	0.88
OS 22	extreme badly sorted	7.18	2.76	0.72
OS 23	extreme badly sorted	7.19	2.76	0.77
OS 24	extreme badly sorted	6.82	2.67	0.94

Tab 4.7. Relative abundances (%) of the most important (> 5% in at least one sample) foraminiferal, dinoflagellate cyst and calcareous nannoplankton taxa.

	OS 1	OS 2	OS 3	OS 4	OS 5	OS 6	OS 7	OS 8	OS 9	OS 10	OS 11	OS 12	OS 13	OS 14
Alabamina tangentialis	2	**6**	**7**	**10**	**14**	4	**9**	5	4	1	1	0	0	1
Ammonia spp.	1	**9**	3	5	2	2	1	0	0	1	0	0	0	0
Amphicoryna ottnangensis	1	2	1	1	1	2	4	0	1	**6**	**8**	**19**	3	4
Astrononion perfossum	3	0	2	5	5	14	7	6	3	2	0	0	0	0
Caucasina cylindrica	**15**	**21**	**20**	**17**	**21**	**21**	**20**	**14**	5	**14**	5	0	0	0
Cibicidoides spp.	3	4	5	2	2	3	3	2	3	**6**	**6**	1	2	4
Fursenkoina acuta	2	3	3	2	4	**8**	**9**	**6**	2	2	2	0	0	0
Gyroidinoides spp.	0	0	0	1	0	0	0	0	0	1	2	**12**	**15**	**10**
Hanzawaia boueana	1	**6**	1	2	1	1	2	0	1	1	0	0	0	0
Laevidentalina spp.	1	1	1	1	2	0	0	0	1	0	2	**17**	**17**	**12**
Lenticulina inornata	**56**	**6**	**39**	**19**	**21**	**19**	**29**	**43**	**55**	**17**	**16**	**9**	**7**	**9**
Marginulina spp.	0	0	0	0	0	0	0	0	0	0	0	0	1	0
Nonion commune	3	**16**	5	5	**6**	5	3	4	2	5	0	4	2	1
Oridorsalis umbonatus	0	0	0	1	0	0	0	0	0	0	3	5	**10**	**6**
Praeglobobulimina spp.	0	0	0	0	0	0	0	0	0	0	0	0	**6**	3
Valvulineria complanata	0	0	0	1	0	0	0	0	0	0	0	5	**10**	**10**
Sigmoilinita tenuis	0	0	0	1	1	0	0	3	1	**6**	**6**	0	0	0
Sigmoilopsis ottnangensis	2	0	0	0	0	2	2	**6**	**6**	4	**6**	2	**9**	3
Spiroloculina spp.	2	**8**	2	**13**	3	5	3	1	1	4	0	3	0	2
Spiroplectamina pectinata	0	0	1	1	5	3	1	3	**9**	**20**	**28**	1	0	2
Apteodinium spp.	**62**	**66**	**60**	**39**	**27**	**39**	**14**	**62**	**57**	**38**	**28**	**26**	**20**	**17**
Achomosphaera/Spiniferites spp.	**8**	4	**7**	**7**	3	**8**	**7**	**8**	**8**	**12**	**12**	**23**	**15**	**21**
Cleistosphaeridium spp.	3	0	1	1	**8**	**10**	2	**6**	3	2	4	4	**6**	4
Cribroperidinium spp.	2	1	2	2	2	0	1	4	5	5	**29**	**13**	**19**	**19**
Exochosphaeridium insigne	1	3	5	2	2	3	1	4	3	**14**	5	**6**	4	1
Glaphyrocysta spp.	7	7	2	7	1	0	1	0	1	0	0	1	0	1
Lejeunecysta spp.	0	1	1	4	2	2	2	2	2	4	1	1	3	3
Lingulodinium machaerophorum	2	0	0	2	0	0	0	1	1	5	2	2	**9**	**10**
Polysphaeridium zoharyi	3	1	4	**13**	**42**	**26**	**55**	0	0	2	0	2	2	1
Round brown cysts	3	3	1	**9**	2	3	4	5	5	3	3	5	4	5
Selenopemphix spp.	2	2	1	2	0	1	2	0	0	2	1	2	3	2
Spiniferites spp.	0	2	0	0	0	0	1	4	4	4	3	3	2	1
Coccolithus pelagicus	**48**	**49**	**56**	**59**	**52**	**59**	**55**	**53**	**48**	**53**	**58**	**48**	**50**	**51**
Cyclicargolithus floridianus	5	**10**	**6**	5	**6**	3	5	5	**8**	5	4	**7**	**7**	4
Helicosphaera ampliaperta	**19**	**16**	**11**	**16**	**17**	**17**	**15**	**15**	**18**	**10**	**10**	**11**	**9**	**12**
Helicosphaera spp.	2	4	**6**	1	2	2	4	2	3	2	2	1	2	1
Reticulofenestra excavata	**12**	**6**	**11**	**6**	**6**	**10**	**11**	**13**	**7**	**11**	**12**	**12**	**9**	**10**
Reticulofenestra minuta	**7**	**9**	**7**	**11**	**14**	**4**	**6**	**6**	**12**	**9**	**7**	**16**	**20**	**19**
Reticulofenestra spp.	4	4	2	2	3	4	3	4	4	5	5	4	1	2

Tab 4.7 (continued).

	OS 15	OS 16	OS 17	OS 18	OS 19	OS 20	OS 21	OS 22	OS 23	OS 24
Alabamina tangentialis	0	0	2	1	0	1	0	1	1	0
Ammonia spp.	0	4	0	1	2	0	1	0	0	1
Amphicoryna ottnangensis	0	5	**19**	**14**	**15**	**11**	**13**	**6**	**9**	**25**
Astrononion perfossum	0	1	0	2	1	3	0	0	0	0
Caucasina cylindrica	0	0	0	1	**6**	3	1	0	0	0
Cibicidoides spp.	**8**	4	2	2	1	3	2	3	3	2
Fursenkoina acuta	0	1	2	1	0	1	0	0	0	0
Gyroidinoides spp.	0	3	2	5	5	**9**	5	4	7	0
Hanzawaia boueana	0	0	0	0	1	0	0	0	0	0
Laevidentalina spp.	**21**	**21**	2	**13**	**8**	**8**	**6**	7	0	1
Lenticulina inornata	**25**	**7**	**12**	**11**	**8**	2	**6**	**9**	**14**	**7**
Marginulina spp.	0	0	0	0	0	0	2	4	**6**	5
Nonion commune	**13**	5	**7**	1	2	**6**	**7**	3	3	**8**
Oridorsalis umbonatus	4	**7**	2	**6**	**10**	4	**9**	**10**	**7**	**9**
Praeglobobulimina spp.	0	2	0	0	0	0	**7**	**9**	**6**	**8**
Valvulineria complanata	0	**14**	0	2	2	**8**	**11**	**14**	**11**	**6**
Sigmoilinita tenuis	0	0	5	**8**	2	3	1	2	3	1
Sigmoilopsis ottnangensis	4	0	5	**7**	5	**7**	3	**7**	**6**	3
Spiroloculina spp.	0	0	0	0	0	0	0	0	0	0
Spiroplectamina pectinata	4	4	**19**	5	**9**	**7**	2	3	5	3
Apteodinium spp.	**12**	**28**	**16**	**34**	**16**	**29**	**11**	**19**	**16**	**37**
Achomosphaera/Spiniferites spp.	**19**	**28**	**43**	**17**	**27**	**17**	**36**	**23**	**23**	**14**
Cleistosphaeridium spp.	5	2	**6**	4	**6**	2	4	**8**	4	2
Cribroperidinium spp.	**14**	5	1	**12**	5	4	3	4	4	4
Exochosphaeridium insigne	3	4	4	4	4	**10**	2	**6**	**7**	2
Glaphyrocysta spp.	0	0	2	0	0	0	0	0	0	0
Lejeunecysta spp.	**7**	3	4	1	2	3	5	3	3	**6**
Lingulodinium machaerophorum	**11**	**9**	4	**8**	**10**	**7**	**12**	**7**	**12**	4
Polysphaeridium zoharyi	0	1	0	0	2	2	1	3	1	0
Round brown cysts	3	1	3	4	3	2	3	3	2	**7**
Selenopemphix spp.	4	2	2	0	3	**6**	3	**6**	**6**	**12**
Spiniferites spp.	**6**	2	5	1	**6**	0	1	0	1	0
Coccolithus pelagicus	**43**	**54**	**46**	**37**	**53**	**59**	**46**	**44**	**38**	**45**
Cyclicargolithus floridianus	4	4	**6**	5	5	**6**	4	3	3	3
Helicosphaera ampliaperta	**18**	**11**	**16**	**8**	**15**	**9**	**12**	**6**	**9**	**9**
Helicosphaera spp.	1	3	2	2	2	1	4	4	4	3
Reticulofenestra excavata	**8**	**14**	**14**	**21**	**14**	**17**	**17**	**15**	**14**	**14**
Reticulofenestra minuta	**21**	**6**	**8**	**20**	**6**	1	**13**	**24**	**27**	**24**
Reticulofenestra spp.	4	5	**6**	3	5	**6**	3	1	3	2

Chapter 5

STRATIGRAPHIC RE-EVALUATION OF THE STRATOTYPE FOR THE REGIONAL OTTNANGIAN STAGE (CENTRAL PARATETHYS, MIDDLE BURDIGALIAN)

Patrick Grunert[a], Ali Soliman[a], Stjepan Ćorić[b], Robert Scholger[c], Mathias Harzhauser[d], Werner E. Piller[a]

[a] Institute for Earth Sciences, University of Graz, Heinrichstraße 26, A-8010 Graz, Austria

[b] Geological Survey of Austria, Neulinggasse 38, A-1030 Vienna, Austria

[c] Department of Applied Geoscience and Geophysics, University of Leoben, Peter-Tunner Straße-5, A-8700 Leoben, Austria

[d] Natural History Museum Vienna, Geological-Paleontological Department, Burgring 7, A-1014 Vienna, Austria

Abstract

The Ottnangian stage represents the middle Burdigalian (c. 18.1-17.2 Ma) within the regional stratigraphic concept for the Central Paratethys. The section Ottnang-Schanze in the North Alpine Foreland Basin of Upper Austria has been defined as its stratotype by Rögl et al. (1973). We present an updated stratigraphic evaluation of the section based on biostratigraphy of foraminifers, dinoflagellate cysts and calcareous nannoplankton as well as magnetostratigraphy.

In agreement with earlier studies, assemblages of benthic foraminifers (co-occurrence of *Amphicoryna ottnangensis* and *Sigmoilopsis ottnangensis*, mass-occurrences of *Lenticulina inornata*) document a late early Ottnangian age. Dinoflagellate cyst *Exochosphaeridium insigne* is recorded for the first time in the early Ottnangian and its occurrence together with *Apteodinium spiridoides*, *Cordosphaeridium cantharellus* and *Glaphyrocysta reticulosa* s.l. extends the regional dinoflagellate zone Ein from the middle to the early Ottnangian. On a global scale, the revealed marker species indicate zone D17a (middle-late Burdigalian). Calcareous nannoplankton assemblages with the very rare occurrence of *Sphenolithus* cf. *belemnos* and *S.* aff. *heteromorphus* show remarkable affinities to Mediterranean nannoplankton zone MNN3b. Together with the frequent occurrence of *Helicosphaera ampliaperta* and the absence of *Triquetrorhabdulus carinatus* an assignment to standard nannoplankton zone NN3 (early-middle Burdigalian) is indicated.

Magnetostratigraphy revealed an inverse polarisation for the outcrop. In combination with the biostratigraphic age constraints and the present correlation of the Ottnangian to the Bur3 sea-level cycle the section belongs to polarity chron C5Dr.2r. For the first time, an absolute age between

17.95-18.056 Ma for the stratotype can be inferred.

5.1. Introduction

Through Oligocene-Miocene the epicontinental Central Paratethys Sea covered major parts of Europe. Its complex paleogeographic evolution is mainly related to tectonic processes of the Alpine orogeny creating a highly dynamic environment (see e.g., Harzhauser and Piller 2007 for details). Changing land-bridges and seaways had a severe impact on the fauna and flora and resulted in distinct biogeographic patterns, recognised already by Laskarev (1924) who was the first to introduce the concept of the Paratethys. With the progress in understanding the unique and complex history of this epicontinental sea, efforts towards a regional stratigraphic concept were taken culminating in the series "Chronostratigraphie und Neostratotypen" (Cicha et al. 1967; Steininger and Seneš 1971; Baldí and Seneš 1975; Papp et al. 1973, 1974, 1978, 1985; Stevanović et al. 1990). This concept paralleling global Oligocene-Miocene stratigraphy has been applied to the Central Paratethys since then and further attempts have been made to correlate the regional stages more and more precisely to the international chronostratigraphic framework (e.g., Rögl 1998; Kováč et al. 2004; Piller et al. 2007; Lirer et al. 2009). For each of the regional stages a holostratotype and several faciostratotypes have been selected. As the later represent characteristic facies reflecting regional environmental changes these sections do not follow the GSSP concept of the International Commission for Stratigraphy which was established somewhat later (Hedberg 1976).

In this study we present a detailed stratigraphical re-evaluation of the section Ottnang-Schanze in Upper Austria, representing the holostratotype for the Ottnangian stage (Early Miocene, middle Burdigalian; Figs. 5.1, 5.2). As for most of the Paratethyan stratotypes, the outcrop lacks a modern examination with respect to the international Cenozoic time-scale (Lourens et al. 2004). Since the initial description by Rögl et al. (1973) only few stratigraphic studies have been carried out on the section mainly focusing on regional aspects (Martini and Müller 1975; Hochuli 1978; Zorn 1995; Rupp and Haunold-Jenke 2003). Some brief overviews on the section have been published in field-trip guide books and in the course of geological mapping in the area (e.g. Roetzel and Nagel 1991; Rupp and van Husen 2007; Rupp et al. 2008). However, up to now, no detailed log or lithological description of the stratotype has been published.

This paper focusing on stratigraphy is the first outcome of an integrated project on the Ottnangian stratotype. The new data come from an evaluation of microfossil assemblages (foraminifers, dinoflagellate cysts, calcareous nannoplankton) and magnetostratigraphy. A detailed facies-analysis based on lithology, sedimentology and paleontology will be published in an accompanying paper.

Fig. 5.1 (right). Log of the stratotype section Ottnang-Schanze and range chart for biostratigraphically relevant species of benthic foraminifers, dinoflagellate cysts and calcareous nannoplankton as revealed in this study. See text for discussion.

Ottnang-Schanze

Ottnangian stratotype

lower Ottnangian / middle Burdigalian

Innviertel Group, Ottnang Fm.

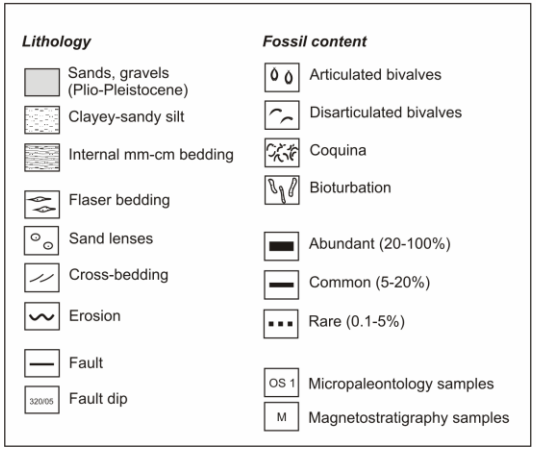

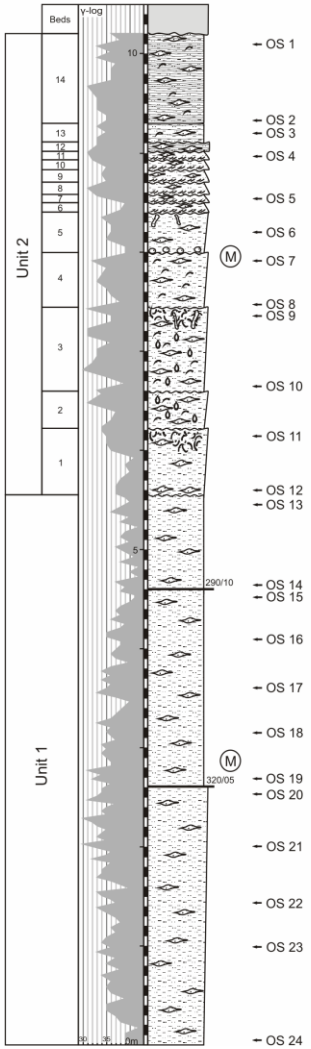

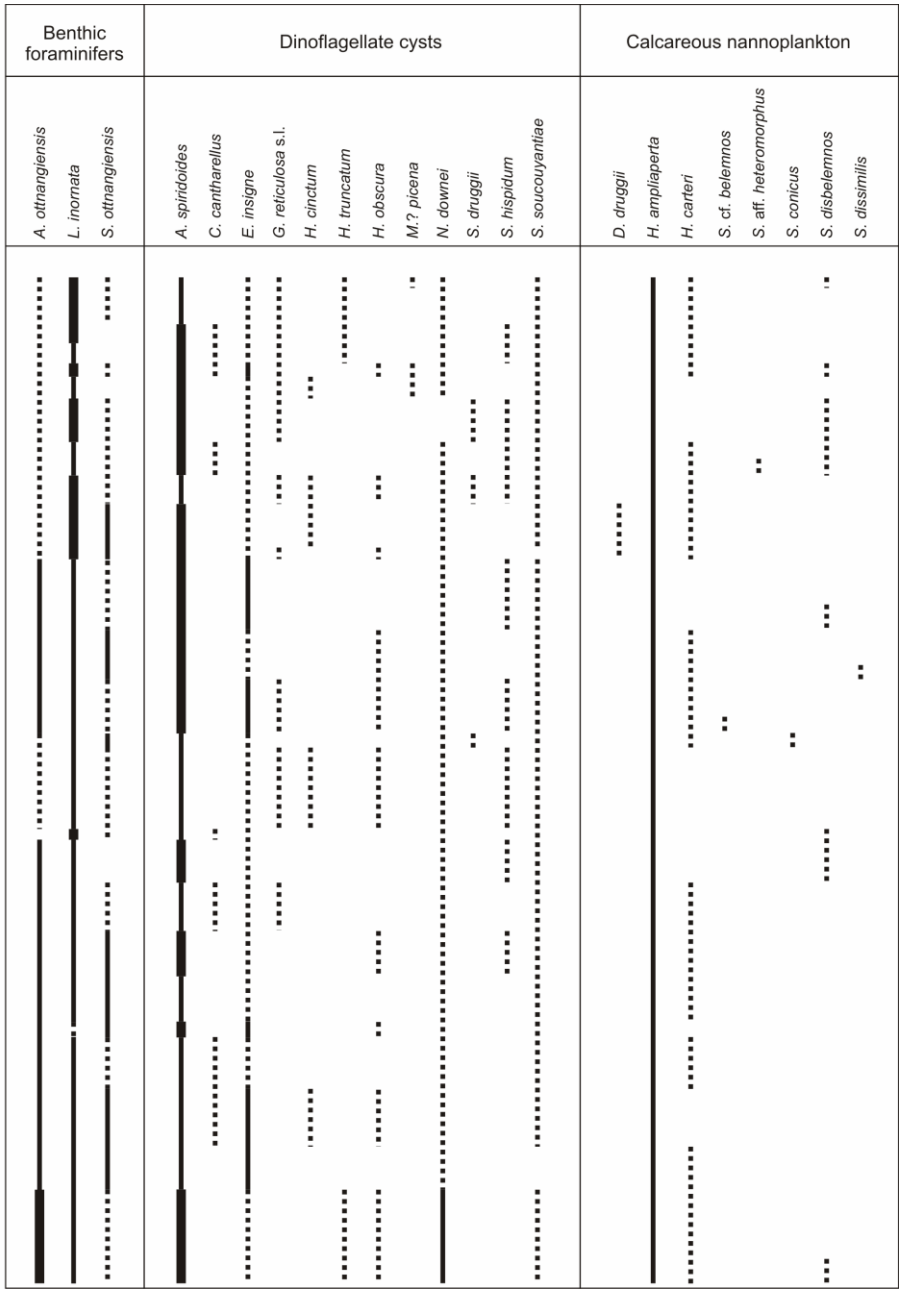

5.2. Regional setting

5.2.1. The Ottnangian stage: stratigraphic and paleogeographic framework

According to the current stratigraphic correlation of the regional Central Paratethyan stages to the international time-scale the Ottnangian corresponds to the 3rd-order sea-level cycle Bur3 of Haq et al. (1998) thus lasting from 18.12-17.23 Ma (Lourens et al. 2004; Piller et al. 2007). Based on lithostratigraphy a threefold internal subdivision of the Ottnangian has been developed (Seneš 1973; Doppler et al. 2005; Rupp et al. 2008). However, in a geochronological context this concept is poorly constrained. While there is some evidence from sequence stratigraphy (Zweigel 1998; Grunert 2009) and Sr-isotope data (Pippèrr et al. 2007) and for an early/middle Ottnangian boundary between 17.8-17.9 Ma, the boundary between middle and late Ottnangian remains unclear due to an asynchronous retreat of the Central Paratethys from the North Alpine Foreland Basin (NAFB) at the time.

Biostratigraphy of the Ottnangian is primarily based on endemic benthic foraminiferal and mollusc species (Cicha and Rögl 1973; Steininger et al. 1973). Ostracods, silicoflagellates, diatoms, dinoflagellate cysts and pollen have been locally used as additional markers (Hochuli 1978; Zorn 1995; Jiménez-Moreno et al. 2006; Roetzel et al. 2006). Due to the high rate of endemism a correlation to the international biostratigraphic zonation schemes proved to be difficult (Harzhauser and Piller 2007; Piller et al. 2007). Although Cicha and Rögl (1973) and Rögl (1985) suggest a possible correlation to the Burdigalian *Globigerinoides trilobus*-zone of the Mediterranean (sensu Iaccarino 1985), planktic foraminiferal assemblages of the Ottnangian generally do not reveal taxa useful for biostratigraphy (Rögl 1985). Only the FAD of the endemic species *Cassigerinella spinata* is documented for the base of the Ottnangian in Bavaria and Upper Austria (Cicha et al. 1998). Studies on dinoflagellate cysts and calcareous nannoplankton seem more promising in this respect (Martini and Müller 1975; Chira 2004; Jiménez-Moreno et al. 2006; Roetzel et al. 2006). However, this work is still in its early stages.

The stratotype section of the Ottnangian is located within the NAFB of Upper Austria (Fig. 5.2a). Reaching from Switzerland via southern Germany to Austria, the NAFB provided the connection between the Central Paratethys and the Atlantic from Oligocene to Early Miocene (Fig. 5.3). Its sedimentary infill is charcaterized by several regressive/transgressive cycles and the final retreat of the Central Paratethys from the basin by the end of the Early Miocene (Rögl 1998; Doppler 2005; Harzhauser and Piller 2007). The Ottnangian is part of the last of these cycles starting in the late Eggenburgian when a transgression re-established the marine pathway towards the Atlantic (Berger 1996). This temporary connection is called the Burdigalian Seaway and persisted throughout the early Ottnangian (Rögl 1998). Early Ottnangian sedimentation was mainly siliciclastic resulting in deposition of characteristic clayey-sandy silts ("Schlier") which are also present at the stratotype section (Harzhauser and Piller 2007). Widespread tidal deposits are reported from the area of the Burdigalian Seaway (Faupl and Roetzel 1987, 1990; Martel et al. 1994; Bieg 2005). Carbonate deposits like the bryozoan-corallinacean limestones of the Zogelsdorf

Formation in Lower Austria are scarce (Nebelsick 1989, 1992). A frequent occurrence of diatomites is reported from the NAFB of Lower and Upper Austria and the Carpathians and has been locally related to upwelling conditions (Kotlarczyk and Kaczmarska 1987; Kotlarczyk 1988; Roetzel et al. 2006; Grunert et al. in press). During late Ottnangian this paleogeographic situation changed distinctly when the seaways towards the Atlantic and Mediterranean seas ceased. Brackish lakes developed in parts of the NAFB and in the Carpathian Foredeep (Rögl 1998; Harzhauser and Mandic 2008).

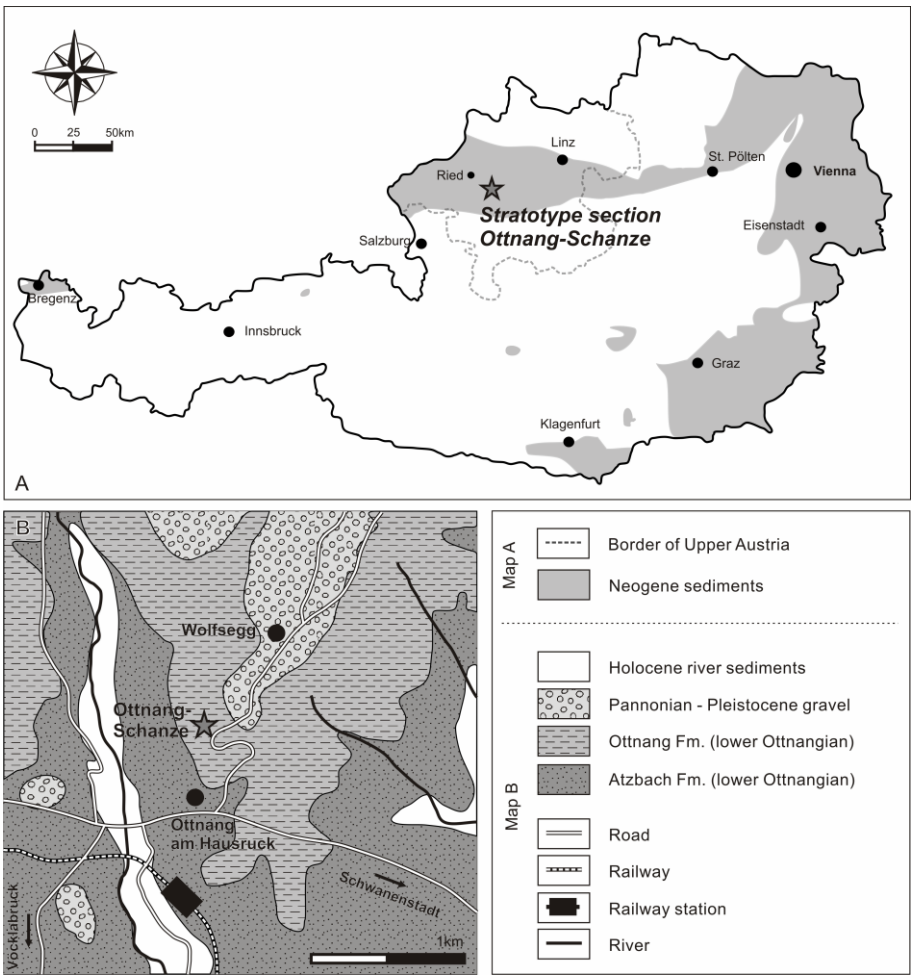

Fig. 5.2. (A) Location of the stratotype section within the Austrian NAFB. (B) Geography and geology of the study area based on Krenmayr and Schnabel (2006) and Rupp et al. (2008).

5.2.2. Study area

The stratotype is located in Upper Austria in the Ried district (Fig. 5.2). In this area the Ottnangian sediments are represented by the Innviertel Group (Papp and Cicha 1973; Rupp et al. 2008; Fig. 5.4). While the lower and middle Ottnangian silts and sands originate from fully marine transgressive and high-stand phases, the brackish-fluvial *Oncophora* beds represent the regressive facies of the late Ottnangian. The sediments of the stratotype section belong to the lower Ottnangian Ottnang Fm. summarizing the pelitic basinal deposits in the area (Rupp et al. 2008). The Ottnang Formation lies above the Atzbach Fm., the Kletzenmarkt-Glaukonit Fm. and the Plesching Fm. and partly interfingers with these units. It is overlain by the middle Ottnangian Ried, Reith and Enzenkirchen Fms. (Rupp and van Husen 2007; Rupp et al. 2008). The average thickness of the Ottnang Fm. is reported with 80-100 m (Kaltbeitzer 1988). The regional geological

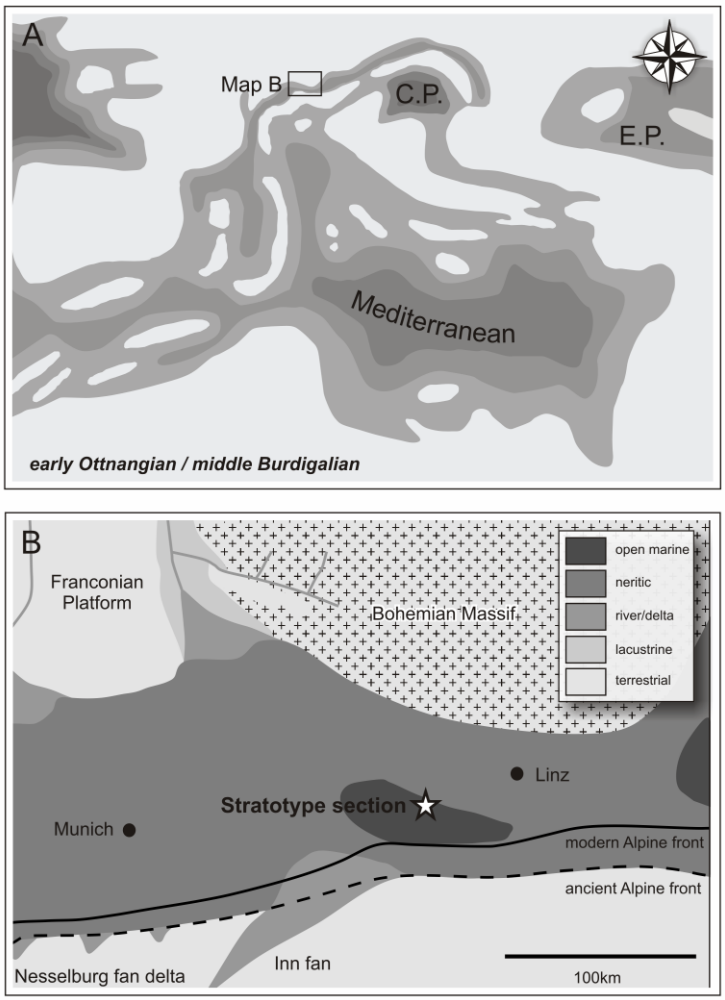

Fig. 5.3. (A) Paleogeography of the early Ottnangian Paratethys and Mediterranean seas based on Rögl (1998) and Harzhauser and Piller (2007). C.P. = Central Paratethys, E.P. = Eastern Paratethys. (B) Paleogeography of the study area based on the reconstruction of Kuhlemann and Kempf (2002).

setting can be found on the Austrian geological maps of ÖK 200 "Upper Austria" (Krenmayr and Schnabel 2006) and ÖK 47 "Ried im Innkreis" (Rupp et al. 2008).

5.2.3. Present outcrop situation

The Ottnangian stratotype Ottnang-Schanze is located 700 m SSW Wolfsegg and 500 m N of the village Ottnang in Upper Austria (48°06'07"N, 13°40'04"E; Fig. 5.2b). It is part of an abandoned pit near a memorial to the Peasant Wars (called "Schanze") and has been declared a natural heritage and geotop (Reiter 1989).

The exposed section comprises 10.2 m of sediments with two faults in the lower part (2.6m, 4.6m; Fig. 5.1). It shows a clear change in sedimentation dividing the section into two lithological units: Unit 1 (0-5.5 m) shows rather homogeneous grey-brown sediments of clayey-sandy silts with sand-lenses and flaser bedding. The sand lenses reach a lateral extension up to 30cm and often contain plant remains. Sediments show no internal bedding but intense bioturbation.

Unit 2 (5.5-10 m) is characterized by 14 beds separated by erosional surfaces and a distinct overall coarsening upward trend. The succession starts with a bed of clayey-sandy silts with flaser bedding similar to Unit 1 which pass into mollusc-rich sediments. Beds 1-11 show internal gradation comprising five coarsening-upward cycles (beds 1-5) and six fining-upward cycles (beds 6-11). Beds with coarsening-upward cycles (thickness: 40-85cm) show indistinct dm-layering often associated with articulated bivalves at the base, passing into bioturbated sediments with bivalve coquinas. Fining-upward cycles (max. thickness: 10 cm) start with cross-bedded sands passing into sandy silts. Finally, the three topmost beds (beds 12-14; thickness: 10-90cm) show a distinct laminated flaser-bedding and disarticulated bivalve shells enriched in sand-lenses.

Only a short part of the Ottnang Fm. crops out at the stratotype section. Based on an evaluation of

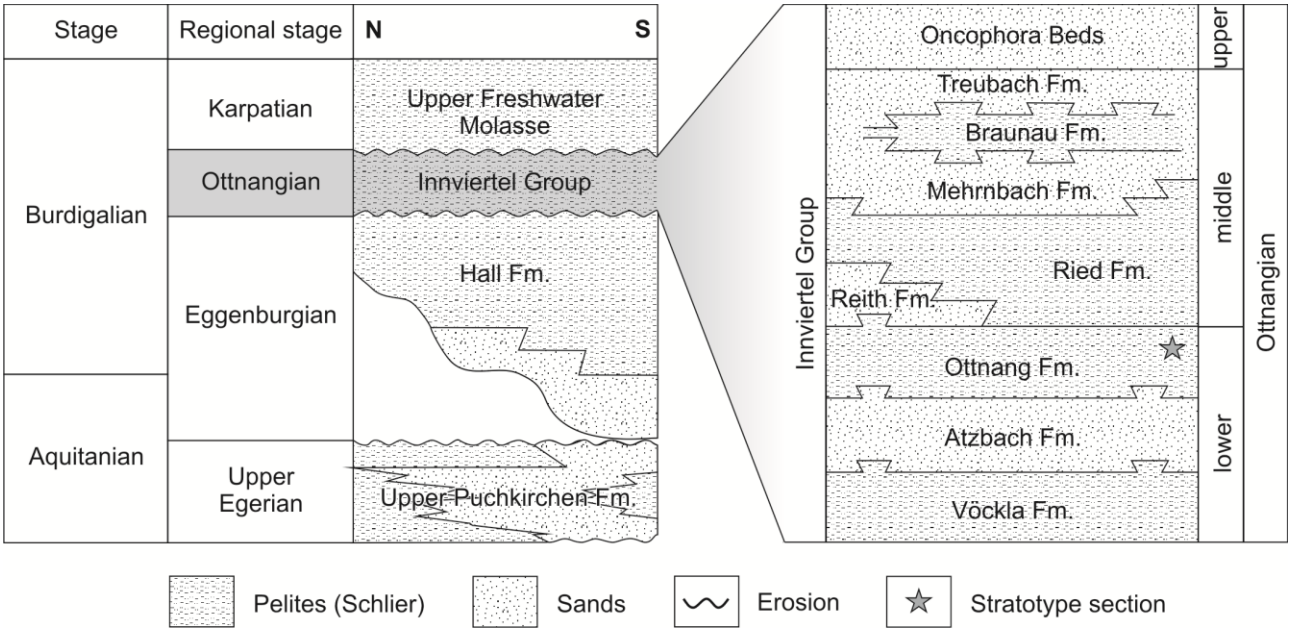

Fig. 5.4. Lithostratigraphy of the Ottnangian Innviertel Group in the Upper Austrian study area based on Rupp and van Husen (2007) and Rupp et al. (2008).

geological maps and information from drill-sites in the vicinity of the stratotype, most of the Innviertel Group in the study area is made up by the Vöckla and Atzbach Fms. with a thickness up to 520 m (Krenmayr and Schnabel 2006; Rupp et al. 2008; personal communication R. Hinsch, RAG). The overlying Ottnang Fm. is only represented by its lowermost part with a thickness of 15-20 m. Its top is eroded and covered by Pliocene-Pleistocene deposits (Rögl et al. 1973).

5.2.4. Historical remarks

By the time the outcrop Ottnang-Schanze was formally defined as the stratotype section for the Ottnangian, stratigraphy of the pelitic deposits near Ottnang ("Schlier of Ottnang") has already been discussed for a long time (Papp and Rögl 1973; Rögl et al. 1973; Rupp and van Husen 2007). Based on mollusc and foraminiferal assemblages collected by Simony (1850) and Ehrlich (1852), Hoernes (1853) and Reuss (1864) correlated the "Schlier of Ottnang" to similar sediments in the Middle Miocene (Langhian/Badenian) of the Vienna Basin. This assessment was supported by Gümbel (1887) who compared deposits from different basins and correlated them to the Middle Miocene ("2. Mediterranstufe"). This interpretation was opposed by Suess (1866), Karrer (1867), Reuss (1867), Hoernes (1875a, b), Suess (1891), Tausch (1896) and Commenda (1900) who favoured an older, Early Miocene age for the deposits.

Hydrocarbon exploration during the first half of the 20th century documented confirmed the Early Miocene age of the "Schlier of Ottnang" and a correlation to the Helvetian stage was established (Götzinger 1926; Hofmann 1932; Petters 1936; Bürgl 1949; Aberer 1958). Recently, the informal lithological units of the Ottnangian Innviertel Group were formalized including the "Schlier of Ottnang" as Ottnang Fm. (Rupp et al. 2008).

5.3. Material and methods

5.3.1. Biostratigraphy

24 samples (OS 1-24) taken from the outcrop during 2007 were used for micropaleontological analyses (Fig. 5.1). For foraminiferal analysis, 100g of each sample were treated with diluted H_2O_2 for several hours and wet sieved under running tap water. Dried samples were split using a splitting device described in Rupp (1986) and at least 200 specimens were counted from size fractions >150µm. Foraminifers were identified after Wenger (1987), Cicha et al. (1998) and Rupp and Haunold-Jenke (2003).

A standard palynological technique for the extraction of organic-wall microplankton from sediments has been applied with slight modifications for dinoflagellate cyst analysis (Green 2001; Grunert et al., in press). 20-30g of sediments were treated with 100ml of HCl (35%) and then macerated in 30-50ml of cold concentrated HF (48%) for 48-72 hours to remove any carbonates and silicates. Before sieving (mesh-sizes: 125µm, 20µm), residues were treated for 30 seconds in an ultrasonic bath and stained with red Safranin "O". Two slides of each sample were prepared by using glycerine jelly as a mounting media and sealed with nail varnish. 250 dinoflagellate cysts were counted in every sample unsing a light microscope; the remainder of the slide(s) was then scanned for rare or exceptionally well-preserved specimens. SEM investigation was additionally used for documentation. Taxonomy follows Fensome et al. (1993, 2008).

Smear slides for nannoplankton investigations were prepared using standard methods and examined under light microscope (cross and parallel nicols) with 1000x magnification. At least 300 specimens were counted from each sample. A further 100 view squares were checked for additional biostratigraphically important nannoplankton taxa.

5.3.2. Magnetostratigraphy

Samples for paleomagnetic investigations were taken from the stratotype section in 2001 and analysis was carried out within the scope of an earlier research project funded by the Austrian Research Fund (FWF-project P13738-TEC; Fig. 5.1). 16 standard paleomagnetic samples from two different positions in the section were subjected to detailed stepwise demagnetisation procedure (alternating field and/or thermal treatment). During thermal demagnetisation, the bulk susceptibility of the samples was routinely measured to observe possible mineral transformations. Paleomagnetic data analyses included principal component analysis based on visual inspection of orthogonal projections. Stepwise saturation, measurements of the coercivity, demagnetisation of the saturation magnetization and Curie-point determinations helped to identify the magnetic minerals in the sediments. All measurements were carried out in the Paleomagnetic Laboratory Gams of the University of Leoben. Natural remanent magnetization was measured on a three-axis cryogenic dc-squid magnetometer with in-line degausser (2G Enterprises). Geofyzika KLY-2 instruments were used for measuring low-field magnetic susceptibility and its anisotropy.

5.4. Results

5.4.1. Biostratigraphy

Micropaleontological analysis revealed useful biostratigraphic marker species from all investigated groups. Their abundance in the samples is summarized in Fig. 5.1, representative images are given in Plates 5.1-5.4.

Foraminiferal assemblages are moderately to well-preserved and revealed over 110 benthic species. The frequently occurring benthic foraminifers *Amphicoryna ottnangensis*, *Sigmoilopsis ottnangensis* and *Lenticulina inornata* represent three marker species important in the context of regional Ottnangian stratigraphy. Planktic assemblages revealed no marker species except for the Early Miocene of the Central Paratethys in general (*Globigerina lentiana*, *G. ottnangiensis*).

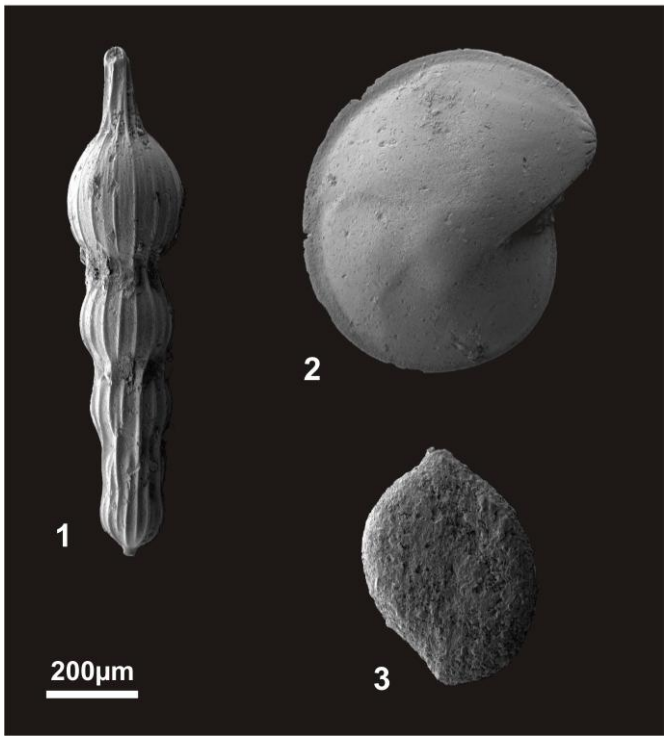

Plate 5.1. Biostratigraphic marker species of benthic foraminifers. 1: *Amphicoryna ottnangensis* (Toula); Sample OS 11. 2: *Lenticulina inornata* (D'Orbigny); Sample OS 11. 3: *Sigmoilopsis ottnangensis* Cicha, Ctyroka & Zapletalova; Sample OS 24.

All samples revealed well-preserved dinoflagellate cysts with over 60 species. The Early Miocene marker species *Apteodinium spiridoides*, *Exochosphaeridium insigne*, *Glaphyrocysta reticulosa* s.l., *Nematosphaeropsis downiei* and *Sumatradinium soucouyantiae* are present throughout the studied samples. *Cordosphaeridium cantharellus*, *Deflandrea phosphoritica*, "*Distatodinium cavatum*", *Hystrichokolpoma cinctum*, *H. truncatum*, *Hystrichosphaeropsis obscura*, *Membranilarnacia? picena*, *Sumatradinium druggii* and *S. hispidum* are recorded sporadically.

Nannoplankton assemblages are moderately to well preserved and frequently contain a variety of autochthonous and reworked taxa. Over 40 autochthonous species have been identified in total. The Burdigalian marker species *Helicosphaera ampliaperta* occurs frequently in all samples. Additionally, the Early Miocene species *Discoaster drugii*, *H. carteri*, *Sphenolithus conicus*, *S. disbelemnos* and *S. dissimilis* are rarely encountered. Single specimens assigned to *Sphenolithus* cf. *belemnos* (OS 12) and *Sphenolithus* aff. *heteromorphus* (OS 6) are present.

5.4.2. Magnetostratigraphy

Mineral magnetic characterisation experiments indicate magnetite as main carrier mineral of the magnetisation: magnetic saturation could be reached at low dc-fields during isothermal remanence

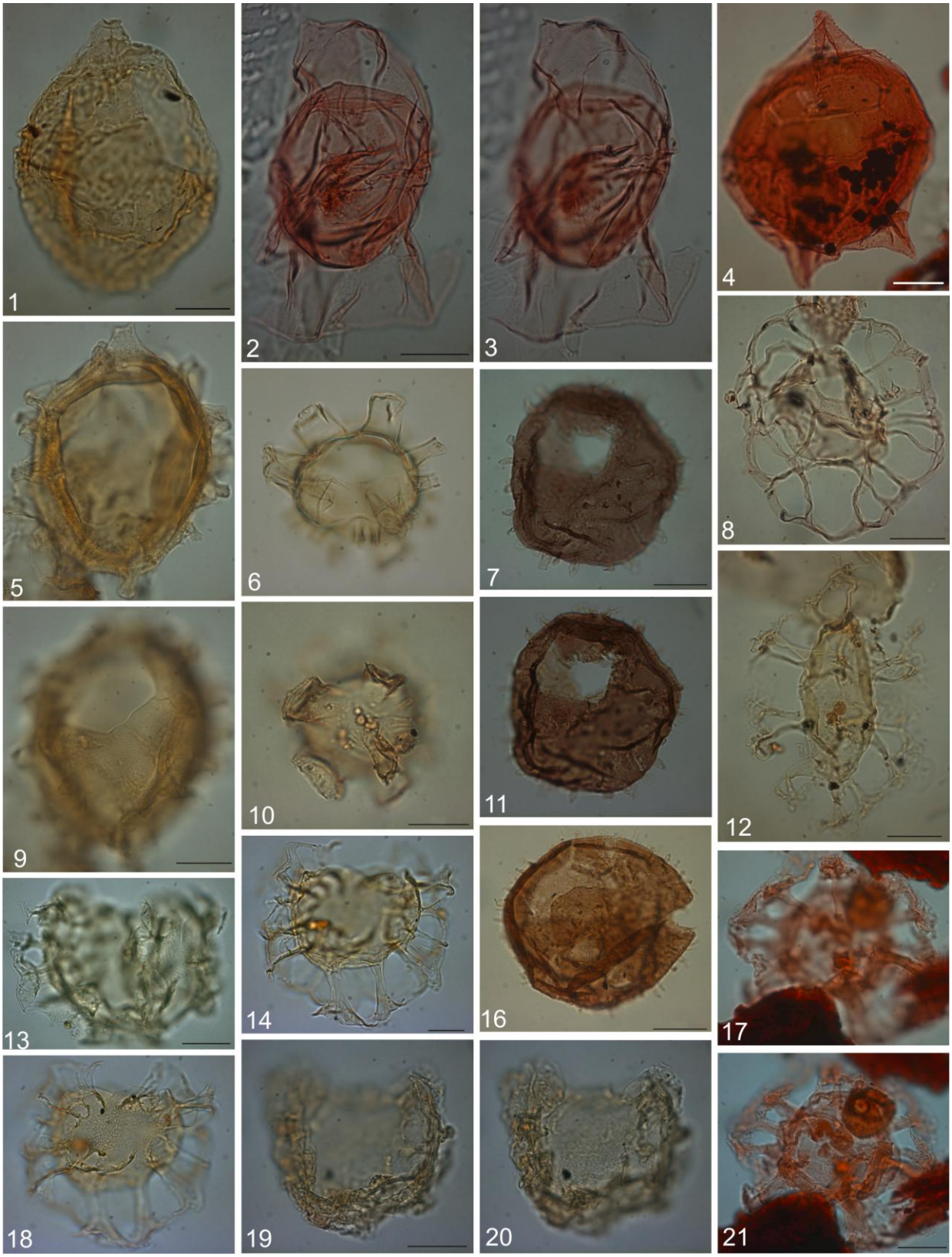

acquisition, and the remanence coercivity derived from back-field analyses was ranging between 30mT and 35mT. Natural remanent magnetization (NRM) was typically fully demagnetised at alternating field strengths of 20mT and temperatures below 400°C, respectively. 8 out of 16 studied samples yielded interpretable demagnetization paths containing two magnetic

Plate 5.2 (left). Biostratigraphic marker species of dinoflagellate cysts. Scale bar = 20µm.
1: *Apteodinium spiridoides* Benedek, 1972; Sample OS 1, Slide B, England Finder F67; later view, mid-focus. 2, 3: *Hystrichosphaeropsis obscura* Habib, 1972; Sample OS 2; Slide B, England Finder, S40/1; successive foci. 4: *Deflandrea phosphoritica* Eisenack, 1938; Sample OS 22, Slide B, England Finder F69/2; dorsal view. 5, 9: *Exochosphaeridium insigne* de Verteuil and Norris, 1996; Sample OS 1, slide B, England Finder G47; ventral and dorsal views respectively. 6, 10: *Hystrichokolpoma truncatum* Biffi and Manum, 1988; Sample OS 1; slide B, England Finder, M37; apical and antapical views respectively. 7, 11*: Sumatradinium soucouyantiae* de Verteuil and Norris, 1992; Sample OS 1, Slide B, England Finder B38; dorsal view, mid and high-focus. 8: *Nematosphaeropsis downiei* Brown, 1986; Sample OS 24; Slide A, England Finder C57/2; dorsal view. 12: *„Distatodinium cavatum"* Zevenboom and Santarelli in Zevenboom, 1995; Sample OS 1; Slide B, England Finder X57; mid-focus. 13: *Membranilarnacia? picena* Biffi and Manum, 1988; Sample OS 4, Slide B, England Finder W23; mid-focus. 14, 18: *Glaphyrocysta reticulosa* (Gerlach, 1961) Stover and Evitt, 1978 sensu lato; Sample OS 3; Slide B, England Finder J60/2; ventral view, mid and high-focus. 16: *Sumatradinium druggii* Lentin, Fensome and Williams, 1994; Sample OS 2, slide B, England Finder O46; dorsal view. 17, 21: *Cordosphaeridium cantharellus* (Brosius) Gocht, 1969;Sample OS 21, slide A; England Finder O43/1; low and high-focus. 19, 20: *Membranophoridium* sp.; Samples OS 1, slide B, England Finder M43/3; ? ventral view, low and high-focus.

components. A randomly distributed viscose component could be removed with alternating fields of less than 5mT. The second magnetic component which was regarded as the characteristic remanent magnetization in both sample groups was characterised by considerably scattering directions, but all vectors yielded inverse polarity. The mean primary magnetization direction from the section Ottnang-Schanze represented a declination of 154° and an inclination of -51°, indicating remanence acquisition during an inverse chron of the Earth's magnetic field.

5.5. Discussion

5.5.1. Foraminiferal biostratigraphy of the Ottnangian

As a correlation with the global planktic zonation fails, regional foraminiferal biostratigraphy relies on the evolution of endemic benthic species. *Amphicoryna ottnangensis* is the only well-established marker for the early Ottnangian in Bavaria and Upper Austria (Cicha and Rögl 1973; Wenger 1987; Cicha et al. 1998; Rupp and Haunold-Jenke 2003). It has its FAD at the Eggenburgian/Ottnangian boundary and lasts until the earliest middle Ottnangian. Another species often used in Ottnangian biostratigraphy is *Sigmoilopsis ottnangensis*. While its FAD in Bavaria has been recorded during late Eggenburgian and LAD at end of early Ottnangian, its records from the Austrian NAFB and Vienna Basin seem to be restricted to the early Ottnangian (Cicha and Rögl 1973; Wenger 1987; Cicha et al. 1998). The FAD of *Pappina breviformis* has been suggested as a marker for the base of the middle Ottnangian (Wenger 1987; Cicha et al. 1998).
Problems occur with other species that seem to have regional value but no superregional significance. *Pappina primiformis* and *Bolivina matejka* have their FAD at the base of the

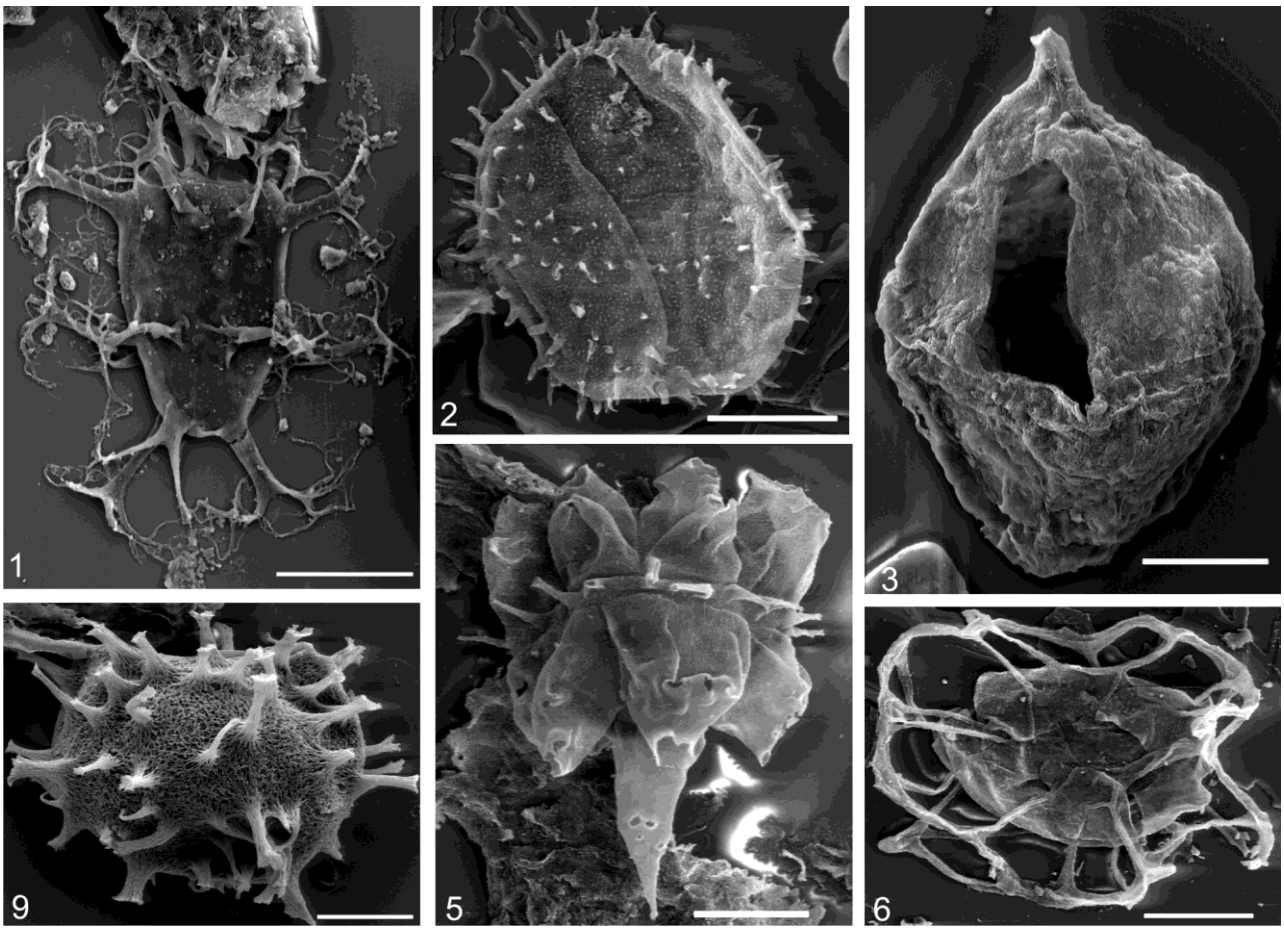

Plate 5.3. Biostratigraphic marker species of dinoflagellate cysts. Scale bar = 20µm. 1: *Distatodinium paradoxum* (Brosius) Eaton 1976: Sample OS 1. 2: *Sumatradinium hispidum* (Drugg) Lentin and Williams emend. Lentin *et al.,* 1994; Sample OS 7; dorsal view. 3: *Apteodinium spiridoides* Benedek, 1972; Sample OS 7; dorsal view. 4: *Exochosphaeridium insigne* de Verteuil and Norris, 1996; Sample OS 4. 5: *Hystrichokolpoma cinctum* Klumpp, 1953; sample OS 4; dorsal view. 6: *Nematosphaeropsis downiei* Brown, 1986; Sample OS 24.

Ottnangian in Bavaria, *B. scitula* is restricted to the early Ottnangian (Wenger 1987). In Croatia, *Elphidium fichtelianum* has its FAD at the base of the Ottnangian (Cicha et al. 1998).

The results from this study with the frequent occurrence of both marker species *A. ottnangensis* and *S. ottnangensis* agree well with results from previous reports (Rögl et al. 1973; Rupp and Haunold-Jenke 2003; Rupp and van Husen 2007; Rupp et al. 2008). Other Ottnangian marker species were not encountered. Accordingly, the outcrop belongs to the late early Ottnangian.

The regional biostratigraphic concept is hampered by the obvious dependency of benthic species on facies distribution (a problem that concerns most of the Paratethys stages). Consequently, *A. ottnangensis* and *S. ottnangensis* have only been described from the NAFB of Bavaria and Austria, the Vienna Basin, Croatia and Slovenia (Cicha et al. 1998). As a result workers locally tend to rely on characteristic composition of foraminiferal assemblages as a whole to identify the Eggenburgian/Ottnangian boundary and to differentiate the internal subdivision of the Ottnangian. In Upper Austria, there is a characteristic development during early Ottnangian from

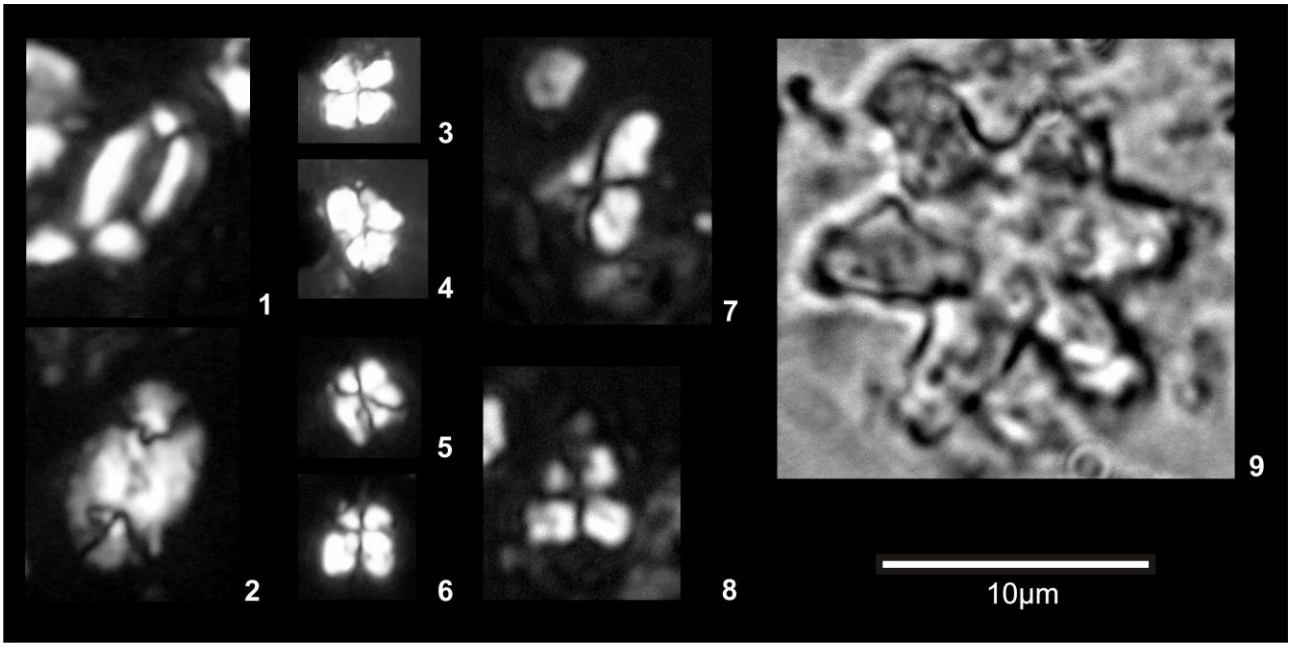

Plate 5.4. Biostratigraphic marker species of calcareous nannoplankton. 1: *Helicosphaera ampliaperta* Bramlette and Wilcoxon, 1967; Sample OS 6. 2: *Helicosphaera carteri* (Wallich, 1877) Kamptner, 1954; Sample OS 6. 3-4: *Sphenolithus* aff. *heteromorphus* Deflandre, 1953; Sample OS 6. 5-6: *Sphenolithus disbelemnos* Fornaciari and Rio, 1996; Sample OS 3. 7-8: *Sphenolithus conicus* Bukry, 1971; Sample OS 13. 9: *Discoaster druggii* Bramlette and Wilcoxon, 1967; Sample OS 9.

an assemblages dominated by *Ammonia parkinsonia*, *Lobatula lobatula* and *Cibicidoides* spp. to a fauna with mass-occurrences of *Lenticulina inornata*. These assemblages become replaced by an *Ammonia parkinsonia* dominated fauna at the beginning of the middle Ottnangian (Bürgl 1949; Aberer 1958; Rupp and Haunold-Jenke 2003; Rupp et al. 2008). Similar faunal successions have been observed in Bavaria (Wenger 1987; Pippèrr et al. 2007). Data of the studied stratotype section correspond to the typical late early Ottnangian *Lenticulina*-pelites.

5.5.2. Dinoflagellate cyst stratigraphy: Central Paratethys and beyond

The composition of the revealed dinoflagellate cyst assemblages is characteristic for an Early Miocene age and allows a biostratigraphic evaluation on the global as well as regional level. While the co-occurrence of *Apteodinium spiridoides*, *Cordosphaeridium cantharellus*, *Exochosphaeridium insigne*, *Hystrichokolpoma truncatum*, *Hystrichosphaeropsis obscura*, *Membranilarnacia? picena*, *Nematosphaeropsis downiei*, *Sumatradinium hispidum* and *S. soucouyantiae* indicates a late Aquitanian to Burdigalian age, the presence of *H. cinctum* and *S. drugii* allows a correlation to D17a dinoflagellate cyst zone (middle-late Burdigalian, 19.03-15.97 Ma; Zevenboom 1995; de Verteuil and Norris 1996; Williams et al. 2004; Lourens et al. 2004; Jiménez-Moreno et al. 2006; Dybkjær and Piasecki 2008). In general, the assemblages are similar to those of the Burdigalian stratotype (Londeix and Jan du Chêne 1998).

Regionally, the species *E. insigne* allows a more precise dating. It has been described as a marker

for early-middle Burdigalian from the western North Atlantic, the North Sea and the Gulf of Suez (de Verteuil and Norris 1996; Köthe 2003; Dybkjær 2004; Soliman 2006; Dybkjær and Piasecki 2008). Earlier occurrences reported for the North Sea are most likely related to caving (Schiøler 2005; Jiménez-Moreno et al. 2006). Notably, *E. insigne* is missing at the Burdigalian stratotype (Londeix and Jan du Chêne 1998). It defines the top of DN2 zone of de Verteuil and Norris (1996) and its last occurrence defines the boundary between D16c and D17a zones in the North Atlantic (Lourens et al. 2004).

In the Upper Austrian NAFB, *E. insigne* has been described from a middle Ottnangian outcrop at Straß-Eberschwang (Jiménez-Moreno et al. 2006). Based on its occurrence together with *A. spiridoides*, *C. cantharellus*, *Glaphyrocysta reticulosa* s.l. and *Membranophoridium* sp. the authors defined the regional dinoflagellate cyst zone Ein. Similar assemblages revealed from Ottnang-Schanze (Hochuli 1978) and ongoing studies on Burdigalian drill-sites (Soliman and Piller 2009) suggest to extend this zone to the entire early Ottnangian.

5.5.3. Calcareous nannoplankton: the link to global stratigraphy

As the Ottnangian spans parts of two standard nannoplankton zones (upper NN3-lower NN4) an exact dating is problematic. In general, the assemblages resemble the results of previous studies on early Ottnangian sediments from the NAFB of Lower Austria (Roetzel et al. 2006) and the Transylvanian Basin (Chira 2004). Martini and Müller (1975) described similar, though less diverse assemblages with *Helicosphaera ampliaperta* and *H. carteri* from the stratotype.

Our new data allow a more precise dating. The frequent occurrences of *Helicosphaera ampliaperta* and the presence of *Discoaster drugii*, *H. carteri* and *Sphenolithus disbelemnos* prove the Early Miocene age of the section. The absence of *Triquetrorhabdulus carinatus* (LAD at NN2/NN3 boundary) indicates a correlation of Ottnang-Schanze with nannoplankton zone NN3 (early-middle Burdigalian; 20.43-17.95 Ma) (Martini 1971; Lourens et al. 2004).

This interpretation is supported by a comparison with the Mediterranean nannoplankton zonation based on quantitative composition of assemblages (Fornaciari and Rio 1996). Nannoplankton assemblages from Ottnang-Schanze with the very rare *S.* cf. *belemnos, S.* aff. *heteromorphus, S. conicus*, *S. dissimilis* and the absence of *Helicosphaera mediterranea* show remarkable similarities in their composition with MNN3b zone (*Sphenolithus belemnos-Sphenolithus heteromorphus* Interval Zone). MNN3b is defined as interval between the last common and continuous occurrence (LCO) of *S. belemnos* and the first common and continuous occurrence (FCO) of *S. heteromorphus* and can be correlated with the upper part of NN3 and lowermost NN4 of Martini (1971) (Fornaciari and Rio 1996).

The suggested correlation to upper NN3 of the standard zonation and to MNN3b of the Mediterranean zonal scheme is in accordance with silicoflagellate *Dictyocha triacantha*-zone earlier recorded from the outcrop (Martini and Müller 1975). The results also confirm the previously assumed correlation of the Ottnangian with the *Globigerinoides trilobus*-Zone (Cicha

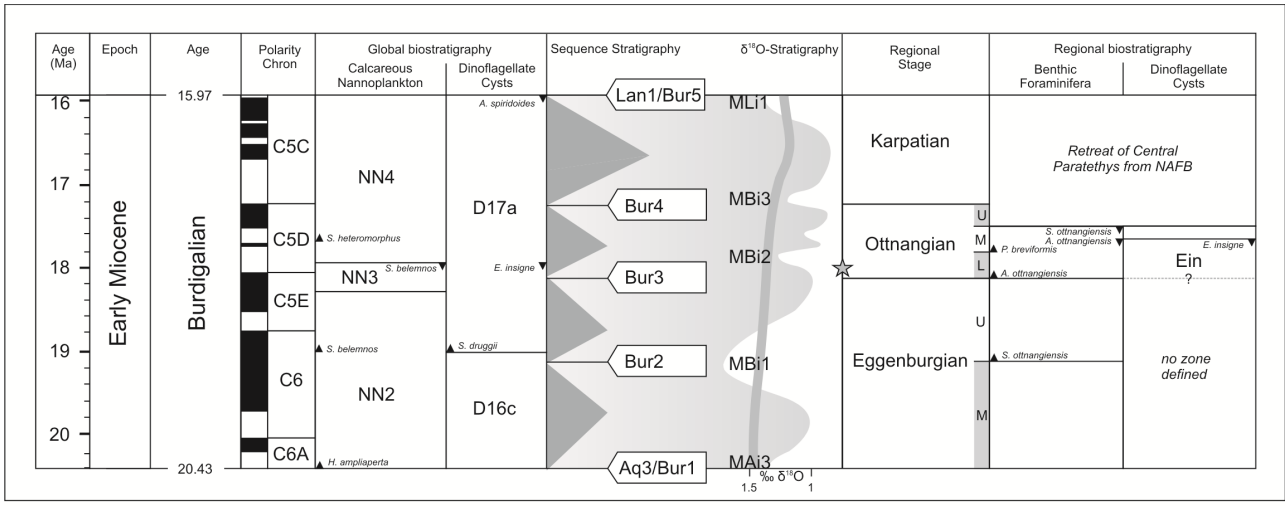

Fig. 5.5. Summary of regional Eggenburgian-Karpatian and international Burdigalian stratigraphy. Asterisk indicates the position of the Ottnangian stratotype. Stratigraphic data are based on Wenger (1987), Cicha et al. (1998), Lourens et al. (2004), Jiménez-Moreno et al. (2006) and Piller et al. (2007). See text for a discussion of the stratigraphic range of *E. insigne*.

and Rögl 1973; Rögl 1985).

5.5.4. Absolute age

Based on the revealed biostratigraphic data, the assessement of an absolute age for the section is possible. Biostratigraphy constrains the time-frame for deposition to an age between 19.03 and 17.95 Ma (lower boundary of D17a – upper boundary of NN3; Lourens et al. 2004). According to the current Central Paratethyan age model based on 3rd-order sequences presented by Kovác et al. (2004) and Piller et al. (2007) the Ottnangian corresponds to cycle Bur3 of Haq et al. (1998) with a lower boundary at 18.12 Ma (Fig. 5.7). Within this temporal limits only chron C5Dr.2r (18.056-17.740 Ma; Lourens et al. 2004) shows reverse polarity. Consequently, Ottnang-Schanze corresponds to a maximum age of 18.056 Ma and a minimum age of 17.95 Ma.

5.6. Conclusions

The section Ottnang-Schanze in the North Alpine Foreland Basin of Upper Austria represents the stratotype for the regional Ottnangian stage (Central Paratethys; middle Burdigalian, c. 18.1-17.2 Ma). In the present study it has been re-evaluated with respect to regional and global stratigraphy based on biostratigraphy (foraminifers, dinoflagellate cysts, calcareous nannoplankton) and magnetostratigraphy.

In agreement with earlier studies, benthic foraminifers (co-occurrence of *Amphicoryna ottnangensis* and *Sigmoilopsis ottnangensis*, mass-occurrences of *Lenticulina inornata*) document a late early Ottnangian age. For the first time, dinoflagellate cyst *Exochosphaeridium insigne* is documented from the early Ottnangian and its occurrence together with *Apteodinium spiridoides*,

Cordosphaeridium cantharellus and *Glaphyrocysta reticulosa* s.l. extends the regional dinoflagellate zone Ein (Jimenéz-Moreno et al. 2006) from the middle to the early Ottnangian. With respect to the international stratigraphic frame-work, the revealed marker species indicate zone D17a (middle-late Burdigalian). Calcareous nannoplankton assemblages with the very rare occurrence of *Sphenolithus* cf. *belemnos* and *S.* aff. *heteromorphus* show remarkable affinities to Mediterranean nannoplankton zone MNN3b. The frequent occurrence of *Helicosphaera ampliaperta* and the absence of *Triquetrorhabdulus carinatus* an assignment to standard nannoplankton zone NN3 (early-middle Burdigalian) is possible.

Magnetostratigraphy revealed an inverse polarisation for the section. In combination with the biostratigraphic age constraints and the present correlation of the Ottnangian to the Bur3 sea-level cycle the section belongs to polarity chron C5Dr.2r. Thus, for the first time, it is possible to propose an absolute age between 18.056-17.95 Ma for the stratotype.

5.7. Acknowledgements

The authors would like to thank Sorin Filipsecu (University of Cluj), Ralph Hinsch (Rohöl-Aufsuchungs AG, Vienna), Bettina Reichenbacher (University of Munich) and Fred Rögl (Natural History Museum Vienna) for comments and discussions. Franz Topka (Natural History Museum Vienna) is thanked for assistance with the field-work. Karl Stingl (Graz) performed paleomagnetic sampling. Peter Pohn (Wolfsegg) kindly provided access to the outcrop. This study was financially supported by the Commission for the Paleontological and Stratigraphical Research of Austria (Austrian Academy of Sciences) and benefited from the cooperation between the universities of Graz and Leoben within UZAG-framework. This paper contributes to the FWF-project 21414-B16.

5.8. References

Aberer, F., 1958. Die Molassezone im westlichen Oberösterreich und in Salzburg. Mitteilungen der Geologischen Gesellschaft Wien 50, 23–94.

Baldí, T., Seneš, J., 1975. OM – Egerien. Die Egerer, Pouzdraner, Puchkirchener Schichtengruppe und die Bretkaer Formation. Chronostratigraphie und Neostratotypen, Miozän der Zentralen Paratethys 5. Verlag der Slowakischen Akademie der Wissenschaften, Bratislava, 577 p.

Berger, J.-P., 1996. Cartes paléogéographiques-palinspastiques du bassin molassique suisse (Oligocène inférieur – Miocène moyen). Neues Jahrbuch für Geologie und Paläontologie 202, 1–44.

Bieg, U., 2005. Palaeooceanographic modelling in global and regional scale: An example from the Burdigalian Seaway. Ph.D. Thesis, Eberhard-Karls-Universität Tübingen, Germany, 108 p.

Bürgl, H., 1949. Zur Stratigraphie und Tektonik des oberösterreichischen Schliers. Verhandlungen der Geologischen Bundesanstalt 1946, 123–151.

Chira, C., 2004. Early Miocene calcareous nannofossils assemblages from Transylvania. Acta Palaeontologica Romaniae 4, 81–88.

Cicha, I., Rögl, F., 1973. Die Foraminiferen des Ottnangien. In: Papp, A., Rögl, F., Seneš, J. (Eds.), Miozän M2 – Ottnangien. Die Innviertler, Salgotarjaner, Bantapusztaer Schichtengruppe und die Rzehakia

Formation. Chronostratigraphie und Neostratotypen, Miozän der Zentralen Paratethys 3. Verlag der Slowakischen Akademie der Wissenschaften, Bratislava, p. 297–355.

Cicha, I., Rögl, F., Rupp, C., Ctyroká, J., 1998. Oligocene-Miocene foraminifers of the Central Paratethys. Abhandlungen der Senckenbergischen Naturforschenden Gesellschaft 549, 1–325.

Cicha, I., Seneš, J., Tejkal, J., 1967. M3 (Karpatien). Die Karpatische Serie und ihr Stratotypus. Chronostratigraphie und Neostratotypen, Miozän der Zentralen Paratethys 1. Verlag der Slowakischen Akademie der Wissenschaften, Bratislava, 312 p.

Commenda, H., 1900. Materialien zur Geognosie Oberösterreichs. Jahresbericht des Museums Francisco-Carolinum 58, 272.

de Verteuil, L., Norris, G., 1996. Miocene dinoflagellate stratigraphy and systematics of Maryland and Virginia. Micropalaeontology 42, 1–172.

Doppler, G., Heissig, K., Reichenbacher, B., 2005. Die Gliederung des Tertiärs im süddeutschen Molassebecken. Newsletters on Stratigraphy 41, 359–375.

Dybkjær, K., 2004. Dinocyst stratigraphy and palynofacies studies used for refining a sequence stratigraphic model – uppermost Oligocene to lower Miocene, Jylland, Denmark. Review of Palaeobotany and Palynology 131, 201–249.

Dybkjær, K., Piasecki, S., 2008. A new Neogene biostratigraphy for Denmark. Geological Survey of Denmark and Greenland Bulletin 15, 29–32.

Ehrlich, C., 1852. Geognostische Wanderungen im Gebiete der nördlichen Alpen. Ein specieller Beitrag zur Kenntniss Oberoesterreich's. Linz, 144 p.

Faupl, P., Roetzel, R., 1987. Gezeitenbeeinflußte Ablagerungen der Innviertler Gruppe (Ottnangien) in der oberösterreichischen Molassezone. Jahrbuch der Geologischen Bundesanstalt 130/4, 415–447.

Faupl, P., Roetzel, R., 1990. Die Phosphoritsande und Fossilreichen Grobsande: Gezeitenbeeinflußte Ablagerungen der Innviertler Gruppe (Ottnangien) in der oberösterreichischen Molasse. Jahrbuch der Geologischen Bundesanstalt 133/2, 157–180.

Fensome, R.A., Mac Rae, R.A., Williams, G.L., 2008. DINOFLAJ2, Version 1. American

Association of Stratigraphic Palynologists, Data Series no. 1.

Fensome, R.A, Taylor, F.J.R., Norris, G., Sarjeant, W.A.S., Wharton, D.I., Williams, G.L., 1993. A classification of living and fossil dinoflagellates. Micropaleontology Special Publication 7, 1–351.

Fornaciari, E., Rio, D., 1996. Latest Oligocene to early middle Miocene quantitative calcareous nannofossil biostratigraphy in the Mediterranean region. Micropaleontology 42, 1–36.

Götzinger, G., 1926. Neueste Erfahrungen über den oberösterreichischen Schlier unter besonderer Berücksichtigung der beiden 1200m-Tiefbohrungen bei Braunau a. I. Montan-Rundschau, 767–774.

Green, O.R., 2001. A manual of practical laboratory and field techniques in palaeobiology. Kluwer Academic Publishers, Dordrecht.

Grunert, P., 2009. Rise and fall of an ancient sea. Initial results from an integrated study on the Central Paratethys. Erstausgabe 2, 157–167.

Grunert, P., Soliman, A., Harzhauser, M., Müllegger, S., Piller, W.E., Roetzel, R., Rögl, F., in press. Upwelling conditions in the Early Miocene Central Paratethys sea. Geologica Carpathica 61/2.

Gümbel, C.W.v., 1887. Die miocänen Ablagerungen im oberen Donaugebiet und die Stellung des Schliers von Ottnang. Sitzungsberichte der Bayerischen Akademie der Wissenschaften, mathematisch-naturwissenschaftliche Klasse 17, 221–325.

Haq, B.U., Hardenbol, J., Vail, P.R., 1998. Mesozoic and Cenozoic chronostratigraphy and cycles of sea-level changes. In: Wilgus, C.K., Hastings, B.S., Kendall, C.G.St.C., Posamentier, H.W., Ross, C.A., van Wagoner, J.C. (Eds.), Sea-level changes – an integrated approach. Society of Economic Paleontologists and Mineralogists, Special Publications 42. p. 71–108.

Harzhauser, M., Mandic, O., 2008. Neogene lake systems of Central and South-Eastern Europe: Faunal diversity, gradients and interrelations. Palaeogeography, Palaeoclimatology, Palaeoecology 260, 417–434.

Harzhauser, M., Piller, W.E., 2007. Benchmark data of a changing sea. – Palaeogeography, Palaeobiogeography and Events in the Central Paratethys during the Miocene. Palaeogeography, Palaeoclimatology, Palaeoecology 253, 8–31.

Hedberg, H.D., 1976. International Stratigraphic Guide. John Wiley & Sons, New York, 200 p.

Hochuli, P.A., 1978. Palynologische Untersuchungen im Oligozän und Untermiozän der Zentralen und Westlichen Paratethys. Beiträge zur Paläontologie von Österreich 4, 1 - 132.

Hoernes, M., 1853. Sitzungsbericht am 11. März 1853. Jahrbuch der Geologischen Reichsanstalt 4, 190.

Hoernes, R., 1875a. Die Fauna des Schliers von Ottnang. Verhandlungen der Geologischen Reichsanstalt 1875, 209–212.

Hoernes, R., 1875b. Die Fauna des Schliers von Ottnang. Jahrbuch der Geologischen Reichsanstalt 25, 333–400.

Hofmann, E., 1932. Tertiäre Pflanzenreste von verschiedenen österreichischen Lagerstätten. Mitteilungen der Geologischen Gesellschaft Wien 24, 144–176.

Iaccarino, S., 1985. Mediterranean Miocene and Pliocene planktic foraminifera. In: Bolli, H.M., Saunders, J.B., Perch-Nielsen, K. (Eds.), Plankton Stratigraphy Volume 1: Planktic foraminifera, calcareous nannoplankton and calpionellids. Cambridge University Press, Cambridge, p. 283–314.

Jiménez-Moreno, G., Head, M.J., Harzhauser, M., 2006. Early and Middle Miocene dionflagellate cyst stratigraphy of the Central Paratethys, Central Europe. Journal of Micropalaeontology 25, 113–139.

Kaltbeitzer, J., 1988. Geologische, sedimentpetrologische und hydrogeologische Untersuchungen im Hausruckgebiet östlich von Eberschwang. Master thesis, Ludwig-Maximilians-Universität, Germany, 81 p.

Karrer, F., 1867. Zur Foraminiferenfauna in Österreich. Sitzungsberichte der Akademie der Wissenschaften, mathematisch-naturwissenschaftliche Classe 55, 331–368.

Kotlarczyk, J., 1988. Geologia Karpat przemiskych – “skicz do portretu”./Geology of the Prezemyśl Carpathians – “a sketch to the portrait”. Prezeglad Geologiczny 6, 325–333.

Kotlarczyk, J., Kaczmarska, I., 1987. Two diatom horizons in the Oligocene and (?) Lower Miocene of the Polish Outer Carpathians. Annales Societatis Geologorum Poloniae 57, 143–188.

Krenmayr, H.G., Schnabel, W., 2006. Geologische Karte von Oberösterreich 1:200.000, 1 sheet, 2 additional maps. Geological Survey of Austria, Vienna.

Köthe, A., 2003. Dinozysten-Zonierung im Tertiär Norddeutschlands. Revue de Paléobiologie 22, 895–923.

Kováč, M., Barath, I., Harzhauser, M., Hlavaty, I. Hudackova, N., 2004. Miocene depositional systems and sequence stratigraphy of the Vienna Basin. Courier Forschungsinstitut Senckenberg 246, 187–212.

Kuhlemann, J., Kempf, O., 2002. Post-Eocene evolution of the North Alpine Foreland Basin and its response to Alpine tectonics. Sedimentary Geology 152, 45–78.

Laskarev, V.N., 1924. Sur les equivalentes du Sarmatien supérieur en Serbie. Recueil de traveaux ofert a M. Jovan Cvijic par ses amis et collaborateurs, p. 73-85.

Lirer, F., Harzhauser, M., Pelosi, N., Piller, W.E., Schmid, H.P., Sprovieri, M., 2009. Astronomically forced teleconnection between Paratethyan and Mediterranean sediments during the Middle and Late Miocene. Palaeogeography, Palaeoclimatology, Palaeoecology 275, 1–13.

Londeix, L., Jan du Chêne, R., 1998. Burdigalian dinocyst stratigraphy of the stratotypic area (Bordeaux, France). Geobios 30, 283–294.

Lourens, L., Hilgen, F., Shackleton, N.J., Laskar, J., Wilson, D., 2004. The Neogene Period. In: Gradstein, F.M., Ogg, J.G., Smith, A.G. (Eds.), A Geologic Time Scale 2004. Cambridge University Press, Cambridge, p. 409-440.

Martel, A.T., Allen, P.A., Slingerland, R., 1994. Use of tidal-circulation modeling of paleogeographical studies: An example from the Tertiary of the Alpine perimeter. Geology 22, 925–928.

Martini, E., 1971. Standard Tertiary and Quaternary Calcareous Nannoplankton Zonation. In: Farinacci, A. (Ed.), Proceedings of the II Planktonic Conference, Roma, 1970. Edizione Tecnoscienza, Roma, p. 738–785.

Martini, E., Müller, C., 1975. Calcareous Nannoplankton and Silicoflagellates from the Type Ottnangian and Equivalent Strata in Austria (Lower Miocene). Proceedings of the Regional Committee on Mediterranean Neogene Stratigraphy 1, 121–124.

Nebelsick, J.H., 1989. Temperate Water Carbonate Facies of the Early Miocene Paratethys (Zogelsdorf Formation, Lower Austria). Facies 21, 11–40.

Nebelsick, J.H., 1992. Component analysis of sediment composition in Early Miocene temperate carbonates from the Austrian Paratethys. Palaeogeography, Palaeoclimatology, Palaeoecology 91, 59–69.

Papp, A., Marinescu, F., Seneš, J., 1974. M5 – Sarmatien (sensu E. Suess, 1866). Die Sarmatische Schichtengruppe und ihr Stratotypus. Chronostratigraphie und Neostratotypen, Miozän der Zentralen Paratethys 4. 707 p.

Papp, A., Rögl, F., 1973. Die Definition der Zeiteinheit M2 – Ottnangien. In: Papp, A., Rögl, F., Seneš, J. (Eds.), Miozän M2 – Ottnangien. Die Innviertler, Salgotarjaner, Bantapusztaer Schichtengruppe und die Rzehakia Formation. Chronostratigraphie und Neostratotypen, Miozän der Zentralen Paratethys 3. Verlag der Slowakischen Akademie der Wissenschaften, Bratislava, p. 39–40.

Papp, A., Rögl, F., Seneš, J., 1973. Miozän M2 – Ottnangien. Die Innviertler, Salgotarjaner, Bantapusztaer Schichtengruppe und die Rzehakia Formation. Chronostratigraphie und Neostratotypen, Miozän der Zentralen Paratethys 3. Verlag der Slowakischen Akademie der Wissenschaften, Bratislava, 841 p.

Papp, A., Cicha, I., 1973. Die Entwicklung der Innviertler Schichtengruppe – $M2_{a\text{-}c(d)}$ – und ihrer Äquivalente in Österreich und anschließenden Gebieten. In: Papp, A., Rögl, F., Seneš, J. (Eds.), Miozän M2 – Ottnangien. Die Innviertler, Salgotarjaner, Bantapusztaer Schichtengruppe und die Rzehakia Formation. Chronostratigraphie und Neostratotypen, Miozän der Zentralen Paratethys 3. Verlag der Slowakischen Akademie der Wissenschaften, Bratislava, p. 54–78.

Papp, A., Cicha, I., Seneš, J., Steininger, F., 1978. M4 – Badenien (Moravien, Wielicien, Kosovien). Chronostratigraphie und Neostratotypen, Miozän der Zentralen Paratethys 6. 594 p.

Papp, A., Jámbor, Á., Steininger, F.F., 1985. M6 – Pannonien (Slavonien und Serbien). Chronostratigraphie und Neostratotypen, Miozän der Zentralen Paratethys 7. 636 p.

Petters, V., 1936. Geologische und mikropaläontologische Untersuchungen der Eurogasco im Schlier Oberösterreichs. Petroleum Zeitschrift 32, 3.

Piller, W.E., Harzhauser, M., Mandic, O., 2007. Miocene Central Paratethys stratigraphy – current status and

future directions. Stratigraphy 4, 151–168.

Pippèrr, M., Reichenbacher, B., Witt, W., Rocholl, A., 2007. The Middle and Upper Ottnangian of the Simssee area (SE Germany): Micropaleontology, biostratigraphy and chronostratigraphy. Neues Jahrbuch für Geologie und Paläontologie 245, 353–378.

Reiter, E., 1989. Das Naturdenkmal „Ottnangien“ zwischen Wolfsegg und Ottnang am Hausruck. Oberösterreichische Heimatblätter 43/3, 262–270.

Reuss, A.E., 1864. Die Foraminiferen des Schliers von Ottnang. Verhandlungen der Geologischen Reichsanstalt 1864, 20–21.

Reuss, A.E., 1867. Die fossile Fauna der Steinsalzablagerungen von Wieliczka in Galizien. Sitzungsberichte der Kaiserlichen Akademie der Wissenschaften, mathematisch-naturwissenschaftliche Classe 55, 17–182.

Roetzel, R., Nagel, D., 1991. Exkursionen im Tertiär Österreichs. Molassezone, Waschbergzone, Korneuburger Becken, Wiener Becken, Eisenstädter Becken. Österreichische Paläontologische Gesellschaft, Wien, 216 p.

Roetzel, R., Ćorić, S., Galović, I., Rögl, F., 2006. Early Miocene (Ottnangian) coastal upwelling conditions along the southeastern scarp of the Bohemian Massif (Parisdorf, Lower Austria, Central Paratethys). Beiträge zur Paläontologie 30, 387–413.

Rögl, F., Schultz, O., Hölzl, O., 1973. Holostratotypus und Faziostratotypen der Innviertler Schichtengruppe. In: Papp, A., Rögl, F., Seneš, J. (Eds.), Miozän M2 – Ottnangien. Die Innviertler, Salgotarjaner, Bantapusztaer Schichtengruppe und die Rzehakia Formation. Chronostratigraphie und Neostratotypen, Miozän der Zentralen Paratethys 3. Verlag der Slowakischen Akademie der Wissenschaften, Bratislava, p. 140–196.

Rögl, F., 1985. Late Oligocene and Miocene planktic foraminifera of the Central Paratethys. In: Bolli, H.M., Saunders, J.B., Perch-Nielsen, K. (Eds.), Plankton Stratigraphy Volume 1: Planktic foraminifera, calcareous nannoplankton and calpionellids. Cambridge University Press, Cambridge, p. 315–328.

Rögl, F., 1998. Palaeogeographic Considerations for Mediterranean and Paratethys Seaways (Oligocene to Miocene). Annalen des Naturhistorischen Museums in Wien 99A, 279–310.

Rupp, C., 1986. Paläoökologie der Foraminiferen in der Sandschalerzone (Badenien, Miozän) des Wiener Beckens. Beiträge zur Paläontologie Österreichs 12, 1–180.

Rupp, C., Haunold-Jenke, Y., 2003. Untermiozäne Foraminiferenfaunen aus dem oberösterreichischen Zentralraum. Jahrbuch der Geologischen Bundesanstalt 143, 227–302.

Rupp, C., Hofmann, T., Jochum, B., Pfleiderer, S., Schedl, A., Schindlbauer, G., Schubert, G., Slapansky, P., Tilch, N., van Husen, D., Wagner, L., Wimmer-Frey, I., 2008. Geologische Karte der Republik Österreich 1:50.000, Blatt 47 Ried im Innkreis. Erläuterungen zu Blatt 47 Ried im Innkreis. Geological Survey of Austria, Vienna.

Rupp, C., van Husen, D., 2007. Zur Geologie des Kartenblattes Ried im Innkreis. In: Egger, H., Rupp, C. (Eds.), Beiträge zur Geologie Oberösterreichs, Arbeitstagung der Geologischen Bundesanstalt 2007. Vienna, p. 73–112.

Seneš, J., 1973. Die Sedimentationsräume und die Schichtengruppen der zentralen Paratethys im Ottnangien. In: Papp, A., Rögl, F., Seneš, J. (Eds.), Miozän M2 – Ottnangien. Die Innviertler, Salgotarjaner, Bantapusztaer Schichtengruppe und die Rzehakia Formation. Chronostratigraphie und Neostratotypen, Miozän der Zentralen Paratethys 3. Verlag der Slowakischen Akademie der Wissenschaften, Bratislava, p. 45–53.

Schiøler, P., 2005. Dinoflagellate cysts and acritarchs form the Oligocene-Lower Miocene interval of the Alma-1 well, Danish North Sea. Journal of Micropalaeontology 24, 1–37.

Simony, F., 1850. Bericht über die Arbeiten der Section V (Reisebericht). Jahrbuch der Geologischen Reichsanstalt 1, 651–657.

Soliman, A., 2006. Lower and middle Miocene dinoflagellate cysts, Gulf of Suez, Egypt. Ph.D. thesis, University of Graz, 327 p.

Soliman, A., Piller, W.E., 2009. Miocene dinoflagellate cysts of the western Central Paratethys. 13th RCMNS-Congress, 2nd-6th September 2009, Naples, Italy. Acta Naturalia de "L'Ateneo Parmense" 45, 229.

Steininger, F., Seneš, J., 1971. M1 – Eggenburgien. Die Eggenburger Schichtengruppe und ihr Stratotypus. Chronostratigraphie und Neostratotypen, Miozän der Zentralen Paratethys 2. Verlag der Slowakischen Akademie der Wissenschaften, Bratislava, 827 p.

Steininger, F., Ctyroky, P., Hölzl, O., Kokay, J., Schlickum, W.R., Schultz, O., Strauch, F., 1973. Die Mollusken des Ottnangien. In: Papp, A., Rögl, F., Seneš, J. (Eds.), Miozän M2 – Ottnangien. Die Innviertler, Salgotarjaner, Bantapusztaer Schichtengruppe und die Rzehakia Formation. Chronostratigraphie und Neostratotypen, Miozän der Zentralen Paratethys 3. Verlag der Slowakischen Akademie der Wissenschaften, Bratislava, p. 380–615.

Stevanović, P., Nevesskaja, L.A., Marinescu, F., Sokac, A., Jámbor, A., 1990. Pl1 – Pontien (sensu F. Le Play, N.P. Barbot, N. I. Andrusov). Chronostratigraphie und Neostratotypen, Neogen der Westlichen ("Zentralen") Paratethys 8. Verlag der Slowakischen Akademie der Wissenschaften, Bratislava, 952 p.

Suess, E., 1866. Untersuchungen über den Charakter der österreichischen Tertiärablagerungen. Sitzungberichte der Akademie der Wissenschaften, mathematisch-naturwissenschaftliche Classe 54, 87–152.

Suess, F.E., 1891. Beobachtungen über den Schlier in Oberösterreich und Bayern. Annalen des Naturhistorischen Museums Wien 6, 407–429.

Tausch, L.v., 1896. Bericht über geologische Beobachtungen bei einigen Tertiärvorkommnissen im Innviertel (Oberösterreich) und in einem Theile von Nieder- und Oberbayern. Verhandlungen der Geologischen Reichsanstalt 1896, 304–311.

Wenger, W.F., 1987. Die Foraminiferen des Miozäns der bayerischen Molasse und ihre stratigraphische sowie paläogeographische Auswertung. Zitteliana 16, 173–340.

Williams, G.L., Brinkhuis, H, Pearce, M.A., Fensome, R.A., Weegink, J.W., 2004. Southern Ocean and global dinoflagellate cyst events compared. Index events for the Late Cretaceous–Neogene. In: Exon, N.F., Kennett, J.P., Malone, M.J. (Eds.), Proceedings of the Ocean Drilling Program, Scientific Results 189, 1–98.

Zevenboom, D., 1995. Dinoflagellate cysts from the Mediterranean Late Oligocene and Miocene. Ph.D. thesis, State University of Utrecht, 221 p.

Zorn, I., 1995. Preliminary report on the ostracodes from the Ottnangian (Early Miocene) of Upper Austria. In: Riha, J. (Ed.), Ostracods and Biostratigraphy. Proceedings of the 12th International Symposium on Ostracoda, Prague, p. 237–243.

Zweigel, J., 1998. Eustatic versus tectonic control on foreland basin fill. Sequence stratigraphy, subsidence analysis, stratigraphic modelling, and reservoir modelling applied to the German Molasse basin. Contributions to Sedimentary Geology 20, 1–140.

CHAPTER 6

INTEGRATED FACIES-ANALYSIS AND STRATIGRAPHY OF THE EARLY MIOCENE NORTH ALPINE FORELAND BASIN OF UPPER AUSTRIA – A SYNOPSIS

The present thesis summarizes the results on facies-analysis and stratigraphy from selected localities in the NAFB of Upper Austria. The Egerian **Pucking** section (chapter 2), the Eggenburgian drill-site **Hochburg 1** (chapter 3) and the Ottnangian stratotype **Ottnang-Schanze** (chapters 4-5) exemplarily document the paleoenvironmental evolution of the study area during the Early Miocene. The achieved integration of bio-, magneto- and sequence stratigraphic constraints allows a correlation of the revealed facies distribution to the global stratigraphic record and the evaluation of the impact of regional and global events on the NAFB. The benthic foraminiferal records additionally provide new insights into regional biostratigraphy.

6.1. Paleoenvironmental development of the Early Miocene NAFB

During the Egerian/late Chattian-**early Aquitanian**, marine deposition in the NAFB was restricted to the Bavarian and Austrian parts of the NAFB (Kuhlemann and Kempf, 2002). The bathyal facies of the Upper Puchkirchen Fm. and the coeval neritic deposits along the northern coastline are well documented in a number of studies (Aberer, 1958, 1959; Küpper and Steininger, 1975; Malzer, 1993; Rögl and Steininger, 1996; Wagner, 1996, 1998; Harzhauser and Mandic, 2002; De Ruig, 2003; Hubbard et al., 2005; De Ruig and Hubbard, 2006; Hinsch, 2008; Covault et al., 2009; Hubbard et al., 2009). In contrast, the transitional outer neritic and upper slope facies of the Ebelsberg Formation has been rarely adressed (Hochuli, 1978; Kovar, 1992; Wagner, 1998; Gregorova et al., 2009). The herein presented evaluation of the lower Aquitanian / upper Egerian deposits of the **Ebelsberg Fm.** near **Pucking** provides new information on the paleoenvironment:

The micropaleontological and geochemical proxies suggest that the finely laminated sediments were deposited along the northern shelf of the Puchkirchen Basin. Upwelling and episodically increased coastal runoff provided large amounts of nutrients stimulating primary productivity. All revealed data suggest dysoxic-anoxic bottom waters of an oxygen minimum zone along the outer shelf and upper slope.

In addition, the Ebelsberg Fm. bears an exceptional *Konservat-Lagerstätte* with a variety of rich macrofossil assemblages. The revealed fossil assemblages show specific associations occurring during distinct intervals within the rather uniform sediments of the section. Different mechanisms are discussed to explain their origin:

- Mass occurrences of pteropods and calcareous nannoplankton occur in several horizons across

the section. These accumulations are interpreted as response to an episodic rise in nutrient availability that results in blooms of productivity. Increased coastal runoff or intensified upwelling activity are considered as the trigger mechanism.

- Allochthonous associations of the nautiloid *Aturia* with brown algae indicate a complex transport mechanism: shells of the offshore-living cephalopods were transported to the coast by surface currents and/or wind currents. Episodic flooding events and storms then mixed the accumulated shells with the algae and drew them offshore again. The latter process also seems to apply to pipefish accumulations observed in the section.
- The multi-species vertebrate accumulations of fish and dolphins are considered as parautochthonous as their habitat is in good agreement with the reconstructed paleoenvironment.
- Benthic mollusc communities are scarce and of low diversity. They mainly consist of bivalves adapted to anoxic environments and thus are regarded as parautochthonous.

During the Eggenburgian/**early Burdigalian**, the interrupted marine connection of the NAFB to the Mediterranean sea in the west is re-established with the formation of the Burdigalian Seaway (Allen et al., 1985; Berger, 1996; Schlunegger et al., 1997; Kuhlemann and Kempf, 2002). Widespread neritic paleoenvironments developed in the course of the transgression throughout the NAFB that have been studied at many localities in Switzerland and Germany (e.g., Wenger, 1987; Schlunegger et al., 1997; Kuhlemann and Kempf, 2002; Pippèrr and Reichenbacher, 2009). Deep-marine Eggenburgian paleoenvironments are restricted to the Puchkirchen Basin (**Hall Fm.**) and along the southeastern Bohemian Massif (Zellerndorf Fm.; Wagner, 1998; Kuhlemann and Kempf, 2002; Roetzel et al., 2006; Grunert et al., 2010). While the paleoenvironment for the later has been described in great detail (Roetzel et al., 2006; Grunert et al., 2010) the pelitic sediments of the Hall Fm. lack a detailed facies and stratigraphic analysis.

A section that comprises the entire Hall Fm. has been chosen from the drill-site **Hochburg 1** for thorough evaluation in the present study. Based on foraminiferal and geochemical proxies, a succession of depositional environments is reavealed: following a major erosional hiatus, the conglomeratic sands at the base of the section contain reworked Chattian and Aquitanian foraminiferal assemblages that document the reactivation of the basin-axial Puchkirchen Channel System. In the course of the transgression the channel was cut off from its sediment sources on the shelf and a deepening bathyal environment was established. Agglutinated foraminiferal assemblages with large amounts of *Bathysiphon filiformis* developed that were adapted to an unstable environment with frequent deposition of turbidites. The middle part of the Hall Fm. contains NE prograding prodeltaic sediments that initiated the upfill of the Puchkirchen Basin. High sedimentation rates and increased input of terrestrial-derived organic matter are documented in low TOC/S and HI values and frequent occurrences of *Ammodiscus* spp. and other opportunistic agglutinating foraminifers. A final major transgression temporarily re-established a eutrophic and

suboxic bathyal environment with foraminiferal assemblages containing high numbers of *Bathysiphon filiformis*. Finally, hyaline foraminiferal faunas with *Lenticulina inornata*, *Ammonia beccharii* and *Cibcidoides* spp. herald the transition into the oxic outer-middle neritic environment of the Ottnangian shelf sea.

Following the upfill of the Puchkirchen Basin, a vast tide-influenced shelf sea developed in the study area during the **middle Burdigalian**/early Ottnangian (Faupl and Roetzel, 1987; 1990; Kuhlemann and Kempf, 2002; Pippèrr and Reichenbacher, 2010; Pippèrr, 2011). During this time, the Burdigalian Seaway reached its maximum extent (Pippèrr, 2011). The herein evaluated section **Ottnang-Schanze** represents the stratotype for the Ottnangian and exemplarily documents the facies development during the late early Ottnangian (Rögl et al., 1973; Rupp et al., 2008). Microfossil assemblages revealed trends in bathymetry, primary productivity, bottom-water oxygenation and water energy that indicate a more diverse paleoenvironment than previously described. Several facies within a eutrophic environment with suboxic bottom-waters are distinguished that document a transition from an outer neritic to upper bathyal towards a middle neritic environment under the influence of storm events and tidal currents.
Earlier studies in eastern Bavaria have shown a regressive trend during late early Ottnangian (Wenger, 1987; Pippèrr, 2011). A comparison of foraminiferal assemblages from the stratotype and other localities in Upper Austria indicates that the outer neritic to upper bathyal facies from the lower part of the stratotype represents the most distal sediments. The upper part together with localities situated closer to the northern coast record inner to middle neritic environments under strong influence of tidal currents. The revealed facies distribution results from the progradation of the tide-influenced northern shelf of the NAFB, heralding the closure of the Burdigalian Seaway and the final regression of the sea towards the East.

6.2. Stratigraphic correlation to ATNTS 2004 and the impact of local and global events

As lined out in chapter 1, many problems exist with the correlation of the regional Paratethyan stages to the global stratigraphic record. In the present study, the age model developed by Piller et al. (2007) is applied to the NAFB. In this stratigraphic framework a correlation of the Paratehyan stages and substages to global 3rd-order sequence stratigraphy is assumed in order to overcome the shortcomings of earlier concepts. For the Early Miocene, Piller et al. (2007) suggest a correlation of the upper Egerian to sequence Aq 1, the lower, middle and upper Eggenburgian correspond to sequences Aq 2, Bur 1 and Bur 2 and the Ottnangian is in accord with sequence Bur 3 (Fig. 1.4.; Abreu and Haddad, 1998; Lourens et al., 2004). The integrated stratigraphic records of the presented thesis allow a correlation of the revealed facies development to the ATNTS 2004 (Lourens et al., 2004) and the age model of Piller et al. (2007).

A review of earlier publications and internal reports by RAG implies that the Upper Puchkichen

and Ebelsberg Fms. follow global 3rd-order sequence stratigraphy (Zweigel, 1998; Peña, 2007; Süss et al., 2007; Hinsch, 2008). Two fining upward cycles can be distinguished in the **Upper Puchkirchen Fm.** that have been correlated to two 3rd-order sequences (Hinsch, 2008). Rögl et al. (1979) report nannoplankton zones NP 25, NN 1 and NN 2a for the Upper Puchkirchen Fm. indicating a correlation to the Ch3 and Aq 1 sequences.
A relation of the second fining upward cycle to sequence Aq 1 is further indicated by the finely laminated fish shales that occur over large areas in Upper Austria (top of Upper Puchkirchen Fm., **Ebelsberg Fm.**) and Bavaria (Obing Beds; Wenger, 1987; Zweigel, 1998). Calcareous nannoplankton assemblages from the **Pucking** section (Gregorova et al., 2009) and the top of the Puchkirchen Fm. (**Hochburg 1**, unpublished) reveal biozones NN 1 and NN 2a which fall within the maximum flooding surface of Aq 1 (Lourens et al., 2004). However, future studies will have to establish a detailed stratigraphic record that integrates the highly variable facies distribution within the Puchkirchen Fm. to confirm these assumptions.

A major **erosional event** occurred between Egerian and Eggenburgian deposits in the NAFB (Papp et al., 1971; Wenger, 1987; Wagner, 1998; Zweigel, 1998; Morend, 2000; Kuhlemann and Kempf, 2002; Holcova, 2007). At **Hochburg 1** the hiatus occurs between the Upper Puchkirchen Fm. and the Hall Fm. Calcareous nannoplankton assemblages reveal the early-middle Burdigalian biozone upper NN2 for the base of the Hall Fm. The correlation of the top of the Upper Puchkirchen Fm. to sequence Aq 1 suggests the absence of the late Aquitanian sequence Aq 2. A duration of c. 1 Ma years is implied for the hiatus in the study area that corresponds to the entire early Eggenburgian.
An evaluation of available records reveals the general scarcity of lower Eggenburgian sediments in the study area: while middle and upper Eggenburgian deposits have been described from many areas in Switzerland, Germany and Upper Austria (e.g., Wenger, 1987; Schlunegger et al., 1997; Wagner, 1998; Rupp and Haunold-Jenke, 2003; Pippèrr and Reichenbacher, 2009), a single locality from southeastern Bavaria (Pechschnaitgraben) has been clearly assigned to the lower Eggenburgian so far (Wenger, 1987).

A relation to **3rd-order sequence stratigraphy** is evident for the Burdigalian deposits in the study area. The integration of the herein revealed facies development with biostratigraphic constraints allows the identification of the 3rd-order sequence boundaries Bur 1-3 in the lower, middle and upper **Hall Fm**. The transgression observed at the base of the Hall Fm. correponds to the early Burdigalian transgression that can be observed in the Central Paratethys (Schlunegger et al., 1997; Mandic and Steininger, 2003) as well as in records all over the world (Haq, 1988; Abreu and Haddad, 1998; Haq and Al-Quathani, 2005; Miller et al., 2005; Kominz et al., 2008). The observations confirm earlier studies that suggest a main control of eustatic sea-level on the NAFB as the basin remained underfilled when thrusting in the eastern Alps ceased followed by viscoelastic relaxation during the early Burdigalian (Zweigel, 1998; Genser, 2007).

In Upper Austria, the **Eggenburgian/Ottnangian boundary** has been correlated to the lithostratigraphic boundary between the Hall Fm. and the Innviertel Group (Papp et al., 1971; Rögl et al., 1979; Cicha et al., 1998; Krenmayr and Schnabel, 2006; Rupp et al., 2008). However, a sharp boundary between the two lithological units is often missing and replaced by a gradational transition (Rupp and Rögl, 1996; Rupp and van Husen, 2007). As a consequence, the top of the Hall Fm. has been defined by the last occurrence of *Lenticulina buergli* and the first occurrence of *Amphicoryna ottnangensis* together with a widespread neritic fauna dominated by *Lenticulina inornata* by some authors (Rupp and Haunold-Jenke, 2003).
The foraminiferal assemblages revealed at **Hochburg 1** exemplarily document the problems related to the identification of the Eggenburgian/Ottnangian boundary due to the facies dependency of the index fossils. Following Piller et al. (2007), the new results place sequence boundary Bur 3 and thus the geochronological boundary c. 190m below the lithostratigraphic boundary indicated by RAG. The boundary occurs directly above the last occurrence of *L. buergli* which is in good agreement with earlier studies (Rupp and Haunold-Jenke, 2003). However, a bathyal agglutinated foraminiferal fauna develops at the base of the Ottnangian and *A. ottnangensis* was not encountered. The characteristic neritic fauna with *L. inornata* was only documented for the topmost samples.

Finally, the new bio- and magnetostratigraphic data for **Ottnang-Schanze** constrain the maximum extent of the Burdigalian Seaway to c. 18 Ma. The subsequent basin-wide regression coincides with isotopic event MBi2 (Abreu and Haddad, 1998) suggesting a combination of global climate cooling and high input of Alpine debris that led to the final retreat of the Central Paratethys from the NAFB.

6.3. Implications for regional biostratigraphy

In contrast to the mollusc-based biostratigraphy developed for the stratotype area in the Lower Austrian part of the NAFB (Steininger and Seneš, 1971; Steininger et al., 1971; Mandic and Steininger, 2003), a biostratigraphic concept based on benthic foraminifers has been developed in eastern Bavaria (Hagn, 1960; Wenger, 1987; Pippèrr and Reichenbacher, 2009). For the early Miocene, five benthic foraminiferal biozones are distinguished that correpond to the upper Egerian, lower-upper Eggenburgian and lower-middle Ottnangian (Wenger, 1987). In Upper Austria, this concept was successfully adopted for the Egerian and Ottnangian when similar facies occurred in the Bavarian and Austrian parts of the basin (Wenger, 1987; Cicha et al., 1998; Rupp and Haunold-Jenke, 2003; Rupp et al., 2008). Problems arose with the correlation of the Eggenburgian shelf deposits of Bavaria with the coeval pelitic Hall Fm. in Upper Austria (Cicha et al., 1998; Rupp and Haunold-Jenke, 2003). The herein presented foraminiferal evaluation of the Hall Fm. contributes new information to these issues.

Uvigerina posthantkeni has been suggested as an index species for the Eggenburgian in the

NAFB by Cicha et al. (1971). Subsequent studies by Cicha et al. (1983, 1986, 1998), Wenger (1987), Kohl and Krenmayr (1997) and Rupp and Haunold-Jenke (2003) challenged the biostratigraphic value of *U. posthantkeni* with reports from upper Egerian and lower Ottnangian deposits. In the latter, specimens are often associated with large amounts of allochthonous taxa and have been considered to be reworked (Kohl and Krenmayr, 1997; Rupp and Haunold-Jenke, 2003). In addition to the uncertain stratigraphic range, Wenger (1987) pointed out the high morphological variability of *U. posthantkeni* that makes the distinction from the closely related species *U. hantkeni* and *U. steyri* difficult.
At Hochburg 1, specimens of *U. posthantkeni* have been recorded in the lower part of the Hall Fm. An allochthonous, most likely reworked origin is indicated by its exceptionally high abundance in the transgressive sands and conglomerates at the base of the Hall Fm. and its association with reworked Egerian index taxa. The tests are often heavily compressed and broken while other, most likely autochthonous hyaline taxa revealed no signs of compression. The observations support earlier studies that strongly question the validity of *U. posthantkeni* as Eggenburgian index species.

The first occurrences of ***Elphidium felsense*** and ***E. ortenburgense*** correspond to the base of the middle Eggenburgian in Bavaria (Wenger, 1987; Pippèrr and Reichenbacher, 2009). In contrast, Cicha et al. (1998) tentatively correlate the occurrence of these elphidiid index species in the Hall Fm. with the base of the Eggenburgian.
The herein presented data strongly suggest that the debate resulted from poor stratigraphic control of the Hall Fm. The correlation of the lower Hall Fm. with the middle Eggenburgian resolves the issue and confirms the validity of *E. felsense* and *E. ortenburgense* as regional index fossils for the base of the middle Eggenburgian.

The stratigraphic range of ***Lenticulina buergli*** has been discussed for a long time. Based on its common occurrence in the Hall Fm. *L. buergli* has been suggested as an Eggenburgian index (Bürgl, 1946; Egger et al., 1996; Cicha et al., 1998; Wagner, 1998; Rupp and Haunold-Jenke, 2003). In contrast, Wenger (1987) correlated the occurrence of *L. buergli* in Bavaria with the base of the Ottnangian. A recent stratigraphic re-evaluation of Eggenburgian and Ottnangian deposits in Bavaria conclusively shows that *L. buergli* is restricted to middle and upper Eggenburgian strata (Pippèrr and Reichenbacher, 2009; Pippèrr, 2011). The herein documented occurrence of several specimens of *L. buergli* in the upper Hall Fm. supports its middle-upper Eggenburgian range.

6.4. References

Abreu, V.S., Haddad, G.A., 1998. Glacioeustatic fluctuations: the mechanism linking stable isotope events and sequence stratigraphy from the Early Oligocene to Middle Miocene. In: Graciansky, C.-P., Hardenbol, J., Jacquin, T., Vail, P.R. (Eds.), Mesozoic and Cenozoic sequence stratigraphy of European basins. Sedimentary Geology Special Publication, vol. 60. Society for Sedimentary Geology, Tulsa, pp. 245–260.

Aberer, F., 1958. Die Molassezone im westlichen Oberösterreich und in Salzburg. Mitteilungen der Geologischen Gesellschaft in Wien 50, 23–93.

Aberer, F., 1959. Das Miozän der westlichen Molassezone Österreichs mit besonderer Berücksichtigung der Untergrenze und seiner Gliederung. Mitteilungen der Geologischen Gesellschaft in Wien 52, 7–16.

Allen, P.A., Mange-Rajetzky, M., Matter, A., Homewood, P., 1985. Dynamic palaeogeography of open Burdigalian sea-way, Swiss Molasse Basin. Eclogae Geologicae Helveticae 79, 351–381.

Berger, J.-P., 1996. Cartes paléogéographiques-palinspastiques du bassin molassique suisse (Oligocène inférieur – Miocène moyen). Neues Jahrbuch für Geologie und Paläontologie 202, 1–44.

Bürgl, H., 1949. Zur Stratigraphie und Tektonik des oberösterreichischen Schliers. Verhandlungen der Geologischen Bundesanstalt 1946, 123–151.

Cicha, I., Zapletalová, I., Papp, A., Čtyroká, J., Lehotayová, R., 1971. Die Foraminiferen der Eggenburger Schichtengruppe. In: Steininger, F., Seneš, J., (Eds.), M1 – Eggenburgien. Die Eggenburger Schichtengruppe und ihr Stratotypus. Chronostratigraphie und Neostratotypen, Miozän der Zentralen Paratethys 2, 234–354. Verlag der Slowakischen Akademie der Wissenschaften, Bratislava.

Cicha, I., Zapletalová, I., Molcikova, V., Brzobohatý, R., 1983. Stratigraphical range of Eggenburgian – Badenian Foraminifera in West Carpathian basins. Plyn Nafta 4, 99–144.

Cicha, I., Krhovský, J., Brzobohatý, R., Čtyroká, J., Daniels von, C.H., Haunold, T., Horvath, M., Luczkowska, E., Reiser, H., Rupp, C., Rijavec, L., Wenger, W., 1986. Oligocene and Miocene *Uvigerina* from the Western and Central Paratethys. Utrecht Micropaleontological Bulletin 35, 121–181.

Cicha, I., Rögl, F., Rupp, C., Ctyroká, J., 1998. Oligocene-Miocene foraminifers of the Central Paratethys. Abhandlungen der Senckenbergischen Naturforschenden Gesellschaft 549, 1–325.

Covault, J.A., Hubbard, S.M., Graham, S.A., Hinsch, R., Linzer, H.-G., 2009. Turbidite-reservoir architecture in complex foredeep-margin and wedge-top depocenters, Tertiary Molasse freeland basin system, Austria. Marine and Petroleum Geology 26, 379–396.

De Ruig, M.J., 2003. Deep Marine Sedimentation and Gas Reservoir Distribution in Upper Austria. Oil Gas European Magazine 29, 64–73.

De Ruig, M.J., Hubbard, S.M., 2006. Seismic facies and reservoir characteristics of a deep marine axial channel belt in the Molasse Basin, Puchkirchen Formation, Upper Austria. AAPG Bulletin 90, 735–752.

Egger, H., Hofmann, T., Rupp, C., 1996. Ein Querschnitt durch die Geologie Oberösterreichs. „Wandertagung Österr. Geol. Ges." 7.–11. Oktober 1996 in Wels. Exkursionsführer 16, Österreichische Geologische Gesellschaft, Wien. 121 pages.

Faupl, P., Roetzel, R., 1987. Gezeitenbeeinflußte Ablagerungen der Innviertler Gruppe (Ottnangien) in der oberösterreichischen Molassezone. Jahrbuch der Geologischen Bundesanstalt 130, 415–447.

Faupl, P., Roetzel, R., 1990. Die Phosphoritsande und Fossilreichen Grobsande: Gezeitenbeeinflußte Ablagerungen der Innviertler Gruppe (Ottnangien) in der oberösterreichischen Molasse. Jahrbuch der Geologischen Bundesanstalt 133/2, 157–180.

Genser, J., Cloetingh, S.A.P.L., Neubauer, F., 2007. Late orogenic rebound and oblique Alpine convergence:

New constraints from subsidence analysis of the Austrian Molasse Basin. Global and Planetary Change 58, 214–223.

Gregorova, R., Schultz, O., Harzhauser, M., Kroh, A., Ćoric, S., 2009. A giant Early Miocene sunfish from the North Alpine Foreland Basin (Austria) and its implication for molid phylogeny. Journal of Vertebrate Paleontology 29, 359–371.

Grunert, P., Soliman, A., Harzhauser, M., Müllegger, S., Piller, W. E., Roetzel, R., Rögl, F., 2010. Upwelling conditions in the Early Miocene Central Paratethys sea. Geologica Carpathica 61, 129–145.

Hagn, H., 1960. Die Gliederung der bayerischen Miozän-Molasse mit Hilfe von Kleinforaminiferen. Mitteilungen der Geologischen Gesellschaft 52, 133–141.

Haq, B.U., Hardenbol, J., Vail, P.R., 1988. Mesozoic and Cenozoic chronostratigraphy and cycles of sea-level change. Society of Economic Paleontologists and Mineralogists 42, 71–108.

Haq, B.U., Al-Qahtani, A.M., 2005. Phanerozoic cycles of sea-level change on the Arabian Platform. GeoArabia 10, 127 – 160.

Harzhauser, M., Mandic, O., 2002. Late Oligocene Gastropods and Bivalves from the Lower and Upper Austrian Molasse Basin, in: Piller, W. E., Rasser, M., (Eds.), The Paleogene of Austria. Österreichische Akademie der Wissenschaften, Schriftenreihe der Erdwissenschaftlichen Kommissionen 14, pp. 671–795.

Hinsch, R., 2008. New Insights into the Oligocene to Miocene Geological Evolution of the Molasse Basin of Austria. Oil Gas European Magazine 34, 138–143.

Hochuli, P.A., 1978. Palynologische Untersuchungen im Oligozän und Untermiozän der Zentralen und Westlichen Paratethys. Beiträge zur Paläontologie von Österreich 4, 1–132.

Holcová, K., 2002. Calcareous nannoplankton from the Eggenburgian stratotype and faciostratotypes (Lower Miocene, Central Paratethys). Geologica Carpathica 53, 381–390.

Hubbard, S.M., de Ruig, M.J., Graham, S.A., 2005. Utilizing outcrop analogs to improve subsurface mapping of natural gas-bearing strata in the Puchkirchen Formation, Molasse Basin, Upper Austria. Austrian Journal of Earth Sciences 98, 52–66.

Hubbard, S.M., de Ruig, M.J., Graham, S.A., 2009. Confined channel-levee complex development in an elongate depo-center: Deep-water Tertiary strata of the Austria Molasse basin. Marine and Petroleum Geology 26, 85–112.

Kohl, H., Krenmayr, H.-G., 1997. Erläuterungen zu Blatt 49 Wels. Geologische Bundesanstalt, Wien. 77 pages.

Kominz, M.A., Browning, J.V., Miller, K.G., Sugarman, P.J., Mizintseva, S., Scotese, C.R., 2008. Late Cretaceous to Miocene sea-level estimates from the New Jersey and Delaware coastal plain coreholes: an error analysis. Basin Research 20, 211–226.

Kovar, J.B., 1982. Eine Blätter-Flora des Egerien (Ober-Oligozän) aus marinen Sedimenten der Zentralen Paratethys im Linzer Raum (Österreich). Beiträge zur Paläontologie von Österreich 9, 1–209.

Krenmayr, H.G., Schnabel, W., 2006. Geologische Karte von Oberösterreich 1:200.000, 1 sheet, 2 additional maps. Geological Survey of Austria, Vienna.

Kuhlemann, J., Kempf, O., 2002. Post-Eocene evolution of the North Alpine Foreland Basin and its response to Alpine tectonics. Sedimentary Geology 152, 45–78.

Küpper, I., Steininger, F., 1975. Faziostratotypen der Puchkirchener Schichtengruppe. In: Baldí, T., Seneš, J. (Eds.), OM – Egerien. Die Egerer, Pouzdraner, Puchkirchener Schichtengruppe und die Bretkaer Formation. Chronostratigraphie und Neostratotypen, Miozän der Zentralen Paratethys, vol. 5. Verlag der Slowakischen Akademie der Wissenschaften, 205–220.

Lourens, L., Hilgen, F., Shackleton, N.J., Laskar, J., Wilson, D., 2004. The Neogene Period. In: Gradstein, F.M., Ogg, J.G., Smith, A.G. (Eds.), A Geologic Time Scale 2004. Cambridge University Press, Cambridge, pp. 409–440.

Malzer, O., Rögl, F., Seifert, P., Wagner, L., Wessely, G., Brix, F., 1993. Die Molassezone und deren Untergrund. In: Brix, F., Schultz, O. (Eds.), Erdöl und Erdgas in Österreich. 281-357.

Mandic, O., Steininger, F.F., 2003. Computer-based mollusc stratigraphy - a case study from the Eggenburgian (Early Miocene) type region (NE Austria) - Palaeogeography, Palaeoclimatology, Palaeoecology 197, 263–291.

Miller, K.G., Kominz, M.A., Brwoning, J.V., Wright, J.D., Mountain, G.S., Katz, M.E., Sugarman, P.J., Cramer, B.S., Christie-Blick, N., Pekar, S.F., 2005. The Phanerozoic record of global sea-level change. Science 310, 1293–1298.

Morend, D., 2000. High-resolution seismic facies of alluvial depositional systems in the Lower Freshwater Molasse (Oligocene–early Miocene, western Swiss Molasse Basin). Terre et Environ 23, 1–97.

Papp, A., Seneš, J., Steininger, F., Cicha, I., Báldi, T., 1971. Die Eggenburger Schichtengruppe – $M_{1(a)b-d}$. In: Steininger, F., Seneš, J., (Eds.), M1 – Eggenburgien. Die Eggenburger Schichtengruppe und ihr Stratotypus. Chronostratigraphie und Neostratotypen, Miozän der Zentralen Paratethys 2, 49–94. Verlag der Slowakischen Akademie der Wissenschaften, Bratislava.

Peña, F.A.C., 2007. The Early Miocene Upper Marine Molasse of the German part of the Molasse Basin - a subsurface study. Sequence Stratigraphy, Depositional Environment and Architecture, 3D Basin Modeling. Ph.D. Thesis, Eberhard-Karls-Universität Tübingen, Germany.

Piller, W.E., Harzhauser, M., Mandic, O., 2007. Miocene Central Paratethys stratigraphy – current status and future directions. Stratigraphy 4, 151–168.

Pippèrr, M., 2011. Characterisation of Ottnangian (middle Burdigalian) palaeoenvironments in the North Alpine Foreland Basin using benthic foraminifera—A review of the Upper Marine Molasse of southern Germany. Marine Micropaleontology 79, 80–99.

Pippèrr, M., Reichenbacher, B., 2009. Biostratigraphy and paleoecology of benthic foraminifera from the Eggenburgian "Ortenburger Meeressande" of southeastern Germany (Early Miocene, Paratethys). Neues Jahrbuch für Geologie und Paläontologie Abhandlungen 254, 41–61.

Pippèrr, M., Reichenbacher, B., 2010. Foraminifera from the borehole Altdorf (SE Germany): Proxies for Ottnangian (early Miocene) palaeoenvironments of the Central Paratethys. Palaeogeography,

Roetzel, R., Ćorić, S., Galović, I., Rögl, F., 2006. Early Miocene (Ottnangian) coastal upwelling conditions along the southeastern scarp of the Bohemian Massif (Parisdorf, Lower Austria, Central Paratethys).

Beiträge zur Paläontologie 30, 387–413.

Rögl, F., Schultz, O., Hölzl, O., 1973. Holostratotypus und Faziostratotypen der Innviertler Schichtengruppe. In: Papp, A., Rögl, F., Seneš, J. (Eds.), Miozän M2 – Ottnangien. Die Innviertler, Salgotarjaner, Bantapusztaer Schichtengruppe und die Rzehakia Formation. Chronostratigraphie und Neostratotypen, Miozän der Zentralen Paratethys 3. Verlag der Slowakischen Akademie der Wissenschaften, Bratislava, p. 140–196.

Rögl, R., Hochuli, P., Muller, C., 1979. Oligocene-Early Miocene stratigraphic correlations in the Molasse Basin of Austria. Annales Geologiques des Pays Helleniques Tome hors series, 1045–1050.

Rögl, F., Rupp, C., 1996. Stratigraphie in der Molassezone Oberösterreichs. Exkursionsführer 16, pp. 66–72. Österreichische Geologische Gesellschaft, Wien.

Rögl, F., Steininger, F., 1996. Miogypsina (Miogypsinoides) formosensis Yabe & Hanzawa 1928 (Foraminiferida) aus den Linzer Sanden (Egerian, Oberoligozän) von Plesching bei Linz. Mitteilungen der Geologischen Gesellschaft 62, 46–54.

Rupp, C., Haunold-Jenke, Y., 2003. Untermiozäne Foraminiferenfaunen aus dem oberösterreichischen Zentralraum. Jahrbuch der Geologischen Bundesanstalt 143, 227–302.

Rupp, C., Hofmann, T., Jochum, B., Pfleiderer, S., Schedl, A., Schindlbauer, G., Schubert, G., Slapansky, P., Tilch, N., Husen, D. van, Wagner, L., Wimmer-Frey, I., 2008. Geologische Karte der Republik Österreich 1:50.000, Blatt 47 Ried im Innkreis. Erläuterungen zu Blatt 47 Ried im Innkreis. Geological Survey of Austria, Vienna.

Rupp, C., Husen, D. van, 2007. Zur Geologie des Kartenblattes Ried im Innkreis. In: Egger, H., Rupp, C. (Eds.), Beiträge zur Geologie Oberösterreichs, Arbeitstagung der Geologischen Bundesanstalt 2007. Geological Survey of Austria, Vienna, 73–112.

Schlunegger, F., Leu, W., Matter, A., 1997. Sedimentary Sequences, Seismic Facies, Subsidence Analysis, and Evolution of the Burdigalian Upper Marine Molasse Group, Central Switzerland. AAPG Bulletin 81, 1185–1207.

Steininger, F., Seneš, J., 1971. M1 – Eggenburgien. Die Eggenburger Schichtengruppe und ihr Stratotypus. Chronostratigraphie und Neostratotypen, Miozän der Zentralen Paratethys 2. Verlag der Slowakischen Akademie der Wissenschaften, Bratislava, 827 p.

Steininger, F., Čtyroký, P., Ondrejíčková, A., Seneš, J., 1971. Die Mollusken der Eggenburger Schichtengruppe. In: Steininger, F., Seneš, J., (Eds.), M1 – Eggenburgien. Die Eggenburger Schichtengruppe und ihr Stratotypus. Chronostratigraphie und Neostratotypen, Miozän der Zentralen Paratethys 2, 356–591. Verlag der Slowakischen Akademie der Wissenschaften, Bratislava.

Süss, M.P., Strauss, C., Hinsch, R., 2008. Sequence stratigraphy and depositional dynamics of the Puchkirchen basin (Upper Austria). Unpublished internal report of RAG, 28pp.

Wagner, L.R., 1996. Stratigraphy and hydrocarbons in Upper Austrian Molasse Foredeep (active margin). European Association of Geoscientists and Engineers Special Publication 5, 217–235.

Wagner, L.R., 1998. Tectono-stratigraphy and hydrocarbons in the Molasse Foredeep of Salzburg, Upper and Lower Austria, in: Mascle, A., Puigdefàbregas, C., Luterbacher H.P., Fernàndez, M. (Eds.), Cenozoic Foreland Basins of Western Europe. Geological Society Special Publications 134. Geological Society, London, pp. 339–369.

Wenger, W.F., 1987. Die Foraminiferen des Miozäns der bayerischen Molasse und ihre stratigraphische sowie paläogeographische Auswertung. Zitteliana 16, 173–340.

Zweigel, J. (1998). Eustatic versus tectonic control on foreland basin fill. Contributions to Sedimentary Geology 20. Schweizerbart, Stuttgart.